Project THEMIS
Technical Report No. 18

RESPONSE OF A TURBULENT BOUNDARY LAYER TO LATERAL ROUGHNESS DISCONTINUITIES

by

Hua Wang

E. C. Nickerson

Prepared under
Office of Naval Research
Contract No. N00014-68-A-0493-0001
Project No. NR 062-414/6-6-68(Code 438)
U. S. Department of Defense
Washington, D. C.

Fluid Dynamics and Diffusion Laboratory
College of Engineering
Colorado State University
Fort Collins, Colorado

July 1972 CER71-72HW-ECN51

ABSTRACT

RESPONSE OF A TURBULENT BOUNDARY LAYER
TO LATERAL ROUGHNESS DISCONTINUITIES

The structure of the turbulent boundary layer on a flat plate consisting of alternate, longitudinal strips of smooth and rough (Sand paper, Grit 4) surfaces parallel to the direction of the flow has been investigated. Measurements of mean velocity, wall shear stress, turbulent intensities, turbulent shear stresses and energy spectra of the streamwise turbulent velocity were obtained.

The flow field can be subdivided into three regions. These are: (a) the "smooth" region along the centerline of each smooth strip; (b) the "rough" region along the centerline of each rough strip; and (c) the "intermediate" region lying between the smooth and the rough regions. In both smooth and rough regions, the flow conditions are found to be nearly analogous to those in two-dimensional boundary layers over smooth and rough walls, respectively. In the intermediate region the wall shear stress was found to adjust itself very rapidly to the local conditions of the wall while going from the smooth to the rough region. The vertical distribution of mean velocity can satisfactorily be expressed by the two-dimensional descriptions for the law of the wall and the velocity-defect law. However, the two laws are not universal but form a family of curves depending on the local wall shear stress. The spanwise change from smooth-wall conditions to rough-wall conditions will induce a weak cross-flow directed from the rough to the smooth region near the wall. A theoretical description of the turbulent

shear stress $-\rho\overline{vw}$ which is responsible for the generation of this cross-flow has been presented. The spanwise adjustment of turbulent quantities to local conditions of the wall takes place at a slower rate than does the wall shear stress. The normalized spectra of the streamwise turbulent velocity remains largely unaffected by the surface configuration investigated here.

TABLE OF CONTENTS

Chapter		Page
	LIST OF TABLES	viii
	LIST OF FIGURES	ix
	LIST OF SYMBOLS	xii
I	INTRODUCTION	1
	1.1 Purpose of Present Investigation	2
	1.2 Scope of Present Investigation	3
	1.3 Effect of Strip Width on Boundary Layer Development	4
	1.4 Effect of Surface Roughness on Boundary Layer Development	6
II	LITERATURE REVIEW	8
	2.1 Turbulent Flow over Smooth Walls	9
	2.2 Turbulent Flow over Rough Walls	13
	2.3 Boundary Layer Flow over Streamwise Roughness Changes	15
III	THEORETICAL DESCRIPTION OF THE FLOW	19
	3.1 Basic Equations	19
	3.2 Mean Velocity Distribution	21
	3.3 Estimation of the Turbulent Shear Stress $-\rho\overline{vw}$	23
IV	EXPERIMENTAL EQUIPMENT AND PROCEDURE	26
	4.1 Experimental Equipment	26
	4.1.1 Wind Tunnel	26
	4.1.2 Flat Plate	27
	4.1.3 Carriage	27

Chapter		Page
	4.1.4 Manometer	28
	4.1.5 Hot-Wire Anemometer Systems	28
	4.1.6 Wave Analyzer	29
	4.2 Experimental Arrangements	30
	4.3 Experimental Procedure	31
	4.3.1 Measurement of Static Pressure	31
	4.3.2 Measurement of Mean Velocity	32
	4.3.3 Measurement of Wall Shear Stress	34
	4.3.4 Measurement of Turbulence	36
	4.3.5 Measurement of Frequency Spectra	42
V	ANALYSIS OF EXPERIMENTAL DATA	44
	5.1 Boundary layer Development	44
	5.2 Determination of Shear Velocity	46
	5.3 Mean Velocity Field	47
	5.3.1 Vertical Distribution of Mean Velocity ..	47
	5.3.2 Spanwise Distribution of Mean Velocity ..	54
	5.4 Turbulence Field	55
	5.5 Energy Spectra of Streamwise Turbulent Velocity	57
VI	CONCLUSIONS	59
	BIBLIOGRAPHY	62
	APPENDIX	70
	TABLES	75
	FIGURES	98

LIST OF TABLES

Table		Page
5.1	Summary of boundary layer parameters	
	a. U_∞ = 20 ft/sec	76
	b. U_∞ = 30 ft/sec	77
5.2	Preston-tube measurement of wall shear stress	
	a. U_∞ = 20 ft/sec	78
	b. U_∞ = 30 ft/sec	79
5.3	Mean velocity data	
	a. U_∞ = 20 ft/sec	80
	b. U_∞ = 30 ft/sec	84
5.4	Turbulence data	
	a. U_∞ = 20 ft/sec	88
	b. U_∞ = 30 ft/sec	90
5.5	Data on one-dimensional spectra	92

LIST OF FIGURES

Figure		Page
1.1	Schematic presentation of boundary layer flow along alternate, longitudinal strips of smooth and rough surfaces	99
1.2	Coordinate system and flow features	100
4.1	Plan view of wind tunnel	101
4.2	Plan view of flat plate	102
4.3	Cross-sectional elevation of flat plate and pressure tap	103
4.4	Experimental arrangement in the test section of wind tunnel	104
4.5	False wind tunnel ceiling to obtain zero streamwise pressure gradient over flat plate	105
4.6	Non-dimensional plot of static pressure distribution at the free-stream along the centerline of the flat plate	106
4.7	Nondimensional plot of wall pressure distribution of the flat plate	107
4.8	Mean velocity distribution at x = 5 ft. to check plane symmetric condition of the flow	108
4.9	Typical comparison of mean velocity profiles measured by hot-wire and pitot tube at x = 6 ft, y = 0 in. ..	109
4.10	Schematic diagram of single hot-wire measurement instrument	110
4.11	Typical calibration curves of the single hot-wire ..	111
4.12	Coordinates of the single and the crossed hot-wires ..	112
5.1	Boundary layer growth over the flat plate	
	a. along the centerline of a smooth strip	113
	b. along the centerline of a rough strip	114
5.2	Displacement thickness as a function of x	115
5.3	Momentum thickness as a function of x	116

Figure		Page
5.17	Spanwise comparison of velocity-defect profiles $-2(U_\infty-U)/(U_{*s}+U_*)$ vs. $zU_{*s}/\delta_s^* U_\infty$	
	a. x = 6 ft, U_∞ = 30 ft/sec	137
	b. x = 10 ft, U_∞ = 30 ft/sec	138
5.18	Spanwise velocity distribution of constant height	
	a. x = 6 ft, U_∞ = 30 ft/sec	139
	b. x = 10 ft, U_∞ = 30 ft/sec	140
5.19	Curves of constant velocity	
	a. x = 6 ft, U_∞ = 30 ft/sec	141
	b. x = 10 ft, U_∞ = 30 ft/sec	142
5.20	Distribution of turbulent intensities	
	a. x = 6 ft and y = 0 in.	143
	b. x = 6 ft and y = 6 in.	144
5.21	Distribution of turbulent shear stresses	
	a. x = 6 ft and y = 0 in.	145
	b. x = 6 ft and y = 6 in.	146
5.22	Spanwise comparison of turbulence quantities	
	a. $\overline{uu}$ profiles	147
	b. $\overline{vv}$ profiles	148
	c. $\overline{ww}$ profiles	149
	d. $-\overline{uv}$ profiles	150
	e. $-\overline{uw}$ profiles	151
	f. $-\overline{vw}$ profiles	152
5.23	Normalized spectra of streamwise turbulent velocity	
	a. x = 6 ft and y = 0 in.	153
	b. x = 6 ft and y = 6 in.	154
5.24	Spanwise comparison of normalized spectra of streamwise turbulent velocity	
	a. x = 6 ft and $z/\delta \simeq 0.03$	155
	b. x = 6 ft and $z/\delta \simeq 0.30$	156
	c. x = 6 ft and $z/\delta \simeq 0.54$	157
A.1	Coordinate system for boundary layer flow over a three-dimensional obstacle	158

Figure		Page
5.4	Shape factor as a function of x	117
5.5	Spanwise variation of shear velocity	118
5.6	Comparison of shear velocity for the smooth surface by various methods	119
5.7	Longitudinal plots of power law profiles - U/U_∞ vs. z/δ	
	a. along the centerline of a smooth strip	120
	b. along the centerline of a rough strip	121
5.8	The parameter m in the power law profile as a function of x	122
5.9	Spanwise comparison of power law profiles - U/U_∞ vs. z/δ	
	a. $x = 6$ ft, $U_\infty = 30$ ft/sec	123
	b. $x = 10$ ft, $U_\infty = 30$ ft/sec	124
5.10	Semi-logarithmic plots of mean velocity data - U/U_∞ vs. z	
	a. $x = 6$ ft, $U_\infty = 30$ ft/sec	125
	b. $x = 10$ ft, $U_\infty = 30$ ft/sec	126
5.11	Spanwise comparison of wall law profiles - U/U_* vs. zU_*/ν	
	a. $x = 6$ ft, $U_\infty = 30$ ft/sec	127
	b. $x = 10$ ft, $U_\infty = 30$ ft/sec	128
5.12	Roughness effect $\Delta U/U_*$ vs. $k_r U_*/\nu$	129
5.13	Spanwise variation of $\Delta U/U_*$	130
5.14	Spanwise comparison of velocity-defect profiles - $(U_\infty-U)/U_*$ vs z/δ	
	a. $x = 6$ ft, $U_\infty = 30$ ft/sec	131
	b. $x = 10$ ft, $U_\infty = 30$ ft/sec	132
5.15	Spanwise comparison of velocity-defect profiles - $(U_\infty-U)/U_*$ vs. $zU_*/\delta^* U_\infty$	
	a. $x = 6$ ft, $U_\infty = 30$ ft/sec	133
	b. $x = 10$ ft, $U_\infty = 30$ ft/sec	134
5.16	Spanwise comparison of velocity-defect profiles - $2(U_\infty-U)/(U_{*s}+U_*)$ vs. z/δ	
	a. $x = 6$ ft, $U_\infty = 30$ ft/sec	135
	b. $x = 10$ ft, $U_\infty = 30$ ft/sec	136

LIST OF SYMBOLS

Symbol	Definition	Dimension
A, A'	Constants	
B, B'	Constants	
B_w	Filter bandwidth	
C, c	Constants	
C_f	Local skin friction coefficient	
D	Constant	
d	Height of rectangular-parallelepiped obstacle	L
d_1	Diameter of Preston tube	L
E	Mean voltage	V
$E(k)$	One-dimensional wave-number spectrum funtion	L^3/T^2
$E(n)$	One-dimensional frequency spectrum function	T
e	Voltage fluctuation	V
F	Function	
f	Funtion	
f_p	Function	
f_r	Function	
G	Function	
g, g_1	Functions	
H	Shape factor	
Δh	Difference between dynamic and static pressure head	M/LT^2
k	One-dimensional wave number	L^{-1}
k_r	Roughness height	L
m	Exponent	
n	Frequency	T^{-1}

Symbol	Definition	Dimension
P	Mean static pressure	M/LT^2
P_∞	Static pressure outside boundary layer	M/LT^2
Δp	Preston-tube reading	M/LT^2
Re_d	Reynolds number based on d	
Re_k	Reynolds number based on k_r	
S_1, S_2	Sensitivities of crossed wire at $\alpha = \pm 45^o$	VT/L
S_U	Sensitivity of voltage with respect to velocity	VT/L
S_α	Sensitivity of voltage with respect to angle	VT/L
U	Streamwise mean-flow velocity	L/T
U_*	Shear velocity	L/T
U_{*s}	Shear velocity corresponds to smooth-wall flow	L/T
U_{*r}	Shear velocity corresponds to rough-wall flow	L/T
U_∞	Free stream velocity	L/T
u,v,w	Velocity fluctuations in x,y,z direction	L/T
V,W	Secondary-flow components in y,z direction	L/T
x,y,z	Streamwise, spanwise, vertical coordinate	L
z_o	Roughness parameter	L
α	Angle of attack	
δ	Boundary layer thickness	L
δ^*	Displacement thickness	L
η	Non-dimensional spanwise coordinate	
ξ	Non-dimensional vertical coordinate	
θ	Momentum thickness	L
κ	Von Kármán constant	

LIST OF SYMBOLS - Continued

Symbol	Definition	Dimension
λ	Strip width	L
ν	Kinematic viscosity	L^2/T
Π	Coles' pressure gradient parameter	
π	3.14159...	
σ	Parameter	
τ	Non-dimensional streamwise coordinate	
τ_w	Wall shear stress	ML/T^2
ϕ	Non-dimensional mean velocity	
ω	Wake function of Coles	

examples of configurations which can produce cross flows. Near a roughness discontinuity the modification of mean velocity and turbulence profiles can be quite appreciable. At great lateral distances from the discontinuity, however, the chracteristics of the flow can be expected to be approximately the same as that over uniformly rough surfaces. A review of literature reveals that very little attention has been devoted to the effect of lateral roughness changes on the development of the atmospheric boundary layer. Neither theoretical treatments nor experimental data are available at the present stage.

The complex nature of atmospheric flow has stimulated efforts to study its characteristics in the laboratory under controlled conditions. In the lower layer of the atmosphere, the characteristics of the flow are found to be nearly analogous to that in the turbulent boundary layer along a flat plate. The feasibility of laboratory simulation of atmospheric flow for a wide range of situations has been established (Cermak, et al., 1966, Hidy, 1966, and Nemoto, 1968). The simulation of atmospheric flow over non-uniform surface conditions poses no new problems provided appropriate scaling relationships are available.

1.1 Purpose of Present Investigation

The objective of the present experimental investigation is to provide qualitative and quantitative information necessary for an analysis of the response of the turbulent boundary layer to lateral changes in surface roughness. In particular, information is sought regarding the boundary layer configuration and structure of the flow over longitudinal strips of alternating surface roughness. The main purposes of this investigation are: (a) to study the effect of lateral roughness changes on mean velocity distribution, wall shear stress, turbulent intensities, turbulent shear stresses and energy spectra of the streamwise turbulent velocity by means of extensive pitot-tube and hot-wire surveys, and (b) to compare the experimental data with available data from two-dimensional flows over uniform surfaces. The experimental results will permit a better understanding of the flow characteristics, will provide a physical basis for developing an analytical model, and will have direct application to the study of atmospheric flows with complex boundary conditions which lead to three-dimensional mean motions.

1.2 Scope of Present Investigation

The present investigation deals with a turbulent boundary layer with zero pressure gradient over a flat plate consisting of alternate, longitudinal strips of smooth and rough surfaces, as shown in Fig. 1.1. The strips which are of equal width are placed in the streamwise direction starting from the leading edge of the plate. The rough strips are uniformly covered with sand grains. The experimental investigation is limited to one type of surface configuration with the free-stream velocity as the only variable.

A detailed survey of literature concerning turbulent boundary layers over both smooth and rough walls and research in the area of boundary layer flows over streamwise roughness changes is given in Chapter II.

The theoretical description of the flow is presented in Chapter III. The present study treats the non-uniform three dimensional surface conditions as a small perturbation about a two-dimensional state. The effect of spanwise roughness changes on the mean velocity distribution is discussed. The distribution of the turbulent shear stress $-\rho\overline{vw}$ which is responsible for the generation of a cross-flow in the boundary layer has been estimated.

The experimental equipment and procedure is described in detail in Chapter IV. Mean velocity profiles through the boundary layer at selected stations were made with a pitot tube and cross-checked by a single hot-wire. Measurement of the wall shear stress along a smooth strip of the flat plate in the boundary layer was obtained using a Preston tube. The intensities of turbulence and the turbulent shear stresses were measured by means of a single hot-wire and a crossed hot-wire. The spectra of the streamwise turbulent velocity were analyzed from the turbulence data.

The experimental results, given in Chapter V, are concentrated on the spanwise variation of mean velocity and turbulence profiles at distances far downstream from the leading edge of the flat plate where the local boundary layer thickness is comparable to the strip width, but is very large compared to roughness height. A summary of these results and discussions is given in Chapter VI.

1.3 Effect of Strip Width on Boundary Layer Development

The entire flow field produced by a surface configuration of the present type is very complicated. Near the leading edge of the plate the roughness elements contained in the rough strips will cause large disturbances in the oncoming flow while the boundary layer forms downstream from these disturbances. Such disturbances associated with strong mixing and momentum diffusion will cause the flow to become turbulent at a shorter downstream distance from the leading edge than occurs naturally. The disturbances fade away gradually as the flow progresses downstream. Nevertheless, continuous production of small localized disturbances persists in a small region along side edges of the rough strips. Additionally, the spanwise inequality of the turbulent normal stresses in the boundary layer, due to the presence of roughness changes, will induce a weak secondary flow in the form of longitudinal vortices (Fig. 1.2). This secondary flow will cause a redistribution of momentum in planes perpendicular to the direction of the mean flow, which results in spanwise distortions of mean velocity and turbulence profiles.

The influence of strip width on the boundary layer characteristics can be determined by introducing the relative width λ/δ, defined as the ratio of the strip width λ to the local boundary layer thickness δ. Near the leading edge of the plate where $\frac{\lambda}{\delta} >> 1$, the flow field is unaffected by the presence of roughness changes except in the proximity of the wall near the roughness discontinuities. For $\frac{\lambda}{\delta} \sim 1$, that is, when the local boundary layer thickness is comparable to the strip width, the flow field will be influenced by the presence of roughness changes. The strip width then becomes a significant length scale and must be introduced as an additional parameter to characteristics of the flow. For $\frac{\lambda}{\delta} << 1$, that is, when the local boundary layer thickness is very much larger than the strip width, the flow is again almost everywhere independent of the width.

1.4 Effect of Surface Roughness on Boundary Layer Development

In turbulent flow, the proximity of the rigid boundary or wall has a direct bearing on the turbulence. For a smooth wall this effect occurs through the action of viscous stresses, for a rough wall through the action of more complicated forces resulting from the flow around the individual roughness elements. The action of the roughness can be interpreted as being equivalent to a reduction of the viscous sublayer. The roughness effect on boundary layer characteristics depends on the ratio of the roughness dimension to the thickness of the viscous sublayer. If the roughness elements are much smaller than the thickness of the viscous sublayer, the surface is considered as hydraulically smooth. For the hydraulically smooth surface, no effect of the roughness is felt. On the other hand, if the roughness elements are so large as to protrude through the viscous sublayer completely, the surface is considered to be completely rough. For the completely rough surface, the turbulent motion produced by the flow around the roughness elements dominates the wall shear stress and the viscous action has comparatively little influence. Between these two extremes there exists a transitional state where only a fraction of the roughness elements disturbs the viscous sublayer. Consequently, the wall shear stress in this case will be affected by both the viscosity and the roughness dimension.

For a surface configuration of the present type, the roughness height representing the scale length of the roughness on each of the rough strips remains constant, while the boundary layer thickness increases downstream. As far as the flow along the centerline of a rough strip in concerned, this circumstance causes the flow characteristics near the leading edge of the flat plate to behave differently from that at very large distances downstream. The completely rough regime occurs over the forward portion, followed by the transition regime and eventually, the rough strip may become hydraulically smooth if the plate is sufficiently long.

CHAPTER II

LITERATURE REVIEW

A survey of the literature reveals that very little progress has been made concerning the structure of the turbulent boundary layer produced by the present surface configuration. Previous investigations have been primarily concerned with the effect of spanwise non-uniformity of surface roughness on turbulence suppression phenomena and on secondary flow phenomena. Concerning turbulence suppression, Liu, Kline and Johnston (1966) investigated the effect of extremely narrow roughness strips having various roughness spacings on a smooth surface using flow visualization techniques. Their results show that neither sufficient suppression of turbulent production nor significant reduction in wall shear stress have been found. The effect of a spanwise change from smooth-wall conditions to rough-wall conditions on secondary flow phenomena were studied by Hinze (1967). He concluded that the lateral change in surface roughness will cause a similar local secondary flow as the side edge of a finite flat plate (Elder,1960).

In working with the turbulent boundary layer consisting of flow parallel to strips of smooth and rough surfaces, it is advantageous to do a parallel study of two-dimensional turbulent boundary layers over both smooth and rough walls. In this chapter, previous investigations of turbulent boundary layers over both smooth and rough walls and research in the area of boundary layer flows over streamwise roughness changes are reviewed.

2.1 Turbulent Flow Over Smooth Walls

Close examination of a two-dimensional turbulent boundary layer over smooth walls reveals a characteristic which allows division of the boundary layer into (i) an inner layer, and (ii) an outer layer. The inner layer, whose thickness is roughly 10 to 20 percent of the boundary layer thickness derives its supply of turbulent energy almost exclusively from the interaction of the turbulent shear stress and the mean velocity gradient within itself. Within the layer the flow is dependent only on local wall conditions and the shear stress is nearly constant. This layer is also referred to as the constant-stress layer. The mean velocity distribution across this layer is determined by the wall shear stress τ_w, the density ρ, the kinematic viscosity ν, and the vertical distance z from the wall. Application of dimensional analysis to these variables on which the mean velocity U depends gives the functional relationship

$$\frac{U}{U_*} = f\left(\frac{zU_*}{\nu}\right) \tag{2-1}$$

where $U_* = \sqrt{\tau_w/\rho}$ is the shear velocity.

Equation (2-1) is known as Prandtl's law of the wall. This law implies that mean velocity profiles are independent of position along the plate when the mean velocity is measured in terms of its scale U_*, and the distance from the wall is measured in terms of its scale ν/U_*.

In the case of a smooth wall there exists a sublayer adjacent to the wall where the flow is predominantly viscous and the turbulent shear stress is negligible. This is called the viscous sublayer, whose thickness is of the order of 0.1 to 1.0 percent of the boundary layer thickness. The mean velocity distribution in this sublayer follows the linear relationship

$$\frac{U}{U_*} = \frac{zU_*}{\nu} . \tag{2-2}$$

The outer layer, which contains 80 to 90 percent of the boundary layer, receives its greatest portion of turbulent energy by diffusion from the constant-stress layer. Within this layer the flow is completely turbulent and the effect of viscosity is negligible. It is practically independent of local wall conditions but depends instead on external conditions and on the upstream history of the flow. The velocity defect $U_\infty - U$ is thus a function of the vertical distance z, the boundary layer thickness δ , and the shear velocity U_*. Dimensional analysis gives

$$\frac{U_\infty - U}{U_*} = g(\frac{z}{\delta}) \tag{2-3}$$

This similarity relation is known as Kármán's velocity-defect law. This law implies that the asymptotic approach of the mean velocity profile to the free-stream velocity U_∞ is uniquely determined by the distance from the wall relative to the boundary layer thickness.

Since the division of the boundary-layer into inner and outer layers is arbitrary, there must be a region in which both Eqs. (2-1) and (2-3) are valid. This overlapping of the two similarity laws indicates that some relationship must exist between two distinct set of parameters used. To satisfy this conditions, the functions f and g must be logarithmic. Therefore, for the overlap region the mean velocity distribution can be expressed as

$$\frac{U}{U_*} = \frac{1}{\kappa} \ln \frac{zU_*}{\nu} + A \tag{2-4}$$

and

$$\frac{U-U_\infty}{U_*} = \frac{1}{\kappa} \ln \frac{z}{\delta} + B \tag{2-5}$$

where κ, A and B are experimentally determined constants. In particular, κ is known as von Kārmān's constant. The value of κ is usually taken as 0.41 for flat plate flows. A summary of the experimental determinations of κ has been made by Slotta (1963).

Telles and Dukler (1968) demonstrated that the law of the wall (Eq. 2-4) is the zeroth-order small perturbation type of solution of the boundary layer equations, but that the velocity-defect law (Eq. 2-5) does not represent a valid similarity type of solution of the boundary layer equations. The law of the wall has been generalized empirically to flows with arbitrary pressure gradients by Ludwieg and Tillmann(1950), and the velocity-defect law to a certain class of equilibrium flows by Clauser (1954).

Usually a single function is sought to describe the mean velocity distribution for the entire boundary layer. One of the earliest empirical descriptions is the power law profiles. The general form of the power law (Schlichting, 1968) is given by

$$\frac{U}{U_\infty} = \left(\frac{z}{\delta}\right)^{\frac{1}{m}} \tag{2-6}$$

where m is an empirical exponent.

Coles (1956) deduced a purely empirical correction function to account for the large observed deviations between the measured mean velocity profiles and the logarithmic form of the "law of the wall" in the outer region of the boundary layer,

$$\frac{U}{U_*} = \frac{1}{\kappa} \ln \frac{zU_*}{\nu} + A + \frac{\Pi}{\kappa} \omega \left(\frac{z}{\delta}\right) \tag{2-7}$$

where Π is a parameter which depends on pressure gradient and turbulence level near the edge of the boundary layer, and $\omega(\frac{z}{\delta})$ is the wake function known as "the law of the wake". Coles originally gave the wake function in numerical form. Hinze (1959) suggested that the wake function can be accurately described by a closed form function

$$\omega\left(\frac{z}{\delta}\right) = 1 - \cos\left(\frac{\pi z}{\delta}\right) \tag{2-8}$$

Telles and Dukler (1968) demonstrated that the first-order small perturbation type solution of the boundary layer equations will generate a correction function similar to Coles' law of the wake.

Minor inconsistencies in Coles' formulation of the wake law were corrected by Bull (1968) who extend Eq. (2-8) by means of a simple power law. The resulting correction function was rather cumbersome and involved two parameters which had to be independently evaluated from experimental data. A similar approach was employed by Allan (1970) who deduced a generalized correction function for pipe flows, flat plate flows and diffusing flows.

There now exists a considerable amount of experimental work on smooth-wall turbulent boundary layers. The experimental results have been accumulated in the past by Baines (1951), Ross (1953), Hama (1954), Clauser (1956), Townsend (1956), Hinze (1959) and Rotta (1962). Methods of computation of the turbulent boundary layers have been collected by Kline, et al. (1968).

2.2 Turbulent Flow over Rough Walls

For a two-dimensional turbulent boundary layer over a rough wall, whose surface is uniformly covered by geometrically similar roughness of size small compared with the boundary layer thickness, there exists a constant-stress layer adjacent to the wall, where the motion is entirely determined by the wall shear stress τ_w, density ρ, kinematic viscosity ν and roughness height k_r (Rotta, 1962). The application of the similarity relation to the mean velocity distribution leads to

$$\frac{U}{U_*} = F\left(\frac{zU_*}{\nu}, \frac{k_r U_*}{\nu}\right) \tag{2-9}$$

Experimental studies by Moore (1950) indicated that the velocity-defect law as expressed in Eq. (2-5) is universal for either smooth or rough walls. Then Eq. (2-9) can thus be expressed for a rough wall by the relation

$$\frac{U}{U_*} = \frac{1}{\kappa} \ln \frac{zU_*}{\nu} + C\left(\frac{k_r U_*}{\nu}\right) \tag{2-10}$$

where $C(\frac{k_r U_*}{\nu})$ is an empirical constant depending upon the roughness geometry.

By virtue of Moore's conclusion, Clauser (1956) suggested that the mean velocity distribution in the constant-stress layer can be expressed generally as

$$\frac{U}{U_*} = \frac{1}{\kappa} \ln \frac{zU_*}{\nu} + A - \frac{\Delta U}{U_*} \tag{2-11}$$

where $\Delta U/U_*$ represents the downward shift of mean velocity profiles in the vicinity of the roughness elements. This shift is a function of the roughness Reynolds number $Re_k = k_r U_*/\nu$. For completely rough flows Clauser (1956) showed that $\Delta U/U_*$ takes the form

$$\frac{\Delta U}{U_*} = \frac{1}{\kappa} \ln \frac{k_r U_*}{\nu} + D \tag{2-12}$$

where D is an empirical constant. However, Bettermann (see Dvorak, 1969) suggested that $\Delta U/U_*$ must also depend upon the roughness spacing.

The "law of the wall" (Eq. 2-10) may be rewritten as

$$\frac{U}{U_*} = \frac{1}{\kappa} \ln \frac{z}{z_o} \tag{2-13}$$

where z_o is a roughness parameter which is independent of the flow conditions and must be given as part of the boundary conditions. Summaries of values of z_o for various surface roughness are presented by Priestley (1959). In general, the value of z_o is an order of magnitude less than the average height of surface roughness elements.

The "power law" (Eq. 2-6) has been used to describe the mean velocity distribution for the turbulent boundary layer over rough walls by many investigators (e.g., Corrsin and Kistler, 1954; Chowdhury, 1966; and Liu, Kline and Johnston, 1966). The "law of the wake" has been modified to include the effect of surface roughness by Allan (1970).

For rough-wall flows, the effective origin of z is undefined due to the presence of roughness elements. Intuitively, the effective origin can be located anywhere between the trough and crest of the roughness elements. Scottron (1967) argued that the location of the effective origin may be presumed to be associated with the generation of turbulence near the wall and depend on roughness geometry and local roughness Reynolds number Re_k. Based on the assumption of the existence of a logarithmic velocity profile near the wall, Perry and Joubert (1963) proposed a method for determining the effective origin of the wall. Their scheme consisted essentially of adjustment of the z origin until a best-fitting straight line could be drawn from a U/U_∞ versus z plot on a semi-logarithmic paper.

Experimental investigations on rough-wall turbulent boundary layers are those of Tillmann (1945), Baines (1950), Moore (1950), Hama (1954), Corrsin and Kistler (1954), Chanda (1958), Liu, Kline and Johnston (1966), Chowdhury (1966) and Perry, Schofield and Joubert (1969) in zero pressure gradient, and those of Perry and Joubert (1963) and Scottron (1967) in adverse pressure gradient. The experimental results of all these investigators indicate the existence of the logarithmic mean velocity profile in the constant-stress layer.

2.3 Boundary Layer Flow over Streamwise Roughness Changes

Significant progress towards an understanding of turbulent boundary layer flow above an abrupt change in surface roughness under neutral stratification has been made in recent years. Al existing studies, which are mainly concerned with the lower layer of the atmosphere, treat the problem in two dimensions, with the line of roughness discontinuity normal to the mean flow direction. The roughness heights on either side of the discontinuity are assumed to correspond to homogeneous terrain of infinite extent. Upstream of the roughness discontinuity the flow is assumed to be in equilibrium with the underlying surface roughness and to have a constant shear stress distribution independent of height and a logarithmic mean velocity profile. Downstream of the discontinuity the flow will gradually adjust itself at all levels to the downstream roughness. The effect of the downstream roughness is assumed to be confined to a so-called "internal boundary layer," which increases with downstream distance from the roughness discontinuity.

Several theories have been proposed for predicting the growth of the internal boundary layer by prescribing mean velocity and shear stress profiles inside the layer. Elliott (1958) assumed a constant shear stress distribution and a logarithmic velocity profile. This led to a discontinuity of shear stress at the edge of the internal boundary layer. Panofsky and Townsend(1964) removed this physically unrealistic discontinuity at the interface by assuming a linear variation of the shear stress with height and a log-linear velocity profile. Townsend (1965a, 1965b, 1966) introduced a self-preserving development of the flow modification induced by the downstream roughness change. The deviations of mean velocity from the upstresm distribution were expressed as the result of a flow acceleration and a vertical displacement of the streamline. Plate and Hidy (1967) added advection to Elliott's technique and incorporated Townsend's theory in a modified form, such that the result could be extended to include a pressure gradient and a non-uniform shear stress at the surface. Blom and Wartena (1969) corrected a minor discrepancy between Townsend's resulting profile and his inner boundary condition, and further extended Townsend's theory to more than one discontinuity in surface roughness.

A different theoretical approach to the internal boundary layer problem was employed by Miyake (1961). He did not explicitly develop a theory for the velocity profile, but derived an expression for the height of the internal boundary layer. Miyake's theory is based on the simple assumption that the slope of the internal boundary layer is proportional to the ratio of the standard deviation of vertical velocity to the upstream velocity.

In conclusion, all theories agree in that an internal boundary layer develops after the roughness change, and the height of which varies approximately with the downstream distance from the roughness discontinuity, raised to the 4/5 power. The theories disagree with each other, however, in the shear stress distribution within the internal boundary layer, further, they differ in the downstream distance required to set up a new equilibrium up to a given height.

For flow from a smooth to a rough surface, the rough surface behaves in an "active" manner. The growth of the internal boundary layer may be dominated by the "wake" from the leading roughness elements. Because of the vigorous generation of turbulence close to the rough surface, adjustment of the wall shear stress to the downstream roughness is very rapid. For flow from a rough to a smooth surface, the smooth surface behaves in a "passive" manner. The growth of the internal boundary layer is inhabited in its growth by diffusion of information from the "active" outer flow back towards the surface. This leads to a slower adjustment of the wall shear stress.

Wind-tunnel studies of the boundary layer flow above an abrupt change in surface roughness were performed by Jacobs (1940), Clauser (1956), Logan and Jones (1963), Plate and Hidy (1967), Yeh (1970), and Antonia and Luxton (1971a,1971b) following a smooth-to-rough change, and by Jacobs (1940) and Taylor (1962) following a rough-to-smooth change. Jacobs, Taylor, Plate and Hidy, and Antonia and Luxton conducted the experiments in channel flows, Logan and Jones in pipe flows, and Clauser and Yeh in flat plate flows. Atmospheric observations were made by Blackadar et al. (1967), Bradley (1968), and Blackadar and Panofsky (1970). The results of all these investigators indicated that the adjustment of the wall shear stress to downstream roughness occurs at a short distance downstream of the roughness discontinuity. A decelerated flow moving from smooth-to-rough surface and an accelerated flow moving from rough-to-smooth surface were observed.

Numerical studies of the internal boundary layer problem were treated by Wagner (1966), Onishi (1966), Nickerson (1968), Estoque and Bhumralkar (1968), Peterson (1969), Taylor (1969, 1970) and Huang (1971). These studies differ from each other mainly in the use of the governing equations and of the boundary conditions. Wagner's model is time-dependent, unlike the other models in which stationary is assumed. Nickerson considers a step change in wall shear stress, Taylor a step change in surface roughness parameter, and Peterson the shear stress proportional to the turbulent energy. Except Peterson's model, all other models depend on the assumed behavior of the mixing length theory or the momentum exchange coefficient.

CHAPTER III

THEORETICAL DESCRIPTION OF THE FLOW

Since turbulent boundary layers involve the complex combination of boundary layer phenomena, non-linear mechanics and turbulence, a direct theoretical solution of the problem throughout the entire region occupied by the boundary-layer flow has not yet been attained. In order to obtain insight into the turbulent boundary layers, one is evitably led to strong dependence on experimental and empirical investigations.

In this chapter, a theoretical description of the flow is presented, and the turbulent shear stress $-\rho\overline{vw}$, which gives rise to a weak cross-flow within the boundary layer, has been estimated.

3.1 Basic Equations

The present analysis considers a steady, incompressible turbulent boundary layer over alternate, longitudinal strips of smooth and rough surfaces with zero streamwise pressure gradient. In order to simplify the analysis and yet still retain the essential physics of the problem, the following assumptions are made:

1) the roughness height is so small compared with the local boundary layer thickness that the mean flow and pressure field outside the boundary layer are not affected by the roughness changes,
2) the disturbances generated along the side edges of each of the rough strips can be neglected,

3) the rates of variation of quantities in the streamwise direction are small with respect to changes of the same quantities in the spanwise and vertical directions,

4) the turbulent fluctuations are small with respect to the mean flow, and

5) the magnitude of the components of the secondary flow is small compared with that of the mean flow.

The Reynolds equation of motion then reduces to

$$U \frac{\partial U}{\partial x} + V \frac{\partial U}{\partial y} + W \frac{\partial U}{\partial z} + \frac{\partial \overline{uv}}{\partial y} + \frac{\partial \overline{uw}}{\partial z} = \nu \frac{\partial^2 U}{\partial z^2} \tag{3-1}$$

$$\frac{\partial \overline{v^2}}{\partial y} + \frac{\partial \overline{vw}}{\partial z} = - \frac{1}{\rho} \frac{\partial P}{\partial y} \tag{3-2}$$

$$\frac{\partial \overline{vw}}{\partial y} + \frac{\partial \overline{w^2}}{\partial z} = - \frac{1}{\rho} \frac{\partial P}{\partial z} \tag{3-3}$$

where x, y, z are the streamwise, spanwise and vertical coordinates of the cartesian coordinate system, as shown in Fig. 1.2. U is the streamwise mean-flow velocity, and V, W are defined as the secondary-flow components in y- and z-directions, respectively. u, v and w are the corresponding turbulent velocity fluctuations in x, y, z directions. P is mean static pressure. The terms $\rho\overline{v^2}$, $\rho\overline{w^2}$, $-\rho\overline{uv}$, $-\rho\overline{uw}$ and $-\rho\overline{vw}$ are known as the turbulent normal and shear stresses, respectively, also known as Reynolds stresses. These stresses are the representation of the rate of momentum transport because of the turbulent velocity fluctuations.

The continuity equation for the mean motion is

$$\frac{\partial U}{\partial x} + \frac{\partial V}{\partial y} + \frac{\partial W}{\partial z} = 0 \tag{3-4}$$

Eqs. (3-1) through (3-4) with the appropriate boundary conditions do not form a complete set of equations from which a solution could be obtained. The closure of the system requires that all statistical quantities of turbulence be specified. So far, no satisfactory solution to this problem has been obtained.

3.2 Mean Velocity Distribution

Cumpsty (1970) in his review of three-dimensional boundary layers made the following statement:

> "When the three-dimensional effects, including cross-flow, are small, the use of two-dimensional descriptions for the flow is nature and needs no justification."

The turbulent boundary layer produced by surface configuration of the present type falls into this category.

The present analysis of the three-dimensional turbulent boundary layer presumes the existence of three different regions, the "smooth" region along the centerline of each smooth strip, the "rough" region along the centerline of each rough strip and the "intermediate" region lying between the smooth and the rough regions. The spanwise variation of the boundary layer thickness is assumed to be negligibly small.

In the smooth region the flow is assumed to behave like a two-dimensional boundary layer over a smooth surface. The mean velocity distribution in this region may be described by the law of the wall

$$\frac{U}{U_{*s}} = \frac{1}{\kappa} \ln \frac{zU_{*s}}{\nu} + A \tag{3-5}$$

and the velocity-defect law

$$\frac{U - U_\infty}{U_{*s}} = \frac{1}{\kappa} \ln \frac{z}{\delta} + B \tag{3-6}$$

where the subscript "s" refers to the smooth wall conditions. Eqs. (3-5) and (3-6) may be combined to give

$$\frac{U_\infty}{U_{*s}} = \frac{1}{\kappa} \ln \frac{\delta U_{*s}}{\nu} + (A - B) \tag{3-7}$$

In the rough region the flow is assumed to behave like a two-dimensional boundary layer over a rough surface of uniform but identical roughness. The law of the wall for the rough-wall flows may be written, after Clauser (1956), as

$$\frac{U}{U_{*r}} = \frac{1}{\kappa} \ln \frac{zU_{*s}}{\nu} + A - \frac{\Delta U}{U_{*r}} \tag{3-8}$$

where the subscript "r" refers to the rough wall conditions, and the term $\Delta U/U_{*r}$ represents the vertical shift of the logarithmic profile caused by roughness. If the roughness elements are small compared with the boundary layer thickness, the universal velocity-defect law may be expressed as

$$\frac{U - U_\infty}{U_{*r}} = \frac{1}{\kappa} \ln \frac{z}{\delta} + B \tag{3-9}$$

From the combination of Eqs. (3-8) and (3-9), it follows that

$$\frac{U_\infty}{U_{*r}} = \frac{1}{\kappa} \ln \frac{\delta U_{*s}}{\nu} + (A - B) - \frac{\Delta U}{U_{*r}} \tag{3-10}$$

Thus, from Eqs. (3-7) and (3-10), there emerges a very significant relation between the smooth and rough regions, viz.,

$$\frac{U_\infty}{U_{*s}} - \frac{U_\infty}{U_{*r}} = \frac{\Delta U}{U_{*r}} \tag{3-11}$$

In the intermediate region the roughness effect tends to increase from zero in the smooth region to a maximum value in the rough region. If the strip width λ is comparable to the boundary layer thickness, the relationship existing among the variables describing the roughness effect may be written, in general, as

$$\frac{\Delta U}{U_{*r}} = f_r \left(\frac{k_r U_{*r}}{\nu} , \frac{y}{\lambda} \right) \tag{3-12}$$

A knowledge of Eq. (3-12) thus permits the evalution of the complete correlation of geometry to roughness effect.

3.3 Estimation of the Turbulent Shear Stress $-\rho\overline{vw}$

Secondary flows in turbulent flow have been separated into two categories by Prandtl (1952). The secondary flow of the first kind is produced by mean flow skewing, while the secondary flow of the second kind is caused by the non-uniformity of anisotropic wall turbulence.

For the present study the secondary flow of Prandtl's second kind, produced by the inequality of turbulent normal stresses, predominates. Along the centerline of a smooth or rough strip, $\overline{vw}$ vanishes by symmetry, so that integrating Eq. (3-3) with respect to z gives

$$\overline{w^2} = \frac{1}{\rho}(P_\infty - P) \tag{3-13}$$

where P_∞ is the mean static pressure outside the boundary layer. Further, the integration of Eq. (3-2) with respect to y gives

$$\int_0^\lambda \frac{\partial \overline{vw}}{\partial z}\, dy = (\overline{v^2} + \frac{P}{\rho})_{y=0} - (\overline{v^2} + \frac{P}{\rho})_{y=\lambda} \tag{3-14}$$

If the flow field outside the boundary layer is assumed to be unaffected by the presence of the roughness changes, it follows from Eq. (3-13) that

$$\int_0^\lambda \frac{\partial \overline{vw}}{\partial z}\, dy = (\overline{v^2} - \overline{w^2})_{y=0} - (\overline{v^2} - \overline{w^2})_{y=\lambda} \tag{3-15}$$

For regions not too close to the wall, the distribution of $(\overline{v^2}-\overline{w^2})$ in a normally two-dimensional boundary layer is strongly dependent on the vertical distance from the wall (Klebanoff, 1954). Non-dimensionalizing the turbulent normal stresses with U_*, the local shear velocity, it should be possible to write

$$\frac{\overline{v^2} - \overline{w^2}}{U_*^2} = G\left(\frac{z}{\delta}\right) \tag{3-16}$$

where G is a universal function. Perkins (1970) suggested that the behavior of the universal function can be adquately demonstrated by the approximation

$$G\left(\frac{z}{\delta}\right) = 1 - \frac{z}{\delta} \quad ; \quad \frac{z}{\delta} > 0.1 \tag{3-17}$$

with the aid of Eqs. (3-16) and (3-17), Eq. (3-15) becomes

$$\int_0^\lambda \frac{\partial \overline{vw}}{\partial z}\, dy = -\,(U_{*r}^2 - U_{*s}^2)\,(1 - \frac{z}{\delta}) \quad ; \quad \frac{z}{\delta} > 0.1 \qquad (3\text{-}18)$$

When the strip width is comparable to the local boundary layer thickness, it is reasonable to assume that $\partial\overline{vw}/\partial z$ has its non-zero values distributed spanwisely between the centerlines of both smooth and rough strips. The distribution of $\partial\overline{vw}/\partial z$ consistent with the symmetry of the flow about the centerlines, following Townsend (1956), is

$$\frac{\partial \overline{vw}}{\partial z} = \begin{cases} \left[\dfrac{\partial \overline{vw}}{\partial z}\right]_{y=\frac{\lambda}{2}} \dfrac{y}{\lambda} & ; \quad 0 \le \dfrac{y}{\lambda} \le \dfrac{1}{2} \\ \left[\dfrac{\partial \overline{vw}}{\partial z}\right]_{y=\frac{\lambda}{2}} (1 - \dfrac{y}{\lambda}) & ; \quad \dfrac{1}{2} \le \dfrac{y}{\lambda} \le 1 \end{cases} \qquad (3\text{-}19)$$

If this is introduced in Eq. (3-18) and by means of integration, we obtain

$$\left[\frac{\partial \overline{vw}}{\partial z}\right]_{y=\frac{\lambda}{2}} = -\,\frac{4}{\lambda}\,(U_{*r}^2 - U_{*s}^2)\,(1 - \frac{z}{\delta}) \quad ; \quad \frac{z}{\delta} > 0.1 \qquad (3\text{-}20)$$

Then Eq. (3-19) upon integration gives

$$\overline{vw} = \begin{cases} \dfrac{2\delta}{\lambda}\,(U_{*r}^2 - U_{*s}^2)\,\dfrac{y}{\lambda}\,(1 - \dfrac{z}{\delta})^2 & ; \quad 0 \le \dfrac{y}{\lambda} \le \dfrac{1}{2} \\ \dfrac{2\delta}{\lambda}\,(U_{*r}^2 - U_{*s}^2)\,(1 - \dfrac{y}{\lambda})\,(1 - \dfrac{z}{\delta})^2 & ; \quad \dfrac{1}{2} \le \dfrac{y}{\lambda} \le 1 \end{cases} \qquad (3\text{-}21)$$

This equation shows that the spanwise distribution of the turbulent shear stress $-\rho\overline{vw}$ cannot be zero in this sort of flow, and the existence of this stress will tend to produce a cross-flow in the boundary layer.

CHAPTER IV

EXPERIMENTAL EQUIPMENT AND PROCEDURE

Experiments were performed in a low-speed wind tunnel located in the Fluid Dynamics and Diffusion Laboratory at Colorado State University. In this chapter, the experimental equipment, arrangement and procedure for this study are described.

4.1 Experimental Equipment

The basic experimental equipment consists of i) a wind tunnel, ii) a flat plate, iii) a carriage, iv) a manometer, v) two hot-wire anemometer systems, and vi) a wave analyzer. A brief description for each of the instruments is given below.

4.1.1 Wind Tunnel

The wind tunnel is a closed circulating type with a test section 30 ft. long, 6 ft. wide, and 6 ft. high. A schematic diagram of the wind tunnel is shown in Fig. 4.1. Air flow in the tunnel is driven by a constant pitch controlled fan. The tunnel can generate wind speeds ranging from 5 ft/sec to about 70 ft/sec. The turbulence level in the free stream is kept within 2 percent by providing damping screen and a 4:1 ratio entrance contraction. There is no arrangement for temperature control in the tunnel. A thermometer showed that the temperature varied from 70^{0}F at the beginning of the test run to 90^{0}F after a few hours of operation. It was thus necessary to warm up the tunnel for at least two hours to achieve a more or less steady temperature before starting the experiments. The temperature was recorded at the beginning and end of each experiment.

4.1.2 Flat Plate

The flat plate used for the experimental investigation was made of smoothed and polished aluminum plate. It is 12 ft. long, 4 1/2 ft. wide and 3/8 inch thick. The plate had a sharp leading edge which resulted in separation of the flow along that edge. The small region of separated flow was followed by reattachment in a transitional region; the flow became increasingly turbulent as it progressed further downstream. The plate was mounted on a steel stand at a height of 2 ft. above the wind tunnel floor in order to avoid the secondary motions resulting from the excessive loss of momentum in the corners of the tunnel, and was leveled accurately with a leveling instrument.

Four rough strips (sand paper, Grit 4), each of 12 ft. long, 1/2 ft. wide and 0.1 inch averaged roughness height, were attached on the plate longitudinally starting from the leading edge of the plate. The spacing between the two adjacent rough strips was kept at 1 foot. A total of fifty-four pressure tape with 1/32 inch in diameter holes, placed on either side of the centerline of the plate, was used to measure the wall static pressure along the plate. A plan view of the plate with pressure taps is shown in Fig. 4.2 and cross-sectional elevation of the plate is shown in Fig. 4.3.

4.1.3 Carriage

Probes were mounted on a wind tunnel carriage located 3 ft. above the wind tunnel floor of the test section. The carriage moved along the wind tunnel on rails which were fastened to the vertical walls of the tunnel. Two small D.C. motors with driving mechanism were used to produce independent vertical and lateral movements. The

Vibration Analyzer and 1521 Graphic Level Recorder. The former consists essentially of a set of passive filters in the range of 2.5 to 25,000 HZ. The filters are of the octave type having 1/3-octave (23%) and 1/10-octave (7%) noise bandwidths. The latter can record automatically the spectrum of a region under analysis.

4.2 Experimental Arrangements

In order to obtain a condition of zero pressure gradient flow along the flat plate, a specially shaped false ceiling was mounted onto the wind tunnel ceiling, as shown in Fig. 4.4. The shape of the false ceiling is shown in Fig. 4.5. A dimensionless plot of static pressure distribution at the free stream along the centerline of the flat plate is shown in Fig. 4.6. The maximum magnitude of streamwise pressure gradients are about 2.42×10^{-6} psi/in. for $U_\infty = 20$ ft/sec and 4.83×10^{-6} psi/in. for $U_\infty = 30$ ft/sec, if the first two-foot section of the plate was excluded. These values are small enough to be considered as zero streamwise pressure gradient. A dimensionless plot of wall pressure distribution on the plate is shown in Fig. 4.7. The result indicates that the wall pressure distribution is of the same order of the corresponding free-stream pressure distribution. It also shows that the spanwise pressure gradient is very small.

For testing plane symmetric flow condition along the centerline of the flat plate, a comparison of similar mean velocity profiles extending to 1 ft on either side of the centerline was made for a streamwise distance of 5 ft. from the leading edge of the plate, as shown in Fig. 4.8. The results show no signs of three-dimensional effects resulting from the whirling motion generated from the corner of the leading edge of the flat plate. It also indicates that a nearly plane symmetric flow about the centerline of the plate has been established.

4.3 Experimental Procedure

The aspect of the experimental procedure consists of measurements of static pressure, mean velocity, wall shear stress, turbulence and frequency spectrum. The procedure of these measurements and the data reduction techniques are presented below.

4.3.1 Measurement of Static Pressure

The static pressure at the free stream along the flat plate was measured by using two pitot tubes with both static heads connected to an electronic pressure meter (MKS Baratron Type 77). Both tubes were first set at the same height, side by side in the free stream, near the leading edge and well above the surface of the plate. At this position, the pressure difference between these tubes is zero. One of the tubes was then used as a reference static pressure and the other tube was moved downstream along the plate. The streamwise pressure gradient, if any, was thus obtained.

The wall static pressure distribution on the surface of the plate were measured through pressure taps embedded in the plate. These pressure taps were connected successively through plastic tubing to the same pressure meter, where they were measured against a reference pressure of the tap located at x=6 ft. and y=1 ft. of the smooth surface of the plate. The accuracy of the static pressure measurement on the rough surface is uncertain due to large local static pressure variations.

4.3.2 Measurement of Mean Velocity

The mean velocity was measured with both a pitot tube and a single hot-wire. The hot-wire was also employed to cross-check the values obtained by pitot tube measurements.

(A) Pitot Tube for Mean Velocity

The pitot tube measurement of mean velocity was made with a 1/16 inch diameter standard pitot-static tube. The dynamic and static pressures were obtained from the dynamic and static taps of the tube, respectively. The two taps of the tube were connected by flexible tubings to the terminal of an electronic pressure meter (MKS Type 77). This instrument was calibrated against a standard micromanometer (Meriam Model 34 FB 2 TM). No detectable difference was observed between the two within the range of the present measurements.

The D.C. output of the pressure meter, which indicates the pressure difference in millimeters of mercury between the dynamic pressure and the static pressure, was connected to the Y-axis of a X-Y recorder (Moseley Type 135). The X-axis of the recorder can be either set in time to obtain the time integration for a point-by-point measurement, or connected to the voltage output of the potentiometer of the carriage to obtain a continuous vertical profile of the pressure difference between the dynamic and the static heads. At each station, the continuous profile was made and later checked by means of point-by-point measurements. After a smoothing process, the continuous profile was later digitized using an optical-traced digitizer, and computed to obtain mean velocities. From a knowledge of the pressure difference between dynamic and static pressures, the barometric pressure, and the temperature, the mean velocity was calculated according to

$$U = 2.36 \sqrt{\Delta h/\rho} \tag{4-1}$$

where U is the mean velocity in ft/sec, ρ is the density of the air in slugs/ft^3, and Δh is the pressure difference between dynamic and static pressures in millimeters of mercury.

Possible sources of errors in pitot tube measurement of mean velocity have been discussed by Goldstein (1938), MacMillan (1956), Davies (1958), Bradshaw (1964) and Sandborn (1966). These errors are caused by the effects of the proximity of the wall, the local shear stress and the turbulence. Except very close to the wall, the possibility of errors due to shear and proximity of the wall are negligible. The turbulence effects can not be overlooked in the inner portion of the turbulent boundary layer where the turbulent intensities are very high. The importance of this effect decreases with distance from the wall. Correction for the turbulence effects of the pitot tube measurements following Goldstein, was found to vary from -1.7 to +0.1% of the local mean velocity. Hinze (1959) has criticized Goldstein's method which assumes that spanwise velocity fluctuations affect the pitot tube reading the same way as streamwise fluctuation, and has suggested that the effect of the former is appreciable less and may be even of opposite nature. For the present investigation no such correction was applied to the pitot tube measurement of mean velocity.

(B) Hot-Wire for Mean Velocity

The hot-wire measurement of mean velocity was made with a $2x10^{-4}$ inch diameter platinum coated tungsten wire, which was held parallel to the flat plate and perpendicular to the direction of the flow. The hot-wire was operated by a constant-temperature anemometer system (DISA 55D01). The voltage output of the anemometer was recorded on a X-Y recorder (Moseley Model 135) for a suitable time interval; later, an average was obtained from the records. The mean velocity was obtained from the D.C. voltage output through a calibration curve of the hot-wire. The procedure of the hot-wire calibration will be discussed in Section 4.3.4.

Fig. 4.9 illustrates a typical comparison of mean velocity profiles measured by the hot-wire and the pitot tube. The hot-wire results were generally in good agreement with pitot tube values, except in a region very close to the wall. This discrepency is primarily due to turbulence effects.

4.3.3 Measurement of Wall Shear Stress

Measurement of local wall shear stress along a smooth strip of the flat plate in the boundary layer was made by Preston's method using a round surface pitot tube attached to the surface (the so-called Preston tube). By assuming that close to the surface there exists a region in which the flow is substantially determined by the wall shear stress and the physical properties of the fluid, Preston (1954) obtained a universal non-dimensional relation between the wall shear stress and the difference between the pressure in the Preston tube and the static pressure on the surface

$$\frac{\tau_w d_1^2}{\rho \nu^2} = f_p \left(\frac{\Delta p d_1^2}{\rho \nu^2} \right) \tag{4-2}$$

where τ_w is the wall shear stress, d_1 is the diameter of the Preston tube, Δp is the Preston tube reading (i.e. the difference between pitot tube and static pressures), and the function f_p is determined from the calibration of the Preston tube.

Experiments by Head and Rechenberg (1962), Ferriss (1965) and Patel (1965) confirmed the assumption of universal wall similarity common to flat-plate boundary layers and fully-developed pipe flows, and provided the convincing evidence of the soundness of Preston's method of measuring wall shear stress. However, Patel found that the Preston's method overestimates the wall shear stress in both strong favourable and adverse pressure gradients. The inaccuracy of the method is caused by large deviations from the wall similarity due to the existence of the pressure gradients.

For the present investigation a homemade pitot tube of diameter 1/16 inch was built and used to measure local wall shear stress in the turbulent boundary layer of nearly zero streamwise pressure gradient. Care was taken to ensure that the mouth of the tube was free from burrs and deformities and that the tube was lying along the surface of the flat plate as closely as possible. Additional pressure taps of 1/16 inch diameter hole at proper locations were constructed for the wall shear stress measurement. The tube was first placed on the surface, parallel to the centerline of the plate, on one side of a static pressure tap, and was 1/4 inch apart between the tube and the pressure tap. The pressure difference between the two was recorded by means of a pressure meter (MKS Baratron Type 77). The same arrangement was repeated again on the other side of the pressure tap. The average value of two readings was used to determine the wall shear stress at the station of the pressure tap. With the calibration formula given, the wall shear stress could be readily calculated. The calibration formula, provided by the staff of the Aerodynamics Division, N. P. L. (1958), for the flat plate

$$\log_{10} \frac{\tau_w d_1^2}{4\rho\nu^2} = \bar{2}.647 + 0.875 \log_{10} \frac{\Delta p d_1^2}{4\rho\nu^2} \qquad (4\text{-}3)$$

was used.

Measurement of wall shear stress using a Preston tube indicates good agreement with other measurements in the turbulent boundary layer along a smooth surface. Along a rough surface, however, the method casts considerable doubt on the accuracy of the measurement. The individual roughness produce local mean velocity fluctuations which in turn produce local static pressure variations near the wall. The surface pitot tube and wall pressure taps can not be used to give meaningful Preston tube readings.

4.3.4 Measurement of Turbulence

Two types of hot-wire probes were used to measure the turbulence quantities. One was a single wire placed normal to the flow, to measure $\overline{u^2}$. The same wire was also used on mean velocity measurement. Another was a crossed wire to measure $\overline{v^2}$, $\overline{w^2}$, $\overline{uv}$ and $\overline{uw}$. The crossed wire was made of two hot-wires mounted on a single probe in the shape of X as in conventional hot-wire anemometry. The measurements of these turbulence quantities depend on the plane of axis in which the wires were operated. All the wires were made of platinum coated tungsten wire of a 2×10^{-4} inch diameter. A schematic diagram of the single wire measurement instrumentation is shown in Fig. 4.10. For crossed wire measurements similar arrangements were made with two hot-wire anemometer systems.

(A) Calibration of Hot-Wires

Prior to the hot-wire calibration, each hot-wire was subjected to the "curing" precess. During the curing process the hot-wire was operated in no flow condition for at least 24 hours. This operation would ensure a stable condition of the hot-wire characteristics before any calibration of measurement was made. The hot-wire was calibrated against a 1/16 inch diameter standard pitot-static tube in the free stream outside the boundary layer. The calibration curve was obtained by measuring D.C. voltage output of the wire for a range of mean velocities.

During the experiments the hot-wire was calibrated every two hours. No detectable change on the calibration curve was found for a properly "cooked" wire. A typical calibration curve of the hot-wire is shown in Fig. 4.11.

(B) Calculations of Turbulent Intensities and Shear Stresses

Baldwin, Sandborn and Lawrence (1960) found that the heat loss from a hot-wire is a function of local velocity, temperature and fluid properties, and angle of attack. For the present investigation, temperature and fluid properties were considered to be constant. Following the derivations given by Sandborn (1967), the response equation of the wire held in the x-z plane at an angle α to the direction of the flow is given by

$$e = \frac{\partial E}{\partial U} u + \frac{1}{U} \frac{\partial E}{\partial \alpha} w \tag{4-4}$$

where e represents the fluctuation output of the wire, and $\frac{\partial E}{\partial U}$ and $\frac{\partial E}{\partial \alpha}$ are respectively the sensitivities of the wire to local velocity and angle of attack.

Letting $\frac{\partial E}{\partial U} = S_U$ and $\frac{1}{U}\frac{\partial E}{\partial \alpha} = S_\alpha$, one obtains

$$e = S_U u + S_\alpha w \tag{4-5}$$

Squaring and averaging this equation results in

$$\overline{e^2} = S_U^2 \overline{u^2} + 2 S_U S_\alpha \overline{uw} + S_\alpha^2 \overline{w^2} \tag{4-6}$$

Arya (1968) found that the relation between S_U and S_α should have the form

$$S_\alpha = c \cot\alpha \, S_U \tag{4-7}$$

and

$$c = \frac{1 - \sigma^2}{1 + \sigma^2 \cot\alpha} \tag{4-8}$$

where σ is a parameter, proposed by Hinze (1959), to indicate the effective heat transfer from the velocity component parallel to the wire. The variation of σ with wire sizes and velocities has been studies by Webster (1962) and Champagne et al. (1967). It is found that σ depends primarily on the wire length-to-diameter ratio. Wires of different materials have less effect in the values of σ .

For the present study $\sigma = 0.2$ is used.

Substituting Eq. (4-7) into (4-6), we obtain

$$\overline{e^2} = S_U^2 \left(\overline{u^2} + 2c\,\overline{uw}\cot\alpha + c^2\overline{w^2}\cot^2\alpha\right) \tag{4-9}$$

In the following discussion different wire configurations are considered for the turbulence quantities that are measured.

(i) <u>Calculating $\overline{u^2}$ from the Single Wire</u>

The streamwise turbulent flux $\overline{u^2}$ was determined from the r.m.s. output to the local mean velocity. When the wire is held in a plane normal to the flow, i.e. $\alpha = 90°$. it follows from Eq. (4-9) that

$$\overline{u^2} = \frac{\overline{e^2}}{S_U^2} \tag{4-10}$$

The velocity sensitivity S_U can be obtained either by measuring the slope of the hot-wire calibration curve, or by differentiating an empirical curve based on King's law. The latter approach has been found to be more convenient and to give better results. If one plots the squared voltage output of the wire E^2 against the square root of corresponding velocity $\sqrt{U}$, a best fit curve can be obtained by a least-square curve fitting process,

$$E^2 = A' + B'\sqrt{U} \tag{4-11}$$

where A' and B' are constants.

The velocity sensitivity S_U is then given by

$$S_U = \frac{\partial E}{\partial U} = \frac{1}{4E}\,\frac{B'}{\sqrt{U}} \tag{4-12}$$

Substituting Eq. (4-12) into Eq. (4-10), one obtains

$$\overline{u^2} = \frac{16U\ (A'+B'\sqrt{U})}{B'^2}\ \overline{e^2} \tag{4-13}$$

(ii) <u>Calculating $\overline{v^2}$, $\overline{w^2}$, $\overline{uv}$ and $\overline{uw}$ from the Crossed Wire</u>

For measuring turbulent quantities $\overline{w^2}$ and $\overline{uw}$, the crossed wire was held in the x-z plane, as shown in Fig. 4.12. For convenience the angles between the direction of mean velocity and the crossed wire are kept at $\alpha = \pm\ 45°$.

Eq. (4-9) follows, when $\alpha = 45°$,

$$\overline{e_1^2} = S_1^2\ (\overline{u^2} + 2c\ \overline{uw} + c^2\ \overline{w^2}) \tag{4-14}$$

and when $\alpha = -45°$,

$$\overline{e_2^2} = S_2^2\ (\overline{u^2} - 2c\ \overline{uw} + c^2\ \overline{w^2}) \tag{4-15}$$

where $\overline{e_1^2}$ and $\overline{e_2^2}$ represent respectively the r.m.s. response of the crossed wire at $\alpha = \pm\ 45°$, and S_1 and S_2 represent respectively the sensitivity of the crossed wire to local velocity at $\alpha = \pm 45°$.

After rearranging Eqs. (4-14) and (4-15), and solving simultaneously for $\overline{w^2}$ and $\overline{uw}$, one obtains

$$\overline{w^2} = \frac{1}{2c^2}\ \{(\ \frac{\overline{e_1^2}}{S_1^2} + \frac{\overline{e_2^2}}{S_2^2}\ ) - 2\ \overline{u^2}\ \} \tag{4-16}$$

$$\overline{uw} = \frac{1}{4c}\ (\ \frac{\overline{e_1^2}}{S_1^2} - \frac{\overline{e_2^2}}{S_2^2}\ ) \tag{4-17}$$

In the same fashion, $\overline{v^2}$ and $\overline{uv}$ can be measured by operating the crossed wire in the x-y plane, and calculating equations similar to Eqs. (4-16) and (4-17).

(C) Errors in Hot-Wire Measurements

Hot-wire measurements of turbulence are subject to various type of errors. Random errors are produced in the process of calibration, reading instruments, alignment of probes, etc. Each of the random errors is independent of the others. The error of measured result can be estimated through the statistical method of repeating the measurements numerous times. The method for calculating the errors in single-sample experiments are discussed by Kline and McClintock (1953). Systematic errors are introduced due to finite length of the hot-wire, proximity of solid boundary, gradients of mean velocity and turbulent intensities, etc. Details of the systematic errors are discussed by Tieleman (1967). Most of these errors become significant only when measurements are made very close to the wall. Errors due to gradients of mean velocity and turbulent intensities are important only in measurements with crossed wires. The crossed wire measurements are furthermore affected by the correlation between the turbulent components over a small separation distance between two wires. In the absence of any suitable technique available for correcting the errors, no correction was applied in the present turbulence measurements.

4.3.5 Measurement of Frequency Spectra

For the purpose of measuring spectrum and various second order correlations of turbulent components, the fluctuating signals of hot-wire anemometers for single wire as well as crossed wire, at selected points in the boundary layer, were recorded on FM magnetic tape. Because of the low fluctuating outputs of the anemometer and a maximum of 1 volt r.m.s. recording limit to the tape recorder (Ampex FM 1300), the signals were required to pass through the low-level preamplifiers (Tektronix Type 122) and a proper attenuating stage before recording.

For the present study only the frequency spectra of the streamwise turbulent velocity were analyzed. The mean-square output between frequencies n and n + dn was automatically recorded by feeding the recorded hot-wire signal into a wave analyzer (General Radio Type 1911) having a set of passive filters from 2.5 to 25,000 Hz and two fixed bandwidths. Only the 1/3-octave (23%) bandwidth was used in the spectrum analyses.

The frequency spectrum of $\overline{u^2}$ is

$$\frac{1}{\overline{u^2}} \int_0^\infty E(n)\, dn = 1 \tag{4-18}$$

where E(n) is the fraction of energy between frequencies n and n + dn, and is known as the frequency-density function. In terms of the mean-square output signal of the wave analyzer, the fraction of energy at each frequency is

$$E(n) = \frac{1}{B_W} \overline{e^2(n, B_W)} \tag{4-19}$$

where $\overline{e^2(n, B_w)}$ is the mean-square output signal of the wave analyzer at any selected frequency n, and B_w is the filter bandwidth.

The spectral measurements are subject to errors due to finite hot-wire length, filter bandwidth, and noise. Due to finite length of the hot-wire, two or more eddies of small size may strike the wire simultaneously with the result that the measured power would be larger than the true power. This will cause the inaccuracy of the spectrum data at the high-frequency end. For a constant-percent bandwidth of 1/3-octave (23%), the side-band effect is negligible if the response time at each frequency (rise and fall time) is short enough.

CHAPTER V

ANALYSIS OF EXPERIMENTAL DATA

Extensive measurements of mean value and turbulence quantities for the turbulent boundary layer over a flat plate consisting of alternate, longitudinal strips of smooth and rough surfaces were obtained. These measurements included mean velocity distribution, wall shear stress, turbulent intensities, turbulent shear stresses and energy spectra of the streamwise turbulent velocity. The experimental investigation was limited to one type of surface configuration, as shown in Fig. 4.2. Two free-stream velocities of 20 and 30 ft/sec were chosen to give different flow conditions. The streamwise pressure gradient in the free stream was adjusted so as to be nearly zero. The spanwise periodic nature of the surface boundary conditions suggested that the entire flow field in the boundary layer is reproducible when the measurements are made in a region bounded by planes of symmetry of a smooth strip and an adjacent rough strip. In the present study, measurements were thus concentrated in a narrow region from the centerline of the smooth strip ($y = 0$ in.) to that of the rough strip ($y = 6$ in.). An analysis of the experimental data is presented in this chapter.

5.1 Boundary Layer Development

Various methods have been used to specify the height of a boundary layer. The boundary layer δ is defined as the vertical distance from the wall where the mean velocity differs by one percent from the free-stream velocity. The displacement thickness δ^* and the momentum thickness θ are defined by

$$\delta^* = \int_0^\infty \left(1 - \frac{U}{U_\infty} \right) dz \tag{5-1}$$

$$\theta = \int_0^\infty \frac{U}{U_\infty} \left(1 - \frac{U}{U_\infty} \right) dz \tag{5-2}$$

The ratio $H = \delta^* / \theta$, known as the shape factor, is usually chosen as a parameter characterizing the mean velocity profile in the boundary layer.

The values of δ^* and θ can be computed with reasonable accuracy by numerical integration of the mean velocity profiles. On the other hand the uncertainty in δ is large because the mean velocity in the boundary layer approaches the free-stream velocity asymptotically. A summary of boundary layer parameters that describe the experimental flow conditions at various locations is given in Tables 5.1a-b.

Figs. 5.1a-b show the boundary layer growth over the flat plate along the centerlines of the smooth strip (y = 0 in.) and the rough strip (y = 6 in.). Figs. 5.2 through 5.4 are the plots of δ^*, θ and H as a function of x, respectively. The various thickness δ, δ^* and θ increase with increasing streamwise distance, but decrease with increasing free-stream velocity. The shape factor H appears to be nearly constant under the same conditions of the wall. The values of δ^*, θ and H for the smooth surface are, in general, smaller than those for the rough surface. However, δ is roughly the same for both smooth and rough surfaces. Since the boundary layer thickness cannot be accurately measured, a spanwise averaged value of δ is used for the analysis of experimental data.

5.2 Determination of Shear Velocity

The shear velocity U_*, which is an important velocity scale used in the analysis of mean velocity data, is defined by

$$U_* = \sqrt{\frac{\tau_w}{\rho}} \tag{5-3}$$

It is also related to the local skin-friction coefficient C_f by the relation

$$\sqrt{\frac{C_f}{2}} = \frac{U_*}{U_\infty} \tag{5-4}$$

The physical basis for the determination of the shear velocity is provided by the postulation of the logarithmic mean velocity profile in the region near the wall. The shear velocity is thus obtained from the slope of the measured logarithmic profiles in accordance with Eq. (2-4) or Eq (2-10). The results, as shown in Fig. 5.5, indicate that the shear velocity reacts rapidly to a lateral change in surface roughness.

For the smooth strip, the Preston-tube method (Section 4.3.3) has been used to measure the wall shear stress. The results are listed in Tables 5.2a-b. The values of the resulting shear velocity are in good agreement with those calculated from the well-known Ludwieg and Tillmann's (1950) empirical formula for two-dimensional turbulent boundary layer over smooth walls,

$$U_* = U_\infty \left\{0.123 \times 10^{-0.678H} \times \left(\frac{U_\infty \theta}{\nu} \right)^{-0.268} \right\}^{1/2} \tag{5-5}$$

but are a bit higher than those obtained using the logarithmic law of mean velocity method, as shown is Fig. 5.6. This is probably due to the small departure of measured mean velocity profiles from a two-dimensional state.

In principle the shear velocity may be obtained by extrapolating the turbulent shear stress $-\rho\overline{uw}$. For the smooth surface the values obtained by the extrapolation of the turbulent shear stress and by the logarithmic law of mean velocity method are in fair agreement. However, for the case of the rough surface such extrapolation of the turbulent shear stress gives considerably lower shear velocities in comparison with those determined from the mean velocity profiles. This is because the pressure distribution on the roughness elements can produce a form drag which may contribute significantly to the total wall shear stress. Therefore, the turbulent shear stress obtained from the crossed hot-wire anemometers does not represent the true wall shear stress on any rough surface.

5.3 Mean Velocity Field

The mean velocity distribution across the boundary layer has been measured at x-stations 1, 2, 3, 4, 6, 8 and 10 ft. with the corresponding y-stations 0, 1, 2, 2.5, 3, 3.5, 4, 5 and 6 inches using two free-stream velocities of 20 and 30 ft/sec. The mean velocity data are tabulated in Tables 5.3a-b.

5.3.1 Vertical Distribution of Mean Velocity

Since the secondary flow generated by the present surface configuration is very small, the two-dimensional descriptions for similarity velocity laws can approximately be applied (Cumpsty, 1970).

Three types of non-dimensional plots have been used to study and compare the mean velocity distribution normal to the wall. They are:

$$\frac{U}{U_\infty} = \left(\frac{z}{\delta} \right)^{1/m} \tag{5-6}$$

$$\frac{U}{U_*} = f\left(\frac{zU_*}{\nu} \right) \tag{5-7}$$

and

$$\frac{U_\infty - U}{U_*} = g\left(\frac{z}{\delta} \right) \tag{5-8}$$

Eqs. (5-6) through (5-8) are known as the power law, the law of the wall and the velocity-defect law, respectively.

(A) Power Law Profiles

To test the validity of the power law (Eq. 5-6), mean velocity data were plotted as U/U_∞ versus z/δ. The resulting velocity profiles along the centerline of the smooth strip (y = 0 in.) and the rough strip (y = 6 in.), as presented in Figs. 5.7a-b, are not similar but form a family of curves for different Reynolds number $Re_x = U_\infty x/\nu$ and degree of roughness of the wall. This result agrees with the findings of Hama (1954) and Clauser (1956). The parameter m in the power law, determined by the method of least squares, is plotted versus the streamwise coordinate x in Fig. 5.8. The value of m for the rough surface is always smaller than that for the smooth surface under the same flow conditions.

Spanwise comparisons of power law profiles at x = 6 and 10 ft. for U_∞ = 30 ft/sec are presented in Figs. 5.9a-b. The resulting velocity profiles are similar in the outer 40 percent of the boundary layer but form a family of curves below this portion. This implies that the spanwise disturbing effect of wall roughness is limited to the inner 60 percent of the boundary layer. The spanwise variation of m in the power law profile takes place gradually from the centerline of the smooth strip to that of the rough strip.

(B) "Law of the Wall" Profiles

From the semi-logarithmic plots of U/U_∞ versus log z as shown in Figs. 5.10a-b, two significant facts are noted. First, all mean velocity profiles coincide for large value of z and diverge near the wall. This indicates that the effect of the spanwise changes of wall roughness depends not only on the distance from the wall but also on the roughness difference between the rough strip and the smooth strip. Secondly, the mean velocity profiles in the inner portion of the boundary layer are logarithmic in character. It follows from this fact that there still exists a wall region where the law of the wall applies, resulting in a logarithmic velocity distribution.

To illustrate the validity of the wall law given in Eq. (5-7), the mean velocity data are plotted in the form U/U_* versus Log zU_*/ν as shown in Figs. 5.11a-b, where U_* is the local shear velocity. Note that the experimental data have been forced to fit the two-dimensional description for the wall law by the prodedure used to determine the shear velocity. Hence, a well-defined logarithmic region exists near the wall. In the wall region all velocity profiles appear to fall onto straight lines with the same logarithmic slope. The range of validity of the wall law extends from $zU_*/\nu = 20$ to

zU_*/ν = 150 in the smooth part of the wall, and from zU_*/ν = 100 to zU_*/ν = 500 in the rough part of the wall. The thickness of the wall law region becomes smaller as it approaches the roughness discontinuity. At the plane of symmetry of the smooth strip (y = 0 in.), the law of the wall can be expressed as

$$\frac{U}{U_*} = \frac{1}{\kappa} \ln \frac{zU_*}{\nu} + A \tag{5-9}$$

where the values of the empirical constants κ and A are 0.41 and 6.6 respectively. For two-dimensional smooth-wall flows, there is appreciable scatter in the values of κ and A because different values of these constants have been proposed by different investigators. Opinions about the value of Kármán's constant κ are less divergent. The value of κ is usually taken as 0.41 for flat-plate flows. The choice of the constant A, however, differs from a value of 4.9 (Clauser, 1956) to that of near 7 (Townsend, 1956). The present suggested value of A which is obtained from the best fit of the experimental data is still within this wide range of choice. It is therefore suggested that the mean velocity distributions along the centerline of the smooth strip is closely analogous to those in two-dimensional smooth-wall flows.

Away from the smooth-wall flow region, the law of the wall can be written, in general, in the following form:

$$\frac{U}{U_*} = \frac{1}{\kappa} n \frac{zU_*}{\nu} + A - \frac{\Delta U}{U_*} \tag{5-10}$$

where $\Delta U/U_*$ represents the downward shift of a profile from the smooth wall profile in the wall-law plot. The absolute value of $\Delta U/U_*$ depends on the shape and distribution of the roughness elements and is a function of $k_r U_*/\nu$, where k_r is the roughness height. A relation exists between $\Delta U/U_*$ and $k_r U_*/\nu$ as given in Fig. 12. The roughness effect $\Delta U/U_*$ measured from Figs. 5.11a-b is plotted versus the spanwise coordinate y in Fig. 5.13. The result indicates that $\Delta U/U_*$ can be well predicted by the relation

$$\frac{\Delta U}{U_*} = U_\infty \left(\frac{1}{U_{*s}} - \frac{1}{U_*} \right) \tag{5-11}$$

where the subscript "s" refers to the wall condition at the plane of symmetry of the smooth strip. It also reveals that the spanwise adjustment from a smooth-wall flow to a rough-wall flow takes place almost immediately in the vicinity of the roughness discontinuity.

(C) Velocity-Defect Profiles

The mean velocity data, in conjuction with local shear velocity, can now be applied to test the validity of the velocity-defect law given in Eq. (5-8). Since δ is not well defined by the experimental data, Rotta (1962) suggested that the velocity-defect law may be expressed as

$$\frac{U_\infty - U}{U_*} = g_1 \left(\frac{zU_*}{\delta^* U_\infty} \right) \tag{5-12}$$

by introducing a non-dimensional wall distance $zU_*/\delta^* U_\infty$ instead of z/δ. The measured velocity data are therefore presented in the form $(U_\infty - U)/U_*$ versus z/δ in Figs. 5.14a-b, and versus $zU_*/\delta^* U_\infty$ in Figs. 5.15a-b. The resulting velocity profiles show considerable but systematic variations depending on the distribution of local wall shear stress. This implies that the universality of the velocity-defect law for the outer region of the boundary layer breaks down for the flow of this kind.

At the plane of symmetry of the smooth strip (y = 0 in.), the straight-line portion of the semi-logarithmic plots of mean velocity data can be described by the relation

$$\frac{U_\infty - U}{U_*} = - \frac{1}{\kappa} \ln \frac{z}{\delta} + 2.5 \tag{5-13}$$

or

$$\frac{U_\infty - U}{U_*} = - \frac{1}{\kappa} \ln \frac{zU_*}{\delta^* U_\infty} - 0.4 \tag{5-14}$$

The velocity profiles show deviations from the straight-line portion at $z/\delta \simeq 0.15$ or $zU_*/\delta^* U_\infty \simeq 0.04$. Apparently this value of z/δ or $zU_*/\delta^* U_\infty$ marks roughly the boundary between the wall region and the outer region of the boundary layer. In the outer region of the boundary layer, the velocity profiles show fair agreement with the empirical relations for two-dimensional smooth-wall flows (Hama, 1954),

$$\frac{U_\infty - U}{U_*} = 9.6 \left(1 - \frac{z}{\delta} \right)^2 \tag{5-15}$$

or

$$\frac{U_\infty - U}{U_*} = 9.6 \left(1 - 3.33 \frac{zU_*}{\delta^* U_\infty} \right)^2 \tag{5-16}$$

The velocity correlations given in Eqs. (5-13) through (5-16) indicate that the outer portion of the boundary layer along the centerline of the smooth strip is also analogous to those in two-dimensional smooth-wall flows.

Away from the smooth-wall flow region, the velocity profiles form a family of curves for different wall shear stress. Several different versions of the velocity-defect plot have been examined. When the mean velocity data are replotted as $2(U_\infty-U)/(U_{*s}+U_*)$ versus z/δ in Figs. 5.16a-b, and versus $zU_{*s}/\delta_s^* U_\infty$ in Figs. 5.17a-b, all velocity profiles fall within a resonably narrow band in an apparently universal fashion. This suggested that all the velocity profiles in the outer portion of the boundary layer may be approximated by a modified velocity-defect expression of the form

$$\frac{U_\infty - U}{U_*} = \frac{1}{2} \left(\frac{U_{*s} + U_*}{U_*} \right) g\left(\frac{z}{\delta} \right) \tag{5-17}$$

or

$$\frac{U_\infty - U}{U_*} = \frac{1}{2} \left(\frac{U_{*s} + U_*}{U_*} \right) g_1\left(\frac{zU_{*s}}{\delta_s^* U_\infty} \right) \tag{5-18}$$

The functions g and g_1 correspond to the velocity-defect distribution in a two-dimensional smooth-wall flow. The effect of spanwise variation of wall roughness enters through the variable $(U_{*s}+U_*)/2U_*$.

5.3.2 Spanwise Distribution of Mean Velocity

Figs. 5.18a-b show the spanwise distribution of mean velocity at constant heights in vertical plane x = 6 and 10 ft. for $U_\infty = 30$ ft/sec. The mean velocity distribution far above the wall is not affected by the presence of spanwise changes of wall roughness. At low elevations, however, the mean velocity varies in the spanwise direction. At very low elevations, only local surface conditions dominate the profile. The present study can thus be treated as a small perturbation about a two-dimensional smooth-wall flow, provided that the secondary flow in the boundary layer is small.

The effect of the transition from smooth-wall conditions to rough-wall conditions on the curves of constant mean velocity (or isovels) is shown in Figs. 5.19a-b. The spanwise distortion of the mean velocity distribution near the roughness discontinuity may be explained by the existence of a secondary flow of Prandtl's second kind (Section 3.3). This secondary flow, as suggested by Hinze (1967), is directed towards the wall in the plane of symmetry of a rough strip, then along the wall towards the smooth part of the wall, and away from the wall in the plane of symmetry of a smooth strip. In the present study, the measurement of secondary-flow components by means of a rotating crossed wire indicates that a weak cross-flow exists and is directed from a rough strip to a smooth strip near the wall. The magnitude of this cross-flow is everywhere less than 3 percent of the free-stream velocity. The strength of the cross-flow decreases with increasing wall distance. Due to various errors introduced in the hot-wire measurements (see Section 4.3.4), the accuracy of the measured secondary flow is poor. The secondary flow data were thus excluded.

5.4 Turbulence Field

The measurements of the turbulent intensities $\sqrt{\overline{u^2}}$, $\sqrt{\overline{v^2}}$ and $\sqrt{\overline{w^2}}$, and the turbulent shear stresses $-\rho\overline{uv}$ and $-\rho\overline{uw}$ were made in the boundary layer at x-stations 6 and 10 ft. with the corresponding y-stations 0, 1, 2, 2.5, 3, 3.5, 4, 5 and 6 inches using two free-stream velocities of 20 and 30 ft/sec. The free stream had a turbulence level within 2 percent. The experimental data are given in Tables 5.4a-b, as well as in Figs. 5.20 through 5.22. No attempt has been made to measure the turbulent shear stress $-\rho\overline{vw}$ in the boundary layer. However, an estimate of the $-\rho\overline{vw}$ distribution based on a theoretical analysis is obtained (Section 3.3).

Figs. 5.20a-b show the intensities of the streamwise, spanwise and vertical turbulent velocities $\sqrt{\overline{u^2}}$, $\sqrt{\overline{v^2}}$ and $\sqrt{\overline{w^2}}$ relative to the free-stream velocity in the boundary layer along the centerline of the smooth strip (y = 0 in.) and of the rough strip (y = 6 in.), respectively. In all cases the values of the turbulent intensities for the smooth strip are smaller than the corresponding values for the rough strip. The turbulent intensities approach the free-stream values at a greater distance from the wall than does the mean velocity. The intensity of the streamwise turbulent velocity reaches a maximum value, while the other two turbulent intensities remain nearly constant, in a region close to the wall. The present high-turbulence data have been compared with the smooth-wall data of Chowdhury (1966) and the curve shows nearly the same trends and locations of maximum values of $\sqrt{\overline{u^2}}/U_\infty$.

However, the measured turbulent intensities in the present case are found to be higher than Chowdhury's experimental data in the identical wind tunnel. This increase in the turbulent intensities may be due to continuous production of disturbances which diffuses outwards from the leading-edge roughness elements and along side edges of each of the rough strips as the flow progresses downstream. It may be noticed that the three turbulent intensities differ appreciably from one another over the inner portion of the boundary layer. The intensity of the streamwise turbulent velocity has the highest value; that of the vertical turbulent velocity has the smallest value. The difference between $\overline{v^2}$ and $\overline{w^2}$ is nearly constant in the region close to the wall, but depends strongly on the vertical distance over much of the whole boundary layer.

The distributions of $-\overline{uv}$ and $-\overline{uw}$ relative to the free-stream velocity in the boundary layer along the centerline of the smooth strip (y = 0 in.) and of the rough strip (y = 6 in.) are shown in Figs. 5.21a-b. The values of $-\overline{uv}$ and $-\overline{uw}$ increase gradually from near the wall to their maximum values at very short distances, then decrease. The value of $-\overline{uv}$, although very small, indicates that the turbulence field at the centerline of each strip is not "strictly" two-dimensional.

Spanwise comparisons of turbulence profiles $\overline{u^2}$, $\overline{v^2}$, $\overline{w^2}$, $-\overline{uv}$, $-\overline{uw}$ and $-\overline{vw}$ are presented in Figs. 5.22a-f, where the $-\overline{vw}$ distribution is estimated theoretically according to Eq. (3-21). The results indicate that the spanwise distributions of these turbulence quantities depend not only on the underlying surface characteristics, but also on the roughness difference between the rough strip and the smooth strip.

The modifications of $\overline{u^2}$, $\overline{v^2}$, $\overline{w^2}$ and $-\overline{uw}$ takes place gradually from the centerline of the smooth strip to that of the rough strip. The values of $-\overline{uv}$ and $-\overline{vw}$ attain their maximum values at the roughness discontinuity, then decrease gradually towards the centerlines of both smooth and rough strips.

5.5 Energy Spectra of Streamwise Turbulent Velocity

It is possible to gain some further insight into the boundary layer flow by examining the energy spectrum of the streamwise turbulent velocity. The energy enters the spectrum through large eddies and is then transferred down the spectrum to smaller eddies where it is finally dissipated.

One-dimensional energy spectra of the streamwise turbulent velocity evaluated at x-stations 6 and 10 ft. with the corresponding y-stations 0, 1, 2, 2.5, 3, 3.5, 4, 5 and 6 inches for the free-stream velocity of 30 ft/sec are given in Table 5.5. The data have been normalized with respect to $\overline{u^2}$ such that

$$\frac{1}{\overline{u^2}} \int_0^\infty E(k)\ dk = 1 \tag{5-19}$$

where $k = 2\pi n/U$ is the one-dimensional wave number, and $E(k)$ is the one-dimensional wave-number spectrum function. Over most of the range, the accuracy is on the order of $\pm$ 10 %. The accuracy is somewhat less at the two extremes because of large-amplitude fluctuations at low frequencies and because of low signal-to-noise ratio at high frequencies. The error due to finite length of hot-wire increases as the scale of the turbulence decreases and becomes significant at the higher frequencies. However, because of the lesser accuracy of measurement in this range, no wire-length corrections were made.

Normalized spectra of the streamwise turbulent velocity at x = 6 ft, y = 0 and 6 inches for U_∞ = 30 ft/sec are shown in Figs. 5.23a-b. The normalized spectra show a strong dependence on z/δ. Far away from the wall where the transfer among eddies predominates, there exists an extensive range where the spectra vary nearly according to $k^{-5/3}$. As the wall is approached where the production of turbulence becomes significant, the spectra show the tendency towards k^{-1} in the wave-number range where $k^{-5/3}$ normally exists when there is no mean-velocity gradient. This indicates a strong interaction between the mean-velocity gradient and the turbulent motion near the wall. The shape of the spectra shows a gradual transition from the -5/3 slope in the outer portion of the boundary layer to a -1 slope near the wall in accordance with the theoretical prediction by Tchen (1953). Nearly all of the spectra indicate the existence of a range varying as k^{-7} at the high wave-number end in agreement with Hisenberg's (1948) theory. The results also reveal that the contribution to the turbulent energy in the low wave-number range, that is, made by the large eddies, decreases as the wall approaches, but that the contribution in the high wave-number range is increased.

Spanwise comparisons of the normalized spectra at x = 6 ft. for approximately equal values of z/δ are given in Figs. 5.24a-c. Except at the low wave-number end, all spectra collapse on a single curve. At the low wave-number end, the turbulent energy contained in large eddies decreases gradually while going from a smooth to a rough strip.

CHAPTER VI

CONCLUSIONS

The present study has been carried out with the specific goal of increasing our knowledge of the flow characteristics of the turbulent boundary layer over a flat plate consisting of alternate, longitudinal strips of smooth and rough surfaces, at zero pressure gradient. The experimental investigation was limited to one type of surface configuration with the free-stream velocity as the only variable. Special attention has been given to mean velocity and turbulence distributions under the combined influence of wall roughness and strip width at distances far downstream from the leading edge of the plate, where the local boundary layer thickness is comparable to the strip width but is very large compared to the roughness height.

Results on measurements have been discussed in the preceding chapter. Several conclusions can be drawn from these results and discussions.

(1) The presence of the streamwise roughness strips in an otherwise two-dimensional smooth-wall flow will indeed perturb the flow. If the roughness height is very small compared to the local boundary layer thickness, the entire flow field can be treated as a small perturbation about a two-dimensional state. At the planes of symmetry of a smooth strip and a rough strip, the flow conditions are nearly analogous to those in two-dimensional boundary layers over a smooth wall and a rough wall, respectively.

(2) The adjustment of the wall shear stress to local conditions of the wall takes place very rapidly while undergoing an abrupt,

spanwise change in surface roughness.

(3) The mean velocity distribution can be represented adquately by a power law, except near the wall. However, the power law profiles do not coincide but form a family of curves for different Reynolds number and degree of wall roughness.

(4) There still exists a wall region where the two-dimensional description for the law of the wall applies, resulting in a logarithmic velocity distribution. The thickness of this wall region becomes smaller as it approaches the roughness discontinuity. Away from the plane of symmetry of a smooth strip, the wall law shows a downward shift of mean velocity profiles from the smooth-wall profile, depending on the distribution of the local wall shear stress. The spanwise adjustment from a smooth-wall flow to a rough-wall flow occurs almost immediately in the vicinity of the roughness discontinuity.

(5) The universality of the two-dimensional velocity-defect law for the outer portion of the boundary breaks down for the flow of this kind. The velocity-defect profiles for the smooth part of the wall are higher than those for the rough part of the wall.

(6) A weak cross-flow which provides strong mixing and momentum transport in the spanwise direction exists near the wall. This cross-flow is directed from a rough strip to a smooth strip.

(7) The intensities of the streamwise, spanwise and vertical turbulent velocities differ appreciable from one another over the inner portion of the boundary. The intensity of the streamwise turbulent velocity has the highest value and that of the vertical turbulent velocity has the smallest value. The values of the turbulent

intensities for the smooth strip are smaller than the corresponding values for the rough strip. The spanwise adjustment of the turbulent intensities takes place at a slower rate than does the wall shear stress.

(8) The turbulent shear stresses $-\rho\overline{uv}$ and $-\rho\overline{vw}$ attain their maximum values at the roughness discontinuity, then decrease gradually towards the centerlines of both smooth and rough strips. However, the turbulent shear stress $-\rho\overline{uw}$ increase gradually from the centerline of the smooth strip to that of the rough strip.

(9) The normalized spectra of the streamwise turbulent velocity show strong dependence on z/δ. The shape of the spectra varies from $k^{-5/3}$ law in the outer portion of the boundary layer to k^{-1} law near the wall. The spectra exhibit the tendency towards k^{-7} law at the high wave-number end. The spanwise distribution of the spectra remains largely unaffected by the surface configuration of the kind investigated here.

BIBLIOGRAPHY

Allan, W. K. (1970), "Velocity Distribution in Turbulent Flow," J. Mech. Eng. Sci., 12, 391-399.

Antonia, R. A. and Luxton, R. E. (1971a), "The Response of a Turbulent Boundary Layer to an Upstanding Step Change in Surface Roughness," J. Basic Eng., Trans. ASME, Ser. D, 93, 22-34.

Antonia, R. A. and Luxton, R. E. (1971b), "The Response of a Turbulent Boundary Layer to a Step Change in Surface Roughness, Part 1: Smooth to Rough," J. Fluid Mech., 48, 721-761.

Arya, S. P. S. (1968), "Structure of Stably Stratified Turbulent Boundary Layer," Ph.D. Dissertation, also Tech. Rept. CER68-69SPS10, Fluid Dynamics and Diffusion Laboratory, Colorado State University.

Baines, W. D. (1950), "An Exploratory Investigation of Boundary-Layer Development on Smooth and Rough Surfaces," Ph.D. Dissertation, State University of Iowa.

Baines, W. D. (1951), "A Literature Survey of Boundary-Layer Development on Smooth and Rough Surfaces at Zero Pressure Gradient," Iowa Institute of Hydraulic Research, State University of Iowa.

Baldwin, L. V., Sandborn, V. A. and Lawrence, J. C. (1960), "Heat Transfer from Transverse and Yawed Cylinders in Contiuum, Slip and Free Module Flow," J. Heat Transfer, Trans. ASME, Ser. C, 82, 77-86.

Blackadar, A. K., et al. (1967), "Determination of the Effect of Roughness Change on Wind Profile, in Boundary Layer and Turbulence," Phys. Fluids, 10, Supplement, S209-S211.

Blackadar, A. K. and Panofsky, H. A. (1970), "The Effects of a Change of Terrain on Wind Profiles," Final Report Contract No. AT(30-1)-3562, Department of Meteorology, Pennsylvania State University.

Blom, J. and Wartena, L. (1969), "The Influence of Changes in Surface Roughness on the Development of the Turbulent Boundary Layer in the Lower Layers of the Atmosphere," J. Atmos. Sci., 26, 255-265.

Bradley, E. F. (1968), "A Micrometeorological Study of Velocity Profiles and Surface Drag in the region Modified by a Change in Surface Roughness," Quart. J. Roy. Meteorol. Soc., 94, 361-379.

Bradshaw, P. (1964), "Experimental Fluid Mechanics," Pergamon Press, Oxford.

Bull, M. K. (1969), "Velocity Profiles of Turbulent Boundary Layers," Aero. J. Roy. Aero. Soc., 73, 143-147.

Carslaw, H. S. and Jaeger, J. C. (1959), "Conduction of Heat in Solids," Oxford University Press, London.

Cermak, J. E., et. al. (1966), "Simulation of Atmospheric Motion by Wind Tunnel Flows," Tech Rept. CER66JEC-VAS-EJP-GJB-HC-RNM-SI17, Fluid Dynamics and Diffusion Laboratory, Colorado State University.

Champagne, F. H., Sleicher, C. H. and Wehrmann, O. H. (1967), "Turbulence Measurements with Inclined Hot Wire," J. Fluid Mech., 28, 153-175.

Chanda, B. (1958), "Turbulent Boundary Layer over Heated and Unheated Plane, Rough Surfaces," Scientific Report No. 1, Department of Civil Engineering, Colorado State University.

Chowdhury, S. (1966), "Turbulent Eddies in Boundary Layer on Smooth and Rough Flat Plate," Tech. Rept. CER65SC-EJP57, Fluid Mechanics Program, College of Engineering, Colorado State University.

Clauser, F. H. (1954), "Turbulent Boundary Layers in Adverse Pressure Gradients," J. Aero. Sci., 21, 91-108.

Clauser, F. H. (1956), "The Turbulent Boundary Layer," Advances in Applied Mechanics, 4, 1-51, Academic Press, New York.

Coles, D. (1956), "The Law of the Wake in the Turbulent Boundary Layer," J. Fluid Mech., 1, 191-226.

Corrsin, S. and Kistler, A. L. (1954), "The Free-Stream Boundaries of Turbulent Flows," NACA TN 3133.

Cumptsy, N. A. (1970), "A Critical Examination of the use of a Two-Dimensional Turbulent Profile Family to Represent Three-Dimensional Boundary Layers," Aero. Res. Counc., Current Paper, C. P. 1068.

Davies, P. O. A. L. (1958), "The Behavior of a Pitot Tube in Transverse Shear," J. Fluid Mech., 3, 441-456.

Dvorak, F. A. (1969), "Calculation of Turbulent Boundary Layers on Rough Surfaces in Pressure Gradient," AIAA J., 7, 1752-1759.

Elder, J. W. (1960), "The Flow Past a Flat Plate of Finite Width," J. Fluid Mech., 5, 133-153.

Elliott, W. P. (1958), "On the Growth of the Internal Boundary Layer in the Lower Atmosphere," Ph.D. Dissertation, A & M College of Texas.

Estoque, M. A. and Bhumralkar, C. M. (1968), "Theoretical Studies of the Atmospheric Boundary Layer," Paper No. 3, Institute of Atmospheric Science, University of Miami (Florida).

Ferriss, D. H. (1965), "Preston Tube Measurement in Turbulent Boundary Layer and Fully Developed Pipe Flow," Aero. Res. Counc., Current Paper, C. P. 831.

Goldstein, S. (1938), "Modern Development in Fluid Dynamics, Vol. 1," Calrendon Press, Oxford.

Hama, F. R. (1954), "Boundary Layer Characteristics for Smooth and Rough Surfaces," Trans. Soc. Naval Architects & Marine Eng., 62, 333-358.

Head, M. R. and Rechenberg, I. (1962), "The Preston Tube as a Meass of Measureing Skin Friction," J. Fluid Mech., 14, 1-17.

Heisenberg, W. (1948), "On the Theory of Statistical and Isotropic Turbulence," Proc. Roy. Soc. (London), Ser. A, 195, 402-406.

Hidy, G. M. (1966), "On the Atmospheric Simulation: A Colloquium," NCAR-TN-22, National Center for Atmospheric Research.

Hinze, J. O. (1959), "Turbulence: An Introduction to its Mechanism and Theory," McGraw-Hill Book Co., New York.

Hinze, J. E. (1967), "Secondary Currents in Wall Turbulence," Phys. Fluids, 10, Supplement, S122-S125.

Huang, C. H. (1971), "Numerical Simulation of Wind, Temperature, Shear Stress and Turbulent Energy over Non-homogeneous Terrain," Ph.D. Dissertation, College of Engineering, Colorado State University.

Jacobs, W. (1940), "Variation in Velocity Profile with Change in Surface Roughness of Boundary," NACA TM 951.

Klebanoff, P. S. (1954), "Characteristics of Turbulence in a Boundary Layer with Zero Pressure Gradient," NACA TN 3178.

Kline, S. J. and McClintock, F. A. (1953), "Describing Uncertainties in Single-Sample Experiments," Mech. Eng., 75, 3-8.

Kline, S. J., et al. (1968), "Proceedings, Computation of Turbulent Boundary Layers-1968, AFOSR-IFP-STANFORD Conference, Vol. 1," Thermosciences Division, Department of Mechanical Engineering, Stanford University.

Liu, C. K., Kline, S. J. and Johnston, J. P. (1966), "An Experimental Study of Turbulent Boundary Layer on Rough Walls," Rept. MD-15, Thermosciences Division, Department of Mechanical Engineering, Stanford University.

Logan, E. and Jones, J. B., (1963), "Flow in a Pipe following an Abrupt Increase in Surface Roughness," J. Basic Engr., Trans. ASME, 35-40.

Ludwieg, H. and Tillmann, W. (1950), "Investigation of the Wall Shearing Stress in Turbulent Boundary Layers," NACA TM 1285.

Lumley, J. L. and Panofsky, H. A. (1964), "The Structure of Atmospheric Turbulence," Interscience Publishers, New York.

MacMillan, F. A. (1956), "Experiments on Pitot-Tubes in Shear Flow," Aero. Res. Counc., Rept. and Memo. 3028.

Miyake, M. (1961), "Transformation of Atmospheric Boundary Layer Induced by Inhomogeneous Surfaces," M. S. Thesis, University of Washington (Seattle).

Moore, W. L. (1950), "An Experimental Investigation of the Boundary Layer Development along a Rough Surface," Ph.D. Dissertation, State University of Iowa.

Nemoto, S. (1968), "Similarity Between Natural Wind in the Atmosphere and Model Wind in a Wind Tunnel," Pap. Meteorol. Geophys., 19, 131-230.

Nickerson, E. C. (1968), "Boundary Layer Adjustment as an Initial Value Problem," J. Atmos. Sci., 25, 207-213.

Onishi, G. (1966), "A Two-Dimensional, Steady State Numerical Model of Atmospheric Boundary Layer Flow over Inhomogeneous Terrain," in Theoretical Studies of the Atmospheric Boundary Layer, Final Report HIG-66-16, Hawaii Institute of Geophysics, University of Hawaii, 81-122.

Panofsky, H. A. and Townsend, A. A. (1964), "Change of Terrain Roughness and the Wind Profile," Quart. J. Roy. Meteorol. Soc., 90, 147-155.

Patel, V. C. (1965), "Calibration of the Preston Tube and Limitations on its Use in Pressure Gradients," J. Fluid Mech., 23, 185-208.

Perkins, H. J. (1970), "The Formulation of Streamwise Vorticity in Turbulent Flow," J. Fluid Mech., 44, 721-740.

Perry, A. E. and Joubert, P. N. (1963), "Rough-Wall Boundary Layers in Adverse Pressure Gradients," J. Fluid Mech., 17, 193-211.

Perry, A. E., Schofield, W. H. and Joubert, P. N. (1969), "Rough Wall Turbulent Boundary Layers," J. Fluid Mech., 37, 383-413.

Peterson, E. W. (1969), "A Numerical Model of the Mean Wind and Turbulent Energy Downstream of a Change in Surface Roughness," Publication No. 102-69, Center for Air Environment Studies, Pennsylvania State University.

Plate, E. J. and Hidy, G. M. (1967), "Laboratory Study of Air Flowing over a Smooth Surface into Small Water Waves," J. Geophys. Res., 72, 4627-4641.

Plate, E. J. (1971), "Aerodynamic Characteristics of Atmospheric Boundary Layer," AEC Critical Review Series, TID-25465, Division of Technical Information, U. S. Atomic Energy Commission.

Prandtl, L. (1951), "Essentials of Fluid Dynamics," Hafner Publishing Co., New York.

Preston, J. H. (1954), "The Determination of Turbulent Skin Friction by Means of Pitot Tubes," J. Roy. Aero. Soc., 58, 109.

Priestley, C. H. B. (1959), "Turbulent Transfer in the Lower Atmosphere," University of Chicago Press, Chicago.

Rose, D. (1953), "A Study of Incompressible Turbulent Boundary Layers," Tech. Memo. ONR Project NR 062-139-1, Ordance Research Laboratory, Pennsylvania State College.

Rotta, J. C. (1962), "Turbulent Boundary Layers in Incompressible Flow," Progress in Aeronautical Sciences, 2, 1-219, Pergamon Press, Oxford.

Sandborn, V. A. (1966), "Metrology of Fluid Mechanics," CER66VAS32, College of Engineering, Colorado State University.

Sandborn, V. A. (1967), "Hot Wire Anemometer Measurement in Large Scale Boundary Layers," Tech. Rept. CER66-67VAS32, Fluid Dynamics and Diffusion Laboratory, Colorado State University.

Schlichting, H. (1968), "Boundary-Layer Theory,' McGraw-Hill Book Co., New York.

Scottron, V. E. (1967), "Turbulent Boundary Layer Characteristics over a Rough Surface in an Adverse Pressure Gradient," Rept. 2659, Hydromechanics Laboratory, Naval Ship Research and Development Center, Washington, D. C.

Slotta, L. S. (1963), "A Critical Investigation of the Universality of Karman's Constant in Turbulent Flow," Studies of the Effects of Variations in Boundary Conditions on the Atmospheric Boundary Layer, Annual Report 1963, Department of Meteorology, University of Wisconsin, 1-36.

Staff of Aerodynamics Division, N.P.L. (1958), "On the Measurements of Local Surface Friction on a Flat Plate by Means of Preston Tubes," Aero. Res. Counc., Rept. and Memo. 3185.

Stewartson, K. and Howarth, L. (1960), "On the Flow past a Quarter Infinite Plate Using Oseen's Equations," J. Fluid Mech., 7, 1-21.

Taylor, P. A. (1969), "On Wind and Shear-Stress Profiles above a Change in Surface Roughness," Quart. J. Roy. Metoeorol. Soc., 95, 77-91.

Taylor, P. A. (1970), "A Model of Airflow above Changes in Surface Heat Flux, Temperature, and Roughness for Neutral and unstable Conditions," Bound. Layer Meteorol., 1, 18-39.

Taylor, R. J. (1962), "Small-Scale Advection and the Neutral Wind Profile," J. Fluid Mech., 13, 529-539.

Tchen, C. M. (1953), "On the Spectrum of Energy in Turbulent Shear Flow," Res. Pap., RP2388, J. Res., National Bureau of Standards, 51, 51-62.

Telles, A. S. and Dukler, A. E. (1968), "Similarity Type of Solution of the Turbulent Boundary Layer Equations for Momentum and Energy, Part I," AICHE J., 14, 440-447.

Tielemann, H. W. (1967), "Viscous Region of Turbulent Boundary Layer," Ph.D. Dissertation, also Tech Rept. CER67-68HWT21, Fluid Dynamics and Diffusion Laboratory, Colorado State University.

Tillmann, W. (1945), "Investigation of Some Particularities of Turbulent Boundary Layer on Plates," Joint Intelligence Objective Agency, Washington, D.C.

Townsend, A. A. (1956), "The Structure of Turbulent Shear Flow," Cambridge University Press, London.

Townsend, A. A. (1965a), "Self-Preserving Flow inside a Turbulent Boundary Layer," J. Fluid Mech., 22, 773-797.

Townsend, A. A. (1965b), "The Response of a Turbulent Boundary Layer to Abrupt Changes in Surface Conditions," J. Fluid Mech., 22, 799-822.

Townsend, A. A. (1966), "The Flow in a Turbulent Boundary Layer after a Change in Surface Roughness," J. Fluid Mech., 26, 255-266.

Wagner, N. K. (1966), "A Two-Dimensional, Time Dependent Numerical Model of Atmospheric Boundary-Layer Flow over Inhomogeneous Terrain," in Theoretical Studies of the Atmospheric Boundary Layer, Final Report, HIG-66-16, Hawaii Institute of Geophysics, University of Hawaii.

Webster, C. A. G. (1964), "An Experimental Study of Turbulence in a Density-Stratified Shear Flow," J. Fluid Mech., 19, 221-245.

Yeh, F. F. and Nickerson, E. C. (1970), "Air Flow over Roughness Discontinuity," Ph.D. Dissertation, also Tech. Rept. CER70-71FFY-ECN6, Fluid Dynamics and Diffusion Laboratory, Colorado State University.

APPENDIX

APPENDIX

BOUNDARY LAYER FLOW OVER A THREE-DIMENSIONAL OBSTACLE

A mathematical model for laminar flow over a semi-infinite, rectangular-parallelepiped obstacle located along the centerline of a flat plate, as shown in Fig. A-1, is formulated. The three-dimensional effects, including cross-flow, is assumed to be small such that the flow field is in a perturbed state about a two-dimensional boundary layer. The essential ideas underlying the solution are based on Oseen's linearization of the boundary layer equation. Far away from the obstacle the flow will approximate the two-dimensional flow past a semi-infinite flat plate. Stewartson and Howarth (1960) solved this two-dimensional flow by building up successively from the potential flow associated with the free-stream velocity and a shear layer introduced to restore the no-slip condition on the plate. Near the obstacle a three-dimensional diffusive flow is determined by introducing a negative volume source to give zero mean velocity inside the obstacle. The solution thus obtained, neglecting the effects of the edges, shall give a first-order approximation of the three-dimensional boundary layer problem.

In the absence of longitudinal pressure gradient, Oseen's linearization of the boundary layer equation with small cross-flow takes the form

$$U_\infty \frac{\partial U}{\partial x} = \nu \nabla^2 U \tag{A-1}$$

where $\nabla^2 \equiv \frac{\partial^2}{\partial y^2} + \frac{\partial^2}{\partial z^2}$ is a Laplace operator.

The coordinates are now non-dimensionalized by the following transformation:

$$\begin{aligned} \phi &= U/U_\infty \\ \tau &= x/d \\ \eta &= y\sqrt{Re_d}\,/d \\ \xi &= z\sqrt{Re_d}\,/d \end{aligned} \tag{A-2}$$

where d is a characteristic length, and $Re_d = U_\infty d/\nu$ is the Reynolds number based on length d. Upon substitution, Eq. (A-1) becomes

$$\frac{\partial^2 \phi}{\partial \tau^2} = \frac{\partial^2 \phi}{\partial \eta^2} + \frac{\partial^2 \phi}{\partial \xi^2} \tag{A-3}$$

For the case of an semi-infinite, rectangular-parallelepiped obstacle of height d and width 2ed placed on a flat plate longitudinally starting from the leading edge of the plate, the boundary conditions are:

$$\begin{aligned} &\tau < 0, \quad \phi = 1 \qquad \text{for all values of } \eta \text{ and } \xi \\ &\tau > 0, \quad \phi = \begin{cases} 0 & |\eta| \leq e\sqrt{Re_d} \text{ and } 0 \leq \xi \leq \sqrt{Re_d} \\ 1 & \text{otherwise} \end{cases} \end{aligned} \tag{A-4}$$

The linearity of Eq. (A-3) with appropriate boundary conditions allows the solution to be separated into the potential flow associated with the free-stream velocity, a two-dimensional shear flow to restore the no-slip condition, and a three-dimensional perturbed, diffusive flow:

$$\phi = 1 + \phi_1 + \phi_2 \tag{A-5}$$

The two-dimensional shear flow is described by the eqaution

$$\frac{\partial \phi_1}{\partial \tau} = \frac{\partial^2 \phi_1}{\partial \xi^2} \tag{A-6}$$

with the boundary conditions:

$$\tau < 0, \qquad \phi_1 = 0 \qquad \text{for all values of } \xi$$

$$\tau > 0, \qquad \phi_1 = \begin{cases} -1 & \text{for } \xi = 0 \\ 0 & \text{as } \xi \to \infty \end{cases} \tag{A-7}$$

This leads to the solution

$$\phi_1 = -\mathrm{erfc}\left(\frac{\xi}{2\sqrt{\tau}}\right) \tag{A-8}$$

where

$$\mathrm{erfc}(z) = \frac{2}{\sqrt{\pi}}\int_z^\infty e^{-t^2}\,dt = 1 - \mathrm{erf}(z)$$

Three-dimensional perturbed flow is described by the equation

$$\frac{\partial \phi_2}{\partial \tau} = \frac{\partial^2 \phi_2}{\partial \eta^2} + \frac{\partial^2 \phi_2}{\partial \xi^2} \tag{A-9}$$

with the boundary conditions:

$$\tau < 0, \qquad \phi_2 = 0 \qquad \text{for all values of } \eta \text{ and } \xi$$

$$\tau > 0, \qquad \phi_2 = \begin{cases} -\mathrm{erf}\left(\frac{\xi}{2\sqrt{\tau}}\right) & |\eta| \le e\sqrt{Re_d} \text{ and } 0 \le \xi \le \sqrt{Re_d} \\ 0 & \text{otherwise} \end{cases} \tag{A-10}$$

Eq. (A-9) with the boundary conditions describes the diffusion from a semi-infinite, rectangular-parallelepiped volume source with variable strength. Following the technique given by Carslaw and Jaeger (1959), the solution of Eq. (A-9) is, in general, given by

$$\phi_2 = \frac{1}{4\pi}\iiint_{-\infty}^{\infty} \frac{\phi_2(t,\alpha,\beta)}{\tau - t}\left\{ e^{-\frac{(\eta-\alpha)^2+(\xi-\beta)^2}{4(\tau-t)}} - e^{-\frac{(\eta-\alpha)^2+(\xi+\beta)^2}{4(\tau-t)}} \right\} dt\,d\alpha\,d\beta$$

Substituting the boundary conditions yields

$$\phi_2 = -\frac{1}{4\pi}\int_{-\sqrt{Re_d}}^{\sqrt{Re_d}}\int_{-e\sqrt{Re_d}}^{e\sqrt{Re_d}}\int_0^\infty \frac{\mathrm{erf}(\frac{\beta}{2\sqrt{t}})}{\tau-t}\{e^{-\frac{(\eta-\alpha)^2+(\xi-\beta)^2}{4(\tau-t)}} - e^{-\frac{(\eta-\alpha)^2+(\xi+\beta)^2}{4(\tau-t)}}\}\, dt d\alpha d\beta$$

or

$$\phi_2 = \frac{1}{4\sqrt{\pi}}\int_0^{\sqrt{Re_d}}\int_0^\infty \frac{\mathrm{erf}(\frac{\beta}{2\sqrt{t}})}{\tau-t}\{\mathrm{erf}(\frac{\eta-e\sqrt{Re_d}}{2\sqrt{\tau-t}}) - \mathrm{erf}(\frac{\eta+e\sqrt{Re_d}}{2\sqrt{\tau-t}})\}\{e^{-\frac{(\xi-\beta)^2}{4(\tau-t)}} - e^{-\frac{(\xi+\beta)^2}{4(\tau-t)}}\} dt d\alpha d\beta \qquad \text{(A-11)}$$

The final solution for the boundary layer flow over the three-dimensional obstacle then reads

$$\frac{U}{U_\infty} = \mathrm{erf}(\frac{\xi}{2\sqrt{\tau}}) + \frac{1}{4\sqrt{\pi}}\int_0^{\sqrt{Re_d}}\int_0^\infty \frac{\mathrm{erf}(\frac{\beta}{2\sqrt{t}})}{\tau-t}\{\mathrm{erf}(\frac{\eta-e\sqrt{Re_d}}{2\sqrt{\tau-t}}) - \mathrm{erf}(\frac{\eta+e\sqrt{Re_d}}{2\sqrt{\tau-t}})\}\{e^{-\frac{(\xi-\beta)^2}{4(\tau-t)}} - e^{-\frac{(\xi+\beta)^2}{4(\tau-t)}}\} dt d\alpha d\beta \qquad \text{(A-12)}$$

Table 5.1a Summary of boundary layer parameters, U_∞ = 20 ft/sec

X (ft)	Y (in.)	δ (in.)	δ^* (in.)	θ (in.)	H
1	0	1.80	.268	.201	1.33
	1	1.90	.284	.213	1.33
	2	1.75	.260	.198	1.31
	2.5	1.86	.300	.223	1.35
	3	1.80	.320	.220	1.45
	3.5	1.86	.307	.216	1.42
	4	1.82	.282	.206	1.37
	5	1.76	.306	.213	1.44
	6	1.81	.316	.216	1.46
2	0	2.56	.349	.268	1.30
	1	2.48	.334	.260	1.28
	2	2.45	.333	.258	1.29
	2.5	2.51	.356	.272	1.31
	3	2.42	.392	.273	1.44
	3.5	2.57	.372	.274	1.36
	4	2.46	.338	.252	1.34
	5	2.61	.387	.281	1.38
	6	2.51	.360	.265	1.36
3	0	3.27	.413	.322	1.28
	1	3.25	.407	.319	1.28
	2	3.33	.409	.319	1.28
	2.5	3.38	.440	.335	1.31
	3	3.00	.451	.324	1.39
	3.5	3.24	.462	.335	1.38
	4	3.26	.444	.326	1.36
	5	3.22	.485	.341	1.42
	6	3.20	.465	.333	1.40
4	0	3.80	.451	.357	1.26
	1	3.72	.452	.357	1.27
	2	3.76	.457	.359	1.27
	2.5	3.72	.486	.373	1.30
	3	3.83	.533	.380	1.40
	3.5	3.85	.504	.375	1.34
	4	3.56	.496	.365	1.36
	5	3.59	.527	.380	1.39
	6	3.62	.528	.381	1.39
6	0	4.34	.544	.418	1.30
	1	4.35	.551	.422	1.31
	2	4.42	.592	.448	1.32
	2.5	4.39	.615	.454	1.35
	3	4.59	.676	.477	1.42
	3.5	4.48	.602	.440	1.37
	4	4.59	.607	.446	1.36
	5	4.41	.605	.441	1.37
	6	4.41	.632	.455	1.39
8	0	5.01	.633	.487	1.30
	1	5.05	.666	.510	1.31
	2	5.20	.679	.518	1.31
	2.5	5.19	.663	.505	1.31
	3	5.30	.734	.538	1.36
	3.5	5.19	.690	.515	1.34
	4	5.22	.730	.528	1.38
	5	5.17	.713	.521	1.37
	6	5.03	.737	.525	1.40
10	0	5.50	.774	.573	1.35
	1	5.70	.805	.595	1.35
	2	5.76	.782	.578	1.35
	2.5	5.57	.765	.571	1.34
	3	5.91	.840	.604	1.39
	3.5	5.77	.773	.571	1.35
	4	5.57	.797	.574	1.39
	5	5.43	.779	.566	1.38
	6	5.24	.825	.580	1.42

Table 5.1b Summary of boundary layer parameters, U_∞ = 30 ft/sec

X (ft)	Y (in.)	δ (in.)	δ^* (in.)	θ (in.)	H
1	0	1.71	.240	.186	1.29
	1	1.58	.222	.173	1.28
	2	1.71	.248	.193	1.28
	2.5	1.70	.246	.190	1.29
	3	1.78	.297	.210	1.41
	3.5	1.76	.269	.196	1.37
	4	1.73	.267	.192	1.39
	5	1.80	.263	.189	1.39
	6	1.82	.297	.207	1.43
2	0	2.46	.308	.241	1.28
	1	2.44	.309	.242	1.28
	2	2.24	.295	.231	1.28
	2.5	2.33	.329	.252	1.31
	3	2.30	.368	.257	1.43
	3.5	2.44	.347	.254	1.37
	4	2.37	.330	.242	1.36
	5	2.38	.364	.257	1.42
	6	2.38	.359	.256	1.40
3	0	3.15	.371	.292	1.27
	1	2.99	.353	.282	1.25
	2	2.97	.371	.291	1.27
	2.5	3.07	.380	.295	1.29
	3	2.95	.441	.315	1.40
	3.5	2.98	.418	.302	1.38
	4	2.95	.449	.316	1.42
	5	2.88	.450	.312	1.44
	6	2.96	.478	.328	1.46
4	0	3.83	.415	.334	1.24
	1	3.63	.418	.336	1.24
	2	3.62	.416	.331	1.26
	2.5	3.46	.434	.336	1.29
	3	3.28	.484	.339	1.43
	3.5	3.53	.474	.346	1.37
	4	3.44	.477	.349	1.37
	5	3.59	.508	.362	1.40
	6	3.53	.502	.359	1.40

X (ft)	Y (in.)	δ (in.)	δ^* (in.)	θ (in.)	H
6	0	3.99	.486	.378	1.29
	1	4.12	.507	.392	1.29
	2	4.08	.534	.407	1.31
	2.5	4.07	.546	.411	1.33
	3	4.13	.596	.427	1.40
	3.5	4.26	.556	.413	1.37
	4	4.22	.594	.426	1.39
	5	4.14	.618	.434	1.42
	6	4.00	.613	.427	1.44
8	0	4.75	.592	.460	1.29
	1	4.94	.632	.486	1.30
	2	4.88	.652	.494	1.32
	2.5	5.02	.646	.493	1.31
	3	4.99	.672	.492	1.37
	3.5	5.07	.675	.496	1.36
	4	5.01	.666	.494	1.39
	5	4.97	.702	.498	1.41
	6	5.18	.701	.503	1.39
10	0	5.19	.740	.546	1.36
	1	5.42	.772	.565	1.37
	2	5.55	.767	.563	1.36
	2.5	5.32	.784	.565	1.39
	3	5.16	.801	.556	1.44
	3.5	5.20	.766	.541	1.42
	4	5.46	.748	.539	1.39
	5	5.30	.772	.541	1.43
	6	5.08	.761	.529	1.44

Table 5.2a Preston tube measurement of wall shear stress, U_∞ = 20 ft/sec

X =3.0 ft, R_x=2.88x10^5				X =4.0 ft, R_x=3.85x10^5				X =5.0 ft, R_x=4.81x10^5			
Y (in.)	U_* (fps)	τ_w (lbs/ft^2)	C_f	Y (in.)	U_* (fps)	τ_w (lbs/ft^2)	C_f	Y (in.)	U_* (fps)	τ_w (lbs/ft^2)	C_f
0.5	.890	1.48×10^{-3}	3.97×10^{-3}	0.5	.868	1.40×10^{-3}	3.78×10^{-3}	0.5	.817	1.24×10^{-3}	3.35×10^{-3}
1.0	.861	1.38×10^{-3}	3.72×10^{-3}	1.0	.827	1.28×10^{-3}	3.43×10^{-3}	1.0	.805	1.21×10^{-3}	3.25×10^{-3}
2.0	.910	1.54×10^{-3}	4.15×10^{-3}	2.0	.867	1.40×10^{-3}	3.77×10^{-3}	2.0	.844	1.33×10^{-3}	3.57×10^{-3}
2.5	.853	1.36×10^{-3}	3.65×10^{-3}	2.5	.816	1.24×10^{-3}	3.34×10^{-3}	2.5	.781	1.14×10^{-3}	3.06×10^{-3}
2.75	.769	1.10×10^{-3}	2.97×10^{-3}	2.75	.755	1.06×10^{-3}	2.86×10^{-3}	2.75	.734	1.01×10^{-3}	2.70×10^{-3}

X =6.0 ft, R_x=5.77x10^5				X =8.0 ft, R_x=7.69x10^5				X =10.0 ft, R_x=9.61x10^5			
Y (in.)	U_* (fps)	τ_w (lbs/ft^2)	C_f	Y (in.)	U_* (fps)	τ_w (lbs/ft^2)	C_f	Y (in.)	U_* (fps)	τ_w (lbs/ft^2)	C_f
0.5	.782	1.14×10^{-3}	3.07×10^{-3}	0.5	.725	9.81×10^{-4}	2.64×10^{-3}	0.5	.679	8.60×10^{-4}	2.31×10^{-3}
1.0	.816	1.12×10^{-3}	3.03×10^{-3}	1.0	.735	1.01×10^{-3}	2.71×10^{-3}	1.0	.695	9.00×10^{-4}	2.42×10^{-3}
2.0	.816	1.24×10^{-3}	3.34×10^{-3}	2.0	.766	1.09×10^{-3}	2.94×10^{-3}	2.0	.731	9.96×10^{-4}	2.68×10^{-3}
2.5	.762	1.08×10^{-3}	2.91×10^{-3}	2.5	.702	9.20×10^{-4}	2.47×10^{-3}	2.5	.674	8.48×10^{-4}	2.28×10^{-3}
2.75	.725	9.81×10^{-4}	2.64×10^{-3}	2.75	.696	9.03×10^{-4}	2.43×10^{-3}	2.75	.668	8.33×10^{-4}	2.24×10^{-3}

Table 5.2b Preston tube measurement of wall shear stress, U_∞ = 30 ft/sec

X = 3.0 ft $R_x=4.36\times10^5$				X = 4.0 ft $R_x=5.31\times10^5$				X = 5.0 ft $R_x=7.26\times10^5$			
Y (in.)	U_* (fps)	τ_w (lbs/ft^2)	C_f	Y (in.)	U_* (fps)	τ_w (lbs/ft^2)	C_f	Y (in.)	U_* (fps)	τ_w (lbs/ft^2)	C_f
0.5	1.36	3.43×10^{-3}	4.00×10^{-3}	0.5	1.32	3.21×10^{-3}	3.74×10^{-3}	0.5	1.28	3.05×10^{-3}	3.55×10^{-3}
1.0	1.36	3.39×10^{-3}	3.95×10^{-3}	1.0	1.31	3.17×10^{-3}	3.69×10^{-3}	1.0	1.28	3.01×10^{-3}	3.50×10^{-3}
2.0	1.35	3.36×10^{-3}	3.91×10^{-3}	2.0	1.32	3.19×10^{-3}	3.72×10^{-3}	2.0	1.25	2.90×10^{-3}	3.38×10^{-3}
2.5	1.30	3.11×10^{-3}	3.62×10^{-3}	2.5	1.26	2.93×10^{-3}	3.41×10^{-3}	2.5	1.23	2.81×10^{-3}	3.27×10^{-3}
2.75	1.19	2.61×10^{-3}	3.04×10^{-3}	2.75	1.17	2.51×10^{-3}	2.93×10^{-3}	2.75	1.13	2.36×10^{-3}	2.75×10^{-3}

X = 6.0 ft $R_x=8.71\times10^5$				X = 8.0 ft $R_x=1.12\times10^6$				X =10.0 ft $R_x=1.45\times10^6$			
Y (in.)	U_* (fps)	τ_w (lbs/ft^2)	C_f	Y (in.)	U_* (fps)	τ_w (lbs/ft^2)	C_f	Y (in.)	U_* (fps)	τ_w (lbs/ft^2)	C_f
0.5	1.24	2.85×10^{-3}	3.32×10^{-3}	0.5	1.18	2.56×10^{-3}	2.98×10^{-3}	0.5	1.10	2.25×10^{-3}	2.62×10^{-3}
1.0	1.24	2.83×10^{-3}	3.30×10^{-3}	1.0	1.17	2.52×10^{-3}	2.94×10^{-3}	1.0	1.11	2.29×10^{-3}	2.67×10^{-3}
2.0	1.22	2.73×10^{-3}	3.18×10^{-3}	2.0	1.15	2.42×10^{-3}	2.82×10^{-3}	2.0	1.08	2.16×10^{-3}	2.52×10^{-3}
2.5	1.19	2.60×10^{-3}	3.02×10^{-3}	2.5	1.14	2.39×10^{-3}	2.79×10^{-3}	2.5	1.10	2.21×10^{-3}	2.58×10^{-3}
2.75	1.12	2.30×10^{-3}	2.68×10^{-3}	2.75	1.08	2.16×10^{-3}	2.52×10^{-3}	2.75	1.06	2.08×10^{-3}	2.43×10^{-3}

Table 5.3a Mean velocity data, U_∞ = 20 ft/sec

X= 1.0 FT Y= 0.0 IN		X= 1.0 FT Y= 1.0 IN		X= 1.0 FT Y= 2.0 IN		X= 1.0 FT Y= 2.5 IN		X= 1.0 FT Y= 3.0 IN		X= 1.0 FT Y= 3.5 IN		X= 1.0 FT Y= 4.0 IN		X= 1.0 FT Y= 5.0 IN		X= 1.0 FT Y= 6.0 IN	
Z (IN)	U (FPS)	Z (IN)	U (FPS)	Z (IN)	U (FPS)	Z (IN)	U (FPS)	Z (IN)	U (FPS)	Z (IN)	U (FPS)	Z (IN)	U (FPS)	Z (IN)	U (FPS)	Z (IN)	U (FPS)
.040	10.049	.037	9.381	.035	9.688	.038	9.533	.038	7.411	.127	9.614	.129	9.962	.128	9.355	.129	8.087
.056	10.466	.050	10.006	.043	10.313	.052	10.323	.063	8.176	.167	9.743	.161	10.253	.167	9.772	.161	8.533
.072	11.074	.066	10.819	.057	11.121	.071	11.008	.088	9.041	.199	10.168	.189	10.814	.197	10.253	.195	9.179
.091	11.846	.084	11.445	.077	11.931	.098	11.723	.114	9.772	.226	10.725	.214	11.449	.224	10.921	.227	10.035
.106	12.378	.107	12.015	.095	12.567	.127	12.550	.145	10.485	.264	11.433	.235	11.983	.259	11.620	.249	10.810
.130	12.947	.126	12.775	.121	13.150	.155	12.813	.171	11.216	.302	12.323	.263	12.620	.296	12.346	.280	11.566
.161	13.443	.158	13.317	.157	13.645	.195	13.328	.201	11.910	.348	12.914	.296	13.150	.334	12.847	.324	12.296
.201	13.831	.208	13.772	.205	14.079	.238	13.758	.231	12.474	.405	13.589	.341	13.610	.381	13.295	.374	12.865
.248	14.184	.258	14.198	.265	14.460	.288	14.195	.266	12.973	.463	14.116	.390	14.004	.449	13.747	.428	13.447
.305	14.510	.315	14.658	.327	14.866	.348	14.480	.320	13.429	.516	14.602	.443	14.390	.500	14.099	.483	13.966
.368	14.834	.389	15.046	.396	15.275	.414	14.769	.385	13.900	.575	15.059	.494	14.785	.568	14.586	.541	14.466
.418	15.082	.457	15.388	.452	15.589	.481	15.046	.445	14.535	.651	15.599	.551	15.218	.633	15.075	.598	14.902
.482	15.378	.527	15.691	.524	15.967	.551	15.363	.501	14.788	.725	16.037	.600	15.531	.701	15.593	.665	15.372
.548	15.706	.604	16.102	.595	16.334	.632	15.828	.565	15.316	.792	16.451	.653	15.862	.753	16.019	.735	15.949
.612	16.054	.675	16.433	.659	16.672	.696	16.186	.631	15.868	.865	16.901	.715	16.254	.815	16.445	.802	16.457
.684	16.445	.761	16.807	.735	17.059	.761	16.524	.706	16.554	.935	17.328	.805	16.746	.889	16.915	.869	16.901
.746	16.807	.844	17.169	.808	17.422	.822	16.830	.772	16.752	1.002	17.690	.872	17.166	.959	17.320	.944	17.311
.808	17.236	.934	17.598	.869	17.701	.897	17.253	.851	17.127	1.090	18.110	.945	17.581	1.033	17.699	1.009	17.644
.863	17.587	1.019	18.016	.946	18.046	.956	17.527	.918	17.603	1.163	18.394	1.028	17.995	1.109	18.104	1.079	18.046
.919	18.003	1.085	18.355	1.026	18.357	1.028	17.864	.999	18.000	1.251	18.697	1.091	18.289	1.186	18.485	1.157	18.446
.989	18.412	1.178	18.813	1.120	18.751	1.121	18.247	1.076	18.365	1.347	19.064	1.178	18.656	1.259	18.871	1.228	18.762
1.062	18.772	1.272	19.240	1.217	19.097	1.205	18.568	1.163	18.772	1.443	19.409	1.247	18.925	1.334	19.280	1.298	18.999
1.169	19.102	1.371	19.483	1.307	19.357	1.280	18.856	1.255	19.142	1.547	19.726	1.316	19.127	1.389	19.538	1.384	19.315
1.269	19.379	1.491	19.726	1.410	19.628	1.363	19.105	1.344	19.417	1.647	19.918	1.403	19.379	1.491	19.799	1.478	19.560
1.372	19.584	1.608	19.915	1.514	19.862	1.453	19.379	1.449	19.704	1.779	20.122	1.522	19.687	1.597	19.997	1.589	19.807
1.497	19.797	1.728	20.072	1.641	20.112	1.569	19.687	1.561	19.944	1.892	20.244	1.647	19.952	1.698	20.141	1.711	20.041
1.635	20.014	1.830	20.186	1.745	20.234	1.676	19.896	1.697	20.096	2.017	20.331	1.749	20.132	1.813	20.279	1.813	20.196
1.788	20.191	1.965	20.315	1.855	20.322	1.793	20.067	1.811	20.220	2.154	20.397	1.854	20.265	1.931	20.364	1.933	20.322
1.953	20.329	2.090	20.418	2.012	20.407	1.953	20.229	1.953	20.322	2.238	20.414	2.033	20.404	2.055	20.397	2.084	20.381
2.080	20.385	2.217	20.447	2.216	20.414	2.084	20.319	2.077	20.393	2.238	20.414	2.234	20.423	2.235	20.402	2.236	20.397
2.220	20.404	2.217	20.447	2.216	20.414	2.218	20.343	2.221	20.412	2.238	20.414	2.234	20.423	2.235	20.402	2.236	20.397

X= 2.0 FT Y= 0.0 IN		X= 2.0 FT Y= 1.0 IN		X= 2.0 FT Y= 2.0 IN		X= 2.0 FT Y= 2.5 IN		X= 2.0 FT Y= 3.0 IN		X= 2.0 FT Y= 3.5 IN		X= 2.0 FT Y= 4.0 IN		X= 2.0 FT Y= 5.0 IN		X= 2.0 FT Y= 6.0 IN	
Z (IN)	U (FPS)	Z (IN)	U (FPS)	Z (IN)	U (FPS)	Z (IN)	U (FPS)	Z (IN)	U (FPS)	Z (IN)	U (FPS)	Z (IN)	U (FPS)	Z (IN)	U (FPS)	Z (IN)	U (FPS)
.056	8.356	.057	9.421	.057	8.816	.059	9.118	.056	4.847	.113	9.371	.133	9.557	.134	9.139	.133	8.982
.077	8.581	.082	9.860	.076	9.406	.083	9.487	.077	5.289	.135	9.646	.158	9.942	.162	9.552	.158	9.325
.090	9.426	.095	10.523	.088	10.113	.093	10.267	.093	6.138	.158	10.202	.176	10.432	.196	10.113	.175	9.885
.106	10.387	.108	11.329	.095	10.901	.104	10.870	.107	7.286	.188	10.905	.202	10.966	.223	10.640	.197	10.505
.120	11.202	.127	12.053	.108	11.619	.127	11.635	.121	8.190	.223	11.500	.226	11.408	.261	11.210	.226	11.134
.140	11.946	.153	12.747	.129	12.202	.149	12.206	.146	9.411	.269	12.167	.258	11.926	.302	11.745	.261	11.765
.160	12.657	.184	13.462	.159	12.844	.177	12.699	.173	10.396	.318	12.725	.298	12.449	.343	12.198	.305	12.384
.189	13.281	.208	13.859	.189	13.313	.218	13.245	.201	11.308	.383	13.334	.339	12.954	.388	12.684	.350	12.943
.229	13.759	.259	14.295	.233	13.821	.255	13.659	.255	12.009	.444	13.787	.387	13.416	.432	13.162	.400	13.430
.279	14.182	.328	14.699	.281	14.212	.333	14.235	.276	12.589	.515	14.262	.436	13.863	.485	13.610	.446	13.852
.329	14.526	.409	15.069	.348	14.601	.402	14.637	.328	13.111	.594	14.750	.493	14.375	.539	14.026	.514	14.335
.393	14.888	.489	15.376	.419	14.952	.478	15.050	.383	13.662	.682	15.258	.555	14.856	.598	14.474	.582	14.799
.459	15.242	.588	15.706	.492	15.286	.545	15.366	.447	14.182	.775	15.715	.620	15.286	.659	14.850	.650	15.204
.537	15.582	.674	16.054	.579	15.621	.644	15.743	.516	14.705	.869	16.145	.681	15.649	.729	15.251	.746	15.706
.613	15.866	.753	16.333	.670	15.982	.720	16.012	.597	15.211	.945	16.481	.754	16.045	.818	15.724	.849	16.154
.707	16.181	.849	16.650	.756	16.333	.805	16.333	.680	15.639	1.034	16.840	.846	16.484	.921	16.187	.961	16.573
.792	16.446	.953	16.964	.844	16.644	.884	16.613	.765	16.039	1.134	17.195	.940	16.894	1.002	16.558	1.075	16.950
.875	16.684	1.067	17.286	.924	16.905	.980	16.933	.862	16.443	1.242	17.557	1.033	17.273	1.104	16.978	1.171	17.369
.957	16.942	1.178	17.611	1.009	17.168	1.094	17.278	.967	16.818	1.358	17.921	1.141	17.659	1.198	17.355	1.267	17.692
1.052	17.229	1.305	17.948	1.117	17.497	1.210	17.597	1.083	17.179	1.488	18.266	1.236	17.948	1.312	17.724	1.387	18.085
1.162	17.527	1.422	18.229	1.226	17.785	1.320	17.895	1.194	17.527	1.611	18.583	1.361	18.284	1.409	18.006	1.491	18.372
1.265	17.796	1.546	18.509	1.342	18.109	1.445	18.235	1.303	17.852	1.755	18.875	1.496	18.593	1.508	18.253	1.629	18.706
1.439	18.180	1.671	18.774	1.487	18.445	1.560	18.532	1.400	18.119	1.853	19.146	1.611	18.858	1.642	18.565	1.761	18.988
1.574	18.470	1.805	19.043	1.638	18.769	1.669	18.787	1.522	18.427	1.984	19.410	1.759	19.125	1.775	18.878	1.893	19.240
1.705	18.744	1.921	19.274	1.772	19.026	1.780	19.024	1.647	18.716	2.124	19.575	1.870	19.314	1.920	19.113	2.017	19.412
1.834	18.986	2.067	19.490	1.953	19.319	1.901	19.252	1.761	18.961	2.260	19.697	2.036	19.544	2.056	19.336	2.147	19.580
1.971	19.203	2.171	19.624	2.121	19.537	2.041	19.463	1.890	19.230	2.428	19.834	2.189	19.723	2.172	19.488	2.280	19.718
2.118	19.414	2.310	19.771	2.330	19.769	2.196	19.670	2.008	19.442	2.575	19.915	2.379	19.906	2.307	19.648	2.458	19.867
2.268	19.605	2.495	19.925	2.514	19.958	2.343	19.836	2.143	19.675	2.759	20.025	2.587	20.051	2.455	19.788	2.657	20.001
2.462	19.839	2.661	20.008	2.696	20.027	2.473	19.949	2.268	19.800	2.923	20.082	2.783	20.122	2.592	19.889	2.798	20.058
2.615	19.944	2.823	20.067	2.891	20.079	2.647	20.098	2.455	19.927	3.131	20.112	2.971	20.160	2.743	19.989	2.957	20.094
2.854	20.063	3.027	20.105	3.025	20.091	2.821	20.146	2.623	19.999	3.131	20.112	3.130	20.164	2.868	20.056	3.131	20.105
3.025	20.105	3.131	20.112	3.130	20.094	3.020	20.179	2.819	20.075	3.131	20.112	3.130	20.164	3.030	20.101	3.131	20.105
3.130	20.108	3.131	20.112	3.130	20.094	3.130	20.186	2.992	20.108	3.131	20.112	3.130	20.164	3.132	20.108	3.131	20.105
3.130	20.108	3.131	20.112	3.130	20.094	3.130	20.186	3.150	20.105	3.131	20.112	3.130	20.164	3.132	20.108	3.131	20.105

Table 5.3a Mean velocity data, U_{∞} = 20 ft/sec -- Continued

X= 3.0 FT Y= 0.0 IN		X= 3.0 FT Y= 1.0 IN		X= 3.0 FT Y= 2.0 IN		X= 3.0 FT Y= 2.5 IN		X= 3.0 FT Y= 3.0 IN		X= 3.0 FT Y= 3.5 IN		X= 3.0 FT Y= 4.0 IN		X= 3.0 FT Y= 5.0 IN		X= 3.0 FT Y= 6.0 IN	
Z (IN)	U (FPS)	Z (IN)	U (FPS)	Z (IN)	U (FPS)	Z (IN)	U (FPS)	Z (IN)	U (FPS)	Z (IN)	U (FPS)	Z (IN)	U (FPS)	Z (IN)	U (FPS)	Z (IN)	U (FPS)
.055	8.351	.038	9.227	.040	8.929	.040	8.531	.042	6.060	.134	8.282	.157	8.598	.133	6.772	.133	9.014
.060	8.740	.068	9.865	.063	9.497	.056	9.087	.065	6.945	.177	8.971	.169	8.982	.156	7.511	.181	9.238
.069	9.345	.086	10.773	.073	10.185	.069	9.651	.083	7.894	.212	9.695	.195	9.651	.180	8.271	.224	9.552
.083	10.066	.111	11.660	.088	10.918	.089	10.281	.099	8.735	.244	10.341	.226	10.442	.210	9.061	.269	10.281
.097	10.733	.140	12.430	.110	11.700	.115	11.022	.128	9.601	.291	11.061	.271	11.210	.244	9.783	.307	10.822
.120	11.466	.178	13.086	.141	12.468	.146	11.745	.167	10.564	.349	11.785	.315	11.870	.287	10.537	.353	11.516
.143	12.147	.230	13.582	.187	13.079	.180	12.318	.203	11.366	.406	12.391	.366	12.445	.336	11.286	.398	12.084
.168	12.810	.303	14.138	.248	13.634	.215	12.799	.250	12.057	.479	13.050	.432	13.068	.396	11.910	.451	12.642
.203	13.306	.378	14.578	.329	14.222	.271	13.256	.306	12.646	.566	13.725	.504	13.564	.462	12.472	.519	13.277
.248	13.763	.469	15.031	.419	14.754	.343	13.714	.372	13.251	.660	14.371	.572	13.999	.538	13.119	.585	13.811
.296	14.135	.574	15.462	.523	15.245	.422	14.178	.447	13.787	.750	14.901	.639	14.395	.619	13.714	.670	14.381
.355	14.533	.701	15.899	.628	15.658	.517	14.660	.527	14.312	.841	15.379	.711	14.799	.701	14.265	.770	14.936
.432	14.965	.850	16.344	.739	16.048	.613	15.075	.629	14.914	.960	15.938	.805	15.270	.789	14.799	.873	15.459
.504	15.301	1.010	16.818	.850	16.423	.759	15.600	.736	15.459	1.063	16.385	.888	15.649	.873	15.233	.981	15.935
.582	15.627	1.149	17.162	.974	16.770	.902	16.089	.874	16.027	1.194	16.911	.977	16.012	.973	15.724	1.104	16.443
.680	15.971	1.333	17.567	1.102	17.104	1.052	16.581	1.016	16.512	1.351	17.344	1.103	16.489	1.090	16.207	1.243	16.922
.830	16.423	1.490	17.857	1.231	17.426	1.216	17.054	1.179	16.909	1.498	17.692	1.220	16.885	1.184	16.564	1.394	17.385
.974	16.778	1.651	18.148	1.398	17.751	1.400	17.558	1.334	17.591	1.647	18.001	1.357	17.328	1.317	17.012	1.542	17.737
1.108	17.090	1.808	18.416	1.558	18.035	1.587	17.995	1.490	17.817	1.817	18.305	1.517	17.834	1.443	17.393	1.726	18.130
1.274	17.429	1.993	18.673	1.743	18.367	1.773	18.406	1.671	18.206	2.020	18.609	1.675	18.227	1.578	17.761	1.893	18.470
1.458	17.729	2.162	18.906	1.938	18.665	1.986	18.734	1.869	18.583	2.247	18.953	1.852	18.573	1.716	18.096	2.078	18.779
1.598	18.004	2.348	19.125	2.121	18.913	2.198	19.006	2.059	18.055	2.428	19.188	2.024	18.858	1.894	18.465	2.244	19.045
1.741	18.237	2.532	19.311	2.320	19.155	2.461	19.267	2.259	19.106	2.626	19.393	2.212	19.118	2.069	18.774	2.422	19.319
1.930	18.517	2.705	19.478	2.558	19.400	2.686	19.463	2.463	19.341	2.868	19.639	2.379	19.306	2.283	19.071	2.625	19.527
2.109	18.759	2.873	19.619	2.781	19.580	2.931	19.624	2.653	19.532	3.100	19.767	2.572	19.488	2.492	19.309	2.832	19.675
2.285	18.971	3.074	19.745	3.040	19.735	3.205	19.733	2.869	19.718	3.296	19.867	2.766	19.610	2.723	19.534	3.003	19.771
2.525	19.250	3.289	19.841	3.224	19.852	3.402	19.827	3.074	19.810	3.493	19.939	2.972	19.728	2.949	19.689	3.177	19.841
2.715	19.432	3.469	19.915	3.469	19.939	3.655	19.915	3.375	19.901	3.697	19.989	3.221	19.855	3.206	19.827	3.386	19.930
2.936	19.622	3.673	19.980	3.687	20.011	3.906	19.982	3.659	19.944	3.947	20.030	3.490	19.946	3.418	19.901	3.612	19.994
3.168	19.779	3.909	20.018	3.901	20.065	4.184	20.020	3.910	19.965	4.200	20.041	3.709	20.003	3.694	19.975	3.825	20.034
3.409	19.889	4.187	20.025	4.186	20.077	4.184	20.020	4.190	19.970	4.200	20.041	3.922	20.041	3.950	20.025	3.988	20.041
3.629	19.958	4.187	20.025	4.186	20.077	4.184	20.020	4.190	19.970	4.200	20.041	4.200	20.070	4.199	20.032	4.204	20.049
3.871	20.008	4.187	20.025	4.186	20.077	4.184	20.020	4.190	19.970	4.200	20.041	4.200	20.070	4.199	20.032	4.204	20.049
4.185	20.025	4.187	20.025	4.186	20.077	4.184	20.020	4.190	19.970	4.200	20.041	4.200	20.070	4.199	20.032	4.204	20.049

X= 4.0 FT Y= 0.0 IN		X= 4.0 FT Y= 1.0 IN		X= 4.0 FT Y= 2.0 IN		X= 4.0 FT Y= 2.5 IN		X= 4.0 FT Y= 3.0 IN		X= 4.0 FT Y= 3.5 IN		X= 4.0 FT Y= 4.0 IN		X= 4.0 FT Y= 5.0 IN		X= 4.0 FT Y= 6.0 IN	
Z (IN)	U (FPS)	Z (IN)	U (FPS)	Z (IN)	U (FPS)	Z (IN)	U (FPS)	Z (IN)	U (FPS)	Z (IN)	U (FPS)	Z (IN)	U (FPS)	Z (IN)	U (FPS)	Z (IN)	U (FPS)
.029	8.628	.031	8.902	.026	8.731	.042	8.418	.036	2.492	.124	8.758	.131	7.175	.129	8.552	.134	7.953
.044	9.023	.046	9.619	.042	9.391	.057	9.059	.051	4.058	.154	9.325	.147	8.076	.166	9.152	.167	8.541
.053	9.495	.061	10.372	.053	10.068	.070	9.750	.065	5.419	.189	10.063	.164	8.854	.207	9.731	.195	9.178
.064	10.077	.079	11.023	.069	10.777	.086	10.340	.093	6.826	.230	10.738	.189	9.692	.256	10.394	.233	9.908
.078	10.667	.098	11.577	.086	11.434	.105	10.959	.110	8.012	.281	11.318	.216	10.503	.314	11.091	.279	10.601
.094	11.280	.126	12.310	.107	12.140	.132	11.686	.130	8.991	.349	11.973	.265	11.171	.380	11.798	.335	11.297
.107	11.878	.157	12.969	.139	12.758	.173	12.175	.150	9.908	.409	12.563	.319	11.782	.462	12.466	.383	11.826
.131	12.533	.195	13.415	.186	13.245	.227	12.716	.174	10.851	.486	13.238	.376	12.333	.544	13.077	.442	12.409
.157	13.095	.256	13.880	.259	13.788	.298	13.263	.208	11.475	.558	13.778	.445	12.892	.634	13.685	.511	12.954
.192	13.526	.346	14.389	.348	14.317	.373	13.775	.268	12.206	.649	14.380	.531	13.499	.757	14.284	.592	13.547
.233	13.904	.441	14.847	.467	14.847	.463	14.265	.333	12.856	.762	15.004	.617	14.005	.851	14.863	.687	14.135
.303	14.350	.529	15.201	.579	15.272	.556	14.729	.415	13.495	.897	15.646	.707	14.533	.961	15.364	.796	14.716
.368	14.761	.633	15.568	.698	15.664	.670	15.204	.524	14.165	1.065	16.254	.821	15.095	1.084	15.888	.893	15.185
.459	15.185	.752	15.959	.848	16.132	.785	15.640	.616	14.646	1.219	16.759	.928	15.571	1.205	16.323	.992	15.601
.553	15.543	.863	16.274	1.018	16.595	.898	16.012	.710	15.111	1.383	17.191	1.041	16.018	1.342	16.814	1.116	16.064
.659	15.882	1.019	16.722	1.173	16.987	1.029	16.412	.845	15.661	1.529	17.540	1.190	16.544	1.497	17.306	1.241	16.484
.782	16.274	1.180	17.111	1.339	17.368	1.165	16.775	1.010	16.219	1.735	17.944	1.335	16.957	1.674	17.738	1.383	16.912
.892	16.564	1.370	17.514	1.520	17.754	1.327	17.166	1.171	16.711	1.944	18.281	1.488	17.316	1.839	18.082	1.561	17.379
1.018	16.856	1.554	17.844	1.707	18.095	1.477	17.476	1.327	17.095	2.138	18.552	1.635	17.666	2.012	18.392	1.767	17.838
1.168	17.177	1.736	18.152	1.880	18.371	1.655	17.833	1.525	17.565	2.313	18.774	1.801	18.009	2.206	18.716	1.956	18.189
1.328	17.460	1.934	18.425	2.092	18.646	1.843	18.202	1.709	17.959	2.493	18.979	1.977	18.328	2.447	19.016	2.175	18.542
1.483	17.725	2.110	19.661	2.305	18.902	2.079	18.552	1.910	18.297	2.685	19.188	2.129	18.603	2.668	19.242	2.405	18.849
1.667	18.020	2.336	18.917	2.537	19.139	2.301	18.812	2.114	18.595	2.926	19.393	2.312	18.894	2.882	19.425	2.601	19.105
1.958	18.433	2.557	19.134	2.760	19.337	2.532	19.058	2.370	18.882	3.123	19.526	2.541	19.156	3.100	19.591	2.834	19.359
2.160	18.691	2.812	19.332	3.007	19.526	2.760	19.269	2.567	19.095	3.354	19.665	2.713	19.327	3.345	19.763	3.049	19.565
2.415	18.976	3.020	19.497	3.304	19.711	3.019	19.471	2.765	19.279	3.649	19.808	2.952	19.514	3.602	19.903	3.241	19.701
2.689	19.245	3.240	19.663	3.549	19.835	3.305	19.661	2.999	19.451	3.925	19.922	3.168	19.689	3.924	20.014	3.527	19.846
2.938	19.446	3.466	19.794	3.846	19.934	3.569	19.818	3.222	19.598	4.171	20.000	3.423	19.816	4.228	20.075	3.828	19.936
3.165	19.630	3.724	19.922	4.132	20.019	3.835	19.951	3.473	19.727	4.393	20.052	3.689	19.922	4.565	20.096	4.077	19.995
3.411	19.773	3.939	19.986	4.454	20.085	4.204	20.021	3.701	19.855	4.632	20.077	3.978	20.016	4.825	20.098	4.362	20.038
3.662	19.908	4.193	20.047	4.650	20.098	4.545	20.077	4.038	19.960	4.828	20.094	4.357	20.042	4.825	20.098	4.607	20.052
3.954	20.005	4.469	20.101	4.816	20.108	4.815	20.087	4.311	20.019	4.828	20.094	4.627	20.056	4.825	20.098	4.829	20.075
4.280	20.096	4.820	20.117	4.816	20.108	4.815	20.087	4.600	20.068	4.828	20.094	4.825	20.070	4.825	20.098	4.829	20.075
4.565	20.141	4.820	20.117	4.816	20.108	4.815	20.087	4.820	20.085	4.828	20.094	4.825	20.070	4.825	20.098	4.829	20.075
4.825	20.157	4.820	20.117	4.816	20.108	4.815	20.087	4.820	20.085	4.828	20.094	4.825	20.070	4.825	20.098	4.829	20.075

Table 5.3a Mean velocity data, U_∞ = 20 ft/sec -- Continued

X= 6.0 FT Y= 0.0 IN		X= 6.0 FT Y= 1.0 IN		X= 6.0 FT Y= 2.0 IN		X= 6.0 FT Y= 2.5 IN		X= 6.0 FT Y= 3.0 IN		X= 6.0 FT Y= 3.5 IN		X= 6.0 FT Y= 4.0 IN		X= 6.0 FT Y= 5.0 IN		X= 6.0 FT Y= 6.0 IN	
Z (IN)	U (FPS)	Z (IN)	U (FPS)	Z (IN)	U (FPS)	Z (IN)	U (FPS)	Z (IN)	U (FPS)	Z (IN)	U (FPS)	Z (IN)	U (FPS)	Z (IN)	U (FPS)	Z (IN)	U (FPS)
.028	8.593	.028	8.526	.030	8.456	.035	8.121	.033	5.380	.125	7.845	.130	8.108	.125	8.373	.120	7.918
.037	9.164	.036	9.159	.043	9.112	.053	8.695	.047	5.949	.146	8.304	.150	8.664	.154	8.708	.138	8.267
.045	9.692	.046	9.712	.055	9.848	.070	9.156	.060	6.680	.165	8.744	.187	9.118	.181	9.082	.157	8.617
.058	10.136	.060	10.216	.076	10.497	.089	9.654	.079	7.365	.197	9.314	.213	9.547	.199	9.492	.176	8.943
.073	10.534	.082	10.754	.118	11.151	.120	10.188	.099	7.931	.232	9.827	.250	10.070	.223	9.909	.195	9.283
.100	11.022	.109	11.207	.152	11.589	.152	10.700	.125	8.504	.269	10.443	.275	10.482	.253	10.355	.219	9.640
.130	11.502	.143	11.687	.192	11.998	.195	11.176	.160	9.116	.309	10.894	.314	10.992	.282	10.720	.255	10.124
.158	11.886	.196	12.255	.244	12.356	.230	11.563	.199	9.688	.348	11.390	.344	11.425	.324	11.210	.294	10.613
.198	12.286	.238	12.544	.313	12.815	.295	12.028	.250	10.248	.405	12.035	.390	11.682	.369	11.733	.332	11.051
.246	12.714	.292	12.960	.379	13.219	.343	12.480	.296	10.885	.464	12.612	.444	12.384	.419	12.217	.386	11.610
.303	13.194	.366	13.534	.451	13.580	.401	12.916	.339	11.504	.534	13.154	.497	12.848	.481	12.714	.448	12.171
.370	13.636	.442	14.058	.544	14.071	.456	13.327	.373	12.023	.608	13.645	.561	13.295	.552	13.155	.505	12.621
.441	14.061	.524	14.549	.619	14.454	.532	13.770	.432	12.559	.684	14.089	.629	13.711	.619	13.526	.579	13.113
.520	14.486	.608	14.894	.723	14.910	.617	14.193	.485	13.025	.763	14.529	.705	14.135	.686	13.914	.653	13.536
.602	14.887	.710	15.205	.819	15.302	.698	14.585	.555	13.389	.858	14.908	.800	14.624	.768	14.318	.744	14.030
.680	15.208	.825	15.565	.931	15.779	.783	14.978	.599	13.800	.919	15.281	.891	15.038	.852	14.702	.854	14.500
.791	15.633	.924	15.852	1.043	16.136	.902	15.433	.684	14.279	1.028	15.694	.960	15.329	.945	15.091	.971	14.978
.917	16.041	1.038	16.174	1.160	16.511	1.034	15.880	.778	14.700	1.143	16.072	1.053	15.685	1.040	15.471	1.101	15.450
1.059	16.467	1.186	16.572	1.285	16.832	1.174	16.283	.881	15.142	1.254	16.436	1.147	16.009	1.142	15.845	1.247	15.914
1.193	16.815	1.355	16.943	1.420	17.156	1.304	16.648	.986	15.522	1.383	16.804	1.276	16.394	1.242	16.178	1.412	16.428
1.330	17.125	1.515	17.333	1.578	17.473	1.446	17.008	1.093	15.898	1.506	17.138	1.402	16.738	1.377	16.578	1.612	16.998
1.501	17.484	1.679	17.678	1.735	17.759	1.568	17.275	1.227	16.360	1.647	17.491	1.544	17.079	1.521	16.981	1.813	17.471
1.666	17.791	1.838	17.986	1.902	18.044	1.734	17.606	1.354	16.755	1.779	17.756	1.679	17.399	1.667	17.325	2.001	17.867
1.846	18.081	1.999	18.237	2.061	18.276	1.893	17.905	1.484	17.068	1.936	18.035	1.834	17.710	1.819	17.659	2.190	18.200
2.018	18.328	2.213	18.564	2.278	18.546	2.048	18.159	1.623	17.372	2.076	18.265	1.990	17.974	2.000	18.019	2.400	18.520
2.196	18.600	2.426	18.848	2.489	18.802	2.270	18.510	1.752	17.620	2.226	18.488	2.214	18.331	2.181	18.310	2.611	18.794
2.394	18.848	2.640	19.080	2.707	19.040	2.478	18.802	1.916	17.915	2.385	18.726	2.424	18.614	2.356	18.571	2.821	19.030
2.667	19.160	2.909	19.317	2.968	19.304	2.692	19.069	2.074	18.184	2.545	18.930	2.638	18.878	2.517	18.767	3.053	19.275
2.931	19.398	3.172	19.509	3.240	19.521	2.905	19.311	2.255	18.418	2.750	19.137	2.849	19.093	2.707	19.006	3.326	19.488
3.195	19.595	3.497	19.709	3.563	19.736	3.170	19.559	2.448	18.687	2.952	19.312	3.121	19.309	2.889	19.222	3.592	19.649
3.517	19.791	3.812	19.866	3.882	19.924	3.441	19.769	2.664	18.917	3.172	19.486	3.387	19.490	3.076	19.378	3.935	19.834
3.836	19.928	4.134	19.962	4.198	20.065	3.699	19.900	2.931	19.187	3.457	19.668	3.659	19.651	3.271	19.520	4.274	19.966
4.319	20.089	4.508	20.067	4.522	20.184	4.020	20.035	3.201	19.454	3.721	19.811	3.969	19.822	3.523	19.663	4.624	20.055
4.800	20.193	4.881	20.134	4.894	20.255	4.341	20.141	3.520	19.687	4.043	19.961	4.298	19.942	3.798	19.812	4.997	20.132
5.337	20.271	5.314	20.196	5.324	20.316	4.711	20.241	3.840	19.896	4.313	20.079	4.617	20.041	4.120	19.942	5.295	20.179
5.607	20.297	5.582	20.226	5.592	20.351	5.080	20.312	4.161	20.060	4.659	20.179	4.994	20.139	4.441	20.044	5.530	20.202
5.904	20.297	5.841	20.226	5.592	20.351	5.349	20.355	4.484	20.174	5.004	20.253	5.527	20.235	4.818	20.124	5.794	20.202
5.904	20.297	5.841	20.226	5.592	20.351	5.614	20.358	4.854	20.255	5.327	20.305	5.795	20.235	5.141	20.186	5.794	20.202
5.904	20.297	5.841	20.226	5.592	20.351	5.614	20.358	5.281	20.338	5.596	20.334	5.795	20.235	5.510	20.235	5.794	20.202
5.904	20.297	5.841	20.226	5.592	20.351	5.614	20.358	5.708	20.385	5.868	20.334	5.795	20.235	5.773	20.235	5.794	20.202
5.904	20.297	5.841	20.226	5.592	20.351	5.614	20.358	6.144	20.402	5.868	20.334	5.795	20.235	5.773	20.235	5.794	20.202

X= 8.0 FT Y= 0.0 IN		X= 8.0 FT Y= 1.0 IN		X= 8.0 FT Y= 2.0 IN		X= 8.0 FT Y= 2.5 IN		X= 8.0 FT Y= 3.0 IN		X= 8.0 FT Y= 3.5 IN		X= 8.0 FT Y= 4.0 IN		X= 8.0 FT Y= 5.0 IN		X= 8.0 FT Y= 6.0 IN	
Z (IN)	U (FPS)	Z (IN)	U (FPS)	Z (IN)	U (FPS)	Z (IN)	U (FPS)	Z (IN)	U (FPS)	Z (IN)	U (FPS)	Z (IN)	U (FPS)	Z (IN)	U (FPS)	Z (IN)	U (FPS)
.029	8.921	.022	7.998	.025	8.491	.032	9.026	.029	5.722	.128	8.491	.128	7.357	.128	7.727	.120	6.554
.032	9.166	.024	8.728	.030	9.120	.049	9.516	.040	6.633	.150	8.915	.148	7.653	.143	8.115	.133	6.974
.039	9.426	.037	9.376	.040	9.644	.065	10.006	.053	7.415	.164	9.310	.164	7.974	.154	8.396	.146	7.415
.044	9.742	.048	9.891	.054	10.104	.085	10.481	.069	8.027	.192	9.776	.185	8.362	.174	8.830	.164	7.950
.056	10.058	.068	10.441	.072	10.517	.100	10.858	.084	8.586	.229	10.313	.211	8.787	.197	9.269	.181	8.357
.069	10.445	.087	11.005	.108	11.010	.138	11.319	.105	9.213	.263	10.762	.244	9.279	.233	9.791	.209	8.921
.092	10.906	.122	11.534	.150	11.493	.187	11.766	.128	9.737	.308	11.255	.277	9.786	.271	10.253	.240	9.386
.117	11.269	.186	12.142	.190	11.810	.245	12.227	.165	10.336	.354	11.657	.321	10.336	.314	10.744	.273	9.834
.150	11.665	.260	12.608	.262	12.281	.309	12.627	.205	10.793	.410	12.111	.367	10.854	.361	11.210	.316	10.350
.196	12.103	.361	13.101	.331	12.694	.390	13.094	.260	11.327	.476	12.578	.412	11.307	.417	11.624	.361	10.771
.244	12.461	.474	13.608	.414	13.145	.473	13.524	.328	11.906	.554	13.069	.466	11.810	.479	12.056	.424	11.361
.300	12.806	.590	14.076	.501	13.563	.573	13.978	.418	12.522	.625	13.451	.517	12.250	.539	12.488	.501	11.937
.365	13.166	.721	14.543	.587	13.945	.674	14.399	.503	13.025	.714	13.860	.583	12.743	.605	12.952	.576	12.442
.443	13.563	.846	14.937	.689	14.349	.781	14.781	.607	13.556	.809	14.290	.653	13.188	.690	13.437	.654	12.861
.540	13.992	.982	15.331	.821	14.807	.907	15.198	.719	14.056	.895	14.624	.736	13.615	.777	13.866	.742	13.345
.675	14.484	1.110	15.658	.955	15.255	1.036	15.594	.822	14.510	.999	14.997	.822	13.982	.882	14.320	.825	13.760
.800	14.918	1.282	16.114	1.069	15.582	1.206	16.037	.933	14.902	1.125	15.420	.904	14.339	1.002	14.772	.931	14.213
.944	15.362	1.448	16.517	1.219	16.015	1.356	16.396	1.058	15.310	1.254	15.814	1.023	14.800	1.128	15.182	1.035	14.620
1.085	15.751	1.620	16.885	1.367	16.416	1.474	16.642	1.189	15.670	1.380	16.178	1.139	15.179	1.278	15.622	1.165	15.082
1.262	16.196	1.795	17.204	1.538	16.798	1.642	16.958	1.361	16.131	1.506	16.508	1.256	15.534	1.432	16.016	1.294	15.485
1.423	16.562	1.962	17.488	1.712	17.121	1.800	17.289	1.529	16.539	1.678	16.916	1.390	15.907	1.579	16.564	1.427	15.868
1.585	16.907	2.174	17.791	1.885	17.417	1.974	17.606	1.698	16.904	1.849	17.254	1.540	16.265	1.727	16.679	1.566	16.225
1.765	17.262	2.387	18.078	2.053	17.655	2.141	17.892	1.867	17.245	2.019	17.569	1.692	16.614	1.899	17.010	1.717	16.594
1.973	17.596	2.597	18.333	2.267	17.939	2.354	18.257	2.058	17.572	2.232	17.894	1.857	16.946	2.072	17.327	1.886	16.969
2.187	17.929	2.814	18.566	2.475	18.175	2.568	18.528	2.251	17.897	2.400	18.107	2.025	17.275	2.240	17.609	2.054	17.322
2.434	18.281	3.067	18.799	2.692	18.392	2.814	18.759	2.466	18.170	2.615	18.351	2.198	17.572	2.451	17.923	2.226	17.633
2.688	18.589	3.323	19.022	2.985	18.693	3.059	18.997	2.676	18.421	2.827	18.589	2.410	17.929	2.666	18.235	2.394	17.894
2.951	18.832	3.576	19.208	3.241	18.915	3.316	19.205	2.890	18.622	3.078	18.827	2.622	18.227	2.874	18.490	2.609	18.188
3.250	19.034	3.834	19.377	3.540	19.149	3.586	19.370	3.143	18.822	3.335	19.047	2.880	18.520	3.127	18.794	2.826	18.446
3.591	19.259	4.086	19.535	3.859	19.350	3.882	19.523	3.400	19.000	3.589	19.237	3.134	18.767	3.382	19.027	3.070	18.701
3.929	19.433	4.384	19.665	4.176	19.545	4.224	19.675	3.654	19.181	3.882	19.435	3.308	18.977	3.675	19.240	3.332	18.950
4.312	19.600	4.639	19.764	4.515	19.697	4.565	19.797	3.953	19.365	4.182	19.615	3.680	19.195	3.975	19.416	3.579	19.178
4.695	19.735	4.936	19.866	4.943	19.852	4.859	19.890	4.249	19.525	4.517	19.769	3.982	19.382	4.271	19.554	3.880	19.396
5.079	19.855	5.277	19.945	5.370	19.961	5.203	19.997	4.588	19.685	4.855	19.885	4.315	19.540	4.612	19.687	4.176	19.591
5.458	19.933	5.613	20.009	5.789	20.047	5.559	20.075	4.925	19.807	5.199	19.997	4.657	19.680	4.947	19.788	4.515	19.725
5.839	19.990	5.875	20.037	6.216	20.096	5.881	20.145	5.550	19.952	5.537	20.075	5.038	19.821	5.372	19.914	4.939	19.840
6.222	20.021	6.248	20.070	6.643	20.120	6.263	20.178	5.776	20.054	5.873	20.141	5.418	19.931	5.800	19.997	5.361	19.928
6.648	20.032	6.633	20.094	6.853	20.120	6.643	20.195	6.198	20.089	6.255	20.176	5.800	20.009	6.220	20.032	5.788	20.002
6.857	20.032	6.847	20.094	6.853	20.120	6.852	20.195	6.622	20.138	6.637	20.197	6.221	20.049	6.640	20.054	6.211	20.049
6.857	20.032	6.847	20.094	6.853	20.120	6.852	20.195	6.834	20.138	6.841	20.197	6.643	20.075	6.876	20.054	6.631	20.061

Table 5.3a Mean velocity data, U_∞ = 20 ft/sec -- Continued

X=10.0 FT Y= 0.0 IN		X=10.0 FT Y= 1.0 IN		X=10.0 FT Y= 2.0 IN		X=10.0 FT Y= 2.5 IN		X=10.0 FT Y= 3.0 IN		X=10.0 FT Y= 3.5 IN		X=10.0 FT Y= 4.0 IN		X=10.0 FT Y= 5.0 IN		X=10.0 FT Y= 6.0 IN	
Z (IN)	U (FPS)	Z (IN)	U (FPS)	Z (IN)	U (FPS)	Z (IN)	U (FPS)	Z (IN)	U (FPS)	Z (IN)	U (FPS)	Z (IN)	U (FPS)	Z (IN)	U (FPS)	Z (IN)	U (FPS)
.050	7.678	.030	6.899	.027	7.148	.042	7.980	.033	5.503	.127	8.362	.123	7.666	.130	8.385	.124	6.349
.040	8.144	.042	7.597	.039	7.678	.055	8.580	.040	6.312	.142	8.765	.146	8.173	.145	8.717	.147	6.954
.053	8.630	.058	8.115	.050	8.340	.077	9.335	.055	7.331	.166	9.295	.168	8.662	.165	9.120	.169	7.554
.077	9.192	.077	8.765	.062	8.958	.099	9.834	.080	8.068	.196	9.766	.196	9.094	.196	9.536	.193	8.039
.102	9.654	.099	9.381	.086	9.649	.122	10.409	.105	8.673	.224	10.151	.222	9.456	.233	9.968	.221	8.519
.135	10.179	.122	9.911	.118	10.281	.159	10.863	.139	9.325	.258	10.585	.277	10.142	.276	10.427	.255	9.073
.177	10.722	.151	10.372	.165	10.984	.207	11.348	.189	10.010	.307	11.074	.344	10.766	.325	10.880	.286	9.486
.222	11.176	.188	10.889	.227	11.530	.265	11.822	.247	10.678	.363	11.547	.428	11.469	.381	11.352	.342	10.076
.285	11.738	.232	11.336	.314	12.126	.339	12.293	.324	11.319	.429	12.056	.521	12.091	.447	11.798	.415	10.823
.347	12.200	.283	11.842	.401	12.608	.436	12.835	.398	11.838	.493	12.472	.626	12.672	.532	12.324	.480	11.361
.428	12.679	.352	12.254	.506	13.069	.541	13.334	.495	12.438	.576	12.960	.731	13.213	.628	12.876	.553	11.894
.515	13.145	.432	12.698	.606	13.454	.633	13.726	.591	12.945	.656	13.384	.857	13.774	.720	13.309	.651	12.518
.602	13.570	.519	13.130	.740	13.948	.755	14.207	.694	13.444	.745	13.784	.985	14.273	.828	13.760	.764	13.105
.727	14.123	.621	13.577	.864	14.412	.835	14.627	.822	13.999	.852	14.217	1.119	14.784	.955	14.273	.869	13.650
.857	14.581	.747	14.043	.997	14.826	.989	15.048	.951	14.510	.958	14.598	1.285	15.359	1.079	14.756	.998	14.200
.980	14.981	.851	14.395	1.159	15.303	1.118	15.445	1.076	14.972	1.084	15.016	1.454	15.877	1.252	15.359	1.103	14.607
1.106	15.374	1.001	14.861	1.328	15.790	1.288	15.892	1.242	15.524	1.208	15.417	1.629	16.367	1.422	15.668	1.233	15.048
1.277	15.805	1.148	15.285	1.500	16.231	1.456	16.300	1.416	15.993	1.359	15.787	1.800	16.767	1.599	16.315	1.360	15.482
1.444	16.222	1.313	15.709	1.716	16.722	1.625	16.719	1.587	16.379	1.507	16.219	2.012	17.210	1.761	16.695	1.490	15.859
1.611	16.617	1.483	16.108	1.927	17.174	1.836	17.158	1.750	16.719	1.678	16.600	2.229	17.593	1.973	17.174	1.660	16.286
1.784	16.960	1.655	16.479	2.140	17.641	2.048	17.509	1.967	17.113	1.893	17.013	2.436	17.915	2.184	17.580	1.829	16.673
1.996	17.322	1.824	16.812	2.389	18.073	2.257	17.895	2.178	17.463	2.103	17.357	2.690	18.263	2.394	17.913	1.997	17.033
2.207	17.671	2.037	17.210	2.644	18.446	2.514	18.227	2.389	17.796	2.319	17.754	2.942	18.579	2.604	18.227	2.211	17.436
2.418	17.992	2.249	17.588	2.856	18.700	2.767	18.536	2.604	18.112	2.575	18.149	3.189	18.860	2.860	18.564	2.421	17.778
2.629	18.302	2.460	17.892	3.107	18.985	3.023	18.787	2.851	18.428	2.852	18.510	3.490	19.134	3.108	18.865	2.654	18.102
2.883	18.622	2.715	18.214	3.404	19.220	3.322	19.074	3.107	18.754	3.085	18.827	3.745	19.352	3.366	19.104	2.847	18.341
3.136	18.875	2.966	18.505	3.745	19.426	3.615	19.306	3.406	19.049	3.336	19.106	4.058	19.545	3.663	19.352	3.086	18.597
3.391	19.094	3.220	18.784	4.082	19.598	3.912	19.525	3.658	19.250	3.634	19.406	4.381	19.723	4.006	19.622	3.360	18.870
3.689	19.335	3.473	19.007	4.419	19.737	4.246	19.725	3.955	19.472	3.929	19.610	4.719	19.871	4.300	19.845	3.657	19.126
3.980	19.528	3.763	19.220	4.762	19.850	4.589	19.909	4.251	19.665	4.228	19.771	5.064	19.978	4.640	20.006	3.950	19.352
4.276	19.697	4.065	19.413	5.136	19.985	4.925	20.037	4.591	19.847	4.521	19.914	5.444	20.117	4.983	20.120	4.248	19.612
4.531	19.831	4.358	19.576	5.517	20.115	5.264	20.115	4.924	19.968	4.860	20.023	5.828	20.190	5.360	20.206	4.589	19.858
4.865	19.971	4.654	19.725	5.899	20.215	5.645	20.253	5.349	20.047	5.202	20.129	6.205	20.277	5.783	20.296	4.927	20.004
5.205	20.089	4.994	19.866	6.279	20.298	6.023	20.323	5.773	20.159	5.539	20.195	6.625	20.314	6.207	20.356	5.266	20.103
5.543	20.178	5.330	19.992	6.658	20.342	6.401	20.381	6.195	20.281	5.923	20.288	7.052	20.344	6.634	20.407	5.604	20.162
5.877	20.253	5.708	20.106	7.038	20.365	6.822	20.409	6.614	20.342	6.305	20.365	7.052	20.344	7.057	20.423	5.982	20.206
6.213	20.307	6.150	20.174	7.463	20.381	7.246	20.430	7.037	20.388	6.685	20.423	7.052	20.344	7.482	20.423	6.366	20.263
6.593	20.328	6.549	20.244	7.463	20.381	7.246	20.430	7.462	20.404	7.066	20.453	7.052	20.344	7.482	20.423	6.746	20.288
6.975	20.351	6.968	20.290	7.463	20.381	7.246	20.430	7.462	20.404	7.492	20.455	7.052	20.344	7.482	20.423	7.130	20.300
7.349	20.370	7.391	20.304	7.463	20.381	7.246	20.430	7.462	20.404	7.492	20.455	7.052	20.344	7.482	20.423	7.468	20.300

Table 5.3b Mean velocity data, U_{∞} = 30 ft/sec

X= 1.0 FT Y= 0.0 IN		X= 1.0 FT Y= 1.0 IN		X= 1.0 FT Y= 2.0 IN		X= 1.0 FT Y= 2.5 IN		X= 1.0 FT Y= 3.0 IN		X= 1.0 FT Y= 3.5 IN		X= 1.0 FT Y= 4.0 IN		X= 1.0 FT Y= 5.0 IN		X= 1.0 FT Y= 6.0 IN	
Z (IN)	U (FPS)	Z (IN)	U (FPS)	Z (IN)	U (FPS)	Z (IN)	U (FPS)	Z (IN)	U (FPS)	Z (IN)	U (FPS)	Z (IN)	U (FPS)	Z (IN)	U (FPS)	Z (IN)	U (FPS)
.031	16.365	.031	16.429	.032	17.024	.034	16.534	.034	12.525	.128	14.916	.128	15.202	.128	13.713	.128	13.259
.055	17.236	.048	17.075	.044	17.566	.050	17.336	.059	13.431	.163	15.476	.162	15.806	.152	14.427	.159	13.962
.075	18.097	.065	17.981	.060	18.281	.075	18.145	.079	14.213	.198	16.106	.191	16.365	.184	15.158	.191	14.638
.095	19.005	.084	18.944	.084	19.145	.093	19.045	.099	15.120	.223	16.747	.216	17.030	.208	16.189	.227	15.963
.118	20.015	.103	19.619	.107	19.798	.115	19.731	.123	16.047	.244	17.783	.248	17.906	.232	17.131	.258	17.103
.149	20.738	.127	20.431	.131	20.408	.152	20.515	.156	17.292	.272	18.741	.284	18.721	.261	18.081	.290	18.028
.186	21.387	.155	21.022	.157	20.917	.187	20.999	.184	18.044	.307	19.609	.317	19.398	.290	18.919	.329	18.818
.229	21.904	.194	21.640	.199	21.445	.232	21.596	.214	18.782	.339	20.295	.358	20.091	.331	19.924	.369	19.570
.281	22.435	.234	22.182	.242	21.843	.283	22.121	.253	19.716	.387	21.131	.400	20.738	.370	20.719	.421	20.417
.331	22.824	.275	22.706	.299	22.371	.334	22.630	.297	20.394	.442	21.956	.449	21.436	.430	21.632	.471	21.090
.391	23.288	.315	23.144	.351	22.849	.385	23.078	.355	21.221	.495	22.630	.501	22.113	.490	22.503	.527	21.782
.456	23.828	.365	23.627	.404	23.276	.436	23.501	.402	21.777	.546	23.194	.554	22.769	.554	23.284	.585	22.494
.519	24.325	.427	24.088	.467	23.716	.508	24.020	.469	22.452	.602	23.812	.616	23.505	.613	23.976	.646	23.239
.586	24.831	.492	24.587	.534	24.171	.568	24.497	.527	23.057	.670	24.403	.678	24.203	.695	24.823	.715	23.944
.661	25.406	.552	25.027	.609	24.668	.628	24.962	.590	23.764	.746	25.091	.737	24.819	.778	25.590	.776	24.552
.730	25.935	.623	25.519	.684	25.145	.692	25.402	.662	24.493	.830	25.709	.818	25.590	.858	26.334	.840	25.187
.804	26.435	.693	25.994	.769	25.668	.773	25.961	.732	25.122	.912	26.279	.896	26.308	.942	27.040	.917	25.898
.884	26.973	.776	26.540	.848	26.166	.857	26.508	.803	25.679	1.011	26.930	.980	27.005	1.020	27.590	.999	26.558
.969	27.426	.861	27.139	.940	26.709	.938	27.107	.877	26.221	1.112	27.579	1.062	27.593	1.122	28.139	1.082	27.227
1.047	27.814	.941	27.635	1.019	27.304	1.021	27.652	.957	26.816	1.215	28.180	1.164	28.204	1.221	28.584	1.163	27.773
1.133	28.214	1.024	28.088	1.103	27.873	1.122	28.200	1.040	27.374	1.318	28.744	1.266	28.754	1.326	28.986	1.245	28.241
1.216	28.561	1.126	28.701	1.184	28.346	1.228	28.691	1.121	27.849	1.420	29.298	1.369	29.193	1.427	29.321	1.323	28.644
1.299	28.894	1.230	29.177	1.290	28.821	1.331	29.102	1.244	28.474	1.520	29.662	1.491	29.581	1.529	29.642	1.426	29.105
1.399	29.288	1.331	29.545	1.392	29.233	1.433	29.464	1.329	28.904	1.622	29.915	1.611	29.851	1.634	29.874	1.529	29.454
1.502	29.610	1.435	29.922	1.494	29.591	1.553	29.842	1.429	29.275	1.725	30.113	1.734	30.087	1.732	30.059	1.630	29.715
1.624	29.909	1.538	30.119	1.617	29.896	1.677	30.091	1.553	29.623	1.827	30.255	1.858	30.240	1.838	30.198	1.746	29.928
1.748	30.141	1.640	30.236	1.740	30.125	1.800	30.240	1.677	29.883	1.927	30.353	1.978	30.315	1.957	30.309	1.873	30.113
1.892	30.271	1.744	30.300	1.863	30.318	1.935	30.347	1.799	30.075	2.031	30.426	2.098	30.378	2.079	30.394	1.987	30.217
2.041	30.341	1.852	30.341	1.989	30.356	2.088	30.391	1.946	30.224	2.152	30.473	2.189	30.391	2.180	30.451	2.104	30.300
2.169	30.382	1.971	30.416	2.133	30.382	2.166	30.429	2.130	30.353	2.152	30.473	2.189	30.391	2.180	30.451	2.198	30.344
2.169	30.382	2.097	30.466	2.133	30.382	2.166	30.429	2.130	30.353	2.152	30.473	2.189	30.391	2.180	30.451	2.198	30.344

X= 2.0 FT Y= 0.0 IN		X= 2.0 FT Y= 1.0 IN		X= 2.0 FT Y= 2.0 IN		X= 2.0 FT Y= 2.5 IN		X= 2.0 FT Y= 3.0 IN		X= 2.0 FT Y= 3.5 IN		X= 2.0 FT Y= 4.0 IN		X= 2.0 FT Y= 5.0 IN		X= 2.0 FT Y= 6.0 IN	
Z (IN)	U (FPS)	Z (IN)	U (FPS)	Z (IN)	U (FPS)	Z (IN)	U (FPS)	Z (IN)	U (FPS)	Z (IN)	U (FPS)	Z (IN)	U (FPS)	Z (IN)	U (FPS)	Z (IN)	U (FPS)
.030	14.876	.030	15.830	.030	15.974	.032	15.066	.033	10.855	.125	14.513	.125	13.787	.125	12.088	.125	12.567
.057	15.360	.055	16.403	.055	16.414	.054	15.582	.064	11.450	.155	15.135	.147	14.447	.151	13.137	.154	13.317
.075	15.727	.076	17.006	.075	16.961	.077	16.210	.089	12.112	.183	15.721	.168	15.148	.176	14.087	.179	14.074
.092	16.356	.096	17.884	.089	17.627	.096	16.854	.119	12.940	.208	16.379	.188	15.878	.202	15.028	.202	14.946
.108	17.062	.113	18.751	.108	18.465	.115	17.535	.141	13.952	.245	17.145	.216	16.707	.231	15.836	.233	15.920
.122	18.001	.140	19.769	.124	19.252	.135	18.284	.157	14.914	.282	17.911	.244	17.388	.263	16.593	.271	16.922
.134	19.043	.176	20.558	.140	19.970	.157	19.103	.175	16.139	.325	18.777	.275	18.048	.294	17.278	.308	17.847
.147	19.836	.215	21.150	.169	20.608	.184	19.745	.199	17.190	.371	19.527	.318	18.853	.322	17.826	.342	18.486
.175	20.608	.261	21.758	.202	21.150	.216	20.329	.222	17.905	.416	20.179	.357	19.493	.365	18.537	.386	19.213
.204	21.226	.319	22.238	.244	21.687	.258	20.901	.257	18.802	.464	20.792	.400	20.150	.406	19.178	.427	19.884
.234	21.749	.380	22.720	.303	22.306	.310	21.480	.298	19.663	.520	21.467	.462	21.046	.448	19.774	.472	20.580
.279	22.310	.443	23.180	.347	22.716	.361	21.940	.340	20.376	.583	22.186	.523	21.827	.496	20.446	.525	21.320
.329	22.812	.523	23.716	.400	23.147	.413	22.412	.393	21.119	.645	22.899	.585	22.480	.541	21.001	.579	21.971
.377	23.197	.607	24.283	.461	23.587	.475	22.883	.443	21.740	.708	23.445	.649	23.127	.592	21.600	.631	22.527
.440	23.611	.687	24.798	.522	24.003	.534	23.283	.497	22.310	.771	23.979	.723	23.824	.641	22.221	.687	23.086
.501	23.999	.770	25.239	.585	24.373	.627	23.880	.557	22.891	.842	24.520	.792	24.470	.695	22.845	.747	23.627
.585	24.501	.872	25.769	.666	24.837	.709	24.392	.618	23.482	.925	25.103	.867	25.005	.758	23.478	.810	24.137
.665	24.902	.975	26.216	.748	25.269	.792	24.871	.687	23.999	1.007	25.599	.938	25.479	.842	24.236	.876	24.613
.767	25.367	1.076	26.651	.833	25.688	.871	25.303	.766	24.559	1.091	26.066	1.020	26.008	.922	24.886	.932	25.027
.869	25.872	1.199	27.090	.933	26.132	.974	25.843	.853	25.122	1.172	26.476	1.103	26.533	1.005	25.520	.998	25.476
.972	26.310	1.321	27.519	1.035	26.558	1.076	26.367	.955	25.717	1.275	26.967	1.208	27.083	1.111	26.165	1.068	25.898
1.075	26.676	1.446	27.961	1.158	27.020	1.200	26.871	1.036	26.139	1.378	27.446	1.311	27.567	1.214	26.715	1.152	26.346
1.199	27.122	1.567	28.346	1.280	27.505	1.322	27.328	1.139	26.697	1.482	27.872	1.414	27.978	1.318	27.209	1.236	26.793
1.321	27.515	1.691	28.697	1.405	28.002	1.445	27.736	1.241	27.171	1.608	28.529	1.517	28.336	1.441	27.718	1.340	27.307
1.444	27.883	1.834	29.059	1.527	28.460	1.570	28.148	1.343	27.563	1.750	28.697	1.641	28.740	1.565	28.191	1.440	27.749
1.586	28.262	1.979	29.342	1.668	28.842	1.712	28.553	1.466	28.005	1.855	29.036	1.766	29.062	1.689	28.620	1.566	28.229
1.731	28.667	2.142	29.575	1.813	29.180	1.855	28.928	1.588	28.420	2.001	29.365	1.891	29.307	1.835	29.019	1.690	28.617
1.872	28.961	2.305	29.754	1.937	29.450	1.998	29.264	1.733	28.849	2.145	29.604	2.034	29.527	1.979	29.316	1.834	28.980
2.058	29.333	2.489	29.933	2.079	29.674	2.143	29.559	1.875	29.232	2.309	29.777	2.180	29.732	2.125	29.578	1.962	29.297
2.220	29.617	2.672	30.057	2.223	29.885	2.307	29.786	2.021	29.523	2.475	29.914	2.325	29.888	2.269	29.761	2.102	29.568
2.405	29.822	2.856	30.117	2.366	30.000	2.477	29.939	2.183	29.767	2.620	30.034	2.489	30.022	2.454	29.933	2.281	29.806
2.606	29.993	3.024	30.167	2.529	30.072	2.669	30.031	2.346	29.949	2.826	30.107	2.676	30.123	2.619	30.057	2.441	29.958
2.773	30.069	3.121	30.189	2.712	30.155	2.819	30.082	2.511	30.053	2.986	30.167	2.863	30.192	2.789	30.117	2.587	30.069
2.948	30.145	3.121	30.189	2.918	30.183	2.996	30.101	2.715	30.151	3.135	30.189	3.046	30.218	2.953	30.161	2.765	30.136
3.122	30.173	3.121	30.189	3.122	30.202	3.122	30.110	2.918	30.183	3.135	30.189	3.127	30.230	3.135	30.167	2.954	30.167
3.122	30.173	3.121	30.189	3.122	30.202	3.122	30.110	3.122	30.202	3.135	30.189	3.127	30.230	3.135	30.167	3.137	30.202

Table 5.3b Mean velocity data, U_∞ = 30 ft/sec -- Continued

X= 3.0 FT Y= 0.0 IN		X= 3.0 FT Y= 1.0 IN		X= 3.0 FT Y= 2.0 IN		X= 3.0 FT Y= 2.5 IN		X= 3.0 FT Y= 3.0 IN		X= 3.0 FT Y= 3.5 IN		X= 3.0 FT Y= 4.0 IN		X= 3.0 FT Y= 5.0 IN		X= 3.0 FT Y= 6.0 IN	
Z (IN)	U (FPS)	Z (IN)	U (FPS)	Z (IN)	U (FPS)	Z (IN)	U (FPS)	Z (IN)	U (FPS)	Z (IN)	U (FPS)	Z (IN)	U (FPS)	Z (IN)	U (FPS)	Z (IN)	U (FPS)
.030	14.033	.030	16.027	.030	15.434	.031	14.721	.032	11.265	.125	12.799	.126	13.331	.126	10.791	.126	11.769
.054	14.933	.055	16.684	.053	16.414	.046	15.416	.056	12.260	.159	13.676	.164	13.828	.163	11.565	.179	12.665
.072	15.872	.073	17.524	.074	17.262	.066	16.216	.080	13.281	.189	14.650	.207	14.421	.195	12.635	.218	13.494
.094	16.922	.096	18.486	.098	18.143	.087	16.973	.117	14.565	.226	15.588	.248	15.229	.225	13.938	.255	14.381
.117	17.985	.120	19.346	.127	18.983	.109	17.761	.149	15.594	.267	16.512	.292	16.116	.271	15.410	.305	15.551
.145	18.983	.153	20.287	.165	19.875	.140	18.685	.180	16.512	.313	17.481	.343	17.023	.311	16.506	.357	16.581
.177	20.013	.187	21.051	.202	20.524	.177	19.668	.230	17.611	.359	18.346	.406	17.985	.365	17.627	.424	17.681
.228	20.935	.251	21.793	.251	21.028	.226	20.413	.296	18.670	.414	19.356	.472	18.918	.434	18.812	.504	18.711
.272	21.520	.339	22.569	.319	21.608	.309	21.298	.356	19.556	.474	20.296	.528	19.711	.492	19.619	.587	19.827
.338	22.208	.426	23.164	.400	22.229	.382	21.927	.420	20.334	.534	21.042	.598	20.557	.566	20.529	.664	20.695
.398	22.762	.534	23.804	.491	22.899	.468	22.602	.482	21.046	.601	21.740	.664	21.356	.644	21.396	.738	21.586
.471	23.311	.648	24.427	.587	23.530	.554	23.221	.560	21.867	.684	22.484	.732	22.074	.737	22.293	.836	22.577
.534	23.740	.773	25.031	.678	24.082	.651	23.852	.655	22.611	.767	23.160	.814	22.862	.837	23.135	.927	23.393
.608	24.173	.899	25.573	.772	24.582	.763	24.505	.732	23.449	.848	23.860	.900	23.595	.941	23.923	1.022	24.169
.672	24.552	1.025	26.063	.867	25.081	.858	25.005	.827	24.137	.945	24.548	.979	24.157	1.037	24.633	1.117	24.806
.756	24.986	1.149	26.526	.992	25.665	.980	25.610	.937	24.875	1.059	25.273	1.073	24.760	1.140	25.303	1.207	25.335
.851	25.393	1.274	26.967	1.118	26.245	1.108	26.172	1.044	25.528	1.195	25.955	1.198	25.491	1.254	25.979	1.317	25.955
.962	25.821	1.400	27.345	1.244	26.783	1.228	26.644	1.173	26.194	1.357	26.694	1.339	26.216	1.390	26.665	1.429	26.515
1.086	26.288	1.525	27.712	1.371	27.213	1.357	27.076	1.296	26.705	1.510	27.293	1.478	26.836	1.539	27.258	1.552	27.048
1.213	26.719	1.682	28.107	1.526	27.667	1.513	27.563	1.451	27.244	1.672	27.818	1.607	27.328	1.698	27.749	1.707	27.560
1.366	27.150	1.837	28.417	1.682	28.053	1.669	28.022	1.641	27.825	1.856	28.360	1.805	28.036	1.855	28.205	1.864	28.036
1.526	27.553	1.992	28.720	1.838	28.390	1.825	28.433	1.828	28.350	2.045	28.858	2.010	28.604	2.039	28.677	2.018	28.440
1.678	27.903	2.150	28.980	2.026	28.740	2.015	28.806	2.014	28.730	2.232	29.199	2.195	28.993	2.229	29.069	2.206	28.865
1.870	28.293	2.340	29.268	2.212	29.033	2.202	29.150	2.202	29.069	2.448	29.514	2.383	29.320	2.445	29.427	2.391	29.199
2.055	28.627	2.525	29.539	2.430	29.381	2.357	29.394	2.419	29.404	2.636	29.742	2.602	29.620	2.632	29.690	2.610	29.517
2.244	28.914	2.713	29.783	2.652	29.665	2.546	29.671	2.640	29.713	2.855	29.923	2.818	29.831	2.858	29.936	2.862	29.856
2.430	29.177	2.932	29.974	2.842	29.863	2.760	29.844	2.892	29.974	3.100	30.082	3.098	29.987	3.082	30.050	3.105	29.977
2.621	29.436	3.153	30.095	3.059	30.038	3.049	30.006	3.143	30.133	3.380	30.189	3.412	30.117	3.347	30.133	3.408	30.114
2.840	29.687	3.372	30.218	3.309	30.151	3.327	30.148	3.392	30.230	3.738	30.293	3.720	30.180	3.607	30.211	3.703	30.183
3.058	29.879	3.561	30.265	3.559	30.215	3.549	30.243	3.643	30.277	3.956	30.306	3.951	30.205	3.817	30.249	3.858	30.208
3.309	30.072	3.780	30.309	3.812	30.259	3.782	30.321	3.787	30.312	3.956	30.306	3.951	30.205	3.817	30.249	3.858	30.208
3.558	30.202	3.780	30.309	3.940	30.271	3.782	30.321	3.787	30.312	3.956	30.306	3.951	30.205	3.817	30.249	3.858	30.208
3.840	30.249	3.780	30.309	3.940	30.271	3.782	30.321	3.787	30.312	3.956	30.306	3.951	30.205	3.817	30.249	3.858	30.208
3.952	30.252	3.780	30.309	3.940	30.271	3.782	30.321	3.787	30.312	3.956	30.306	3.951	30.205	3.817	30.249	3.858	30.208

X= 4.0 FT Y= 0.0 IN		X= 4.0 FT Y= 1.0 IN		X= 4.0 FT Y= 2.0 IN		X= 4.0 FT Y= 2.5 IN		X= 4.0 FT Y= 3.0 IN		X= 4.0 FT Y= 3.5 IN		X= 4.0 FT Y= 4.0 IN		X= 4.0 FT Y= 5.0 IN		X= 4.0 FT Y= 6.0 IN	
Z (IN)	U (FPS)	Z (IN)	U (FPS)	Z (IN)	U (FPS)	Z (IN)	U (FPS)	Z (IN)	U (FPS)	Z (IN)	U (FPS)	Z (IN)	U (FPS)	Z (IN)	U (FPS)	Z (IN)	U (FPS)
.031	14.791	.031	15.276	.031	14.797	.030	14.016	.030	5.689	.128	13.209	.131	13.894	.131	12.366	.129	12.111
.056	16.043	.048	16.622	.040	16.219	.049	15.709	.065	7.915	.173	13.989	.168	14.539	.167	13.159	.171	13.007
.072	17.066	.070	17.697	.054	17.193	.069	16.724	.084	9.728	.206	14.804	.209	15.362	.200	14.157	.200	14.130
.096	18.115	.097	18.701	.080	18.094	.096	17.617	.107	12.126	.242	15.925	.247	16.114	.242	15.238	.234	15.145
.121	19.067	.142	19.816	.116	19.057	.138	18.503	.128	14.076	.278	16.747	.294	16.944	.291	16.196	.275	16.055
.151	19.840	.194	20.731	.164	19.916	.182	19.151	.151	15.606	.327	17.590	.341	17.751	.346	17.133	.313	16.820
.187	20.575	.275	21.484	.227	20.704	.234	19.835	.180	16.730	.382	18.508	.392	18.487	.410	17.995	.364	17.671
.238	21.312	.363	22.250	.303	21.453	.302	20.520	.218	17.724	.426	19.176	.447	19.303	.484	18.922	.425	18.518
.305	21.976	.465	22.991	.386	22.156	.363	21.133	.265	18.630	.486	19.954	.509	20.072	.552	19.769	.491	19.401
.373	22.529	.571	23.624	.479	22.788	.441	21.786	.313	19.343	.566	20.859	.571	20.786	.629	20.667	.556	20.167
.466	23.183	.697	24.276	.576	23.403	.523	22.382	.377	20.129	.644	21.572	.656	21.590	.715	21.572	.630	20.913
.547	23.672	.826	24.926	.698	24.131	.615	23.011	.456	20.954	.739	22.377	.729	22.220	.805	22.474	.702	21.541
.640	24.229	.952	25.437	.825	24.777	.707	23.572	.529	21.616	.833	23.064	.806	22.867	.906	23.244	.788	22.301
.731	24.678	1.075	25.890	.953	25.374	.827	24.202	.625	22.377	.925	23.688	.885	23.431	1.012	23.946	.871	22.974
.858	25.235	1.199	26.297	1.142	26.098	.958	24.854	.720	23.069	1.050	24.458	.975	24.013	1.121	24.578	.975	23.704
.983	25.729	1.356	26.721	1.297	26.643	1.081	25.422	.815	23.664	1.176	25.246	1.071	24.590	1.224	25.130	1.072	24.396
1.139	26.289	1.513	27.129	1.453	27.139	1.209	25.938	.928	24.299	1.332	26.051	1.171	25.092	1.349	25.806	1.201	25.164
1.295	26.739	1.702	27.558	1.611	27.555	1.366	26.497	1.033	24.880	1.486	26.697	1.293	25.711	1.471	26.394	1.323	25.854
1.454	27.139	1.889	27.957	1.797	27.987	1.523	27.028	1.142	25.463	1.644	27.261	1.411	26.235	1.598	26.891	1.479	26.540
1.639	27.565	2.075	28.330	1.982	28.340	1.680	27.527	1.270	26.040	1.798	27.739	1.537	26.736	1.785	27.531	1.636	27.153
1.828	27.940	2.264	28.656	2.175	28.695	1.866	27.967	1.392	26.537	1.985	28.223	1.710	27.337	1.939	28.004	1.793	27.671
2.048	28.317	2.482	29.062	2.363	29.016	2.055	28.354	1.555	27.129	2.172	28.629	1.879	27.831	2.126	28.497	1.979	28.186
2.266	28.675	2.706	29.380	2.578	29.325	2.246	28.698	1.712	27.647	2.359	28.958	2.065	28.293	2.314	28.925	2.166	28.613
2.489	28.994	2.925	29.630	2.767	29.547	2.463	29.091	1.868	28.089	2.578	29.289	2.255	28.712	2.533	29.302	2.387	29.033
2.738	29.270	3.175	29.846	2.988	29.757	2.715	29.383	2.057	28.503	2.795	29.534	2.441	29.033	2.751	29.623	2.604	29.357
3.020	29.595	3.428	30.039	3.237	29.941	2.966	29.614	2.275	28.889	3.044	29.764	2.628	29.318	3.003	29.856	2.853	29.649
3.303	29.827	3.704	30.177	3.521	30.099	3.214	29.802	2.497	29.225	3.293	29.928	2.845	29.617	3.249	30.020	3.101	29.878
3.586	30.001	4.022	30.293	3.804	30.190	3.498	29.963	2.744	29.553	3.544	30.073	3.064	29.824	3.521	30.146	3.412	30.121
3.865	30.117	4.355	30.358	4.116	30.274	3.782	30.089	3.027	29.833	3.792	30.199	3.313	30.001	3.841	30.265	3.726	30.265
4.337	30.227	4.648	30.393	4.461	30.318	4.063	30.155	3.309	30.007	4.044	30.290	3.563	30.127	4.184	30.365	4.038	30.355
4.648	30.318	4.958	30.424	4.804	30.380	4.346	30.190	3.626	30.136	4.354	30.305	3.872	30.243	4.496	30.430	4.348	30.411
4.963	30.393	5.273	30.442	5.116	30.424	4.655	30.218	3.906	30.215	4.662	30.321	4.186	30.302	4.806	30.452	4.721	30.467
5.276	30.408	5.273	30.442	5.274	30.433	4.970	30.237	4.237	30.237	4.972	30.346	4.495	30.327	5.121	30.477	5.125	30.480
5.276	30.408	5.273	30.442	5.274	30.433	5.286	30.246	4.578	30.259	5.287	30.368	4.835	30.349	5.121	30.477	5.125	30.480
5.276	30.408	5.273	30.442	5.274	30.433	5.286	30.246	4.854	30.287	5.287	30.368	5.122	30.371	5.121	30.477	5.125	30.480
5.276	30.408	5.273	30.442	5.274	30.433	5.286	30.246	5.278	30.290	5.287	30.368	5.122	30.371	5.121	30.477	5.125	30.480

Table 5.3b Mean velocity data, U_∞ = 30 ft/sec -- Continued

X= 6.0 FT Y= 0.0 IN		X= 6.0 FT Y= 1.0 IN		X= 6.0 FT Y= 2.0 IN		X= 6.0 FT Y= 2.5 IN		X= 6.0 FT Y= 3.0 IN		X= 6.0 FT Y= 3.5 IN		X= 6.0 FT Y= 4.0 IN		X= 6.0 FT Y= 5.0 IN		X= 6.0 FT Y= 6.0 IN	
Z (IN)	U (FPS)	Z (IN)	U (FPS)	Z (IN)	U (FPS)	Z (IN)	U (FPS)	Z (IN)	U (FPS)	Z (IN)	U (FPS)	Z (IN)	U (FPS)	Z (IN)	U (FPS)	Z (IN)	U (FPS)
.028	14.035	.030	13.435	.028	13.330	.033	13.196	.035	9.620	.128	11.638	.130	11.447	.128	11.597	.130	10.856
.037	14.699	.043	14.028	.034	14.075	.046	13.995	.053	10.700	.133	12.153	.141	11.954	.146	12.050	.141	11.397
.043	15.323	.052	14.731	.040	14.718	.062	14.725	.062	11.554	.148	12.737	.152	12.363	.166	12.486	.152	11.809
.057	15.922	.062	15.341	.050	15.317	.076	15.286	.078	12.327	.164	13.403	.158	12.714	.189	13.048	.167	12.371
.064	16.477	.072	15.946	.070	16.045	.107	15.916	.095	13.109	.184	14.078	.174	13.129	.210	13.531	.190	12.931
.088	16.992	.088	16.477	.084	16.579	.135	16.483	.120	13.784	.219	15.145	.190	13.622	.245	14.159	.211	13.545
.110	17.577	.110	17.068	.105	17.063	.164	17.056	.144	14.454	.255	15.849	.218	14.300	.290	14.993	.244	14.247
.129	18.081	.132	17.619	.131	17.592	.198	17.587	.168	15.082	.303	16.592	.254	14.999	.351	15.933	.274	14.903
.163	18.621	.162	18.132	.162	18.132	.238	18.101	.190	15.709	.359	17.435	.295	15.776	.407	16.712	.315	15.464
.201	19.088	.189	18.641	.204	18.616	.285	18.611	.227	16.329	.415	18.150	.337	16.429	.488	17.680	.363	16.219
.252	19.615	.234	19.215	.258	19.113	.343	19.210	.258	16.876	.475	18.843	.387	17.125	.568	18.551	.398	16.758
.297	20.068	.275	19.630	.328	19.630	.428	19.937	.311	17.536	.563	19.731	.420	17.561	.651	19.438	.453	17.341
.347	20.539	.336	20.110	.383	20.092	.509	20.620	.370	18.240	.645	20.538	.470	18.150	.733	20.238	.502	17.933
.401	20.972	.412	20.738	.440	20.548	.536	21.235	.455	19.181	.732	21.302	.531	18.828	.825	21.031	.552	18.464
.494	21.644	.501	21.427	.529	21.220	.681	21.805	.542	20.044	.839	22.160	.595	19.457	.923	21.790	.606	19.005
.589	22.266	.584	22.004	.596	21.657	.763	22.413	.625	20.849	.962	22.978	.657	20.082	1.034	22.617	.681	19.665
.690	22.913	.668	22.517	.664	22.076	.850	22.962	.725	21.690	1.094	23.780	.759	20.784	1.142	23.342	.760	20.281
.796	23.518	.755	23.007	.749	22.584	.936	23.410	.794	22.267	1.222	24.462	.810	21.360	1.266	24.151	.838	20.940
.907	24.111	.843	23.458	.836	23.051	1.017	23.834	.877	22.834	1.353	25.133	.888	21.961	1.394	24.850	.943	21.693
1.034	24.683	.923	23.865	.921	23.478	1.143	24.455	.958	23.342	1.495	25.728	.972	22.592	1.539	25.496	1.033	22.332
1.183	25.298	1.030	24.362	1.049	24.127	1.277	25.030	1.048	23.831	1.666	26.330	1.063	23.189	1.694	26.086	1.119	22.870
1.320	25.803	1.135	24.842	1.171	24.710	1.399	25.519	1.155	24.229	1.836	26.841	1.163	23.792	1.862	26.626	1.210	23.395
1.491	26.338	1.263	25.290	1.303	25.246	1.528	25.935	1.260	24.812	2.048	27.402	1.277	24.399	2.028	27.082	1.324	24.084
1.693	26.866	1.391	25.727	1.432	25.716	1.658	26.370	1.387	25.299	2.260	27.921	1.395	24.946	2.200	27.500	1.424	24.587
1.912	27.391	1.557	26.285	1.554	26.142	1.826	26.800	1.510	25.729	2.470	28.339	1.506	25.417	2.411	27.931	1.542	25.175
2.169	27.912	1.733	26.775	1.686	26.561	1.997	27.198	1.649	26.210	2.726	28.731	1.636	25.924	2.623	28.329	1.672	25.761
2.366	28.239	1.941	27.233	1.858	27.040	2.205	27.568	1.810	26.679	2.982	29.056	1.766	26.352	2.880	28.724	1.797	26.261
2.584	28.558	2.156	27.642	1.979	27.370	2.418	27.915	1.978	27.119	3.231	29.314	1.953	26.919	3.131	29.042	1.942	26.780
2.812	28.836	2.361	28.006	2.155	27.757	2.625	28.222	2.191	27.586	3.530	29.529	2.108	27.364	3.385	29.324	2.102	27.308
3.070	29.110	2.575	28.328	2.323	28.076	2.880	28.552	2.406	28.008	3.873	29.729	2.273	27.766	3.684	29.568	2.325	27.886
3.329	29.322	2.745	28.555	2.532	28.424	3.177	28.939	2.617	28.390	4.209	29.893	2.442	28.098	4.019	29.806	2.534	28.322
3.704	29.608	2.996	28.839	2.742	28.706	3.434	29.207	2.827	28.679	4.589	30.030	2.613	28.393	4.402	29.970	2.772	28.711
4.045	29.750	3.250	29.059	2.956	28.946	3.728	29.437	3.076	28.977	4.973	30.148	2.826	28.694	4.785	30.078	3.021	29.042
4.556	29.922	3.509	29.255	3.202	29.200	4.152	29.668	3.333	29.218	5.353	30.195	3.076	28.933	5.164	30.129	3.295	29.334
4.979	29.991	3.716	29.399	3.463	29.437	4.573	29.819	3.584	29.431	5.774	30.214	3.332	29.174	5.590	30.160	3.572	29.571
5.405	30.029	4.050	29.589	3.799	29.652	5.084	29.910	3.842	29.633	5.774	30.214	3.631	29.425	5.590	30.160	3.886	29.749
5.826	30.029	4.353	29.728	4.106	29.832	5.656	29.922	4.095	29.773	5.774	30.214	3.885	29.616	5.590	30.160	4.227	29.883
5.826	30.029	4.774	29.847	4.517	29.963	5.656	29.922	4.431	29.919	5.774	30.214	4.227	29.822	5.590	30.160	4.553	29.998
5.826	30.029	5.200	29.900	4.985	30.097	5.656	29.922	4.734	30.007	5.774	30.214	4.644	30.001	5.590	30.160	5.016	30.059
5.826	30.029	5.625	29.919	5.414	30.116	5.656	29.922	5.284	30.089	5.774	30.214	5.157	30.116	5.590	30.160	5.394	30.094
5.826	30.029	5.625	29.919	5.414	30.116	5.656	29.922	5.284	30.089	5.774	30.214	5.509	30.122	5.590	30.160	5.394	30.094
5.826	30.029	5.625	29.919	5.414	30.116	5.656	29.922	5.284	30.089	5.774	30.214	5.513	30.122	5.590	30.160	5.394	30.094

X= 8.0 FT Y= 0.0 IN		X= 8.0 FT Y= 1.0 IN		X= 8.0 FT Y= 2.0 IN		X= 8.0 FT Y= 2.5 IN		X= 8.0 FT Y= 3.0 IN		X= 8.0 FT Y= 3.5 IN		X= 8.0 FT Y= 4.0 IN		X= 8.0 FT Y= 5.0 IN		X= 8.0 FT Y= 6.0 IN	
Z (IN)	U (FPS)	Z (IN)	U (FPS)	Z (IN)	U (FPS)	Z (IN)	U (FPS)	Z (IN)	U (FPS)	Z (IN)	U (FPS)	Z (IN)	U (FPS)	Z (IN)	U (FPS)	Z (IN)	U (FPS)
.032	14.094	.032	13.430	.031	12.918	.030	13.086	.034	10.460	.126	12.414	.127	11.720	.124	11.597	.125	11.160
.038	14.637	.037	13.986	.040	13.634	.043	13.821	.041	11.172	.151	13.020	.145	12.208	.149	12.223	.146	11.946
.041	15.016	.048	14.618	.052	14.262	.055	14.408	.050	11.922	.168	13.529	.161	12.654	.169	12.707	.176	12.960
.045	15.366	.064	15.304	.066	14.799	.069	14.959	.067	12.514	.197	14.182	.182	13.129	.192	13.250	.208	13.755
.053	15.854	.081	16.015	.084	15.403	.091	15.800	.082	13.245	.223	14.767	.208	13.699	.234	14.050	.235	14.467
.066	16.315	.099	16.512	.104	16.009	.120	16.547	.094	13.773	.249	15.236	.239	14.374	.269	14.683	.278	15.258
.084	16.888	.123	17.184	.138	16.627	.156	17.377	.120	14.461	.282	15.830	.274	14.935	.321	15.445	.319	15.951
.109	17.470	.153	17.724	.184	17.366	.203	18.206	.150	15.135	.321	16.437	.317	15.636	.366	16.100	.376	16.798
.141	18.096	.185	18.206	.215	17.826	.258	18.853	.183	15.752	.359	17.012	.372	16.476	.415	16.781	.428	17.402
.177	18.645	.242	18.817	.258	18.326	.354	19.697	.232	16.547	.393	17.486	.431	17.225	.463	17.380	.490	18.108
.218	19.118	.292	19.321	.304	18.787	.446	20.422	.290	17.550	.441	18.090	.497	18.013	.518	17.965	.556	18.751
.275	19.692	.345	19.798	.363	19.326	.557	21.145	.342	18.054	.492	18.670	.558	18.746	.569	18.603	.614	19.329
.348	20.334	.411	20.306	.434	19.970	.673	21.880	.398	18.650	.546	19.193	.620	19.438	.634	19.260	.701	20.062
.426	20.947	.492	20.865	.496	20.473	.785	22.476	.457	19.237	.601	19.755	.688	20.058	.700	19.823	.790	20.756
.507	21.507	.574	21.396	.577	21.046	.919	23.119	.528	19.856	.672	20.329	.770	20.770	.780	20.510	.872	21.360
.603	22.036	.658	21.880	.665	21.582	1.067	23.776	.634	20.487	.732	20.814	.854	21.391	.864	21.153	.954	21.895
.705	22.577	.768	22.463	.752	22.079	1.212	24.341	.692	21.123	.792	21.316	.945	21.983	.956	21.812	1.046	22.456
.811	23.127	.873	22.924	.842	22.552	1.382	24.898	.786	21.784	.878	21.914	1.027	22.465	1.046	22.405	1.125	22.903
.952	23.736	.990	23.425	.941	23.036	1.553	25.438	.864	22.378	.961	22.361	1.117	22.937	1.123	22.886	1.233	23.464
1.069	24.184	1.108	23.892	1.047	23.545	1.763	26.011	.954	22.887	1.045	22.833	1.239	23.611	1.246	23.542	1.339	23.972
1.201	24.656	1.253	24.431	1.180	24.062	1.974	26.565	1.074	23.502	1.135	23.283	1.366	24.215	1.373	24.187	1.467	24.564
1.332	25.100	1.379	24.852	1.301	24.517	2.189	27.076	1.212	24.125	1.257	23.860	1.493	24.754	1.505	24.773	1.596	25.099
1.488	25.569	1.509	25.266	1.427	24.965	2.446	27.660	1.332	24.629	1.387	24.376	1.628	25.251	1.672	25.421	1.720	25.612
1.657	26.055	1.680	25.773	1.560	25.382	2.704	28.124	1.505	25.251	1.510	24.840	1.751	25.664	1.847	26.038	1.867	26.148
1.834	26.547	1.888	26.331	1.725	25.890	2.956	28.537	1.669	25.784	1.637	25.292	1.921	26.214	2.015	26.558	2.014	26.644
1.975	26.886	2.065	26.790	1.896	26.371	3.208	28.958	1.846	26.342	1.764	25.688	2.092	26.720	2.183	27.104	2.190	27.118
2.146	27.293	2.232	27.199	2.068	26.786	3.509	29.186	2.018	26.804	1.939	26.201	2.267	27.167	2.391	27.631	2.354	27.506
2.315	27.660	2.401	27.588	2.284	27.279	3.719	29.371	2.180	27.185	2.110	26.651	2.435	27.531	2.607	28.115	2.525	27.869
2.570	28.178	2.609	28.039	2.492	27.681	4.017	29.597	2.398	27.657	2.278	27.072	2.603	27.873	2.823	28.490	2.695	28.156
2.825	28.547	2.828	28.373	2.708	28.043	4.400	29.860	2.612	27.975	2.448	27.470	2.814	28.221	3.075	28.880	2.910	28.524
3.039	28.812	3.037	28.650	2.955	28.447	4.736	29.936	2.822	28.299	2.660	27.872	3.072	28.611	3.332	29.164	3.161	28.827
3.293	29.088	3.246	28.891	3.212	28.799	5.078	30.114	3.076	28.637	2.914	28.276	3.322	28.933	3.584	29.363	3.416	29.105
3.589	29.388	3.508	29.144	3.470	29.088	5.461	30.208	3.330	28.928	3.168	28.650	3.579	29.200	3.879	29.597	3.670	29.327
3.881	29.645	3.760	29.391	3.769	29.371	5.843	30.274	3.581	29.144	3.463	28.977	3.874	29.428	4.178	29.806	3.966	29.565
4.225	29.860	4.011	29.591	4.108	29.645	6.222	30.337	3.882	29.388	3.764	29.261	4.176	29.629	4.518	30.005	4.309	29.781
4.526	30.012	4.310	29.758	4.445	29.853	6.649	30.359	4.222	29.633	4.100	29.507	4.513	29.813	4.895	30.154	4.650	29.970
4.945	30.180	4.610	29.911	4.738	30.009	7.074	30.396	4.560	29.806	4.460	29.751	4.893	29.966	5.321	30.290	4.990	30.094
5.370	30.280	4.946	30.047	5.170	30.161	7.074	30.396	4.940	29.965	4.865	29.927	5.278	30.078	5.748	30.378	5.367	30.208
5.797	30.362	5.370	30.177	5.589	30.268	7.074	30.396	5.368	30.133	5.249	30.044	5.701	30.176	6.214	30.451	5.795	30.360
6.218	30.403	5.800	30.271	6.015	30.351	7.074	30.396	5.787	30.233	5.670	30.189	6.169	30.265	6.643	30.482	6.217	30.435
6.645	30.406	6.264	30.337	6.482	30.362	7.074	30.396	6.218	30.277	6.138	30.268	6.635	30.303	6.643	30.482	6.653	30.457
6.645	30.406	6.645	30.350	6.482	30.362	7.074	30.396	6.658	30.287	6.736	30.293	6.856	30.303	6.643	30.482	6.851	30.457

Table 5.3b Mean velocity data, U_{∞} = 30 ft/sec -- Continued

X=10.0 FT Y= 0.0 IN		X=10.0 FT Y= 1.0 IN		X=10.0 FT Y= 2.0 IN		X=10.0 FT Y= 2.5 IN		X=10.0 FT Y= 3.0 IN		X=10.0 FT Y= 3.5 IN		X=10.0 FT Y= 4.0 IN		X=10.0 FT Y= 5.0 IN		X=10.0 FT Y= 6.0 IN	
Z (IN)	U (FPS)	Z (IN)	U (FPS)	Z (IN)	U (FPS)	Z (IN)	U (FPS)	Z (IN)	U (FPS)	Z (IN)	U (FPS)	Z (IN)	U (FPS)	Z (IN)	U (FPS)	Z (IN)	U (FPS)
.030	11.554	.030	11.874	.032	12.064	.031	11.786	.031	9.371	.130	9.021	.136	11.469	.128	11.057	.126	9.421
.037	12.079	.040	12.472	.043	12.824	.034	12.255	.051	9.977	.146	9.737	.155	12.150	.150	11.600	.143	10.202
.049	12.571	.055	13.058	.060	13.493	.051	12.638	.069	10.531	.162	10.656	.170	12.668	.170	12.056	.164	11.040
.060	13.029	.081	13.866	.086	14.243	.075	13.094	.091	11.185	.185	11.551	.206	13.479	.190	12.480	.188	11.914
.074	13.598	.100	14.369	.114	14.893	.097	13.563	.117	11.842	.223	12.661	.258	14.552	.207	12.905	.212	12.608
.087	14.103	.127	14.931	.160	15.625	.142	14.409	.143	12.586	.254	13.451	.322	15.703	.237	13.521	.249	13.479
.111	14.772	.159	15.564	.204	16.271	.194	15.120	.169	13.202	.297	14.329	.387	16.594	.273	14.157	.293	14.369
.139	15.546	.200	16.283	.271	17.061	.239	15.745	.213	14.130	.339	15.120	.466	17.612	.309	14.720	.341	15.170
.176	16.283	.265	17.116	.328	17.735	.283	16.381	.262	14.975	.392	15.942	.558	18.569	.355	15.356	.392	15.919
.222	17.121	.331	17.894	.408	18.492	.329	16.916	.302	15.661	.456	17.066	.632	19.269	.405	16.013	.448	16.702
.273	17.820	.415	18.671	.500	19.328	.392	17.639	.345	16.318	.517	17.910	.711	19.983	.460	16.713	.524	17.553
.323	18.477	.496	19.352	.594	20.016	.478	18.528	.391	16.971	.602	18.862	.817	20.731	.540	17.644	.595	18.287
.398	19.166	.578	19.954	.709	20.763	.566	19.289	.450	17.671	.687	19.687	.913	21.405	.627	18.472	.678	19.057
.490	19.864	.680	20.575	.809	21.383	.650	19.978	.517	18.369	.687	19.687	1.025	22.071	.714	19.245	.778	19.864
.583	20.506	.791	21.232	.915	21.929	.759	20.754	.566	18.947	.798	20.598	1.150	22.726	.806	20.002	.873	20.603
.679	21.102	.908	21.838	1.043	22.575	.857	21.383	.636	19.557	.899	21.378	1.276	23.330	.916	20.795	.969	21.290
.818	21.795	1.040	22.428	1.167	23.138	.954	21.950	.721	20.213	1.029	22.182	1.403	23.875	1.019	21.480	1.086	22.045
.951	22.382	1.163	22.937	1.290	23.668	1.069	22.521	.805	20.781	1.198	23.060	1.569	24.555	1.147	22.288	1.191	22.646
1.075	22.920	1.292	23.499	1.454	24.326	1.191	23.069	.903	21.383	1.366	23.795	1.745	25.246	1.306	23.208	1.297	23.224
1.219	23.503	1.461	24.127	1.626	24.911	1.319	23.628	1.018	22.084	1.584	24.639	1.912	25.843	1.483	24.017	1.415	23.764
1.358	24.041	1.627	24.724	1.818	25.504	1.460	24.174	1.142	22.738	1.794	25.321	2.083	26.307	1.654	24.686	1.548	24.334
1.530	24.616	1.841	25.444	2.005	26.014	1.612	24.708	1.267	23.350	2.009	25.934	2.294	26.863	1.872	25.470	1.656	24.774
1.698	25.156	2.044	26.101	2.211	26.562	1.778	25.276	1.389	23.926	2.216	26.462	2.496	27.355	2.081	26.130	1.798	25.310
1.909	25.777	2.261	26.689	2.423	27.063	1.949	25.777	1.558	24.597	2.470	27.052	2.762	27.916	2.335	26.873	1.944	25.846
2.114	26.361	2.467	27.185	2.635	27.506	2.118	26.246	1.729	25.228	2.721	27.575	3.013	28.347	2.592	27.586	2.120	26.504
2.363	27.024	2.724	27.698	2.886	27.950	2.322	26.810	1.897	25.784	3.019	28.149	3.268	28.705	2.843	28.095	2.295	27.073
2.614	27.623	2.972	28.153	3.137	28.404	2.535	27.279	2.104	26.394	3.315	28.632	3.564	29.062	3.099	28.543	2.508	27.599
2.862	28.109	3.222	28.583	3.391	28.807	2.744	27.719	2.320	26.912	3.655	29.091	3.907	29.383	3.442	29.016	2.718	28.011
3.155	28.586	3.472	28.896	3.683	29.182	2.951	28.078	2.529	27.400	3.950	29.396	4.250	29.655	3.781	29.380	2.972	28.430
3.486	29.072	3.724	29.176	4.017	29.521	3.204	28.473	2.741	27.818	4.290	29.690	4.584	29.881	4.163	29.665	3.226	28.781
3.821	29.434	4.019	29.421	4.440	29.767	3.456	28.791	2.945	28.189	4.626	29.909	4.929	30.039	4.545	29.849	3.482	29.121
4.197	29.732	4.355	29.646	4.855	29.950	3.708	29.101	3.199	28.580	5.005	30.089	5.309	30.158	4.929	30.036	3.779	29.457
4.615	29.995	4.694	29.856	5.279	30.102	3.962	29.344	3.447	28.889	5.428	30.243	5.687	30.268	5.268	30.149	4.121	29.716
5.115	30.212	5.032	30.020	5.702	30.259	4.215	29.553	3.700	29.199	5.851	30.355	6.113	30.389	5.691	30.284	4.420	29.903
5.533	30.355	5.409	30.180	6.122	30.386	4.547	29.789	3.948	29.460	6.313	30.421	6.535	30.470	6.116	30.396	4.803	30.108
6.081	30.439	5.744	30.290	6.537	30.470	4.885	29.963	4.285	29.722	6.730	30.446	6.962	30.508	6.539	30.442	5.183	30.218
6.700	30.542	6.120	30.377	7.006	30.508	5.266	30.121	4.620	29.950	7.157	30.464	7.383	30.508	6.966	30.455	5.565	30.280
7.328	30.542	6.539	30.452	7.379	30.508	5.683	30.202	4.996	30.136	7.373	30.464	7.383	30.508	7.390	30.464	6.029	30.414
7.328	30.542	6.957	30.486	7.379	30.508	6.098	30.299	5.417	30.262	7.373	30.464	7.383	30.508	7.390	30.464	6.455	30.464
7.328	30.542	7.379	30.489	7.379	30.508	6.522	30.371	5.841	30.402	7.373	30.464	7.383	30.508	7.390	30.464	6.966	30.492
7.328	30.542	7.379	30.489	7.379	30.508	6.946	30.436	6.298	30.418	7.373	30.464	7.383	30.508	7.390	30.464	6.966	30.492
7.328	30.542	7.379	30.489	7.379	30.508	7.360	30.436	6.763	30.452	7.373	30.464	7.383	30.508	7.390	30.464	6.966	30.492
7.328	30.542	7.379	30.489	7.379	30.508	7.360	30.436	7.145	30.489	7.373	30.464	7.383	30.508	7.390	30.464	6.966	30.492
7.328	30.542	7.379	30.489	7.379	30.508	7.360	30.436	7.370	30.489	7.373	30.464	7.383	30.508	7.390	30.464	6.966	30.492

Table 5.4a Turbulence data at x = 6 ft, U_∞ = 20 ft/sec

Y=0.0 (IN)

Z (IN)	$\overline{UU}$ $(FPS)^2$	$\overline{VV}$ $(FPS)^2$	$\overline{WW}$ $(FPS)^2$	$-\overline{UV}$ $(FPS)^2$	$-\overline{UW}$ $(FPS)^2$
.060	5.72				
.139	4.78				
.206	4.07				
.300	3.75	1.37	.86	-.16	.58
.363	3.58	1.42	.87	-.17	.60
.461	3.33	1.48	.92	-.18	.62
.608	3.15	1.37	.95	-.22	.60
.797	2.91	1.34	.97	-.23	.57
.964	2.66	1.26	.91	-.24	.52
1.107	2.52	1.13	.89	-.23	.48
1.326	2.33	1.05	.83	-.22	.41
1.868	1.81	.93	.74	-.20	.25
2.207	1.51	.87	.71	-.19	.23
3.172	1.03	.40	.57	-.16	.14
4.452	.40	.12	.21	-.05	.05
5.445	.15	.06	.13	-.02	.02

Y=1.0 (IN)

Z (IN)	$\overline{UU}$ $(FPS)^2$	$\overline{VV}$ $(FPS)^2$	$\overline{WW}$ $(FPS)^2$	$-\overline{UV}$ $(FPS)^2$	$-\overline{UW}$ $(FPS)^2$
.036	5.76				
.085	5.12				
.156	4.19				
.290	3.61	1.96	1.04	-.26	.52
.348	3.44	1.99	1.12	-.28	.54
.413	3.25	2.03	1.25	-.30	.56
.522	3.14	1.92	1.20	-.31	.58
.631	3.01	1.86	1.16	-.33	.54
.739	2.83	1.81	1.15	-.31	.52
.956	2.53	1.70	1.07	-.30	.48
1.173	2.37	1.52	1.00	-.28	.44
1.607	1.88	1.43	.91	-.23	.34
2.474	1.29	1.05	.81	-.19	.22
3.342	.90	.78	.54	-.15	.11
4.426	.39	.31	.29	-.08	.03
5.511	.15	.05	.13	-.01	.01

Y=2.0 (IN)

Z (IN)	$\overline{UU}$ $(FPS)^2$	$\overline{VV}$ $(FPS)^2$	$\overline{WW}$ $(FPS)^2$	$-\overline{UV}$ $(FPS)^2$	$-\overline{UW}$ $(FPS)^2$
.045	5.88				
.098	5.35				
.161	4.53				
.290	3.86	2.18	1.57	-.41	.65
.348	3.77	2.20	1.59	-.36	.66
.413	3.67	2.23	1.60	-.33	.68
.522	3.46	2.26	1.58	-.31	.68
.631	3.24	2.20	1.55	-.28	.67
.739	3.09	2.12	1.48	-.26	.65
.956	2.80	2.00	1.41	-.24	.60
1.173	2.57	1.79	1.35	-.22	.55
1.607	2.09	1.52	.98	-.15	.44
2.474	1.38	1.21	.85	-.10	.21
3.342	.89	.84	.77	-.06	.16
4.426	.45	.18	.25	-.03	.05
5.511	.15	.06	.13	-.01	.01

Y=2.5 (IN)

Z (IN)	$\overline{UU}$ $(FPS)^2$	$\overline{VV}$ $(FPS)^2$	$\overline{WW}$ $(FPS)^2$	$-\overline{UV}$ $(FPS)^2$	$-\overline{UW}$ $(FPS)^2$
.035	5.62				
.081	5.29				
.147	4.81				
.290	4.11	3.74	2.65	-.46	1.05
.348	4.02	3.78	2.68	-.41	1.06
.413	3.92	3.76	2.71	-.37	1.07
.522	3.72	3.72	2.75	-.30	1.09
.631	3.51	3.67	2.70	-.26	1.07
.739	3.34	3.28	2.62	-.23	1.05
.956	3.00	3.17	2.29	-.21	1.00
1.173	2.68	2.78	2.19	-.18	.92
1.607	2.18	2.46	1.80	-.14	.74
2.474	1.46	1.65	1.39	-.10	.47
3.342	1.00	.95	.93	-.06	.18
4.426	.49	.36	.24	-.03	.06
5.511	.16	.19	.13	-.01	.01

Y=3.0 (IN)

Z (IN)	$\overline{UU}$ $(FPS)^2$	$\overline{VV}$ $(FPS)^2$	$\overline{WW}$ $(FPS)^2$	$-\overline{UV}$ $(FPS)^2$	$-\overline{UW}$ $(FPS)^2$
.085	5.44				
.128	5.74				
.192	5.90				
.299	5.97				
.348	5.88	3.45	1.62	-.53	.95
.413	5.75	3.54	1.64	-.56	.97
.522	5.35	3.62	1.67	-.54	.94
.631	4.79	3.38	1.65	-.50	.89
.739	4.38	3.04	1.56	-.47	.82
.956	3.78	2.84	1.45	-.37	.74
1.173	3.20	2.48	1.20	-.33	.64
1.607	2.52	1.66	.98	-.23	.47
2.474	1.66	.93	.80	-.13	.26
3.342	1.14	.58	.47	-.07	.14
4.426	.52	.21	.28	-.03	.06
5.511	.16	.02	.13	-.01	.01

Y=3.5 (IN)

Z (IN)	$\overline{UU}$ $(FPS)^2$	$\overline{VV}$ $(FPS)^2$	$\overline{WW}$ $(FPS)^2$	$-\overline{UV}$ $(FPS)^2$	$-\overline{UW}$ $(FPS)^2$
.130	5.41				
.177	5.66				
.251	5.84				
.371	5.67	3.16	1.68	-.52	1.28
.435	5.46	3.12	1.73	-.54	1.29
.544	5.09	3.02	1.66	-.52	1.30
.652	4.71	2.93	1.61	-.49	1.34
.761	4.39	2.83	1.55	-.46	1.26
.978	3.86	2.44	1.40	-.36	1.18
1.195	3.37	2.19	1.16	-.29	1.02
1.628	2.61	1.63	.92	-.25	.88
2.496	1.61	1.34	.78	-.15	.57
3.364	1.05	.70	.47	-.08	.22
4.448	.46	.27	.27	-.03	.08
5.533	.16	.05	.13	-.01	.01

Y=4.0 (IN)

Z (IN)	$\overline{UU}$ $(FPS)^2$	$\overline{VV}$ $(FPS)^2$	$\overline{WW}$ $(FPS)^2$	$-\overline{UV}$ $(FPS)^2$	$-\overline{UW}$ $(FPS)^2$
.140	5.35				
.185	5.25				
.251	5.18				
.371	5.20	3.29	1.69	-.38	.97
.435	5.17	3.26	1.71	-.42	.99
.544	4.99	3.02	1.74	-.39	.96
.652	4.77	2.95	1.70	-.37	.92
.761	4.53	2.88	1.65	-.34	.88
.978	3.99	2.53	1.33	-.31	.77
1.195	3.47	2.21	1.15	-.27	.68
1.628	2.68	1.81	1.00	-.23	.52
2.496	1.68	1.08	.86	-.15	.28
3.364	1.03	.77	.64	-.07	.17
4.448	.43	.25	.26	-.03	.06
5.533	.15	.03	.13	-.01	.01

Y=5.0 (IN)

Z (IN)	$\overline{UU}$ $(FPS)^2$	$\overline{VV}$ $(FPS)^2$	$\overline{WW}$ $(FPS)^2$	$-\overline{UV}$ $(FPS)^2$	$-\overline{UW}$ $(FPS)^2$
.135	5.41				
.180	5.33				
.244	5.15				
.371	5.09	4.02	2.05	-.26	1.03
.435	5.15	3.86	2.07	-.29	1.04
.544	5.22	3.56	2.08	-.27	1.05
.652	5.02	3.25	1.91	-.25	1.03
.761	4.81	3.05	1.83	-.23	.98
.978	4.31	2.85	1.75	-.21	.89
1.195	3.76	2.10	1.37	-.18	.83
1.628	2.92	1.93	1.04	-.13	.57
2.496	1.84	1.05	.79	-.09	.26
3.364	1.09	.74	.44	-.06	.16
4.448	.43	.31	.23	-.03	.06
5.533	.15	.06	.12	-.01	.01

Y=6.0 (IN)

Z (IN)	$\overline{UU}$ $(FPS)^2$	$\overline{VV}$ $(FPS)^2$	$\overline{WW}$ $(FPS)^2$	$-\overline{UV}$ $(FPS)^2$	$-\overline{UW}$ $(FPS)^2$
.135	5.34				
.180	5.20				
.240	5.13				
.371	5.37	3.67	2.16	-.25	1.09
.435	5.34	3.57	2.21	-.28	1.12
.544	5.21	3.48	2.26	-.26	1.14
.652	5.04	3.43	2.15	-.24	1.08
.761	4.81	3.11	2.00	-.22	1.04
.978	4.27	2.73	1.90	-.19	.90
1.195	3.77	2.34	1.59	-.17	.83
1.628	2.99	1.91	1.40	-.15	.67
2.496	1.69	1.34	.94	-.13	.29
3.364	.98	.76	.48	-.09	.16
4.448	.39	.25	.32	-.03	.05
5.533	.14	.07	.12	-.01	.01

Table 5.4a Turbulence data at x = 10 ft, U_∞ = 20 ft/sec

Y=0.0 (IN)

Z (IN)	$\overline{UU}$ $(FPS)^2$	$\overline{VV}$ $(FPS)^2$	$\overline{WW}$ $(FPS)^2$	$-\overline{UV}$ $(FPS)^2$	$-\overline{UW}$ $(FPS)^2$
.035	8.42				
.084	5.88				
.170	4.16				
.296	3.88	2.09	1.35	-.18	.59
.387	3.79	2.11	1.38	-.21	.61
.533	3.70	2.12	1.39	-.18	.63
.701	3.54	2.08	1.42	-.16	.64
.912	3.30	2.06	1.43	-.15	.62
1.229	2.95	1.77	1.44	-.14	.58
1.653	2.51	1.61	1.25	-.12	.49
2.284	1.93	1.32	1.12	-.10	.34
3.340	1.12	1.25	.87	-.07	.21
4.817	.62	.33	.30	-.04	.08
6.084	.25	.16	.16	-.01	.02

Y=1.0 (IN)

Z (IN)	$\overline{UU}$ $(FPS)^2$	$\overline{VV}$ $(FPS)^2$	$\overline{WW}$ $(FPS)^2$	$-\overline{UV}$ $(FPS)^2$	$-\overline{UW}$ $(FPS)^2$
.035	6.79				
.084	5.01				
.170	4.39				
.311	3.91	2.75	1.13	-.23	.61
.385	3.89	2.80	1.15	-.27	.62
.533	3.81	2.73	1.17	-.24	.64
.704	3.65	2.61	1.26	-.20	.66
.912	3.36	2.55	1.29	-.19	.62
1.229	2.96	2.48	1.31	-.14	.61
1.651	2.56	1.87	1.26	-.12	.53
2.284	1.93	1.44	.89	-.10	.26
3.340	1.15	1.38	.61	-.07	.15
4.817	.55	.64	.38	-.04	.10
6.084	.25	.17	.16	-.01	.02

Y=2.0 (IN)

Z (IN)	$\overline{UU}$ $(FPS)^2$	$\overline{VV}$ $(FPS)^2$	$\overline{WW}$ $(FPS)^2$	$-\overline{UV}$ $(FPS)^2$	$-\overline{UW}$ $(FPS)^2$
.035	8.11				
.084	6.42				
.168	4.92				
.324	4.45	2.48	1.19	-.28	.54
.385	4.33	2.56	1.21	-.27	.54
.533	4.21	2.39	1.28	-.26	.58
.704	3.99	2.37	1.40	-.25	.65
.912	3.69	2.26	1.42	-.20	.59
1.229	3.27	1.96	1.44	-.16	.52
1.651	2.78	1.78	1.04	-.12	.47
2.284	2.08	1.52	.92	-.09	.28
3.340	1.17	1.29	.86	-.07	.22
4.817	.65	.47	.56	-.05	.08
6.084	.27	.21	.22	-.02	.03

Y=2.5 (IN)

Z (IN)	$\overline{UU}$ $(FPS)^2$	$\overline{VV}$ $(FPS)^2$	$\overline{WW}$ $(FPS)^2$	$-\overline{UV}$ $(FPS)^2$	$-\overline{UW}$ $(FPS)^2$
.031	8.53				
.084	6.69				
.170	5.63				
.365	5.19	2.16	1.09	-.37	.66
.401	5.14	2.21	1.12	-.36	.67
.549	4.86	2.27	1.14	-.34	.68
.717	4.52	2.36	1.30	-.26	.69
.929	4.09	2.41	1.39	-.23	.72
1.245	3.48	2.17	1.44	-.19	.64
1.667	2.75	2.11	1.35	-.14	.54
2.301	1.93	1.51	1.21	-.08	.31
3.356	1.24	1.05	.93	-.06	.23
4.834	.59	.52	.57	-.04	.07
6.100	.21	.23	.21	-.01	.02

Y=3.0 (IN)

Z (IN)	$\overline{UU}$ $(FPS)^2$	$\overline{VV}$ $(FPS)^2$	$\overline{WW}$ $(FPS)^2$	$-\overline{UV}$ $(FPS)^2$	$-\overline{UW}$ $(FPS)^2$
.105	8.35				
.168	6.47				
.274	5.94				
.390	5.68	2.15	1.52	-.37	.84
.549	5.34	2.27	1.70	-.45	.86
.717	4.91	2.32	1.80	-.41	.88
.929	4.27	2.34	1.85	-.31	.80
1.245	3.46	2.28	1.90	-.16	.76
1.667	2.77	2.06	1.53	-.13	.58
2.301	1.82	1.45	1.44	-.09	.37
3.356	1.18	1.12	.91	-.07	.24
4.834	.51	.43	.39	-.04	.08
6.100	.21	.18	.17	-.01	.02

Y=3.5 (IN)

Z (IN)	$\overline{UU}$ $(FPS)^2$	$\overline{VV}$ $(FPS)^2$	$\overline{WW}$ $(FPS)^2$	$-\overline{UV}$ $(FPS)^2$	$-\overline{UW}$ $(FPS)^2$
.126	7.76				
.170	7.46				
.276	6.80				
.443	6.21	3.10	1.22	-.47	.90
.549	5.86	3.19	1.31	-.45	.92
.717	5.28	3.39	1.43	-.39	.94
.929	4.68	3.37	1.46	-.27	.80
1.245	3.92	2.90	1.33	-.22	.68
1.667	2.98	2.47	1.21	-.11	.52
2.301	2.05	1.97	1.10	-.09	.33
3.356	1.25	1.43	.54	-.06	.18
4.836	.61	.67	.37	-.03	.09
6.100	.21	.22	.17	-.01	.03

Y=4.0 (IN)

Z (IN)	$\overline{UU}$ $(FPS)^2$	$\overline{VV}$ $(FPS)^2$	$\overline{WW}$ $(FPS)^2$	$-\overline{UV}$ $(FPS)^2$	$-\overline{UW}$ $(FPS)^2$
.126	7.36				
.170	6.90				
.276	6.60				
.445	6.06	2.69	1.35	-.35	.94
.549	5.67	2.74	1.43	-.33	.93
.717	5.31	2.88	1.54	-.30	.91
.929	4.75	2.92	1.67	-.27	.85
1.245	3.90	2.71	1.63	-.22	.78
1.667	3.12	2.25	1.23	-.16	.61
2.301	2.22	1.66	.93	-.10	.34
3.356	1.29	1.24	.67	-.05	.22
4.836	.54	.57	.43	-.03	.10
6.100	.21	.19	.16	-.01	.02

Y=5.0 (IN)

Z (IN)	$\overline{UU}$ $(FPS)^2$	$\overline{VV}$ $(FPS)^2$	$\overline{WW}$ $(FPS)^2$	$-\overline{UV}$ $(FPS)^2$	$-\overline{UW}$ $(FPS)^2$
.126	7.77				
.168	7.52				
.274	7.42				
.401	7.23	2.48	1.42	-.25	1.06
.549	6.87	2.50	1.47	-.26	1.04
.717	6.27	2.74	1.52	-.28	1.03
.929	5.61	2.77	1.56	-.30	1.01
1.245	4.72	2.73	1.60	-.25	.93
1.667	3.56	2.43	1.47	-.20	.70
2.301	2.42	1.72	1.33	-.12	.40
3.356	1.37	1.33	.91	-.07	.27
4.836	.59	.58	.38	-.04	.11
6.100	.22	.19	.14	-.01	.02

Y=6.0 (IN)

Z (IN)	$\overline{UU}$ $(FPS)^2$	$\overline{VV}$ $(FPS)^2$	$\overline{WW}$ $(FPS)^2$	$-\overline{UV}$ $(FPS)^2$	$-\overline{UW}$ $(FPS)^2$
.126	8.16				
.168	7.61				
.274	6.85				
.443	6.62	2.23	1.63	-.27	1.04
.549	6.51	2.34	1.84	-.25	1.09
.717	6.12	2.38	2.11	-.21	1.17
.929	5.67	2.11	2.02	-.18	1.08
1.245	4.96	2.00	1.82	-.14	1.03
1.667	3.69	1.84	1.78	-.10	.77
2.301	2.47	1.72	1.56	-.08	.44
3.356	1.57	1.12	.92	-.05	.28
4.836	.69	.51	.21	-.03	.10
6.100	.24	.10	.11	-.01	.04

Table 5.4b Turbulence data at x = 6 ft, U_∞ = 30 ft/sec

Y=0.0 (IN)

Z (IN)	$\overline{UU}$ (FPS)^2	$\overline{VV}$ (FPS)^2	$\overline{WW}$ (FPS)^2	$-\overline{UV}$ (FPS)^2	$-\overline{UW}$ (FPS)^2
.030	14.53				
.075	11.91				
.131	9.95				
.244	8.93				
.300	8.64	2.52	1.18	-.39	1.06
.365	8.32	2.61	1.21	-.41	1.06
.461	7.83	2.67	1.25	-.43	1.05
.608	7.12	2.63	1.28	-.46	1.01
.797	6.25	2.58	1.24	-.44	.98
.964	5.71	2.51	1.19	-.40	.91
1.107	5.32	2.46	1.08	-.36	.84
1.326	4.79	2.39	.98	-.32	.64
1.868	3.69	1.92	.89	-.27	.39
2.207	3.08	1.69	.67	-.21	.31
3.172	1.92	1.28	.37	-.15	.17
4.454	.72	.25	.10	-.08	.04
5.445	.26	.12	.02	-.02	.01

Y=1.0 (IN)

Z (IN)	$\overline{UU}$ (FPS)^2	$\overline{VV}$ (FPS)^2	$\overline{WW}$ (FPS)^2	$-\overline{UV}$ (FPS)^2	$-\overline{UW}$ (FPS)^2
.025	15.10				
.061	12.91				
.127	10.61				
.258	9.21				
.290	8.87	3.79	1.27	-.71	1.13
.348	8.50	3.78	1.31	-.75	1.15
.413	8.15	3.71	1.34	-.72	1.16
.522	7.75	3.58	1.37	-.68	1.18
.631	7.33	3.47	1.33	-.64	1.15
.739	6.87	3.33	1.29	-.60	1.10
.956	6.07	3.18	1.21	-.53	1.05
1.173	5.39	2.89	1.13	-.48	.89
1.607	4.40	2.18	.97	-.36	.59
2.474	2.88	1.25	.82	-.24	.36
3.342	1.83	.73	.56	-.18	.24
4.426	.75	.31	.15	-.09	.05
5.511	.24	.12	.03	-.02	.02

Y=2.0 (IN)

Z (IN)	$\overline{UU}$ (FPS)^2	$\overline{VV}$ (FPS)^2	$\overline{WW}$ (FPS)^2	$-\overline{UV}$ (FPS)^2	$-\overline{UW}$ (FPS)^2
.030	13.67				
.071	12.17				
.137	11.06				
.244	10.00				
.290	9.76	3.60	1.68	-.76	1.32
.348	9.45	3.72	1.72	-.80	1.34
.413	9.14	3.78	1.77	-.83	1.36
.522	8.80	3.84	1.81	-.78	1.37
.631	8.42	3.73	1.64	-.72	1.33
.739	7.87	3.60	1.55	-.65	1.29
.956	6.88	3.21	1.30	-.52	1.23
1.173	6.07	2.63	1.21	-.44	1.10
1.607	4.84	2.13	1.11	-.29	.86
2.474	2.96	1.50	.93	-.10	.42
3.342	1.87	.80	.64	-.07	.24
4.426	.84	.41	.18	-.04	.07
5.511	.27	.12	.06	-.02	.02

Y=2.5 (IN)

Z (IN)	$\overline{UU}$ (FPS)^2	$\overline{VV}$ (FPS)^2	$\overline{WW}$ (FPS)^2	$-\overline{UV}$ (FPS)^2	$-\overline{UW}$ (FPS)^2
.030	14.46				
.071	12.60				
.137	11.68				
.244	10.73				
.290	10.54	3.78	1.83	-.86	1.48
.348	10.31	3.75	1.88	-.89	1.50
.413	10.06	3.81	1.94	-.92	1.51
.522	9.61	3.75	2.12	-.95	1.51
.631	9.17	3.52	1.95	-.86	1.44
.739	8.68	3.30	1.87	-.76	1.38
.956	7.68	2.88	1.65	-.59	1.24
1.173	6.63	2.62	1.53	-.47	1.11
1.607	5.14	2.09	1.24	-.29	.81
2.474	3.10	1.59	1.12	-.13	.40
3.342	1.86	.80	.64	-.07	.22
4.426	.83	.41	.20	-.04	.07
5.511	.28	.12	.07	-.02	.02

Y=3.0 (IN)

Z (IN)	$\overline{UU}$ (FPS)^2	$\overline{VV}$ (FPS)^2	$\overline{WW}$ (FPS)^2	$-\overline{UV}$ (FPS)^2	$-\overline{UW}$ (FPS)^2
.080	11.49				
.123	11.98				
.185	12.59				
.292	12.34				
.413	11.96	4.77	2.62	-1.61	1.82
.522	11.22	4.73	2.67	-1.58	1.82
.631	10.32	4.65	2.71	-1.51	1.81
.739	9.59	4.58	2.54	-1.44	1.74
.956	8.22	3.61	2.32	-1.16	1.54
1.173	6.86	3.41	2.19	-.95	1.37
1.607	5.10	2.55	1.82	-.71	.95
2.474	3.06	1.72	1.37	-.43	.45
3.342	1.77	.95	.82	-.19	.27
4.426	.75	.22	.21	-.07	.07
5.511	.24	.13	.06	-.03	.02

Y=3.5 (IN)

Z (IN)	$\overline{UU}$ (FPS)^2	$\overline{VV}$ (FPS)^2	$\overline{WW}$ (FPS)^2	$-\overline{UV}$ (FPS)^2	$-\overline{UW}$ (FPS)^2
.135	12.51				
.176	13.13				
.242	14.23				
.347	13.45				
.413	12.73	4.82	3.50	-1.41	2.29
.522	11.76	4.76	3.64	-1.36	2.29
.631	11.08	4.57	3.45	-1.31	2.21
.739	10.46	4.35	3.11	-1.25	2.18
.956	9.35	3.86	2.71	-1.06	1.73
1.173	7.75	3.23	2.10	-.91	1.46
1.607	5.66	2.54	1.84	-.71	1.08
2.474	3.05	1.75	1.41	-.42	.51
3.342	1.83	1.00	.79	-.18	.21
4.426	.73	.23	.15	-.07	.07
5.511	.24	.14	.06	-.03	.02

Y=4.0 (IN)

Z (IN)	$\overline{UU}$ (FPS)^2	$\overline{VV}$ (FPS)^2	$\overline{WW}$ (FPS)^2	$-\overline{UV}$ (FPS)^2	$-\overline{UW}$ (FPS)^2
.135	13.02				
.176	13.22				
.242	13.45				
.371	13.33	6.20	3.52	-.72	2.02
.435	13.06	6.31	3.57	-.75	2.04
.544	12.63	6.14	3.46	-.73	2.02
.652	12.22	5.97	2.98	-.68	1.98
.761	11.62	5.42	2.72	-.62	1.84
.978	10.17	4.81	2.14	-.55	1.62
1.195	8.43	4.51	1.83	-.48	1.36
1.628	6.01	3.45	1.58	-.34	1.01
2.496	3.29	2.80	1.18	-.23	.41
3.364	1.88	1.15	.64	-.11	.25
4.448	.75	.44	.14	-.06	.07
5.553	.24	.12	.05	-.01	.02

Y=5.0 (IN)

Z (IN)	$\overline{UU}$ (FPS)^2	$\overline{VV}$ (FPS)^2	$\overline{WW}$ (FPS)^2	$-\overline{UV}$ (FPS)^2	$-\overline{UW}$ (FPS)^2
.135	13.89				
.182	14.37				
.248	14.03				
.371	13.73	6.39	3.54	-.75	2.25
.435	13.55	6.43	3.61	-.78	2.27
.544	13.42	6.22	3.24	-.80	2.29
.652	13.31	5.73	2.83	-.75	2.23
.761	12.89	5.14	2.46	-.71	2.17
.978	11.24	4.36	1.98	-.65	1.83
1.195	9.55	3.37	1.57	-.50	1.65
1.628	6.72	2.72	1.27	-.36	1.20
2.496	3.66	1.61	1.18	-.23	.48
3.364	1.98	.82	.51	-.12	.23
4.448	.76	.49	.15	-.05	.07
5.533	.23	.13	.06	-.01	.02

Y=6.0 (IN)

Z (IN)	$\overline{UU}$ (FPS)^2	$\overline{VV}$ (FPS)^2	$\overline{WW}$ (FPS)^2	$-\overline{UV}$ (FPS)^2	$-\overline{UW}$ (FPS)^2
.135	11.40				
.180	12.01				
.242	12.40				
.371	12.57	6.58	3.81	-.45	2.43
.435	12.76	6.67	3.86	-.49	2.46
.544	12.73	6.34	3.70	-.52	2.50
.652	12.53	5.87	3.41	-.54	2.45
.761	12.07	5.47	3.03	-.47	2.36
.978	10.83	4.81	2.57	-.42	2.00
1.195	9.40	3.87	2.24	-.31	1.81
1.628	6.79	3.00	1.63	-.21	1.52
2.496	3.54	1.58	1.21	-.16	.48
3.364	1.92	.78	.58	-.10	.27
4.448	.72	.36	.17	-.05	.07
5.533	.22	.12	.06	-.02	.02

Table 5.4b Turbulence data at x = 10 ft, U_∞ = 30 ft/sec

Y=0.0 (IN)

Z (IN)	$\overline{UU}$ (FPS)^2	$\overline{VV}$ (FPS)^2	$\overline{WW}$ (FPS)^2	$-\overline{UV}$ (FPS)^2	$-\overline{UW}$ (FPS)^2
.035	13.20				
.084	9.44				
.170	8.55				
.311	8.29	4.68	2.56	-.39	1.15
.385	8.22	4.87	2.58	-.40	1.17
.533	8.16	5.20	2.60	-.39	1.19
.701	7.79	4.92	2.66	-.37	1.23
.912	7.15	4.83	2.72	-.35	1.21
1.229	6.36	4.50	2.55	-.33	1.19
1.651	5.54	3.92	2.20	-.23	1.02
2.284	4.08	2.83	1.76	-.19	.69
3.340	2.14	2.37	1.48	-.14	.38
4.817	.97	1.04	.52	-.06	.11
6.084	.46	.48	.21	-.02	.02

Y=1.0 (IN)

Z (IN)	$\overline{UU}$ (FPS)^2	$\overline{VV}$ (FPS)^2	$\overline{WW}$ (FPS)^2	$-\overline{UV}$ (FPS)^2	$-\overline{UW}$ (FPS)^2
.035	15.69				
.084	10.87				
.168	9.43				
.311	9.22	4.89	1.96	-.55	1.10
.387	9.13	4.97	2.26	-.58	1.12
.533	8.68	5.12	2.45	-.56	1.14
.701	8.22	5.18	2.54	-.51	1.19
.912	7.90	4.66	2.16	-.42	1.17
1.229	7.43	3.64	1.88	-.36	1.15
1.651	6.18	3.27	1.75	-.31	1.02
2.284	4.42	2.67	1.66	-.21	.75
3.340	2.64	1.70	1.21	-.16	.31
4.817	1.23	.78	.47	-.10	.09
6.084	.51	.38	.17	-.03	.02

Y=2.0 (IN)

Z (IN)	$\overline{UU}$ (FPS)^2	$\overline{VV}$ (FPS)^2	$\overline{WW}$ (FPS)^2	$-\overline{UV}$ (FPS)^2	$-\overline{UW}$ (FPS)^2
.035	16.26				
.084	11.80				
.170	9.64				
.343	9.26	5.76	2.88	-.75	1.26
.387	9.20	5.85	2.94	-.77	1.26
.533	8.84	6.10	3.05	-.79	1.26
.704	8.57	6.38	3.12	-.75	1.25
.912	8.20	5.31	2.58	-.61	1.23
1.229	7.50	4.70	1.87	-.45	1.13
1.651	6.23	3.81	1.71	-.33	.93
2.284	4.41	3.11	1.58	-.17	.64
3.340	2.51	2.55	1.19	-.10	.38
4.817	1.20	.93	.43	-.04	.12
6.084	.50	.33	.20	-.02	.03

Y=2.5 (IN)

Z (IN)	$\overline{UU}$ (FPS)^2	$\overline{VV}$ (FPS)^2	$\overline{WW}$ (FPS)^2	$-\overline{UV}$ (FPS)^2	$-\overline{UW}$ (FPS)^2
.035	14.58				
.084	10.89				
.168	9.05				
.365	8.72	6.06	3.62	-.88	1.34
.401	8.68	6.11	3.67	-.89	1.35
.549	8.50	6.37	3.78	-.91	1.37
.717	8.30	6.42	3.73	-.85	1.35
.929	8.08	5.28	3.15	-.71	1.33
1.245	7.42	4.29	2.41	-.46	1.25
1.667	5.98	3.40	2.03	-.31	1.09
2.301	4.33	2.20	1.58	-.23	.62
3.356	2.19	1.56	1.07	-.17	.37
4.834	.89	.98	.44	-.07	.11
6.100	.36	.41	.21	-.02	.02

Y=3.0 (IN)

Z (IN)	$\overline{UU}$ (FPS)^2	$\overline{VV}$ (FPS)^2	$\overline{WW}$ (FPS)^2	$-\overline{UV}$ (FPS)^2	$-\overline{UW}$ (FPS)^2
.105	16.52				
.168	13.56				
.274	11.72				
.401	11.30	5.48	3.89	-.84	1.74
.549	10.92	5.89	3.94	-.86	1.82
.717	10.58	5.52	3.74	-.87	1.78
.929	9.42	5.29	3.56	-.79	1.64
1.245	7.53	4.77	3.34	-.64	1.46
1.667	6.30	3.73	2.93	-.45	1.25
2.301	4.41	2.41	1.88	-.26	.78
3.356	2.69	1.58	1.11	-.18	.46
4.834	1.04	.70	.41	-.07	.26
6.100	.37	.36	.13	-.01	.02

Y=3.5 (IN)

Z (IN)	$\overline{UU}$ (FPS)^2	$\overline{VV}$ (FPS)^2	$\overline{WW}$ (FPS)^2	$-\overline{UV}$ (FPS)^2	$-\overline{UW}$ (FPS)^2
.126	13.42				
.168	14.03				
.276	13.96				
.443	13.36	5.58	3.18	-.88	1.92
.549	13.15	5.76	3.24	-.87	1.96
.717	12.86	5.37	3.16	-.85	1.97
.929	12.33	4.95	2.92	-.78	1.72
1.245	10.28	4.26	2.54	-.68	1.45
1.667	7.96	3.47	2.12	-.36	1.23
2.301	5.27	2.87	1.65	-.25	.77
3.356	2.73	2.06	.93	-.16	.44
4.836	1.04	.76	.39	-.07	.21
6.100	.42	.33	.11	-.01	.03

Y=4.0 (IN)

Z (IN)	$\overline{UU}$ (FPS)^2	$\overline{VV}$ (FPS)^2	$\overline{WW}$ (FPS)^2	$-\overline{UV}$ (FPS)^2	$-\overline{UW}$ (FPS)^2
.126	16.46				
.170	17.92				
.276	15.88				
.443	14.90	4.86	2.83	-.82	2.09
.549	14.37	4.94	3.07	-.86	2.12
.717	13.92	5.13	3.30	-.81	2.16
.929	12.87	4.84	2.87	-.76	2.05
1.245	10.69	4.51	2.31	-.71	1.71
1.667	8.12	3.85	1.92	-.38	1.33
2.301	5.14	3.01	1.52	-.22	.85
3.356	2.74	1.95	1.19	-.12	.39
4.836	1.04	.85	.49	-.08	.17
6.100	.42	.41	.13	-.01	.03

Y=5.0 (IN)

Z (IN)	$\overline{UU}$ (FPS)^2	$\overline{VV}$ (FPS)^2	$\overline{WW}$ (FPS)^2	$-\overline{UV}$ (FPS)^2	$-\overline{UW}$ (FPS)^2
.126	15.95				
.168	16.31				
.274	15.71				
.401	14.67	4.83	3.06	-.76	2.06
.549	14.31	4.92	3.13	-.80	2.07
.717	13.83	5.08	3.34	-.72	2.09
.929	12.54	4.69	2.52	-.66	2.04
1.245	10.28	4.32	2.11	-.54	1.72
1.667	8.06	3.64	1.73	-.36	1.40
2.301	5.03	2.94	1.44	-.21	.88
3.356	2.48	1.86	1.07	-.12	.39
4.836	.98	.77	.39	-.08	.16
6.100	.41	.31	.13	-.01	.03

Y=6.0 (IN)

Z (IN)	$\overline{UU}$ (FPS)^2	$\overline{VV}$ (FPS)^2	$\overline{WW}$ (FPS)^2	$-\overline{UV}$ (FPS)^2	$-\overline{UW}$ (FPS)^2
.126	15.28				
.168	15.93				
.274	14.87				
.401	13.90	4.76	3.84	-.45	2.18
.549	13.49	4.84	3.96	-.47	2.23
.717	13.17	4.89	4.17	-.42	2.26
.929	12.25	4.46	3.73	-.38	2.15
1.245	10.39	4.14	3.25	-.33	1.83
1.667	7.99	3.47	2.50	-.27	1.51
2.301	5.24	2.78	1.92	-.20	.88
3.356	2.26	1.63	1.04	-.11	.46
4.836	.87	.75	.50	-.06	.16
6.100	.32	.26	.13	-.01	.04

Table 5.5 Data on one-dimensional spectra at x = 6 ft, U_∞ = 30 ft/sec

Y=0.0 IN Z= .073 IN		Y=0.0 IN Z= .131 IN		Y=0.0 IN Z= .244 IN		Y=0.0 IN Z= .602 IN		Y=0.0 IN Z=1.162 IN		Y=0.0 IN Z=2.238 IN	
K (1/FT)	E(K)/$\overline{UU}$ (FT)	K (1/FT)	E(K)/$\overline{UU}$ (FT)	K (1/FT)	E(K)/$\overline{UU}$ (FT)	K (1/FT)	E(K)/$\overline{UU}$ (FT)	K (1/FT)	E(K)/$\overline{UU}$ (FT)	K (1/FT)	E(K)/$\overline{UU}$ (FT)
1.35E+00	8.55E-03	1.15E+00	1.76E-02	1.06E+00	2.37E-02	9.21E-01	3.80E-02	8.26E-01	4.24E-02	6.87E-01	6.95E-02
1.95E+00	2.05E-02	1.49E+00	2.06E-02	1.49E+00	2.81E-02	1.34E+00	5.22E-02	1.16E+00	4.92E-02	1.10E+00	5.79E-02
2.55E+00	2.28E-02	2.27E+00	2.34E-02	2.15E+00	2.37E-02	1.68E+00	4.77E-02	1.55E+00	3.89E-02	1.55E+00	5.79E-02
3.42E+00	1.90E-02	3.72E+00	1.81E-02	2.82E+00	2.50E-02	2.34E+00	4.16E-02	2.14E+00	3.72E-02	1.87E+00	5.51E-02
4.89E+00	1.55E-02	4.66E+00	1.85E-02	4.05E+00	2.31E-02	3.45E+00	3.22E-02	2.95E+00	4.92E-02	2.76E+00	4.16E-02
7.60E+00	1.24E-02	6.15E+00	1.69E-02	6.05E+00	1.59E-02	5.75E+00	2.38E-02	5.08E+00	2.88E-02	4.20E+00	3.95E-02
9.61E+00	1.02E-02	9.35E+00	1.07E-02	8.59E+00	1.25E-02	8.26E+00	1.79E-02	7.29E+00	2.37E-02	6.35E+00	3.41E-02
1.58E+01	6.03E-03	1.24E+01	9.00E-03	1.37E+01	8.28E-03	1.26E+01	1.05E-02	9.92E+00	1.85E-02	9.92E+00	1.96E-02
1.95E+01	5.45E-03	1.75E+01	7.22E-03	2.10E+01	5.68E-03	1.67E+01	7.54E-03	1.63E+01	8.35E-03	1.24E+01	1.48E-02
2.79E+01	4.43E-03	2.24E+01	5.58E-03	2.73E+01	4.76E-03	2.55E+01	4.66E-03	2.22E+01	5.00E-03	2.04E+01	7.35E-03
3.54E+01	3.68E-03	3.07E+01	4.02E-03	4.26E+01	3.01E-03	3.48E+01	3.18E-03	3.13E+01	3.45E-03	2.74E+01	4.86E-03
5.01E+01	2.65E-03	4.65E+01	2.85E-03	6.87E+01	1.75E-03	5.62E+01	1.97E-03	4.11E+01	2.47E-03	4.04E+01	2.42E-03
6.82E+01	2.15E-03	8.95E+01	1.75E-03	8.89E+01	1.35E-03	7.86E+01	1.19E-03	7.31E+01	1.35E-03	5.61E+01	1.34E-03
1.11E+02	1.31E-03	1.31E+02	9.17E-04	1.33E+02	8.25E-04	1.07E+02	7.27E-04	1.00E+02	7.74E-04	7.90E+01	8.86E-04
1.48E+02	8.71E-04	2.15E+02	4.96E-04	1.72E+02	6.55E-04	1.56E+02	4.72E-04	1.26E+02	5.25E-04	1.14E+02	5.36E-04
1.90E+02	5.81E-04	2.86E+02	3.55E-04	2.30E+02	4.01E-04	2.30E+02	3.40E-04	1.62E+02	3.85E-04	1.52E+02	3.86E-04
3.70E+02	2.84E-04	4.01E+02	2.45E-04	3.30E+02	2.96E-04	3.20E+02	2.72E-04	2.22E+02	3.11E-04	2.07E+02	2.64E-04
5.46E+02	1.80E-04	4.48E+02	1.89E-04	4.46E+02	1.49E-04	3.95E+02	1.31E-04	3.25E+02	1.21E-04	2.74E+02	1.69E-04
6.77E+02	5.86E-05	5.50E+02	5.29E-05	5.78E+02	2.52E-05	4.91E+02	2.64E-05	4.26E+02	2.55E-05	3.86E+02	2.61E-05
9.16E+02	7.86E-07	7.59E+02	4.19E-06	7.45E+02	2.02E-06	6.32E+02	2.12E-06	5.51E+02	2.28E-06	5.10E+02	1.30E-06

Y=1.0 IN Z= .061 IN		Y=1.0 IN Z= .127 IN		Y=1.0 IN Z= .238 IN		Y=1.0 IN Z= .598 IN		Y=1.0 IN Z=1.179 IN		Y=1.0 IN Z=2.138 IN	
K (1/FT)	E(K)/$\overline{UU}$ (FT)	K (1/FT)	E(K)/$\overline{UU}$ (FT)	K (1/FT)	E(K)/$\overline{UU}$ (FT)	K (1/FT)	E(K)/$\overline{UU}$ (FT)	K (1/FT)	E(K)/$\overline{UU}$ (FT)	K (1/FT)	E(K)/$\overline{UU}$ (FT)
1.31E+00	8.74E-03	1.12E+00	1.31E-02	1.06E+00	2.47E-02	8.39E-01	3.00E-02	7.47E-01	2.33E-02	6.97E-01	3.68E-02
1.80E+00	1.34E-02	1.65E+00	2.21E-02	1.45E+00	2.31E-02	1.22E+00	2.37E-02	1.10E+00	3.59E-02	1.00E+00	3.86E-02
2.93E+00	1.70E-02	2.22E+00	1.89E-02	2.07E+00	3.27E-02	1.84E+00	4.15E-02	1.72E+00	5.62E-02	1.72E+00	3.54E-02
4.22E+00	1.81E-02	3.76E+00	2.29E-02	3.18E+00	3.25E-02	2.87E+00	3.84E-02	2.77E+00	4.17E-02	2.26E+00	4.23E-02
5.81E+00	1.48E-02	4.86E+00	1.83E-02	5.02E+00	2.09E-02	3.60E+00	3.17E-02	4.90E+00	2.84E-02	3.20E+00	4.15E-02
7.85E+00	1.34E-02	7.26E+00	1.34E-02	6.97E+00	1.61E-02	4.87E+00	2.42E-02	6.47E+00	2.30E-02	4.27E+00	3.52E-02
1.04E+01	1.21E-02	1.01E+01	1.00E-02	8.99E+00	1.32E-02	7.35E+00	1.57E-02	8.74E+00	1.84E-02	5.87E+00	2.84E-02
1.52E+01	8.55E-03	1.77E+01	5.73E-03	1.15E+01	1.04E-02	9.29E+00	1.24E-02	1.21E+01	1.07E-02	7.88E+00	2.37E-02
2.06E+01	6.47E-03	3.29E+01	3.47E-03	1.66E+01	7.28E-03	1.29E+01	1.00E-02	1.62E+01	7.43E-03	1.10E+01	1.48E-02
2.68E+01	5.06E-03	4.38E+01	2.74E-03	2.47E+01	4.73E-03	1.82E+01	6.79E-03	2.40E+01	4.93E-03	1.52E+01	7.72E-03
3.87E+01	3.70E-03	6.83E+01	1.82E-03	4.10E+01	2.96E-03	2.44E+01	4.69E-03	3.30E+01	3.28E-03	1.93E+01	5.22E-03
5.25E+01	3.00E-03	9.31E+01	1.37E-03	6.14E+01	2.20E-03	3.55E+01	3.18E-03	4.45E+01	2.22E-03	3.27E+01	2.93E-03
6.29E+01	2.45E-03	1.28E+02	9.67E-04	8.62E+01	1.53E-03	7.77E+01	1.15E-03	6.94E+01	1.22E-03	4.56E+01	1.99E-03
1.19E+02	1.13E-03	1.87E+02	5.68E-04	1.33E+02	8.55E-04	1.11E+02	6.72E-04	9.94E+01	7.88E-04	6.25E+01	1.32E-03
1.73E+02	6.86E-04	2.58E+02	3.65E-04	1.84E+02	5.60E-04	1.62E+02	4.37E-04	1.54E+02	4.50E-04	8.53E+01	8.25E-04
2.32E+02	4.07E-04	3.30E+02	2.80E-04	2.81E+02	3.61E-04	2.72E+02	2.61E-04	2.37E+02	2.91E-04	1.15E+02	4.76E-04
3.09E+02	2.38E-04	4.45E+02	1.39E-04	3.73E+02	2.51E-04	3.66E+02	1.38E-04	3.42E+02	1.14E-04	2.10E+02	2.41E-04
5.16E+02	9.42E-05	5.88E+02	3.07E-05	4.96E+02	6.82E-05	4.39E+02	4.72E-05	4.17E+02	2.64E-05	2.66E+02	1.40E-04
6.50E+02	2.58E-05	6.94E+02	6.32E-06	6.01E+02	1.31E-05	5.21E+02	8.90E-06	5.05E+02	4.33E-06	4.04E+02	1.14E-05
9.76E+02	4.17E-07	8.21E+02	1.41E-06	7.43E+02	1.98E-06	6.34E+02	1.72E-06	5.87E+02	1.06E-06	5.08E+02	1.42E-06

Y=2.0 IN Z= .071 IN		Y=2.0 IN Z= .137 IN		Y=2.0 IN Z= .244 IN		Y=2.0 IN Z= .608 IN		Y=2.0 IN Z=1.191 IN		Y=2.0 IN Z=2.259 IN	
K (1/FT)	E(K)/$\overline{UU}$ (FT)	K (1/FT)	E(K)/$\overline{UU}$ (FT)	K (1/FT)	E(K)/$\overline{UU}$ (FT)	K (1/FT)	E(K)/$\overline{UU}$ (FT)	K (1/FT)	E(K)/$\overline{UU}$ (FT)	K (1/FT)	E(K)/$\overline{UU}$ (FT)
1.24E+00	7.98E-03	1.13E+00	1.04E-02	9.62E-01	1.58E-02	8.32E-01	2.61E-02	7.69E-01	3.29E-02	6.86E-01	4.96E-02
1.84E+00	2.51E-02	1.64E+00	1.81E-02	1.40E+00	3.77E-02	1.13E+00	4.69E-02	1.09E+00	5.77E-02	9.13E-01	4.93E-02
2.74E+00	2.30E-02	2.45E+00	2.92E-02	2.32E+00	3.53E-02	2.00E+00	3.20E-02	1.67E+00	5.80E-02	1.44E+00	5.33E-02
3.90E+00	2.40E-02	3.46E+00	2.63E-02	3.23E+00	3.17E-02	3.12E+00	3.12E-02	2.50E+00	4.18E-02	2.29E+00	5.15E-02
5.97E+00	1.88E-02	4.98E+00	2.14E-02	4.98E+00	2.41E-02	5.08E+00	3.05E-02	3.36E+00	3.26E-02	3.25E+00	4.41E-02
8.73E+00	1.43E-02	6.67E+00	1.65E-02	6.73E+00	1.77E-02	6.99E+00	2.27E-02	4.76E+00	2.65E-02	4.25E+00	3.84E-02
1.27E+01	1.00E-02	9.91E+00	1.08E-02	8.45E+00	1.42E-02	8.98E+00	1.65E-02	6.39E+00	2.25E-02	5.88E+00	3.10E-02
1.60E+01	8.16E-03	1.32E+01	8.22E-03	1.23E+01	9.88E-03	1.47E+01	9.37E-03	8.56E+00	1.80E-02	7.37E+00	2.70E-02
2.91E+01	4.90E-03	1.74E+01	7.17E-03	1.68E+01	7.40E-03	1.95E+01	6.95E-03	1.20E+01	1.22E-02	1.03E+01	1.61E-02
3.77E+01	4.31E-03	2.64E+01	4.70E-03	2.29E+01	5.98E-03	2.37E+01	5.20E-03	1.71E+01	7.62E-03	1.50E+01	8.93E-03
5.20E+01	3.51E-03	3.55E+01	4.09E-03	3.10E+01	4.41E-03	3.64E+01	3.21E-03	2.30E+01	5.60E-03	1.92E+01	5.74E-03
7.97E+01	2.21E-03	4.75E+01	2.96E-03	4.64E+01	2.62E-03	5.37E+01	2.21E-03	3.08E+01	3.99E-03	2.49E+01	3.98E-03
1.15E+02	1.29E-03	6.82E+01	1.96E-03	6.56E+01	1.85E-03	5.62E+01	1.85E-03	4.78E+01	2.27E-03	3.92E+01	2.44E-03
1.54E+02	8.89E-04	9.18E+01	1.49E-03	8.63E+01	1.24E-03	7.81E+01	1.18E-03	6.16E+01	1.60E-03	5.90E+01	1.36E-03
2.34E+02	4.32E-04	1.47E+02	7.83E-04	1.33E+02	7.75E-04	1.14E+02	7.09E-04	1.00E+02	7.64E-04	9.22E+01	6.22E-04
3.13E+02	2.52E-04	2.21E+02	4.51E-04	2.02E+02	4.99E-04	1.70E+02	4.19E-04	1.50E+02	4.04E-04	1.36E+02	3.79E-04
4.77E+02	1.27E-04	3.13E+02	2.87E-04	2.86E+02	3.37E-04	2.41E+02	3.14E-04	2.13E+02	3.05E-04	1.79E+02	3.07E-04
5.92E+02	3.95E-05	4.61E+02	1.10E-04	4.21E+02	1.32E-04	3.55E+02	1.42E-04	3.13E+02	1.46E-04	2.94E+02	1.48E-04
7.41E+02	6.87E-06	6.45E+02	1.69E-05	5.09E+02	2.00E-05	4.97E+02	2.22E-05	4.38E+02	2.52E-05	3.74E+02	2.68E-05
9.50E+02	1.37E-06	8.29E+02	1.44E-06	7.57E+02	1.69E-06	6.59E+02	1.81E-06	5.63E+02	2.02E-06	5.01E+02	1.81E-06

Table 5.5 Data on one-dimensional spectra at x = 6 ft, U_∞ = 30 ft/sec -- Continued

Y=2.5 IN Z= .071 IN		Y=2.5 IN Z= .157 IN		Y=2.5 IN Z= .244 IN		Y=2.5 IN Z= .627 IN		Y=2.5 IN Z=1.184 IN		Y=2.5 IN Z=2.148 IN	
K (1/FT)	E(K)/$\overline{UU}$ (FT)	K (1/FT)	E(K)/$\overline{UU}$ (FT)	K (1/FT)	E(K)/$\overline{UU}$ (FT)	K (1/FT)	E(K)/$\overline{UU}$ (FT)	K (1/FT)	E(K)/$\overline{UU}$ (FT)	K (1/FT)	E(K)/$\overline{UU}$ (FT)
1.39E+00	1.20E-02	1.15E+00	2.37E-02	1.01E+00	1.55E-02	9.10E-01	2.21E-02	7.45E-01	2.25E-02	6.72E-01	2.91E-02
1.79E+00	1.65E-02	1.56E+00	2.57E-02	1.44E+00	2.44E-02	1.30E+00	2.95E-02	9.67E-01	7.37E-02	9.95E-01	3.91E-02
2.94E+00	2.07E-02	2.51E+00	2.78E-02	2.01E+00	3.19E-02	1.98E+00	3.35E-02	1.50E+00	5.26E-02	1.71E+00	4.26E-02
4.60E+00	1.86E-02	4.16E+00	1.95E-02	3.45E+00	2.18E-02	3.05E+00	3.09E-02	2.21E+00	4.82E-02	2.38E+00	4.39E-02
6.81E+00	1.39E-02	7.68E+00	1.22E-02	4.76E+00	2.02E-02	3.99E+00	2.86E-02	3.47E+00	3.92E-02	3.28E+00	3.74E-02
8.89E+00	1.09E-02	9.51E+00	1.15E-02	6.52E+00	1.66E-02	5.25E+00	2.37E-02	4.81E+00	3.14E-02	4.21E+00	3.34E-02
1.15E+01	9.66E-03	1.39E+01	8.32E-03	9.48E+00	1.17E-02	7.11E+00	1.80E-02	6.55E+00	2.44E-02	6.04E+00	2.58E-02
1.54E+01	7.65E-03	1.66E+01	7.19E-03	1.27E+01	9.28E-03	1.31E+01	9.75E-03	8.84E+00	1.66E-02	7.58E+00	2.12E-02
2.38E+01	5.70E-03	2.52E+01	4.96E-03	1.65E+01	8.35E-03	1.75E+01	7.95E-03	1.21E+01	1.08E-02	1.14E+01	1.15E-02
2.99E+01	4.65E-03	3.57E+01	3.56E-03	2.05E+01	6.37E-03	2.36E+01	6.47E-03	1.52E+01	8.35E-03	1.57E+01	6.51E-03
3.93E+01	3.53E-03	4.01E+01	3.45E-03	3.19E+01	3.96E-03	2.67E+01	4.98E-03	2.12E+01	5.38E-03	2.29E+01	4.30E-03
5.09E+01	2.77E-03	5.54E+01	2.58E-03	3.96E+01	3.08E-03	3.85E+01	2.91E-03	3.10E+01	3.40E-03	3.05E+01	2.77E-03
8.41E+01	1.65E-03	7.64E+01	1.76E-03	6.66E+01	1.85E-03	5.14E+01	1.92E-03	4.91E+01	2.11E-03	3.94E+01	2.11E-03
1.11E+02	1.20E-03	9.62E+01	1.28E-03	8.96E+01	1.18E-03	7.17E+01	1.37E-03	6.30E+01	1.48E-03	5.66E+01	1.46E-03
1.77E+02	6.19E-04	1.55E+02	6.58E-04	1.39E+02	7.15E-04	1.16E+02	7.32E-04	1.01E+02	7.87E-04	9.05E+01	7.56E-04
2.65E+02	2.94E-04	2.29E+02	3.87E-04	2.08E+02	4.12E-04	1.75E+02	4.26E-04	1.51E+02	4.31E-04	1.36E+02	4.18E-04
3.76E+02	1.65E-04	3.25E+02	2.74E-04	2.95E+02	2.94E-04	2.46E+02	3.08E-04	2.14E+02	3.12E-04	1.92E+02	2.92E-04
5.53E+02	5.80E-05	4.77E+02	1.07E-04	4.34E+02	1.25E-04	3.61E+02	1.35E-04	3.15E+02	1.45E-04	2.83E+02	1.29E-04
7.74E+02	6.71E-06	6.68E+02	1.40E-05	6.07E+02	3.90E-05	5.06E+02	2.06E-05	4.41E+02	2.30E-05	4.19E+02	1.93E-05
9.96E+02	4.95E-07	8.59E+02	1.10E-06	7.81E+02	8.86E-06	6.50E+02	1.79E-06	5.67E+02	1.75E-06	5.09E+02	1.86E-06

Y=3.0 IN Z= .080 IN		Y=3.0 IN Z= .123 IN		Y=3.0 IN Z= .292 IN		Y=3.0 IN Z= .656 IN		Y=3.0 IN Z=1.264 IN		Y=3.0 IN Z=2.326 IN	
K (1/FT)	E(K)/$\overline{UU}$ (FT)	K (1/FT)	E(K)/$\overline{UU}$ (FT)	K (1/FT)	E(K)/$\overline{UU}$ (FT)	K (1/FT)	E(K)/$\overline{UU}$ (FT)	K (1/FT)	E(K)/$\overline{UU}$ (FT)	K (1/FT)	E(K)/$\overline{UU}$ (FT)
1.64E+00	3.36E-03	1.47E+00	7.34E-03	1.15E+00	9.85E-03	9.24E-01	2.20E-02	7.64E-01	3.76E-02	6.26E-01	3.10E-02
2.40E+00	9.84E-03	2.06E+00	7.89E-03	1.72E+00	1.79E-02	1.25E+00	3.69E-02	1.07E+00	5.25E-02	1.01E+00	4.80E-02
4.00E+00	1.35E-02	3.19E+00	1.25E-02	2.44E+00	2.45E-02	1.99E+00	2.89E-02	1.78E+00	3.64E-02	1.46E+00	7.35E-02
5.72E+00	1.31E-02	5.42E+00	1.03E-02	3.77E+00	2.07E-02	2.84E+00	3.62E-02	2.38E+00	4.67E-02	2.14E+00	6.41E-02
1.01E+01	8.14E-03	6.82E+00	1.03E-02	5.19E+00	1.82E-02	4.55E+00	2.46E-02	3.57E+00	3.55E-02	3.45E+00	4.85E-02
1.74E+01	5.07E-03	9.63E+00	8.85E-03	8.27E+00	1.26E-02	6.28E+00	1.76E-02	5.05E+00	2.66E-02	4.60E+00	3.81E-02
2.25E+01	4.85E-03	1.26E+01	7.75E-03	9.99E+00	1.18E-02	7.36E+00	2.08E-02	6.40E+00	2.06E-02	6.00E+00	2.85E-02
2.85E+01	4.31E-03	1.74E+01	6.35E-03	1.44E+01	8.48E-03	1.02E+01	1.52E-02	8.21E+00	1.64E-02	8.56E+00	1.91E-02
3.89E+01	3.40E-03	2.18E+01	5.54E-03	1.87E+01	6.90E-03	1.35E+01	9.38E-03	1.12E+01	1.28E-02	1.18E+01	1.29E-02
4.58E+01	3.05E-03	3.17E+01	3.86E-03	2.89E+01	4.55E-03	2.15E+01	5.95E-03	1.57E+01	7.94E-03	1.55E+01	9.04E-03
5.59E+01	2.65E-03	4.20E+01	3.20E-03	3.67E+01	3.78E-03	2.66E+01	4.18E-03	2.15E+01	5.51E-03	2.05E+01	5.85E-03
7.61E+01	2.26E-03	6.27E+01	2.38E-03	4.91E+01	2.99E-03	3.55E+01	2.78E-03	3.52E+01	3.05E-03	2.71E+01	3.86E-03
1.15E+02	1.55E-03	9.48E+01	1.66E-03	6.59E+01	2.11E-03	5.05E+01	1.98E-03	4.84E+01	1.89E-03	4.46E+01	2.12E-03
1.48E+02	1.11E-03	1.30E+02	1.21E-03	1.00E+02	1.30E-03	7.54E+01	1.24E-03	6.63E+01	1.18E-03	6.51E+01	1.08E-03
2.29E+02	6.08E-04	2.01E+02	6.88E-04	1.56E+02	7.01E-04	1.20E+02	6.72E-04	1.02E+02	7.59E-04	9.25E+01	7.07E-04
3.45E+02	3.22E-04	3.01E+02	3.48E-04	2.34E+02	3.80E-04	1.79E+02	4.12E-04	1.55E+02	4.46E-04	1.65E+02	3.69E-04
4.86E+02	1.87E-04	4.27E+02	2.25E-04	3.32E+02	2.75E-04	2.54E+02	3.17E-04	2.17E+02	3.11E-04	2.28E+02	2.34E-04
7.15E+02	6.01E-05	6.27E+02	8.48E-05	4.88E+02	1.28E-04	3.74E+02	1.42E-04	3.19E+02	1.42E-04	3.31E+02	8.72E-05
1.00E+03	6.98E-06	8.78E+02	1.05E-05	6.83E+02	1.89E-05	5.24E+02	1.99E-05	4.46E+02	2.39E-05	4.21E+02	1.44E-05
1.29E+03	5.22E-07	1.13E+03	8.03E-07	8.78E+02	1.25E-06	6.75E+02	1.79E-06	5.79E+02	1.95E-06	5.22E+02	2.06E-06

Y=3.5 IN Z= .135 IN		Y=3.5 IN Z= .242 IN		Y=3.5 IN Z= .692 IN		Y=3.5 IN Z=1.270 IN		Y=3.5 IN Z=2.233 IN	
K (1/FT)	E(K)/$\overline{UU}$ (FT)	K (1/FT)	E(K)/$\overline{UU}$ (FT)	K (1/FT)	E(K)/$\overline{UU}$ (FT)	K (1/FT)	E(K)/$\overline{UU}$ (FT)	K (1/FT)	E(K)/$\overline{UU}$ (FT)
1.65E+00	7.88E-03	1.27E+00	1.12E-02	8.37E-01	1.94E-02	7.64E-01	2.17E-02	6.42E-01	4.96E-02
2.41E+00	8.02E-03	1.84E+00	1.61E-02	1.28E+00	3.49E-02	9.50E-01	2.55E-02	1.03E+00	4.07E-02
3.63E+00	9.71E-03	2.50E+00	1.50E-02	1.76E+00	2.46E-02	1.60E+00	3.50E-02	1.38E+00	4.25E-02
5.26E+00	1.34E-02	4.50E+00	1.11E-02	2.62E+00	3.29E-02	2.25E+00	3.89E-02	2.22E+00	4.93E-02
8.24E+00	9.39E-03	5.89E+00	1.48E-02	3.78E+00	3.45E-02	2.94E+00	3.38E-02	3.14E+00	4.83E-02
1.21E+01	8.11E-03	8.14E+00	1.35E-02	5.96E+00	2.28E-02	4.75E+00	2.17E-02	4.12E+00	3.83E-02
1.49E+01	7.49E-03	1.41E+01	7.94E-03	7.93E+00	1.82E-02	6.67E+00	1.80E-02	6.33E+00	2.73E-02
1.78E+01	7.86E-03	1.66E+01	7.54E-03	1.06E+01	1.65E-02	9.32E+00	1.67E-02	8.40E+00	1.96E-02
2.85E+01	4.99E-03	2.16E+01	7.56E-03	1.44E+01	1.25E-02	1.28E+01	1.16E-02	1.14E+01	1.29E-02
3.72E+01	4.01E-03	2.75E+01	6.36E-03	1.88E+01	8.39E-03	1.57E+01	8.97E-03	1.50E+01	8.90E-03
4.61E+01	3.61E-03	4.30E+01	3.37E-03	2.53E+01	5.34E-03	2.07E+01	5.60E-03	1.91E+01	6.12E-03
7.41E+01	2.27E-03	5.33E+01	2.69E-03	3.52E+01	3.63E-03	3.17E+01	3.15E-03	2.85E+01	3.50E-03
1.02E+02	1.71E-03	8.62E+01	1.72E-03	5.06E+01	2.08E-03	4.67E+01	1.78E-03	4.51E+01	1.78E-03
1.43E+02	9.39E-04	1.11E+02	1.30E-03	7.33E+01	1.31E-03	6.41E+01	1.21E-03	6.35E+01	1.29E-03
1.77E+02	6.30E-04	1.73E+02	6.61E-04	1.19E+02	6.75E-04	1.02E+02	7.29E-04	8.42E+01	8.02E-04
3.34E+02	2.90E-04	2.60E+02	3.75E-04	1.79E+02	3.99E-04	1.53E+02	4.42E-04	1.28E+02	4.01E-04
4.75E+02	1.90E-04	3.68E+02	2.62E-04	2.53E+02	3.14E-04	2.17E+02	3.00E-04	2.16E+02	1.72E-04
6.96E+02	7.11E-05	5.41E+02	1.05E-04	3.72E+02	1.48E-04	3.19E+02	1.45E-04	2.80E+02	1.02E-04
9.75E+02	7.74E-06	7.58E+02	1.41E-05	5.21E+02	2.32E-05	4.47E+02	2.47E-05	3.62E+02	3.20E-05
1.25E+03	6.55E-07	9.74E+02	1.55E-06	6.70E+02	2.03E-06	5.75E+02	1.99E-06	4.55E+02	8.19E-06

Table 5.5 Data on one-dimensional spectra at x = 6 ft, U_∞ = 30 ft/sec -- Continued

Y=4.0 IN Z= .135 IN		Y=4.0 IN Z= .242 IN		Y=4.0 IN Z= .692 IN		Y=4.0 IN Z=1.268 IN		Y=4.0 IN Z=2.232 IN	
K (1/FT)	E(K)/$\overline{UU}$ (FT)	K (1/FT)	E(K)/$\overline{UU}$ (FT)	K (1/FT)	E(K)/$\overline{UU}$ (FT)	K (1/FT)	E(K)/$\overline{UU}$ (FT)	K (1/FT)	E(K)/$\overline{UU}$ (FT)
1.69E+00	8.51E-03	1.41E+00	6.76E-03	8.90E-01	3.72E-02	7.99E-01	3.70E-02	6.66E-01	3.14E-02
2.45E+00	1.29E-02	1.98E+00	1.99E-02	1.26E+00	4.04E-02	1.10E+00	6.17E-02	9.60E-01	4.73E-02
4.52E+00	7.04E-03	3.05E+00	1.68E-02	1.93E+00	4.34E-02	1.65E+00	5.27E-02	1.51E+00	6.42E-02
5.89E+00	7.21E-03	3.96E+00	1.84E-02	2.69E+00	4.14E-02	2.38E+00	3.60E-02	2.56E+00	4.11E-02
7.81E+00	8.45E-03	5.92E+00	1.61E-02	3.71E+00	3.37E-02	3.01E+00	4.42E-02	3.52E+00	3.59E-02
1.01E+01	8.35E-03	9.04E+00	1.09E-02	5.79E+00	2.27E-02	4.78E+00	3.03E-02	4.74E+00	3.50E-02
1.48E+01	6.16E-03	1.06E+01	1.01E-02	8.08E+00	1.60E-02	8.17E+00	1.80E-02	5.84E+00	2.70E-02
1.85E+01	5.39E-03	1.52E+01	7.66E-03	1.04E+01	1.40E-02	1.14E+01	1.24E-02	8.69E+00	1.84E-02
2.44E+01	4.53E-03	2.12E+01	5.94E-03	1.36E+01	1.03E-02	1.67E+01	8.61E-03	1.21E+01	1.24E-02
3.83E+01	3.36E-03	3.08E+01	4.37E-03	2.33E+01	5.39E-03	2.28E+01	5.31E-03	1.66E+01	8.04E-03
5.65E+01	2.51E-03	3.99E+01	3.21E-03	3.11E+01	3.74E-03	3.14E+01	3.17E-03	1.91E+01	6.41E-03
7.70E+01	1.92E-03	5.53E+01	2.49E-03	4.25E+01	2.09E-03	3.97E+01	2.40E-03	2.83E+01	3.60E-03
1.11E+02	1.45E-03	8.56E+01	1.65E-03	6.03E+01	1.70E-03	5.21E+01	1.64E-03	4.10E+01	2.22E-03
1.44E+02	1.08E-03	1.12E+02	1.15E-03	7.60E+01	1.26E-03	7.59E+01	1.08E-03	5.77E+01	1.24E-03
2.26E+02	5.57E-04	1.73E+02	6.27E-04	1.21E+02	6.87E-04	1.14E+02	5.73E-04	8.64E+01	7.26E-04
3.40E+02	2.87E-04	2.59E+02	3.59E-04	1.81E+02	4.33E-04	1.52E+02	4.05E-04	1.49E+02	3.92E-04
4.81E+02	1.82E-04	3.68E+02	2.53E-04	2.56E+02	3.02E-04	2.15E+02	3.29E-04	2.20E+02	2.26E-04
7.08E+02	5.73E-05	5.40E+02	9.25E-05	3.77E+02	1.20E-04	3.16E+02	1.40E-04	2.98E+02	9.65E-05
9.91E+02	5.12E-06	7.57E+02	9.40E-06	5.28E+02	1.58E-05	4.43E+02	1.85E-05	3.79E+02	2.41E-05
1.27E+03	4.77E-07	9.73E+02	7.50E-07	6.79E+02	1.34E-06	5.69E+02	1.56E-06	5.12E+02	1.34E-06

Y=5.0 IN Z= .135 IN		Y=5.0 IN Z= .248 IN		Y=5.0 IN Z= .692 IN		Y=5.0 IN Z=1.266 IN		Y=5.0 IN Z=2.229 IN	
K (1/FT)	E(K)/$\overline{UU}$ (FT)	K (1/FT)	E(K)/$\overline{UU}$ (FT)	K (1/FT)	E(K)/$\overline{UU}$ (FT)	K (1/FT)	E(K)/$\overline{UU}$ (FT)	K (1/FT)	E(K)/$\overline{UU}$ (FT)
1.76E+00	6.04E-03	1.31E+00	1.62E-02	9.29E-01	2.10E-02	7.49E-01	5.19E-02	6.44E-01	5.36E-02
2.80E+00	8.84E-03	1.75E+00	2.43E-02	1.33E+00	4.10E-02	1.09E+00	5.79E-02	9.39E-01	6.10E-02
3.89E+00	1.01E-02	2.80E+00	2.15E-02	2.03E+00	3.40E-02	1.78E+00	5.63E-02	1.36E+00	5.32E-02
5.58E+00	1.02E-02	4.26E+00	1.88E-02	3.10E+00	3.62E-02	2.67E+00	5.47E-02	2.28E+00	4.49E-02
8.15E+00	9.30E-03	6.45E+00	1.64E-02	4.39E+00	2.87E-02	3.65E+00	4.34E-02	3.56E+00	3.81E-02
1.13E+01	9.71E-03	7.96E+00	1.41E-02	5.47E+00	2.59E-02	5.23E+00	3.14E-02	4.74E+00	3.69E-02
1.37E+01	9.31E-03	1.10E+01	1.21E-02	8.00E+00	1.83E-02	6.83E+00	2.58E-02	6.24E+00	2.93E-02
1.94E+01	6.94E-03	1.38E+01	1.04E-02	1.09E+01	1.23E-02	8.76E+00	1.66E-02	7.85E+00	2.22E-02
2.95E+01	4.74E-03	2.01E+01	6.98E-03	1.42E+01	8.98E-03	1.15E+01	1.17E-02	1.03E+01	1.64E-02
4.49E+01	3.13E-03	2.82E+01	4.82E-03	1.99E+01	5.23E-03	1.63E+01	8.06E-03	1.50E+01	8.37E-03
5.70E+01	2.61E-03	3.92E+01	3.22E-03	3.64E+01	2.95E-03	2.20E+01	5.63E-03	1.93E+01	5.31E-03
6.61E+01	2.33E-03	5.80E+01	2.30E-03	4.87E+01	1.98E-03	2.49E+01	4.32E-03	2.73E+01	3.35E-03
1.16E+02	1.38E-03	8.31E+01	1.48E-03	8.27E+01	1.01E-03	3.27E+01	3.03E-03	4.27E+01	2.08E-03
1.51E+02	1.10E-03	1.13E+02	1.07E-03	1.05E+02	7.78E-04	4.85E+01	2.21E-03	6.76E+01	9.95E-04
2.28E+02	5.50E-04	1.73E+02	5.99E-04	1.35E+02	5.85E-04	6.50E+01	1.40E-03	1.08E+02	5.64E-04
3.42E+02	2.75E-04	2.60E+02	3.54E-04	1.80E+02	4.10E-04	9.19E+01	8.79E-04	1.77E+02	2.82E-04
4.85E+02	1.64E-04	3.68E+02	2.36E-04	2.56E+02	2.96E-04	1.35E+02	5.83E-04	2.55E+02	1.86E-04
7.13E+02	4.85E-05	5.41E+02	7.81E-05	3.76E+02	1.20E-04	2.72E+02	2.38E-04	2.93E+02	1.17E-04
9.98E+02	4.58E-06	8.01E+02	7.62E-06	5.26E+02	1.57E-05	4.44E+02	1.83E-05	3.85E+02	1.44E-05
1.28E+03	4.22E-07	9.74E+02	7.11E-07	6.76E+02	2.77E-06	5.71E+02	1.53E-06	4.92E+02	2.13E-06

Y=6.0 IN Z= .135 IN		Y=6.0 IN Z= .242 IN		Y=6.0 IN Z= .692 IN		Y=6.0 IN Z=1.274 IN		Y=6.0 IN Z=2.244 IN	
K (1/FT)	E(K)/$\overline{UU}$ (FT)	K (1/FT)	E(K)/$\overline{UU}$ (FT)	K (1/FT)	E(K)/$\overline{UU}$ (FT)	K (1/FT)	E(K)/$\overline{UU}$ (FT)	K (1/FT)	E(K)/$\overline{UU}$ (FT)
1.71E+00	1.00E-02	1.34E+00	9.62E-03	8.85E-01	1.80E-02	8.03E-01	1.66E-02	7.16E-01	3.56E-02
2.61E+00	9.40E-03	1.93E+00	2.96E-02	1.36E+00	2.92E-02	1.18E+00	2.49E-02	1.10E+00	4.20E-02
3.80E+00	9.97E-03	3.10E+00	2.55E-02	2.11E+00	3.74E-02	1.79E+00	3.00E-02	1.60E+00	4.52E-02
5.67E+00	1.01E-02	4.32E+00	2.22E-02	3.10E+00	3.81E-02	4.47E+00	2.23E-02	2.39E+00	3.56E-02
7.85E+00	1.24E-02	6.41E+00	1.58E-02	4.36E+00	3.66E-02	3.66E+00	3.51E-02	3.35E+00	3.18E-02
1.09E+01	9.38E-03	8.59E+00	1.27E-02	5.77E+00	2.64E-02	5.02E+00	2.97E-02	4.41E+00	2.76E-02
1.53E+01	7.25E-03	1.06E+01	1.20E-02	8.04E+00	1.88E-02	7.01E+00	2.81E-02	5.76E+00	2.76E-02
2.11E+01	6.02E-03	1.56E+01	8.50E-03	1.10E+01	1.19E-02	9.18E+00	1.91E-02	8.29E+00	2.05E-02
2.78E+01	4.85E-03	2.18E+01	6.01E-03	1.55E+01	8.13E-03	1.26E+01	1.26E-02	1.15E+01	1.25E-02
4.01E+01	3.73E-03	3.50E+01	3.50E-03	2.02E+01	6.00E-03	1.85E+01	7.40E-03	1.42E+01	9.07E-03
4.83E+01	3.62E-03	4.45E+01	2.88E-03	2.89E+01	3.56E-03	2.37E+01	5.17E-03	1.91E+01	6.32E-03
8.02E+01	2.50E-03	5.92E+01	2.38E-03	3.69E+01	2.68E-03	3.45E+01	2.96E-03	2.80E+01	3.57E-03
1.10E+02	1.77E-03	8.37E+01	1.55E-03	5.89E+01	1.51E-03	4.65E+01	1.99E-03	4.18E+01	2.23E-03
1.50E+02	1.26E-03	1.14E+02	1.06E-03	7.92E+01	1.11E-03	6.51E+01	1.33E-03	7.62E+01	9.60E-04
2.31E+02	6.23E-04	1.78E+02	6.10E-04	1.25E+02	6.41E-04	1.05E+02	7.35E-04	1.06E+02	6.73E-04
3.46E+02	2.95E-04	2.67E+02	3.40E-04	1.87E+02	3.86E-04	1.57E+02	4.50E-04	1.61E+02	3.88E-04
4.91E+02	1.81E-04	3.78E+02	2.32E-04	2.65E+02	2.51E-04	2.22E+02	3.45E-04	2.05E+02	2.93E-04
7.22E+02	5.99E-05	5.57E+02	9.13E-05	3.90E+02	1.24E-04	3.27E+02	1.53E-04	3.05E+02	1.49E-04
1.01E+03	6.25E-06	7.79E+02	1.18E-05	5.45E+02	1.81E-05	4.57E+02	2.42E-05	4.09E+02	1.53E-05
1.30E+03	5.47E-07	1.00E+03	8.90E-07	7.01E+02	1.53E-06	5.88E+02	2.16E-06	5.12E+02	2.28E-06

Table 5.5 Data on one-dimensional spectra at x = 10 ft, U_∞ = 30 ft/sec

Y=0.0 IN Z= .035 IN		Y=0.0 IN Z= .274 IN		Y=0.0 IN Z= .591 IN		Y=0.0 IN Z=1.119 IN		Y=0.0 IN Z=2.175 IN	
K (1/FT)	E(K)/$\overline{UU}$ (FT)	K (1/FT)	E(K)/$\overline{UU}$ (FT)	K (1/FT)	E(K)/$\overline{UU}$ (FT)	K (1/FT)	E(K)/$\overline{UU}$ (FT)	K (1/FT)	E(K)/$\overline{UU}$ (FT)
1.60E+00	8.12E-03	1.01E+00	2.74E-02	9.29E-01	3.04E-02	7.85E-01	5.24E-02	6.44E-01	6.10E-02
2.35E+00	1.66E-02	1.52E+00	3.65E-02	1.38E+00	4.45E-02	1.25E+00	6.60E-02	9.97E-01	5.90E-02
3.46E+00	1.77E-02	2.25E+00	3.45E-02	2.21E+00	4.07E-02	1.85E+00	6.58E-02	1.45E+00	5.77E-02
4.95E+00	1.65E-02	3.31E+00	3.04E-02	3.06E+00	3.02E-02	2.70E+00	5.18E-02	2.38E+00	4.94E-02
7.42E+00	1.46E-02	5.07E+00	2.62E-02	4.00E+00	2.48E-02	3.85E+00	3.77E-02	3.45E+00	4.20E-02
1.01E+01	1.26E-02	6.88E+00	1.70E-02	5.97E+00	1.89E-02	5.28E+00	2.82E-02	4.67E+00	3.25E-02
1.55E+01	8.90E-03	9.72E+00	1.14E-02	8.12E+00	1.64E-02	6.79E+00	2.05E-02	5.91E+00	2.68E-02
1.94E+01	7.39E-03	1.27E+01	8.52E-03	1.16E+01	1.06E-02	9.75E+00	1.32E-02	7.68E+00	1.95E-02
2.57E+01	8.70E-03	1.61E+01	7.02E-03	1.42E+01	8.58E-03	1.32E+01	8.98E-03	1.12E+01	1.27E-02
3.35E+01	4.81E-03	2.34E+01	4.89E-03	2.02E+01	5.12E-03	1.81E+01	6.45E-03	1.60E+01	7.62E-03
4.55E+01	3.40E-03	3.14E+01	3.25E-03	2.66E+01	3.76E-03	2.54E+01	4.04E-03	2.01E+01	5.14E-03
6.79E+01	2.15E-03	4.86E+01	1.97E-03	4.45E+01	2.10E-03	3.56E+01	2.64E-03	2.96E+01	2.89E-03
1.01E+02	1.25E-03	6.31E+01	1.50E-03	5.35E+01	1.60E-03	5.15E+01	1.49E-03	4.15E+01	1.67E-03
1.40E+02	7.24E-04	8.87E+01	1.02E-03	7.60E+01	1.06E-03	7.12E+01	9.94E-04	6.30E+01	1.05E-03
1.88E+02	3.71E-04	1.42E+02	5.45E-04	1.25E+02	5.38E-04	1.10E+02	5.22E-04	9.01E+01	6.32E-04
3.41E+02	1.36E-04	2.15E+02	2.92E-04	1.85E+02	2.80E-04	1.64E+02	2.84E-04	1.26E+02	3.94E-04
4.67E+02	3.41E-05	3.02E+02	1.99E-04	2.62E+02	1.86E-04	2.35E+02	1.89E-04	1.72E+02	2.25E-04
6.75E+02	1.08E-05	4.45E+02	1.07E-04	3.85E+02	1.00E-04	3.42E+02	1.02E-04	2.50E+02	1.52E-04
9.35E+02	1.75E-06	6.21E+02	2.30E-05	5.38E+02	2.28E-05	4.79E+02	2.28E-05	4.05E+02	3.58E-05
1.17E+03	1.40E-06	7.98E+02	1.81E-06	6.92E+02	2.05E-06	6.16E+02	1.76E-06	5.37E+02	2.28E-06

Y=1.0 IN Z= .035 IN		Y=1.0 IN Z= .276 IN		Y=1.0 IN Z= .591 IN		Y=1.0 IN Z=1.119 IN		Y=1.0 IN Z=2.177 IN	
K (1/FT)	E(K)/$\overline{UU}$ (FT)	K (1/FT)	E(K)/$\overline{UU}$ (FT)	K (1/FT)	E(K)/$\overline{UU}$ (FT)	K (1/FT)	E(K)/$\overline{UU}$ (FT)	K (1/FT)	E(K)/$\overline{UU}$ (FT)
1.50E+00	1.36E-02	1.12E+00	3.08E-02	9.71E-01	3.45E-02	9.66E-01	4.71E-02	7.45E-01	2.94E-02
2.15E+00	2.10E-02	1.60E+00	3.95E-02	1.38E+00	3.31E-02	1.61E+00	5.36E-02	1.00E+00	6.57E-02
3.60E+00	2.25E-02	2.17E+00	4.01E-02	1.95E+00	6.01E-02	2.21E+00	4.08E-02	1.65E+00	5.65E-02
5.68E+00	1.95E-02	3.69E+00	2.66E-02	3.05E+00	4.39E-02	3.35E+00	3.20E-02	2.28E+00	5.70E-02
8.47E+00	1.31E-02	5.19E+00	1.92E-02	4.12E+00	3.35E-02	4.21E+00	3.24E-02	3.02E+00	5.89E-02
1.08E+01	1.07E-02	7.27E+00	1.55E-02	6.16E+00	2.27E-02	6.17E+00	2.35E-02	4.55E+00	3.77E-02
1.39E+01	1.01E-02	9.64E+00	1.21E-02	9.09E+00	1.46E-02	7.56E+00	1.95E-02	5.97E+00	2.64E-02
1.81E+01	9.24E-03	1.35E+01	8.25E-03	1.32E+01	9.60E-03	9.99E+00	1.45E-02	8.35E+00	1.72E-02
2.55E+01	7.15E-03	1.85E+01	5.28E-03	1.69E+01	7.07E-03	1.42E+01	8.56E-03	1.25E+01	1.02E-02
3.08E+01	5.52E-03	2.51E+01	3.74E-03	2.16E+01	5.05E-03	1.88E+01	6.20E-03	1.62E+01	6.31E-03
4.81E+01	3.54E-03	3.25E+01	2.82E-03	2.74E+01	3.76E-03	2.34E+01	4.67E-03	2.30E+01	3.75E-03
7.08E+01	2.19E-03	4.71E+01	2.11E-03	4.31E+01	2.32E-03	3.27E+01	3.02E-03	3.55E+01	2.16E-03
9.97E+01	1.28E-03	6.79E+01	1.37E-03	6.22E+01	1.42E-03	5.09E+01	1.65E-03	4.66E+01	1.47E-03
1.31E+02	9.49E-04	9.50E+01	9.77E-04	8.11E+01	1.08E-03	7.14E+01	1.08E-03	6.78E+01	8.85E-04
2.04E+02	4.04E-04	1.46E+02	5.15E-04	1.26E+02	5.35E-04	1.11E+02	5.56E-04	1.05E+02	4.46E-04
3.18E+02	1.30E-04	2.19E+02	2.80E-04	1.89E+02	2.91E-04	1.66E+02	2.95E-04	1.67E+02	2.25E-04
4.96E+02	4.47E-05	3.10E+02	1.91E-04	2.67E+02	1.95E-04	2.35E+02	2.01E-04	2.45E+02	1.72E-04
6.46E+02	1.75E-05	4.56E+02	9.41E-05	3.95E+02	9.74E-05	3.46E+02	1.12E-04	3.52E+02	7.09E-05
8.68E+02	1.92E-06	6.39E+02	1.87E-05	5.50E+02	2.00E-05	4.84E+02	2.47E-05	4.40E+02	1.15E-05
1.16E+03	1.40E-07	8.22E+02	1.45E-06	7.07E+02	1.75E-06	6.25E+02	2.08E-06	5.55E+02	2.19E-06

Y=2.0 IN Z= .035 IN		Y=2.0 IN Z= .276 IN		Y=2.0 IN Z= .591 IN		Y=2.0 IN Z=1.119 IN		Y=2.0 IN Z=2.175 IN	
K (1/FT)	E(K)/$\overline{UU}$ (FT)	K (1/FT)	E(K)/$\overline{UU}$ (FT)	K (1/FT)	E(K)/$\overline{UU}$ (FT)	K (1/FT)	E(K)/$\overline{UU}$ (FT)	K (1/FT)	E(K)/$\overline{UU}$ (FT)
1.69E+00	1.71E-02	1.04E+00	1.51E-02	9.45E-01	3.27E-02	8.24E-01	6.75E-02	6.92E-01	3.90E-02
2.28E+00	1.77E-02	1.58E+00	4.82E-02	1.36E+00	5.31E-02	1.21E+00	6.46E-02	9.09E-01	7.39E-02
3.20E+00	1.74E-02	2.62E+00	4.54E-02	2.25E+00	4.19E-02	1.77E+00	5.48E-02	1.55E+00	6.32E-02
5.18E+00	1.76E-02	4.25E+00	2.85E-02	3.28E+00	3.17E-02	2.91E+00	4.31E-02	2.45E+00	5.25E-02
6.82E+00	1.95E-02	5.67E+00	2.25E-02	4.54E+00	2.44E-02	4.34E+00	3.39E-02	3.54E+00	4.95E-02
9.17E+00	1.77E-02	7.25E+00	1.85E-02	5.98E+00	2.04E-02	5.65E+00	2.76E-02	4.81E+00	4.25E-02
1.30E+01	1.24E-02	1.04E+01	1.26E-02	8.88E+00	1.49E-02	7.05E+00	2.20E-02	6.14E+00	2.91E-02
1.95E+01	8.89E-03	1.37E+01	9.60E-03	1.11E+01	1.49E-02	9.55E+00	1.48E-02	8.66E+00	1.66E-02
2.41E+01	8.05E-03	2.07E+01	6.22E-03	1.56E+01	9.24E-03	1.28E+01	9.78E-03	1.10E+01	1.25E-02
3.45E+01	5.31E-03	2.85E+01	4.58E-03	2.05E+01	5.99E-03	1.75E+01	6.55E-03	1.47E+01	7.67E-03
4.76E+01	3.95E-03	3.48E+01	3.56E-03	2.78E+01	4.34E-03	2.47E+01	4.08E-03	2.00E+01	4.98E-03
8.25E+01	2.01E-03	4.95E+01	2.50E-03	4.28E+01	2.40E-03	3.65E+01	2.46E-03	2.90E+01	3.52E-03
1.21E+02	1.05E-03	7.06E+01	1.59E-03	6.11E+01	1.51E-03	5.28E+01	1.61E-03	4.47E+01	1.75E-03
1.77E+02	4.07E-04	9.64E+01	1.09E-03	8.09E+01	9.71E-04	6.87E+01	1.20E-03	6.16E+01	1.14E-03
2.45E+02	1.47E-04	1.47E+02	5.47E-04	1.26E+02	5.78E-04	1.10E+02	5.82E-04	1.02E+02	4.82E-04
3.26E+02	6.18E-05	2.21E+02	3.25E-04	1.89E+02	3.22E-04	1.65E+02	3.36E-04	1.59E+02	2.87E-04
4.47E+02	2.64E-05	3.15E+02	2.25E-04	2.68E+02	2.19E-04	2.34E+02	2.29E-04	2.59E+02	1.59E-04
6.41E+02	9.10E-06	4.60E+02	9.65E-05	3.94E+02	1.09E-04	3.45E+02	1.10E-04	3.38E+02	7.35E-05
8.92E+02	3.20E-06	6.44E+02	1.55E-05	5.51E+02	1.95E-05	4.81E+02	2.09E-05	4.12E+02	2.17E-05
1.14E+03	2.25E-06	8.28E+02	1.24E-06	7.09E+02	1.40E-06	6.18E+02	1.55E-06	5.25E+02	2.28E-06

Table 5.5 Data on one-dimensional spectra at x = 10 ft, U_∞ = 30 ft/sec -- Continued

Y=2.5 IN Z= .035 IN		Y=2.5 IN Z= .276 IN		Y=2.5 IN Z= .591 IN		Y=2.5 IN Z=1.119 IN		Y=2.5 IN Z=2.175 IN	
K (1/FT)	E(K)/$\overline{UU}$ (FT)	K (1/FT)	E(K)/$\overline{UU}$ (FT)	K (1/FT)	E(K)/$\overline{UU}$ (FT)	K (1/FT)	E(K)/$\overline{UU}$ (FT)	K (1/FT)	E(K)/$\overline{UU}$ (FT)
1.58E+00	6.29E-03	1.29E+00	2.45E-02	9.14E-01	3.84E-02	8.74E-01	3.01E-02	6.96E-01	5.49E-02
2.55E+00	1.09E-02	1.85E+00	3.65E-02	1.24E+00	5.34E-02	1.17E+00	5.85E-02	1.05E+00	6.49E-02
3.68E+00	1.70E-02	2.95E+00	3.97E-02	2.52E+00	4.51E-02	1.81E+00	6.55E-02	1.60E+00	7.86E-02
5.40E+00	1.72E-02	3.96E+00	2.97E-02	3.46E+00	3.43E-02	2.64E+00	4.85E-02	2.31E+00	7.02E-02
7.04E+00	1.47E-02	5.62E+00	2.00E-02	4.20E+00	2.89E-02	3.63E+00	3.90E-02	3.36E+00	5.31E-02
1.01E+01	1.12E-02	7.31E+00	1.81E-02	6.80E+00	1.82E-02	5.39E+00	2.55E-02	4.88E+00	3.57E-02
1.39E+01	9.36E-03	9.02E+00	1.06E-02	8.40E+00	1.48E-02	6.65E+00	2.09E-02	6.42E+00	2.56E-02
1.90E+01	8.01E-03	1.58E+01	9.69E-03	1.07E+01	1.36E-02	9.73E+00	1.47E-02	8.93E+00	1.77E-02
2.44E+01	6.70E-03	1.72E+01	8.72E-03	1.60E+01	8.79E-03	1.34E+01	1.10E-02	1.16E+01	1.09E-02
3.29E+01	4.91E-03	2.74E+01	5.82E-03	2.01E+01	6.36E-03	1.70E+01	7.39E-03	1.68E+01	6.95E-03
4.59E+01	3.37E-03	3.45E+01	4.37E-03	2.78E+01	3.91E-03	2.52E+01	4.50E-03	2.16E+01	5.16E-03
5.91E+01	2.29E-03	4.65E+01	2.57E-03	3.98E+01	2.67E-03	3.66E+01	2.70E-03	3.17E+01	3.24E-03
9.74E+01	9.98E-04	7.15E+01	1.52E-03	6.48E+01	1.42E-03	4.81E+01	1.76E-03	4.55E+01	2.02E-03
1.35E+02	5.04E-04	9.39E+01	1.11E-03	8.15E+01	1.09E-03	6.21E+01	1.39E-03	6.11E+01	1.34E-03
2.09E+02	1.58E-04	1.54E+02	5.48E-04	1.28E+02	5.68E-04	1.10E+02	6.29E-04	9.69E+01	6.21E-04
3.06E+02	4.39E-05	2.31E+02	2.96E-04	1.92E+02	3.12E-04	1.65E+02	3.40E-04	1.58E+02	2.79E-04
4.40E+02	1.44E-05	3.27E+02	2.01E-04	2.73E+02	2.10E-04	2.34E+02	2.26E-04	2.68E+02	1.74E-04
6.47E+02	2.56E-06	4.81E+02	1.05E-04	4.01E+02	1.09E-04	3.44E+02	1.24E-04	3.58E+02	7.17E-05
8.87E+02	3.76E-07	6.73E+02	2.05E-05	5.61E+02	2.20E-05	4.81E+02	2.84E-05	4.50E+02	1.33E-05
1.15E+03	1.55E-07	8.66E+02	1.64E-06	7.22E+02	1.72E-06	6.19E+02	2.21E-06	5.45E+02	3.21E-06

Y=3.0 IN Z= .105 IN		Y=3.0 IN Z= .274 IN		Y=3.0 IN Z= .591 IN		Y=3.0 IN Z=1.119 IN		Y=3.0 IN Z=2.175 IN	
K (1/FT)	E(K)/$\overline{UU}$ (FT)	K (1/FT)	E(K)/$\overline{UU}$ (FT)	K (1/FT)	E(K)/$\overline{UU}$ (FT)	K (1/FT)	E(K)/$\overline{UU}$ (FT)	K (1/FT)	E(K)/$\overline{UU}$ (FT)
1.72E+00	4.47E-03	1.20E+00	1.75E-02	1.01E+00	3.31E-02	7.87E-01	6.10E-02	7.66E-01	6.50E-02
2.32E+00	8.45E-03	1.72E+00	2.33E-02	1.42E+00	3.24E-02	1.20E+00	8.70E-02	1.08E+00	6.39E-02
3.52E+00	1.37E-02	2.44E+00	3.15E-02	2.05E+00	3.70E-02	1.79E+00	7.19E-02	1.55E+00	7.12E-02
5.54E+00	1.36E-02	4.05E+00	2.24E-02	3.00E+00	2.68E-02	2.80E+00	4.80E-02	2.36E+00	6.25E-02
7.87E+00	1.15E-02	5.82E+00	2.28E-02	5.33E+00	1.86E-02	4.38E+00	3.06E-02	3.37E+00	4.67E-02
1.12E+01	9.05E-03	8.21E+00	1.62E-02	6.80E+00	1.52E-02	5.71E+00	2.42E-02	4.76E+00	3.06E-02
1.52E+01	7.21E-03	1.14E+01	1.26E-02	9.61E+00	1.40E-02	7.23E+00	2.29E-02	5.75E+00	2.45E-02
1.94E+01	6.15E-03	1.46E+01	9.79E-03	1.21E+01	1.38E-02	9.09E+00	1.90E-02	8.82E+00	1.45E-02
2.79E+01	4.91E-03	2.17E+01	6.69E-03	1.58E+01	9.45E-03	1.25E+01	1.41E-02	1.34E+01	9.45E-03
3.70E+01	4.20E-03	2.51E+01	5.77E-03	2.08E+01	6.22E-03	1.63E+01	9.00E-03	1.73E+01	6.34E-03
4.78E+01	3.50E-03	3.53E+01	4.27E-03	2.71E+01	4.42E-03	2.52E+01	4.71E-03	2.13E+01	5.26E-03
6.35E+01	2.55E-03	5.20E+01	2.71E-03	3.92E+01	2.61E-03	3.38E+01	3.34E-03	3.02E+01	3.15E-03
1.13E+02	1.40E-03	7.63E+01	1.74E-03	6.41E+01	1.47E-03	5.10E+01	1.85E-03	4.27E+01	1.97E-03
1.57E+02	9.02E-04	1.08E+02	1.17E-03	8.47E+01	9.70E-04	6.90E+01	1.24E-03	5.87E+01	1.22E-03
2.36E+02	3.89E-04	1.65E+02	5.52E-04	1.31E+02	5.54E-04	1.11E+02	6.38E-04	1.05E+02	7.02E-04
3.46E+02	1.78E-04	2.48E+02	2.99E-04	1.96E+02	3.00E-04	1.66E+02	3.57E-04	1.60E+02	4.07E-04
5.21E+02	7.55E-05	3.51E+02	2.06E-04	2.78E+02	2.09E-04	2.35E+02	2.46E-04	2.13E+02	2.26E-04
7.11E+02	3.20E-05	5.16E+02	9.97E-05	4.09E+02	1.11E-04	3.46E+02	1.31E-04	2.90E+02	1.51E-04
9.39E+02	4.37E-06	7.22E+02	1.78E-05	5.72E+02	2.20E-05	4.85E+02	2.82E-05	4.13E+02	2.54E-05
1.22E+03	3.68E-07	9.28E+02	1.58E-06	7.56E+02	1.69E-06	6.25E+02	2.08E-06	5.31E+02	1.85E-06

Y=3.5 IN Z= .126 IN		Y=3.5 IN Z= .276 IN		Y=3.5 IN Z= .591 IN		Y=3.5 IN Z=1.119 IN		Y=3.5 IN Z=2.175 IN	
K (1/FT)	E(K)/$\overline{UU}$ (FT)	K (1/FT)	E(K)/$\overline{UU}$ (FT)	K (1/FT)	E(K)/$\overline{UU}$ (FT)	K (1/FT)	E(K)/$\overline{UU}$ (FT)	K (1/FT)	E(K)/$\overline{UU}$ (FT)
2.14E+00	6.98E-03	1.24E+00	1.92E-02	9.61E-01	5.21E-02	8.60E-01	4.70E-02	7.28E-01	8.45E-02
2.87E+00	8.82E-03	1.97E+00	2.85E-02	1.59E+00	5.34E-02	1.26E+00	4.76E-02	1.19E+00	7.42E-02
4.69E+00	7.63E-03	2.99E+00	2.28E-02	2.21E+00	4.61E-02	1.72E+00	4.50E-02	1.60E+00	6.30E-02
7.41E+00	5.20E-03	4.69E+00	1.69E-02	3.36E+00	3.59E-02	2.90E+00	3.65E-02	2.27E+00	5.15E-02
1.05E+01	6.31E-03	6.76E+00	1.25E-02	4.67E+00	2.62E-02	3.95E+00	2.78E-02	3.46E+00	4.38E-02
1.54E+01	7.25E-03	8.50E+00	1.14E-02	6.12E+00	2.33E-02	5.09E+00	2.52E-02	4.39E+00	3.64E-02
2.09E+01	5.47E-03	1.19E+01	8.89E-03	8.97E+00	1.74E-02	7.05E+00	2.17E-02	6.14E+00	2.63E-02
2.44E+01	4.97E-03	1.65E+01	6.93E-03	1.19E+01	1.34E-02	9.34E+00	1.53E-02	8.51E+00	1.63E-02
2.89E+01	4.75E-03	2.37E+01	5.69E-03	1.55E+01	9.05E-03	1.33E+01	9.73E-03	1.06E+01	1.23E-02
5.11E+01	3.01E-03	3.04E+01	4.55E-03	2.28E+01	4.97E-03	1.80E+01	6.33E-03	1.62E+01	6.94E-03
6.76E+01	2.29E-03	4.20E+01	3.30E-03	3.03E+01	3.59E-03	2.40E+01	4.33E-03	2.16E+01	4.36E-03
9.85E+01	1.61E-03	5.42E+01	2.26E-03	4.03E+01	2.61E-03	3.48E+01	2.76E-03	2.92E+01	2.94E-03
1.40E+02	1.10E-03	8.13E+01	1.26E-03	5.98E+01	1.57E-03	5.20E+01	1.50E-03	4.60E+01	1.75E-03
1.73E+02	7.25E-04	1.13E+02	8.81E-04	7.85E+01	1.14E-03	6.74E+01	1.18E-03	6.26E+01	1.27E-03
2.79E+02	3.35E-04	1.84E+02	5.00E-04	1.34E+02	6.12E-04	1.11E+02	5.87E-04	1.08E+02	5.55E-04
4.19E+02	1.63E-04	2.76E+02	2.59E-04	2.02E+02	3.50E-04	1.66E+02	3.38E-04	1.57E+02	3.27E-04
5.94E+02	9.24E-05	3.91E+02	1.81E-04	2.86E+02	2.39E-04	2.35E+02	2.33E-04	2.34E+02	2.38E-04
8.73E+02	3.40E-05	5.74E+02	8.75E-05	4.20E+02	1.22E-04	3.46E+02	1.25E-04	3.08E+02	1.63E-04
1.22E+03	4.95E-06	8.04E+02	1.49E-05	5.88E+02	2.52E-05	4.84E+02	2.70E-05	3.86E+02	4.52E-05
1.57E+03	4.01E-07	1.05E+03	1.02E-06	7.56E+02	1.89E-06	6.22E+02	1.90E-06	5.10E+02	6.31E-06

Table 5.5 Data on one-dimensional spectra at x = 10 ft, U_∞ = 30 ft/sec -- Continued

Y=4.0 IN Z= .126 IN		Y=4.0 IN Z= .276 IN		Y=4.0 IN Z= .591 IN		Y=4.0 IN Z=1.119 IN		Y=4.0 IN Z=2.175 IN	
K (1/FT)	E(K)/$\overline{UU}$ (FT)	K (1/FT)	E(K)/$\overline{UU}$ (FT)	K (1/FT)	E(K)/$\overline{UU}$ (FT)	K (1/FT)	E(K)/$\overline{UU}$ (FT)	K (1/FT)	E(K)/$\overline{UU}$ (FT)
1.66E+00	1.29E-02	1.22E+00	2.22E-02	9.95E-01	4.20E-02	8.37E-01	6.20E-02	7.39E-01	6.35E-02
2.54E+00	1.24E-02	1.79E+00	1.87E-02	1.40E+00	4.51E-02	1.20E+00	6.30E-02	1.14E+00	6.25E-02
4.08E+00	9.41E-03	2.75E+00	1.94E-02	1.95E+00	4.56E-02	2.07E+00	5.39E-02	1.58E+00	6.88E-02
5.84E+00	9.80E-03	4.54E+00	2.08E-02	3.22E+00	3.52E-02	2.99E+00	4.55E-02	2.54E+00	4.62E-02
8.71E+00	8.71E-03	6.85E+00	1.55E-02	4.96E+00	2.50E-02	3.82E+00	4.21E-02	3.46E+00	5.20E-02
1.11E+01	7.99E-03	8.70E+00	1.42E-02	6.92E+00	2.08E-02	5.57E+00	3.31E-02	4.50E+00	3.31E-02
1.57E+01	6.79E-03	1.16E+01	1.18E-02	8.84E+00	1.61E-02	7.70E+00	2.50E-02	6.07E+00	2.38E-02
1.85E+01	6.36E-03	1.54E+01	8.56E-03	1.21E+01	1.20E-02	1.02E+01	1.56E-02	8.97E+00	1.99E-02
3.09E+01	3.99E-03	2.07E+01	6.65E-03	1.63E+01	9.58E-03	1.42E+01	9.09E-03	1.19E+01	1.16E-02
3.60E+01	3.69E-03	2.85E+01	5.22E-03	2.18E+01	6.40E-03	1.98E+01	5.74E-03	1.56E+01	7.31E-03
4.97E+01	3.12E-03	3.63E+01	4.56E-03	3.07E+01	4.06E-03	2.62E+01	4.48E-03	2.09E+01	4.83E-03
7.08E+01	2.46E-03	4.87E+01	2.93E-03	4.30E+01	2.75E-03	3.35E+01	3.31E-03	3.15E+01	3.07E-03
1.08E+02	1.56E-03	7.27E+01	1.79E-03	6.82E+01	1.32E-03	5.37E+01	1.89E-03	4.71E+01	2.00E-03
1.51E+02	9.80E-04	1.07E+02	1.16E-03	8.54E+01	9.73E-04	6.95E+01	1.15E-03	5.93E+01	1.52E-03
2.35E+02	4.64E-04	1.68E+02	5.25E-04	1.32E+02	5.90E-04	1.11E+02	6.42E-04	9.41E+01	6.75E-04
3.85E+02	1.80E-04	2.52E+02	2.71E-04	1.99E+02	3.20E-04	1.66E+02	3.46E-04	1.41E+02	3.58E-04
5.96E+02	7.76E-05	3.57E+02	1.80E-04	2.81E+02	2.25E-04	2.35E+02	2.41E-04	2.00E+02	2.44E-04
8.54E+02	1.51E-05	5.25E+02	7.78E-05	4.14E+02	1.05E-04	3.46E+02	1.32E-04	2.94E+02	1.32E-04
1.05E+03	3.17E-06	7.35E+02	1.28E-05	5.79E+02	1.88E-05	4.85E+02	2.68E-05	4.12E+02	2.87E-05
1.22E+03	9.77E-07	9.45E+02	1.21E-06	7.45E+02	1.55E-06	6.23E+02	1.96E-06	5.30E+02	2.42E-06

Y=5.0 IN Z= .126 IN		Y=5.0 IN Z= .274 IN		Y=5.0 IN Z= .591 IN		Y=5.0 IN Z=1.119 IN		Y=5.0 IN Z=2.175 IN	
K (1/FT)	E(K)/$\overline{UU}$ (FT)	K (1/FT)	E(K)/$\overline{UU}$ (FT)	K (1/FT)	E(K)/$\overline{UU}$ (FT)	K (1/FT)	E(K)/$\overline{UU}$ (FT)	K (1/FT)	E(K)/$\overline{UU}$ (FT)
1.67E+00	1.62E-02	1.42E+00	1.71E-02	9.62E-01	4.88E-02	8.31E-01	4.05E-02	7.09E-01	6.44E-02
2.48E+00	1.99E-02	1.86E+00	2.67E-02	1.95E+00	4.38E-02	1.25E+00	5.77E-02	9.74E-01	7.82E-02
3.92E+00	1.47E-02	2.91E+00	2.56E-02	2.36E+00	4.44E-02	1.86E+00	4.96E-02	1.51E+00	6.04E-02
6.18E+00	1.09E-02	4.91E+00	2.03E-02	3.54E+00	3.41E-02	3.10E+00	3.61E-02	2.29E+00	5.18E-02
8.05E+00	1.11E-02	6.27E+00	1.98E-02	5.35E+00	2.76E-02	4.34E+00	2.68E-02	3.55E+00	3.60E-02
1.07E+01	9.58E-03	8.59E+00	1.48E-02	6.87E+00	2.22E-02	6.42E+00	1.88E-02	4.92E+00	3.01E-02
1.57E+01	7.06E-03	1.16E+01	1.12E-02	9.90E+00	1.41E-02	7.61E+00	1.75E-02	6.57E+00	2.42E-02
2.03E+01	6.00E-03	1.62E+01	8.08E-03	1.29E+01	1.09E-02	1.04E+01	1.32E-02	8.63E+00	1.65E-02
2.71E+01	4.94E-03	2.22E+01	5.84E-03	1.67E+01	7.57E-03	1.39E+01	1.02E-02	1.14E+01	1.17E-02
3.75E+01	3.96E-03	2.81E+01	4.61E-03	2.24E+01	5.36E-03	1.87E+01	5.81E-03	1.69E+01	7.69E-03
4.96E+01	3.13E-03	4.05E+01	2.94E-03	3.20E+01	3.48E-03	2.34E+01	4.28E-03	2.14E+01	5.48E-03
6.91E+01	2.15E-03	6.09E+01	2.00E-03	4.61E+01	2.18E-03	3.58E+01	2.41E-03	3.14E+01	3.06E-03
1.17E+02	1.19E-03	8.68E+01	1.33E-03	6.36E+01	1.45E-03	5.13E+01	1.61E-03	4.33E+01	1.87E-03
1.48E+02	8.60E-04	1.17E+02	9.08E-04	8.97E+01	7.99E-04	7.04E+01	1.09E-03	6.41E+01	1.10E-03
2.25E+02	4.05E-04	1.94E+02	4.20E-04	1.37E+02	5.17E-04	1.13E+02	5.76E-04	1.05E+02	4.96E-04
3.37E+02	1.76E-04	2.85E+02	2.38E-04	2.06E+02	3.02E-04	1.69E+02	3.31E-04	1.38E+02	3.78E-04
4.77E+02	9.77E-05	3.97E+02	1.60E-04	2.92E+02	2.05E-04	2.39E+02	2.40E-04	1.86E+02	2.72E-04
7.02E+02	3.63E-05	5.22E+02	1.11E-04	4.30E+02	9.51E-05	3.52E+02	1.46E-04	2.51E+02	2.08E-04
9.83E+02	4.89E-06	6.62E+02	3.05E-05	6.01E+02	1.80E-05	4.93E+02	3.31E-05	3.97E+02	1.13E-04
1.26E+03	3.60E-07	9.29E+02	4.39E-06	7.73E+02	1.91E-06	6.34E+02	1.99E-06	5.20E+02	2.20E-05

Y=6.0 IN Z= .126 IN		Y=6.0 IN Z= .274 IN		Y=6.0 IN Z= .591 IN		Y=6.0 IN Z=1.119 IN		Y=6.0 IN Z=2.175 IN	
K (1/FT)	E(K)/$\overline{UU}$ (FT)	K (1/FT)	E(K)/$\overline{UU}$ (FT)	K (1/FT)	E(K)/$\overline{UU}$ (FT)	K (1/FT)	E(K)/$\overline{UU}$ (FT)	K (1/FT)	E(K)/$\overline{UU}$ (FT)
1.96E+00	6.44E-03	1.35E+00	1.42E-02	1.05E+00	2.01E-02	8.70E-01	4.79E-02	6.99E-01	6.66E-02
2.80E+00	1.35E-02	2.07E+00	2.88E-02	1.48E+00	3.77E-02	1.22E+00	5.81E-02	1.10E+00	8.55E-02
4.81E+00	1.09E-02	2.96E+00	3.27E-02	2.24E+00	3.89E-02	1.92E+00	5.86E-02	1.57E+00	8.12E-02
6.81E+00	1.27E-02	4.60E+00	2.89E-02	3.49E+00	3.49E-02	2.92E+00	4.67E-02	2.36E+00	5.64E-02
1.03E+01	9.93E-03	6.36E+00	2.45E-02	4.65E+00	2.89E-02	3.79E+00	4.10E-02	3.39E+00	4.16E-02
1.29E+01	9.07E-03	9.01E+00	1.60E-02	6.73E+00	2.14E-02	5.30E+00	3.10E-02	4.79E+00	3.35E-02
1.69E+01	8.25E-03	1.13E+01	1.19E-02	8.75E+00	1.64E-02	6.85E+00	2.26E-02	6.10E+00	2.86E-02
2.26E+01	6.45E-03	1.56E+01	8.39E-03	1.16E+01	1.21E-02	9.23E+00	1.65E-02	7.71E+00	2.13E-02
2.98E+01	5.15E-03	2.00E+01	6.45E-03	1.53E+01	8.96E-03	1.37E+01	1.00E-02	1.15E+01	1.24E-02
4.06E+01	4.44E-03	2.61E+01	4.75E-03	2.21E+01	5.71E-03	1.84E+01	7.37E-03	1.59E+01	8.45E-03
5.75E+01	3.14E-03	4.02E+01	3.24E-03	2.76E+01	4.16E-03	2.43E+01	4.98E-03	2.17E+01	5.39E-03
8.99E+01	1.84E-03	5.40E+01	2.52E-03	4.41E+01	2.50E-03	3.37E+01	3.17E-03	2.97E+01	3.46E-03
1.19E+02	1.33E-03	8.03E+01	1.55E-03	6.80E+01	1.59E-03	5.50E+01	1.57E-03	4.25E+01	2.00E-03
1.81E+02	7.01E-04	1.16E+02	9.33E-04	8.96E+01	1.07E-03	7.30E+01	1.01E-03	5.75E+01	1.40E-03
2.81E+02	3.14E-04	1.76E+02	5.11E-04	1.37E+02	5.21E-04	1.12E+02	6.01E-04	9.55E+01	6.95E-04
4.23E+02	1.23E-04	2.60E+02	2.61E-04	2.05E+02	2.85E-04	1.68E+02	3.37E-04	1.40E+02	3.73E-04
6.51E+02	4.16E-05	3.79E+02	1.64E-04	2.91E+02	1.95E-04	2.38E+02	2.41E-04	1.99E+02	2.51E-04
9.05E+02	1.06E-05	5.58E+02	6.72E-05	4.27E+02	1.25E-04	3.51E+02	1.18E-04	2.92E+02	1.57E-04
1.18E+03	1.43E-06	7.81E+02	1.03E-05	5.96E+02	2.69E-05	4.91E+02	2.10E-05	4.09E+02	2.94E-05
1.49E+03	2.00E-07	1.00E+03	7.91E-07	7.69E+02	1.20E-06	6.31E+02	9.34E-05	5.26E+02	2.19E-06

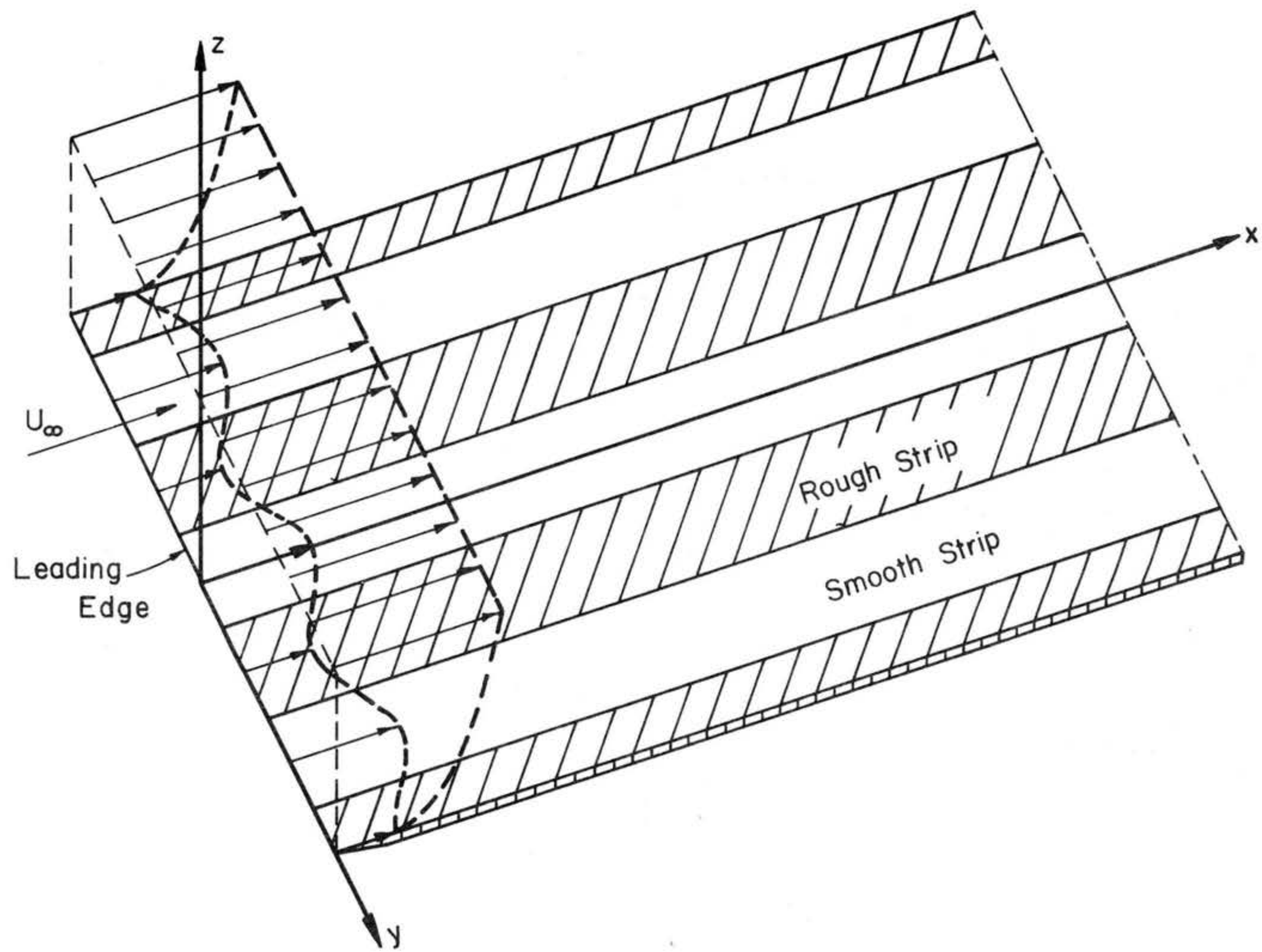

Fig. 1.1 Schematic presentation of boundary layer flow along alternate, longitudinal strips of smooth and rough surfaces

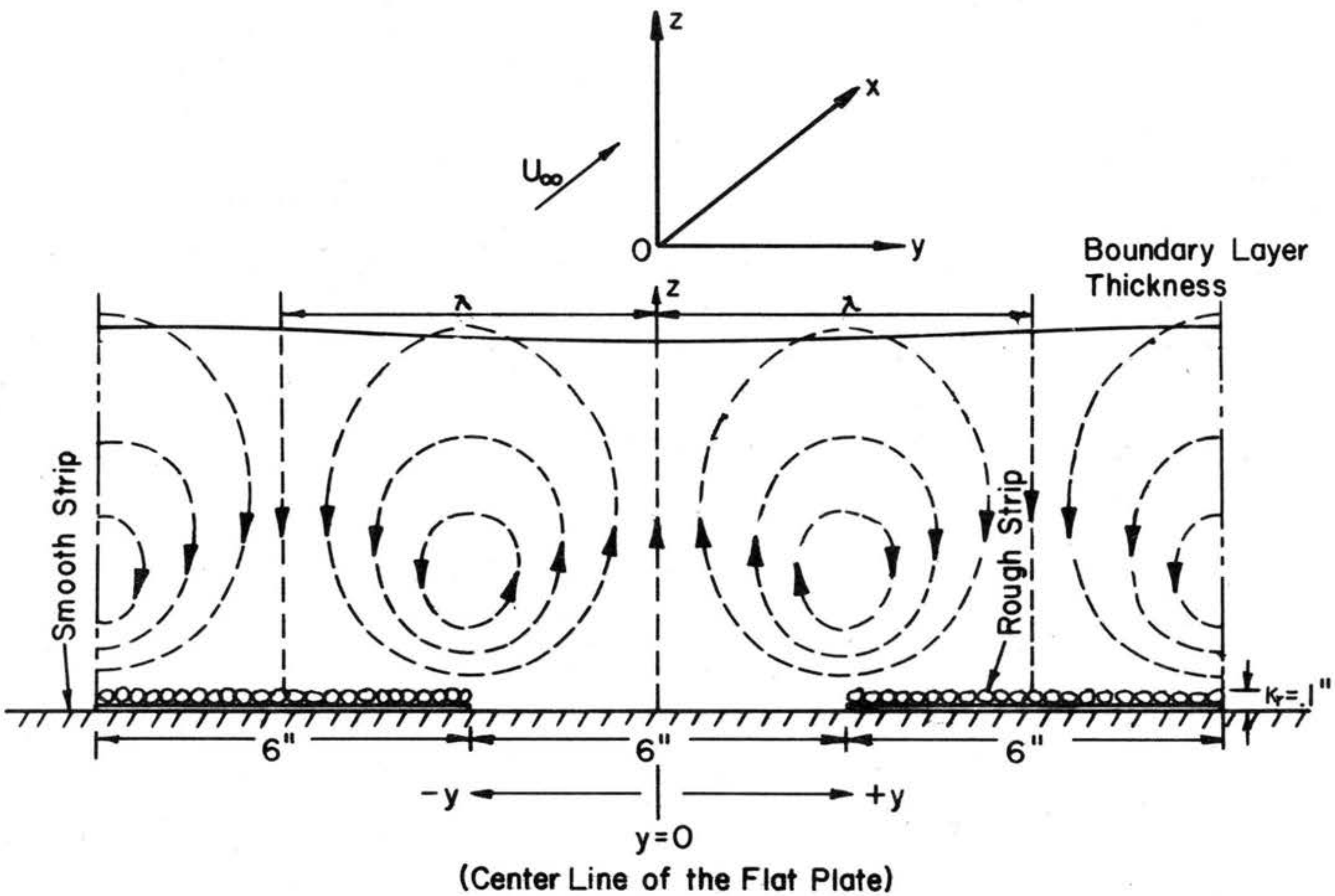

Fig. 1.2 Coordinate system and flow features

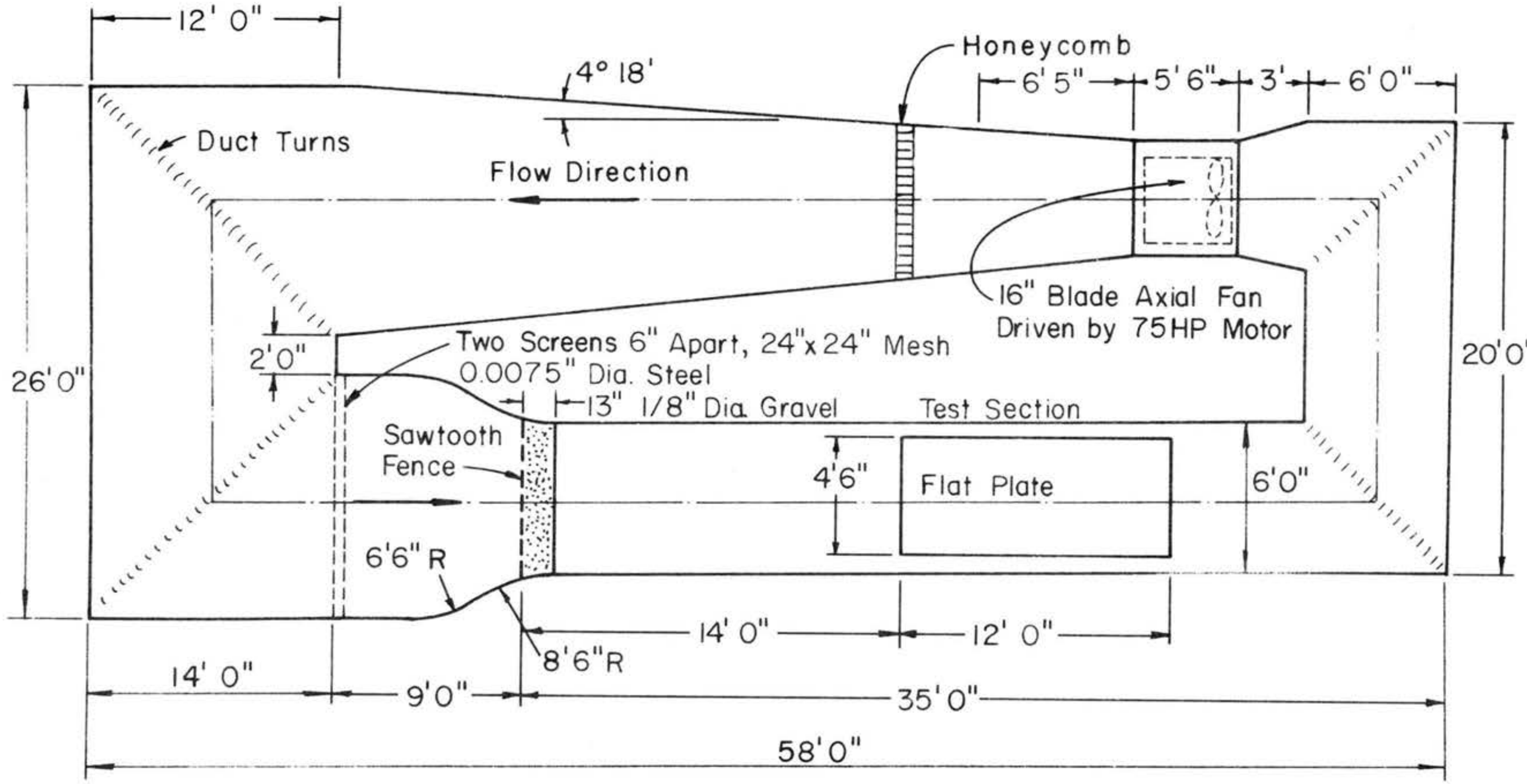

Fig. 4.1 Plan view of wind tunnel

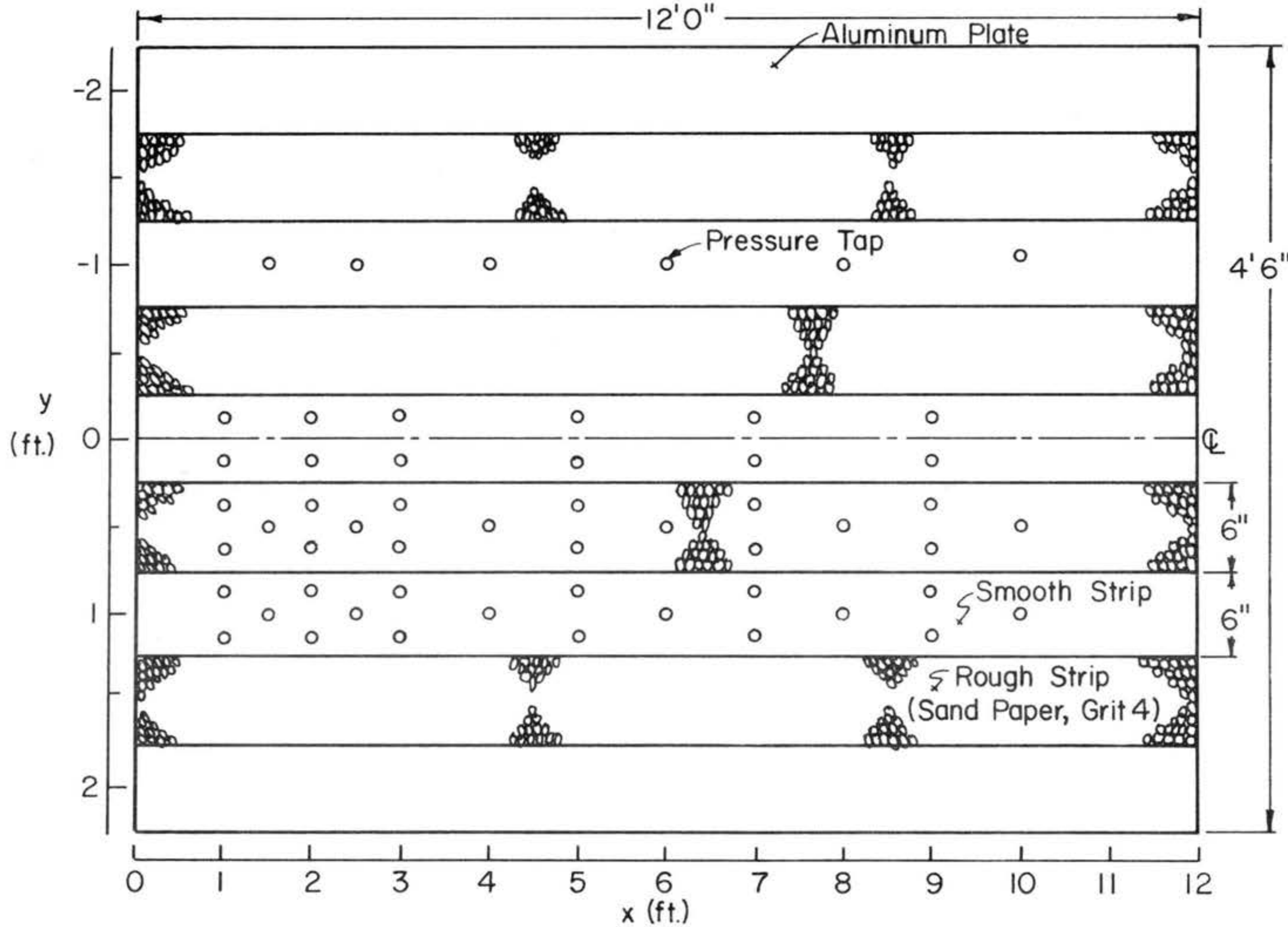

Fig. 4.2 Plan view of flat plate

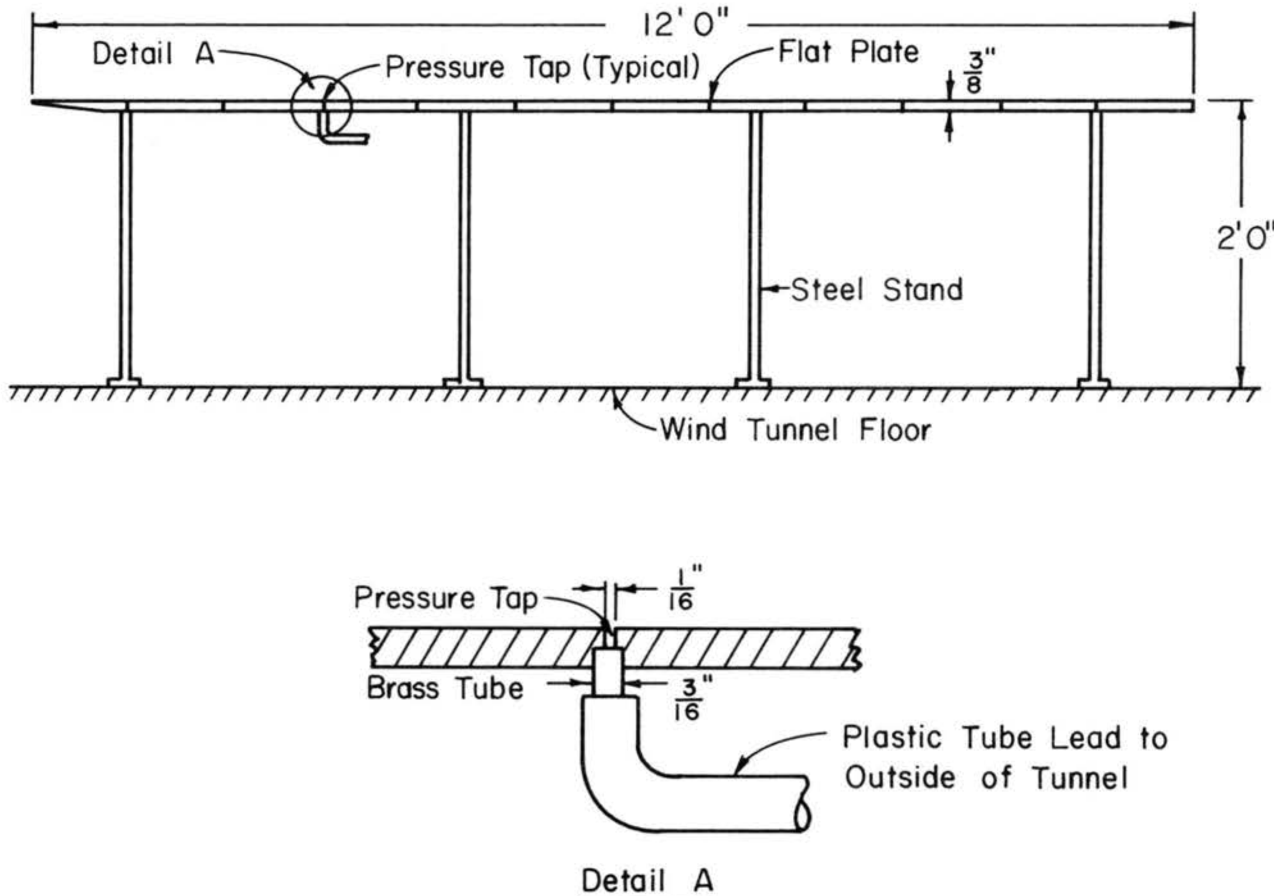

Fig. 4.3 Cross-sectional elevation of flat plate and pressure tape

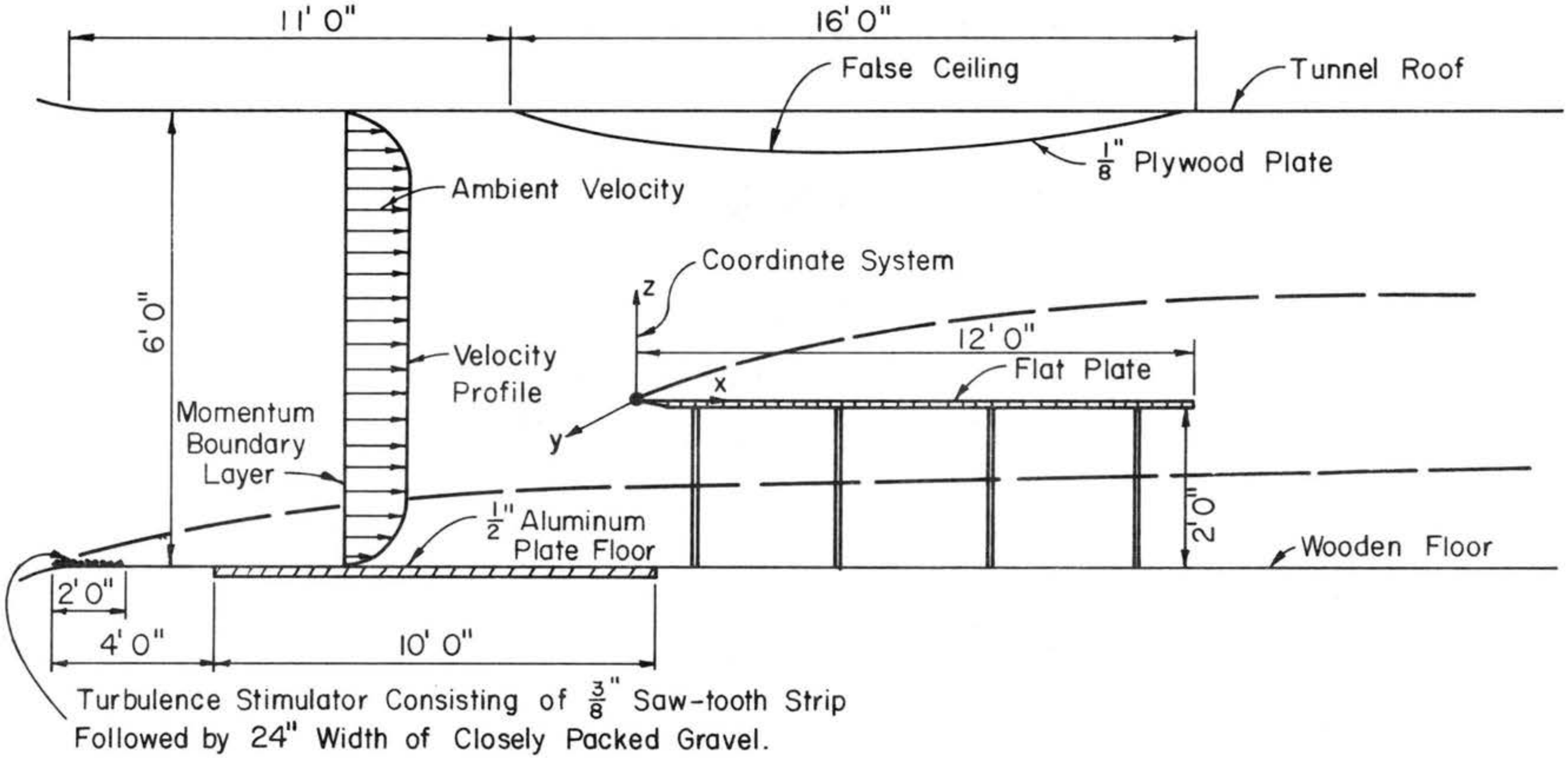

Fig. 4.4 Experimental arrangement in the test section of wind tunnel

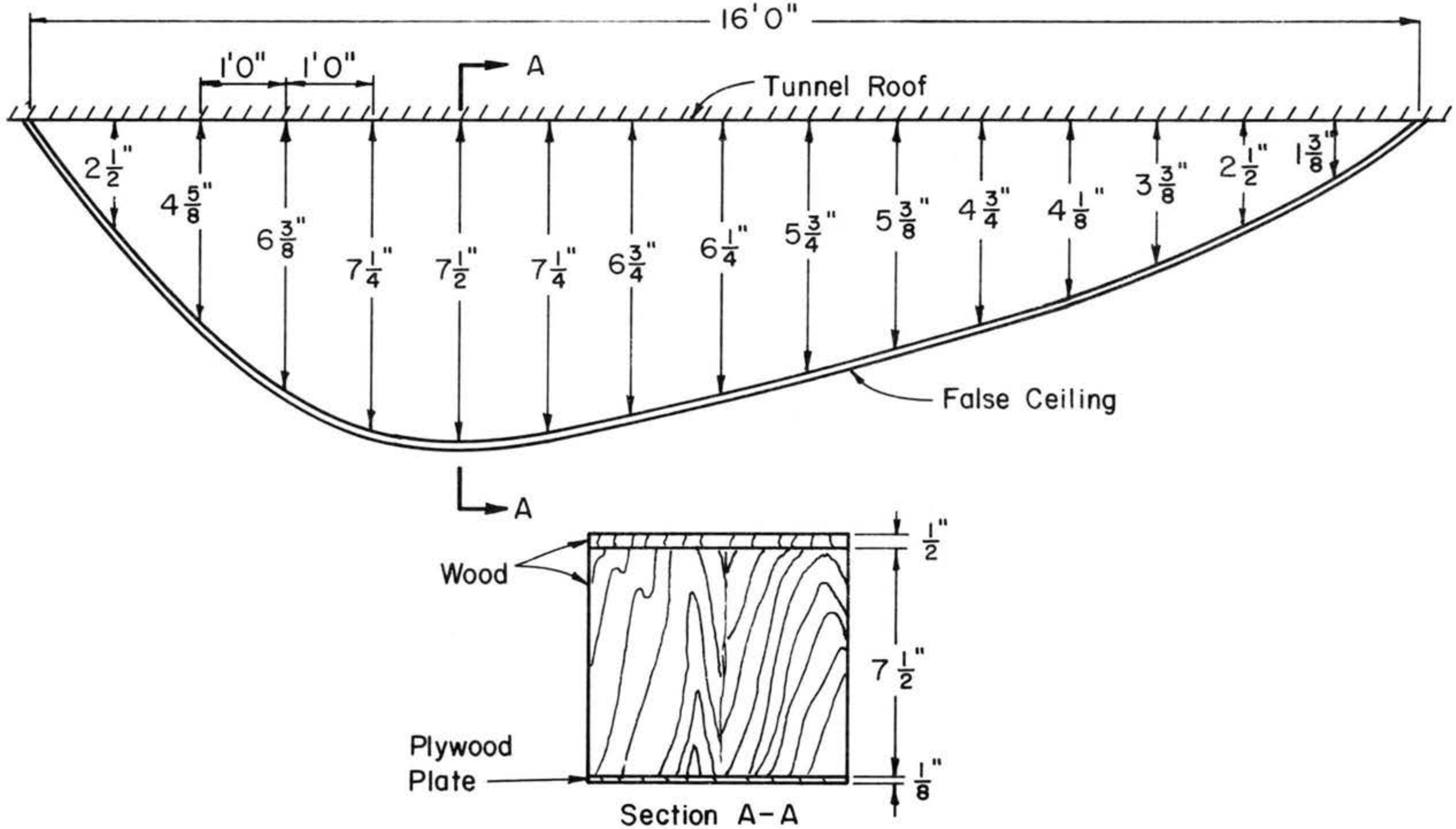

Fig. 4.5 False wind tunnel ceiling to obtain zero streamwise pressure gradient over flat plate

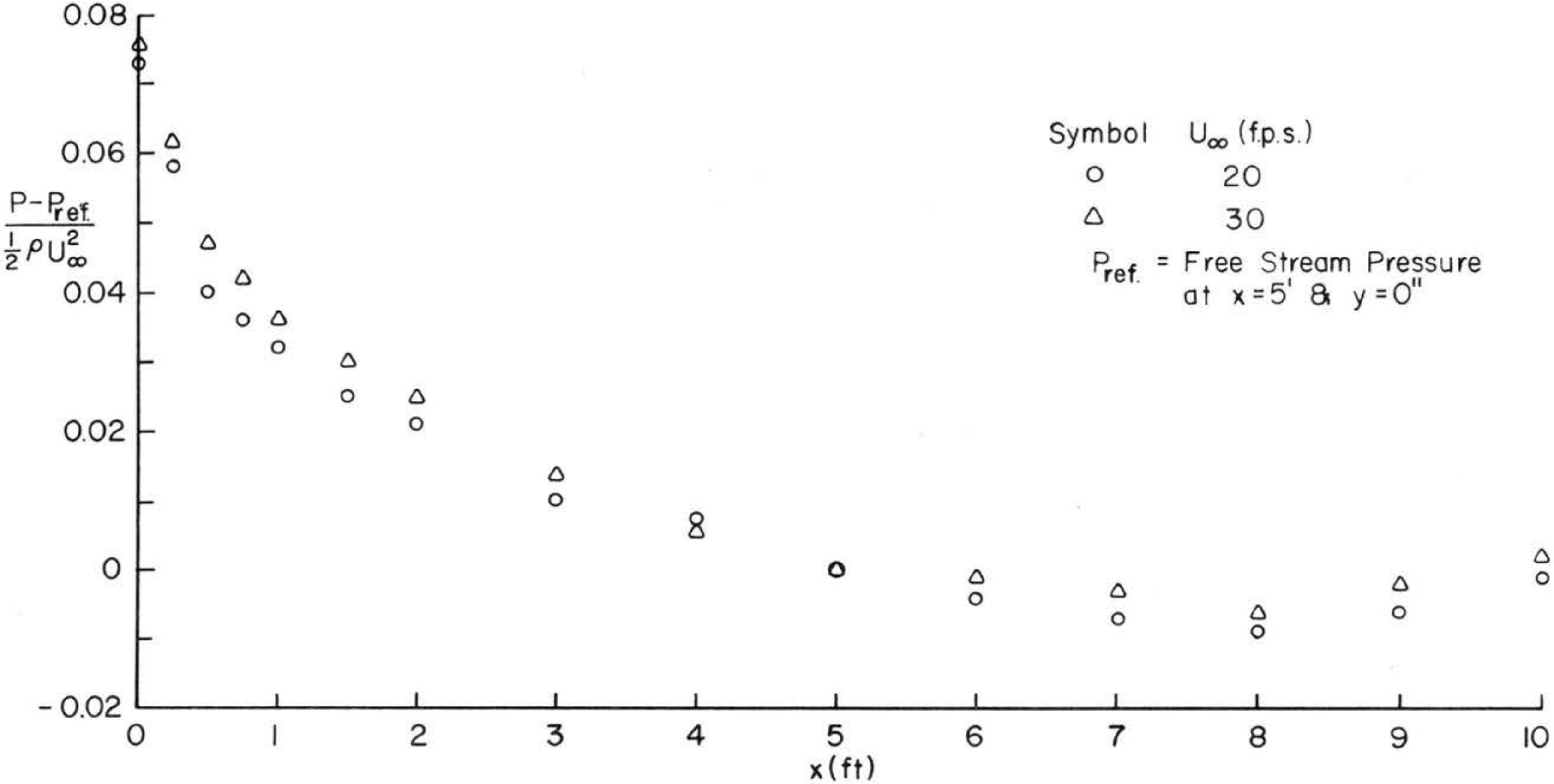

Fig. 4.6 Non-dimensional plot of static pressure distribution at the free stream along the centerline of the flat plate

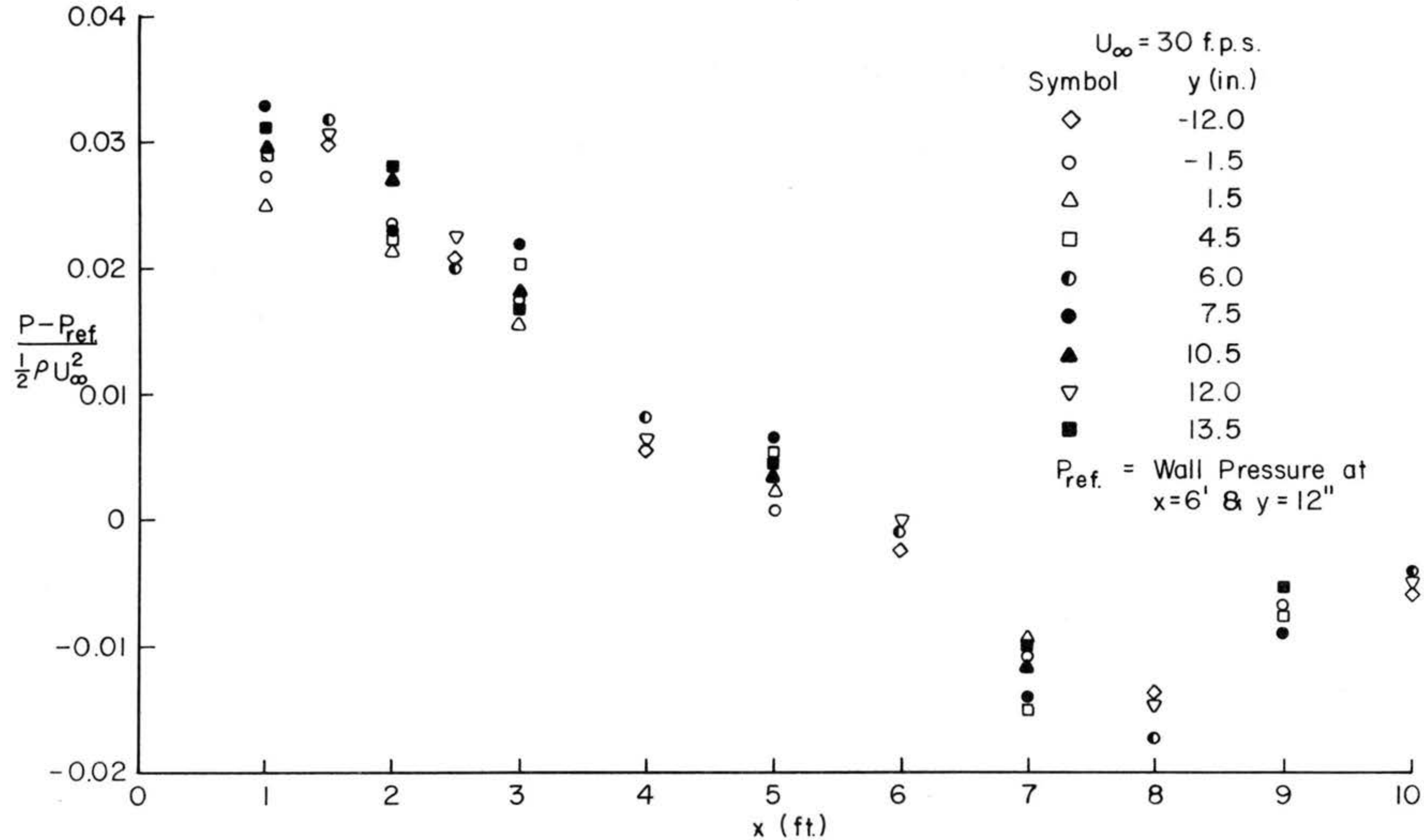

Fig. 4.7 Non-dimensional plot of wall pressure distribution of the flat plate

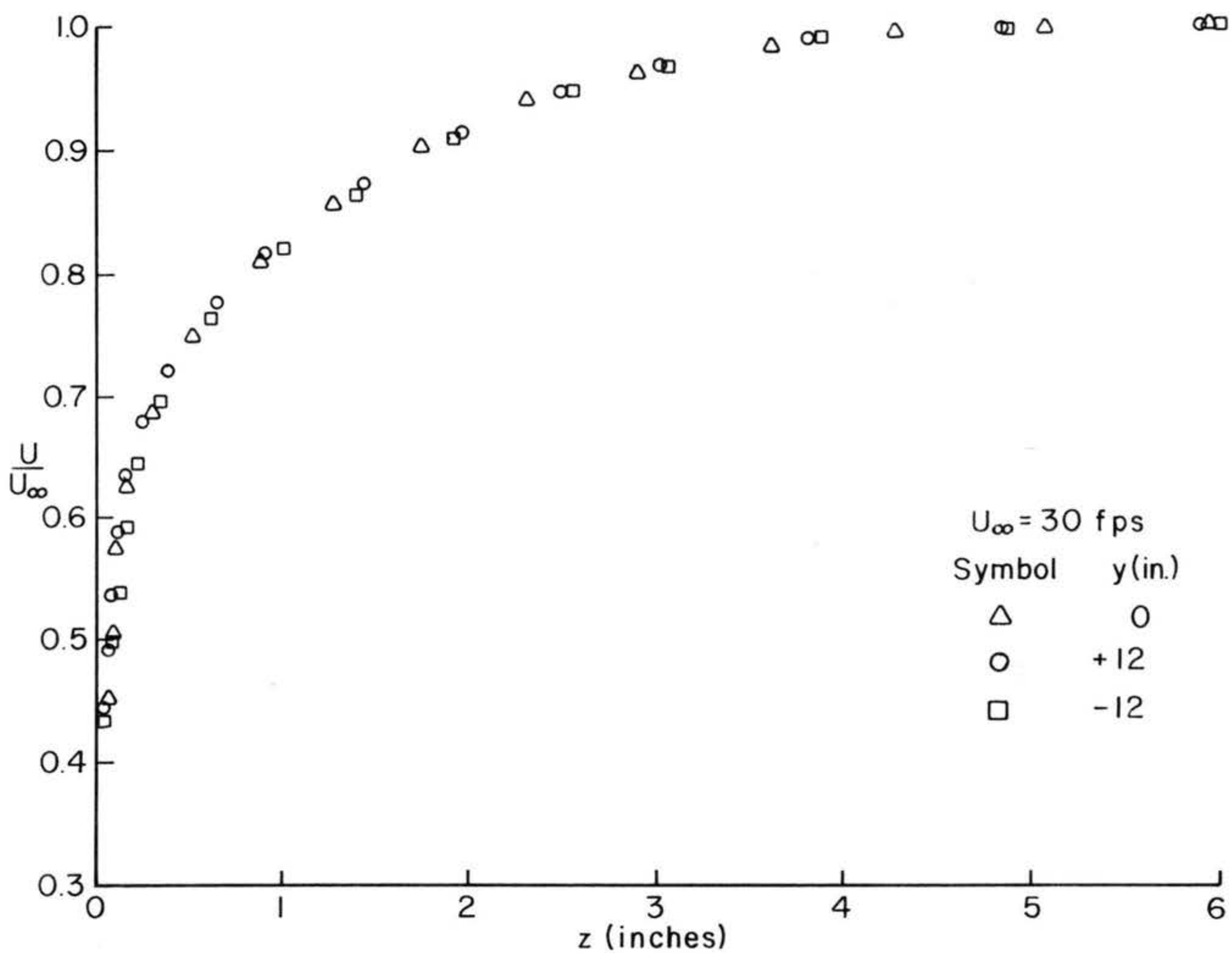

Fig. 4.8 Mean velocity distribution at x = 5 ft. to check plane symmetric condition of the flow

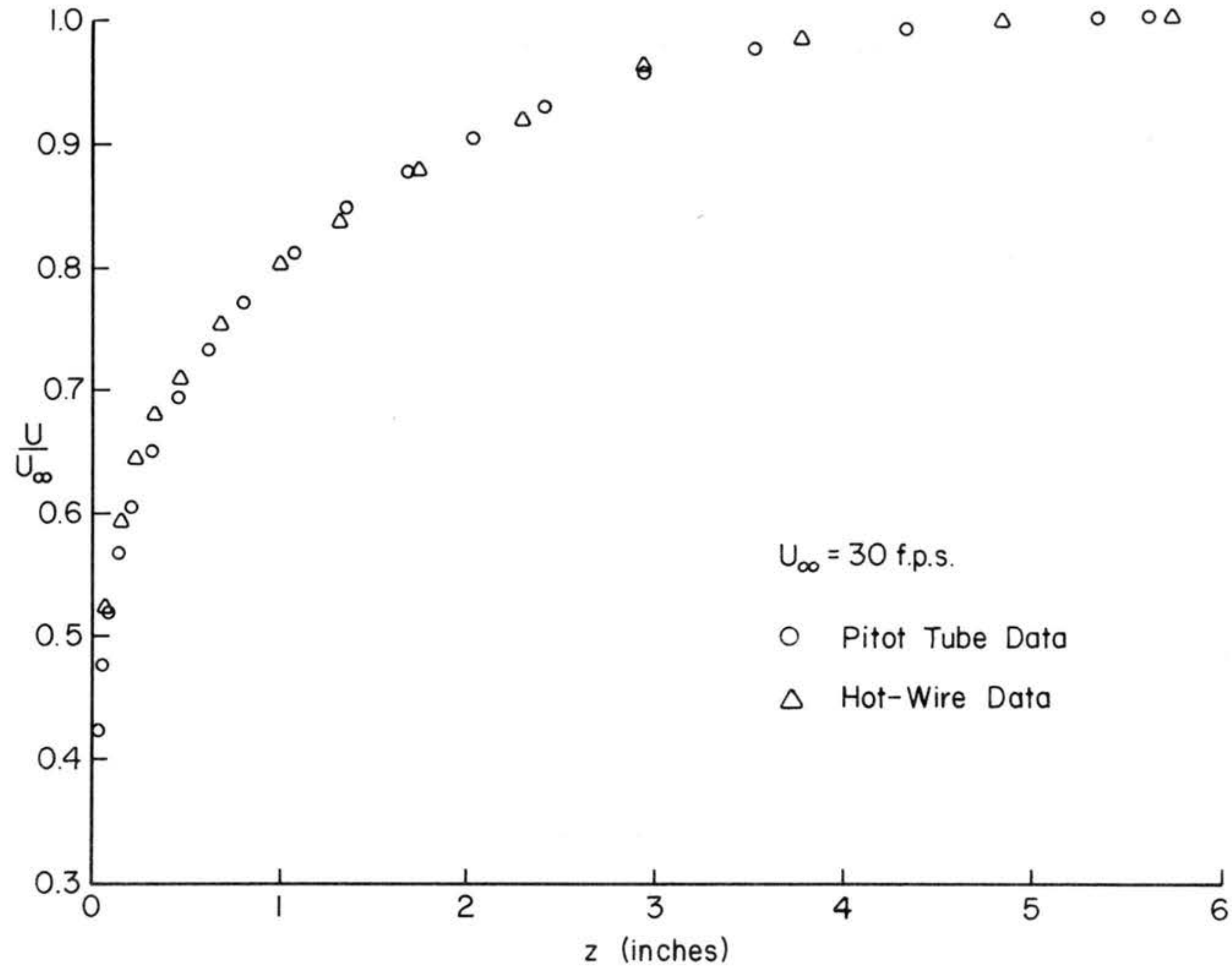

Fig. 4.9 Typical comparison of mean velocity profiles measured by hot-wire and pitot tube at x = 6 ft, y = o in.

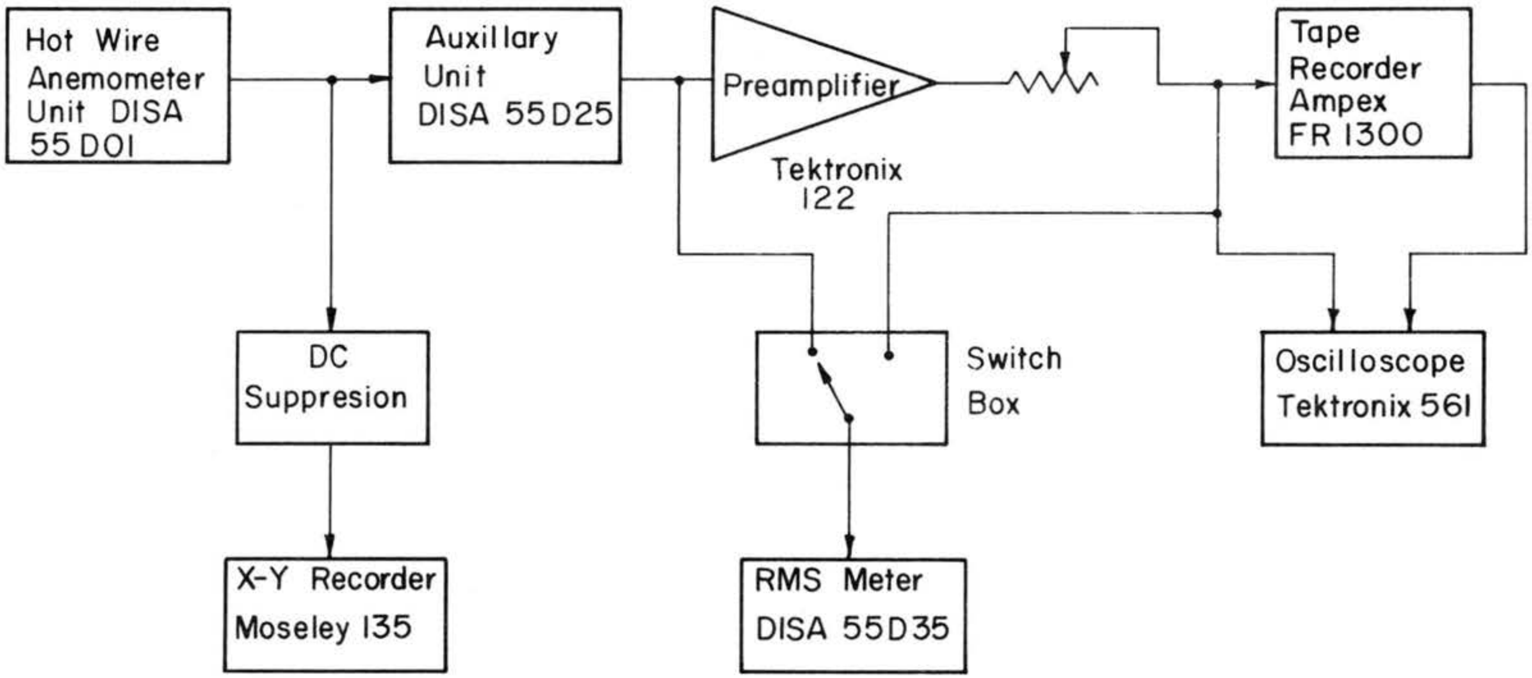

Fig. 4.10 Schematic diagram of single hot-wire measurement instrument

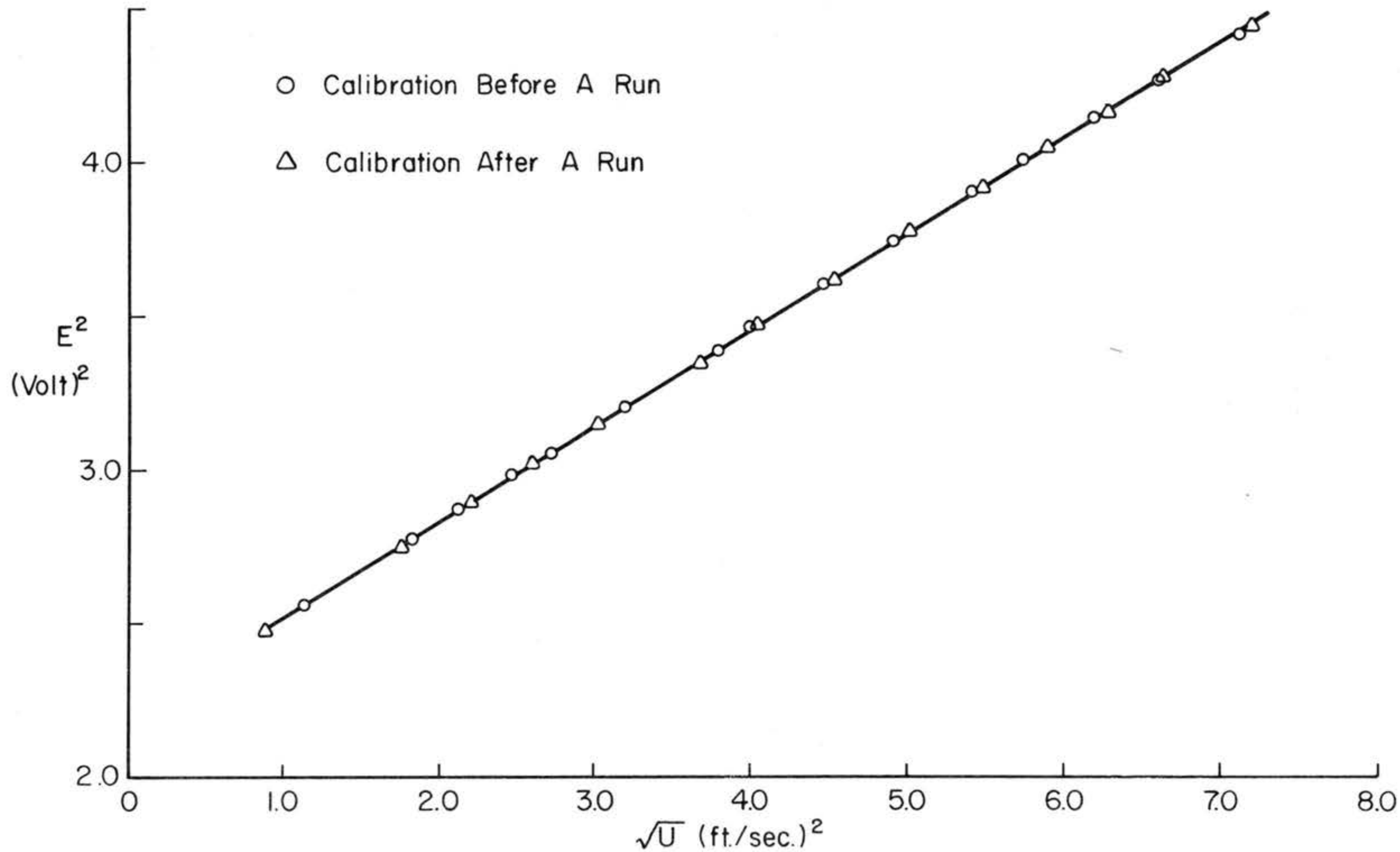

Fig. 4.11 Typical calibration curves of the single hot-wire

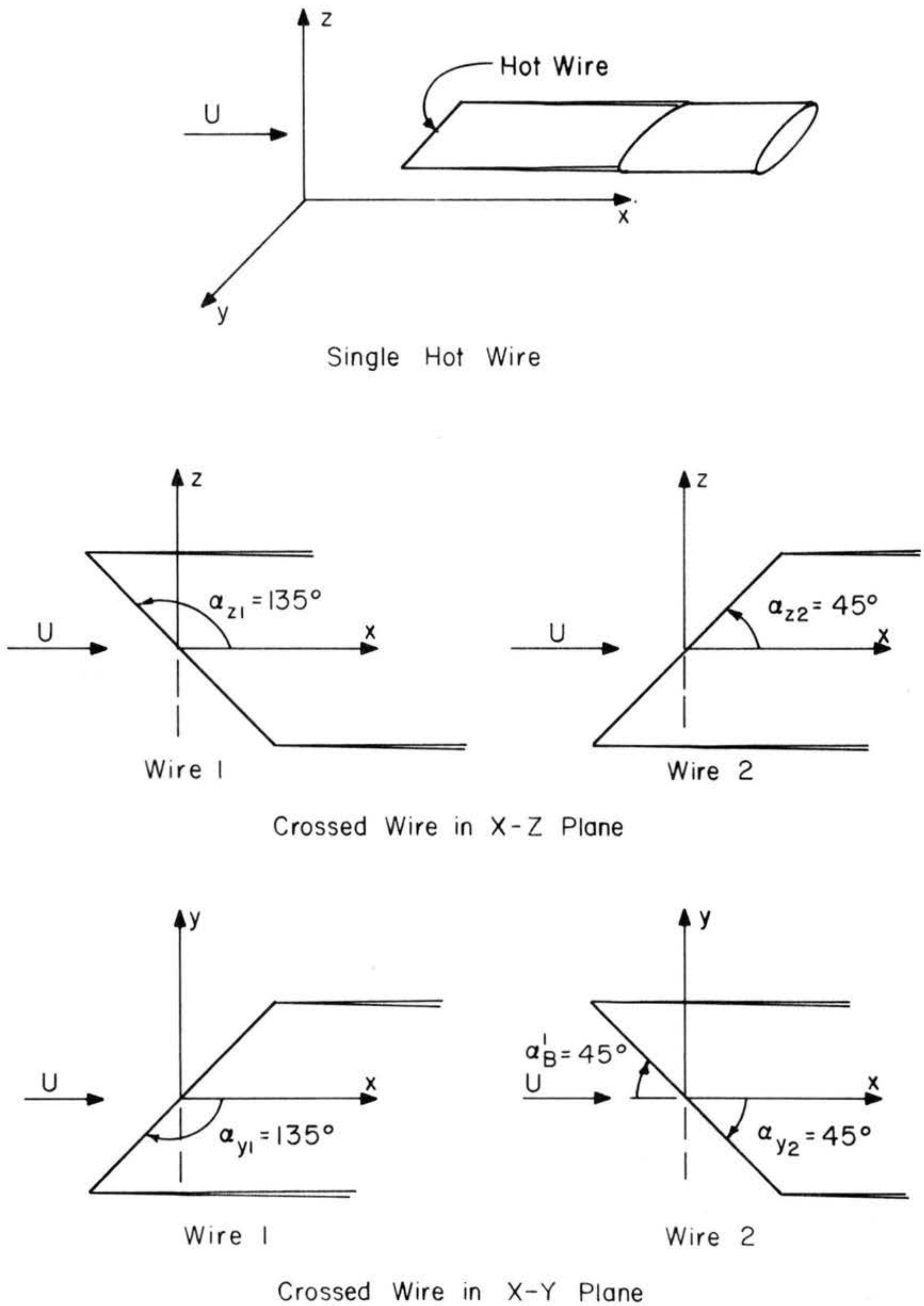

Fig. 4.12 Coordinates of the single and the crossed hot-wires

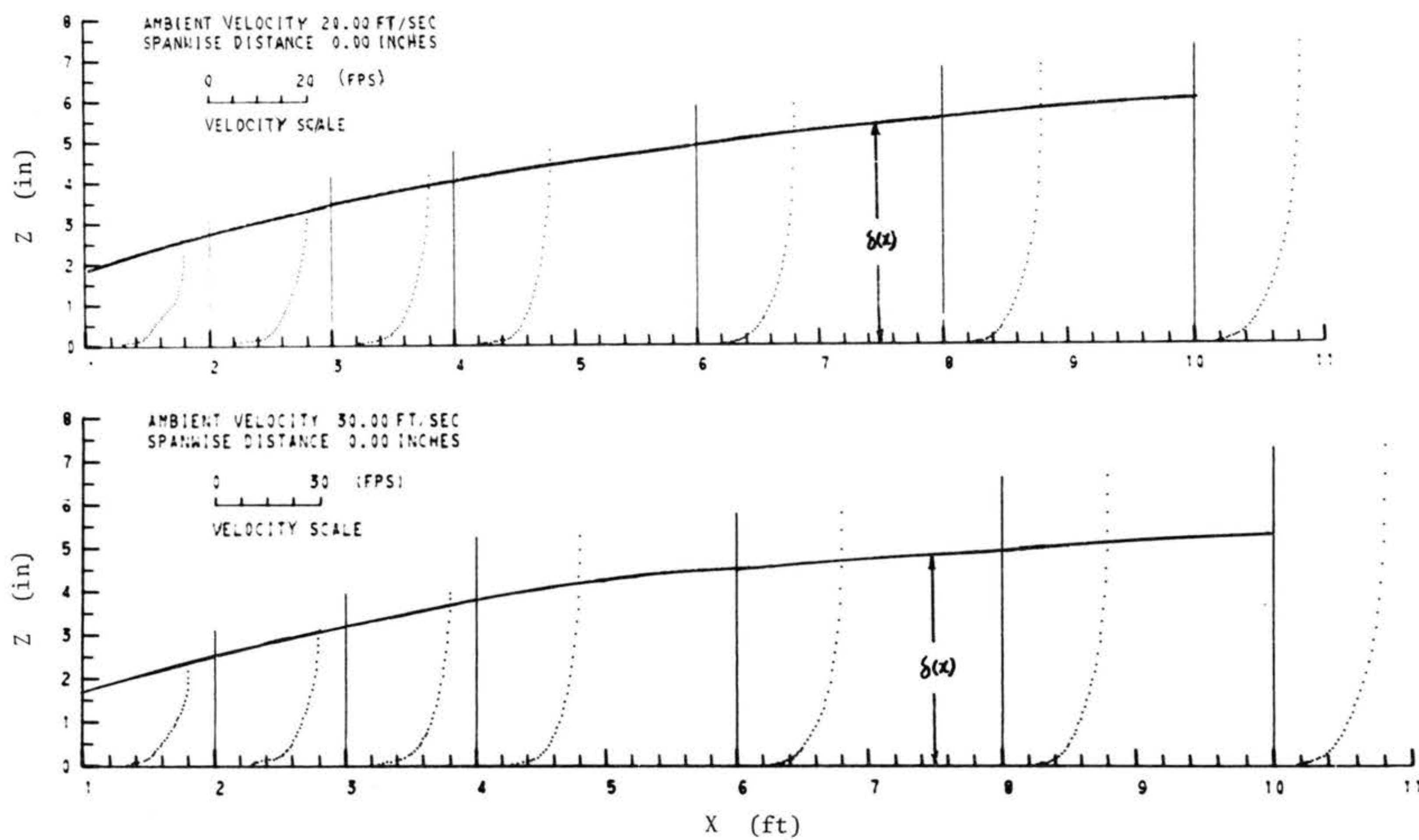

Fig. 5.1a Boundary layer growth over the flat plate along the centerline of a smooth strip

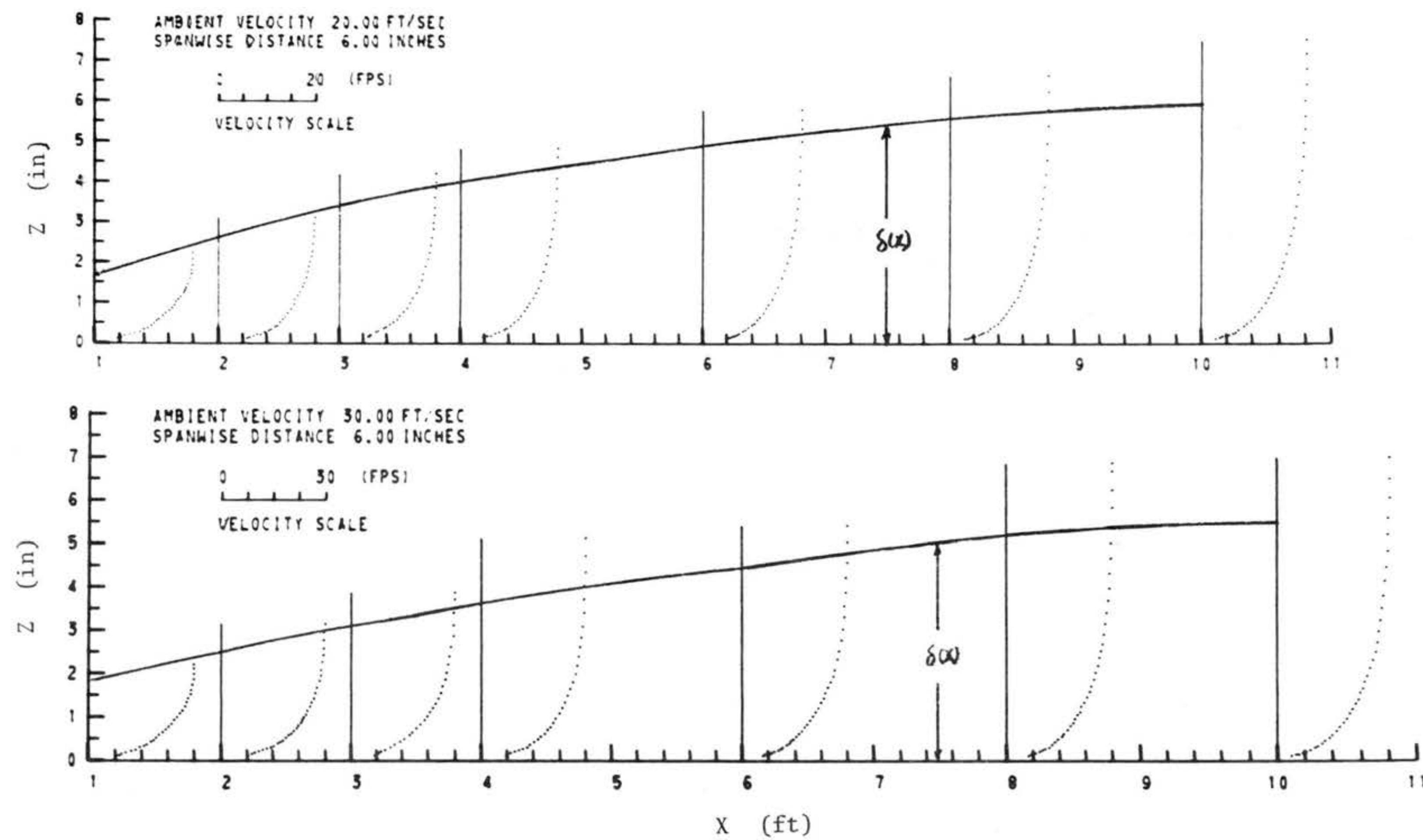

Fig. 5.1b Boundary layer growth over the flat plate along the centerline of a rough strip

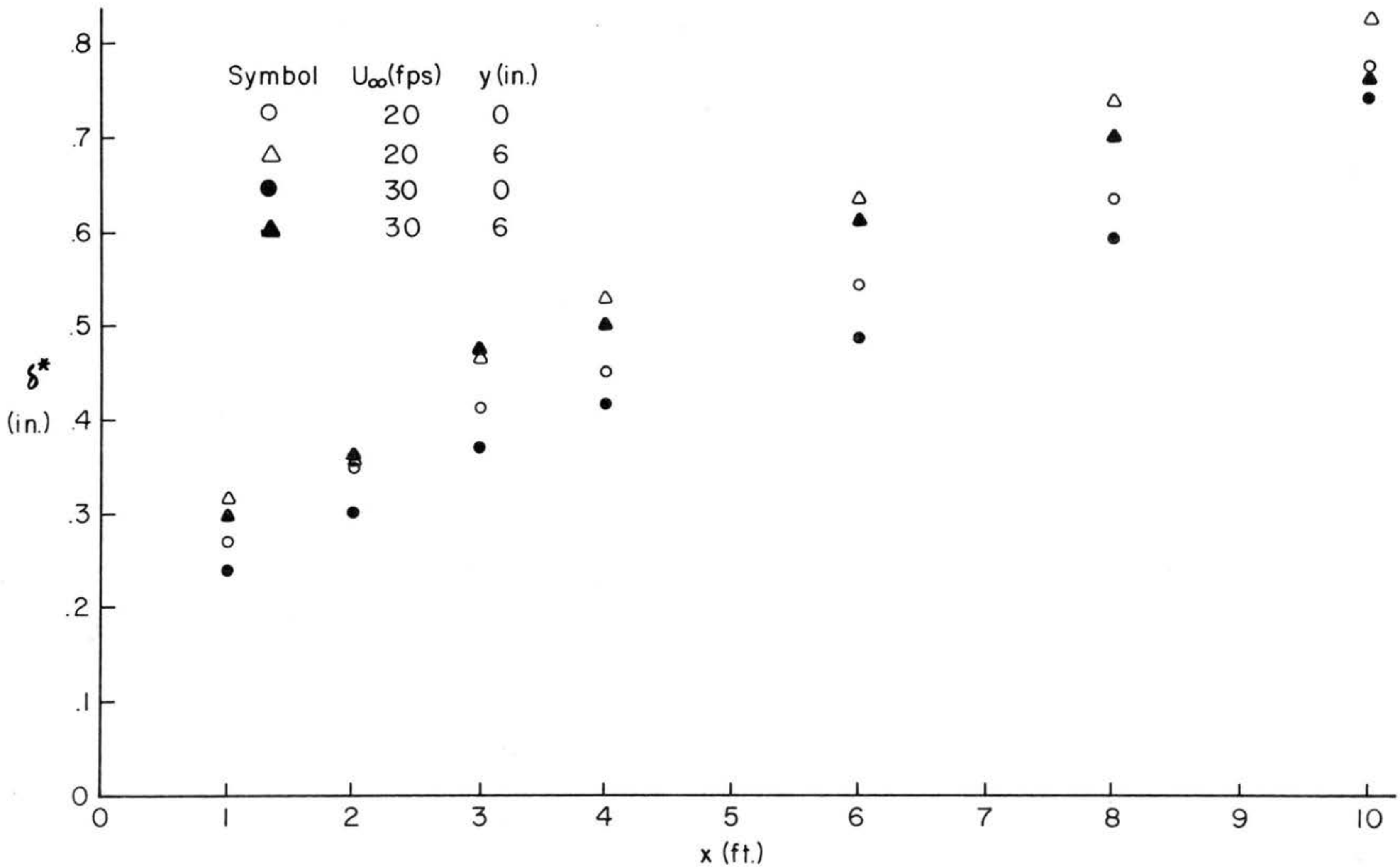

Fig. 5.2 Displacement thickness as a function of x

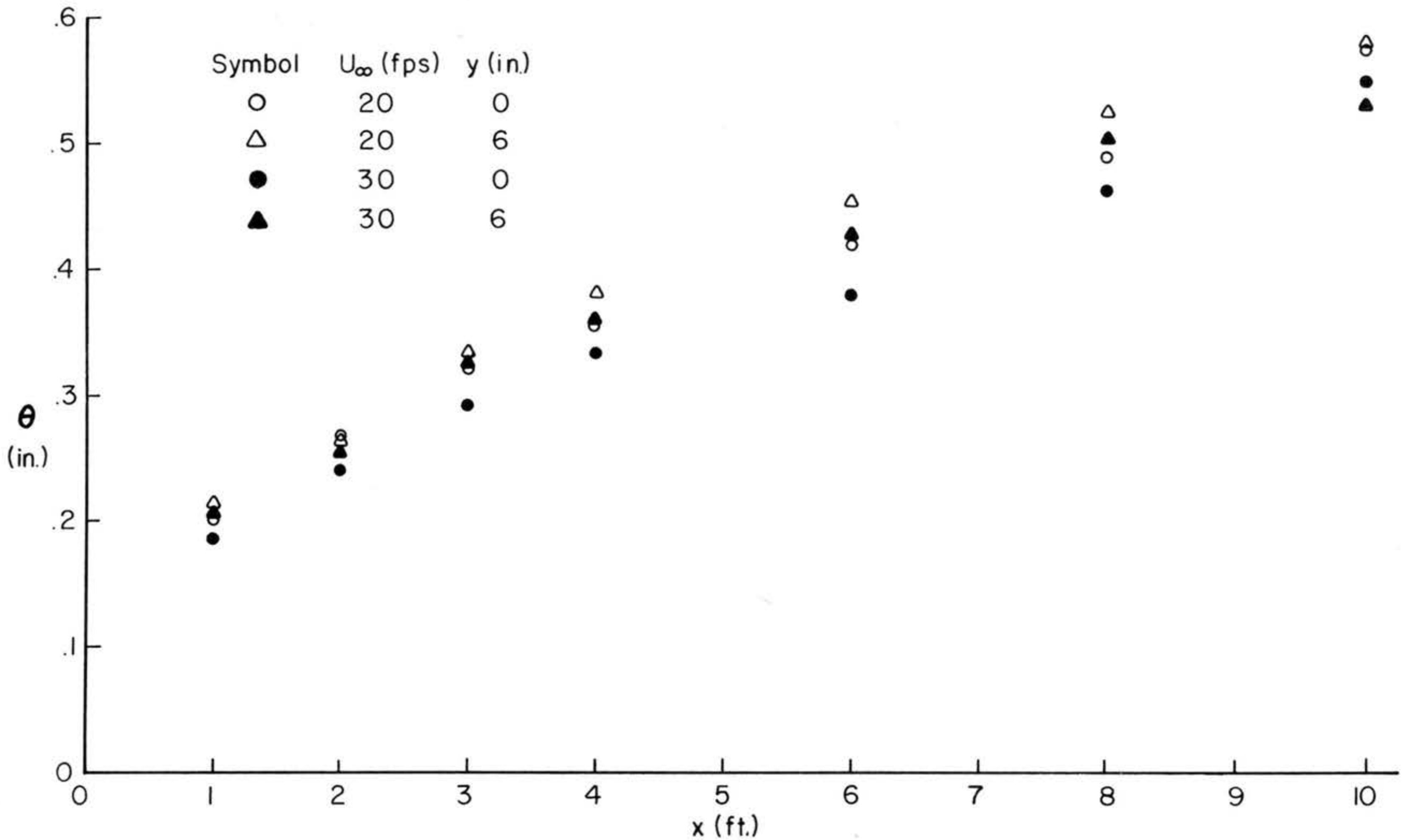

Fig. 5.3 Momentum thickness as a function of x

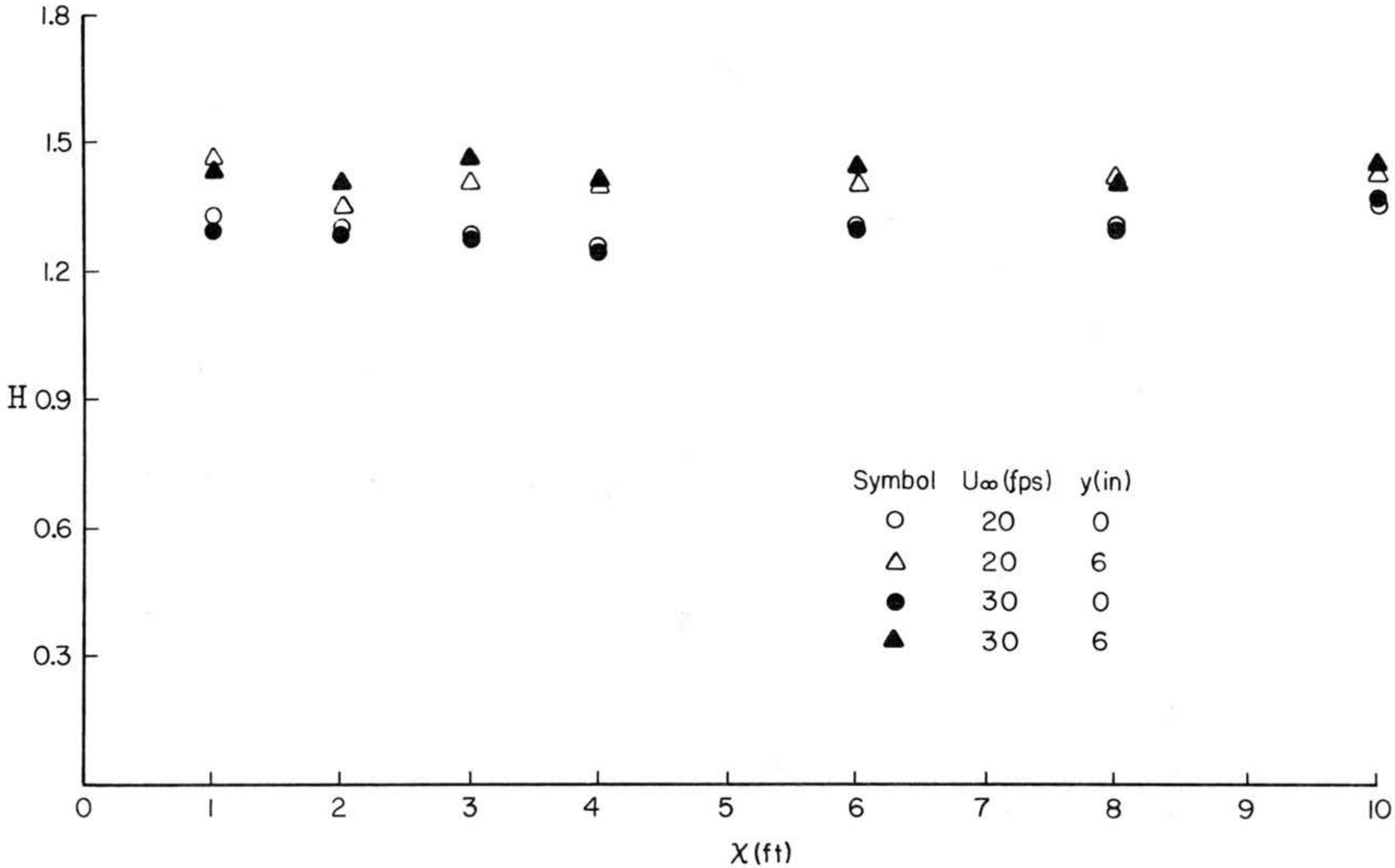

Fig. 5.4 Shape factor as a function of x

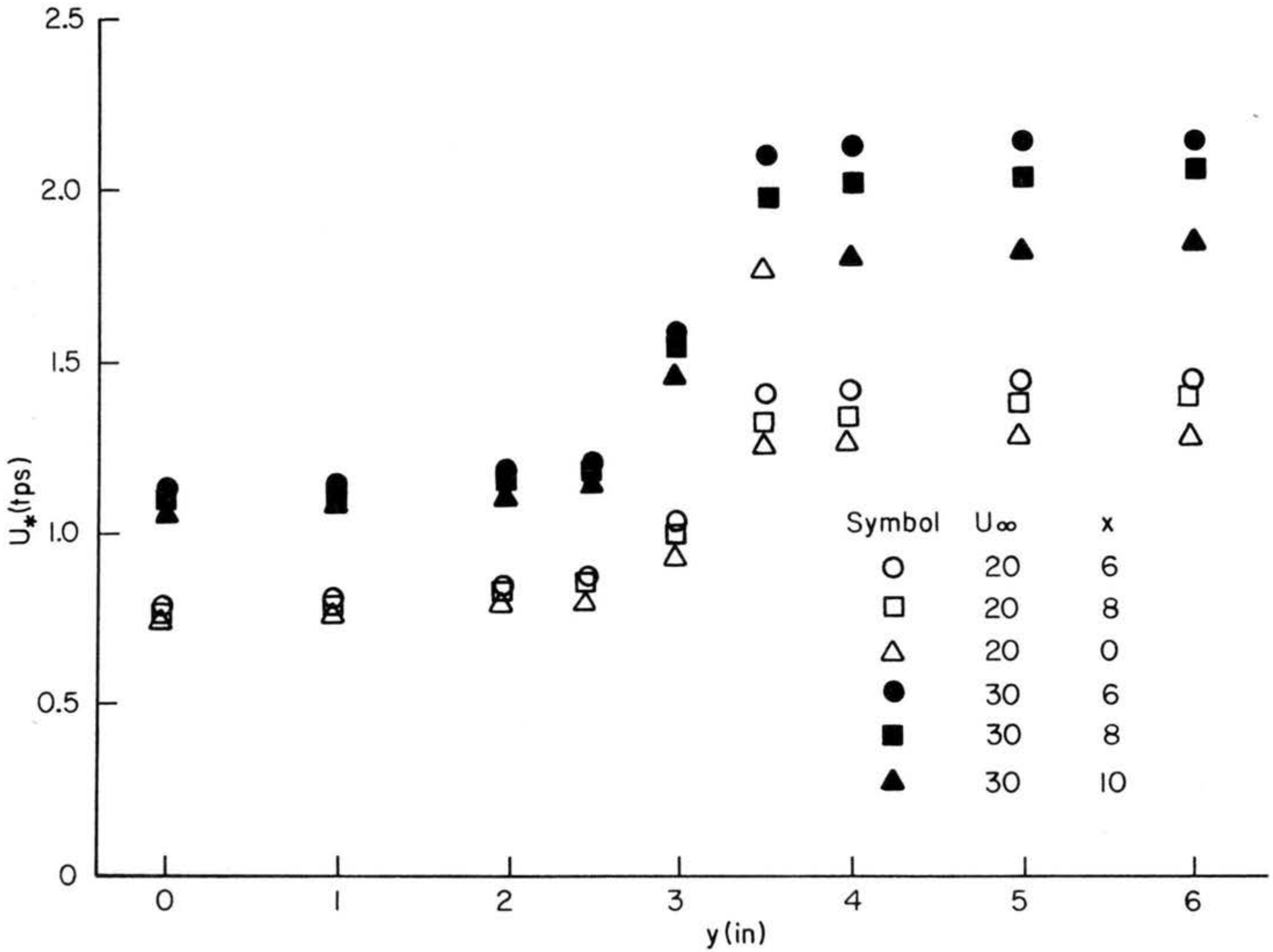

Fig. 5.5 Spanwise variation of shear velocity

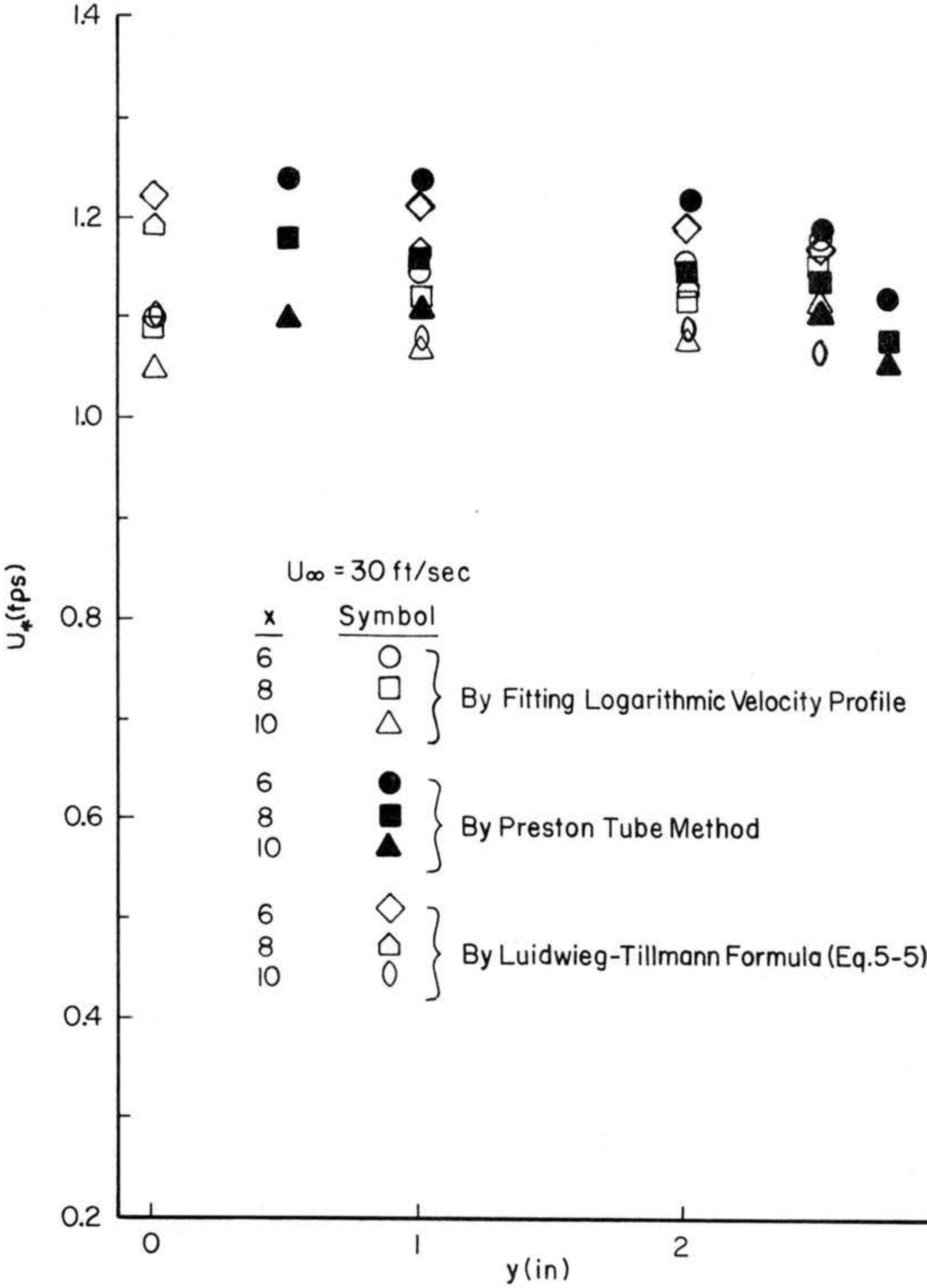

Fig. 5.6 Comparison of shear velocity for the smooth strip by various methods

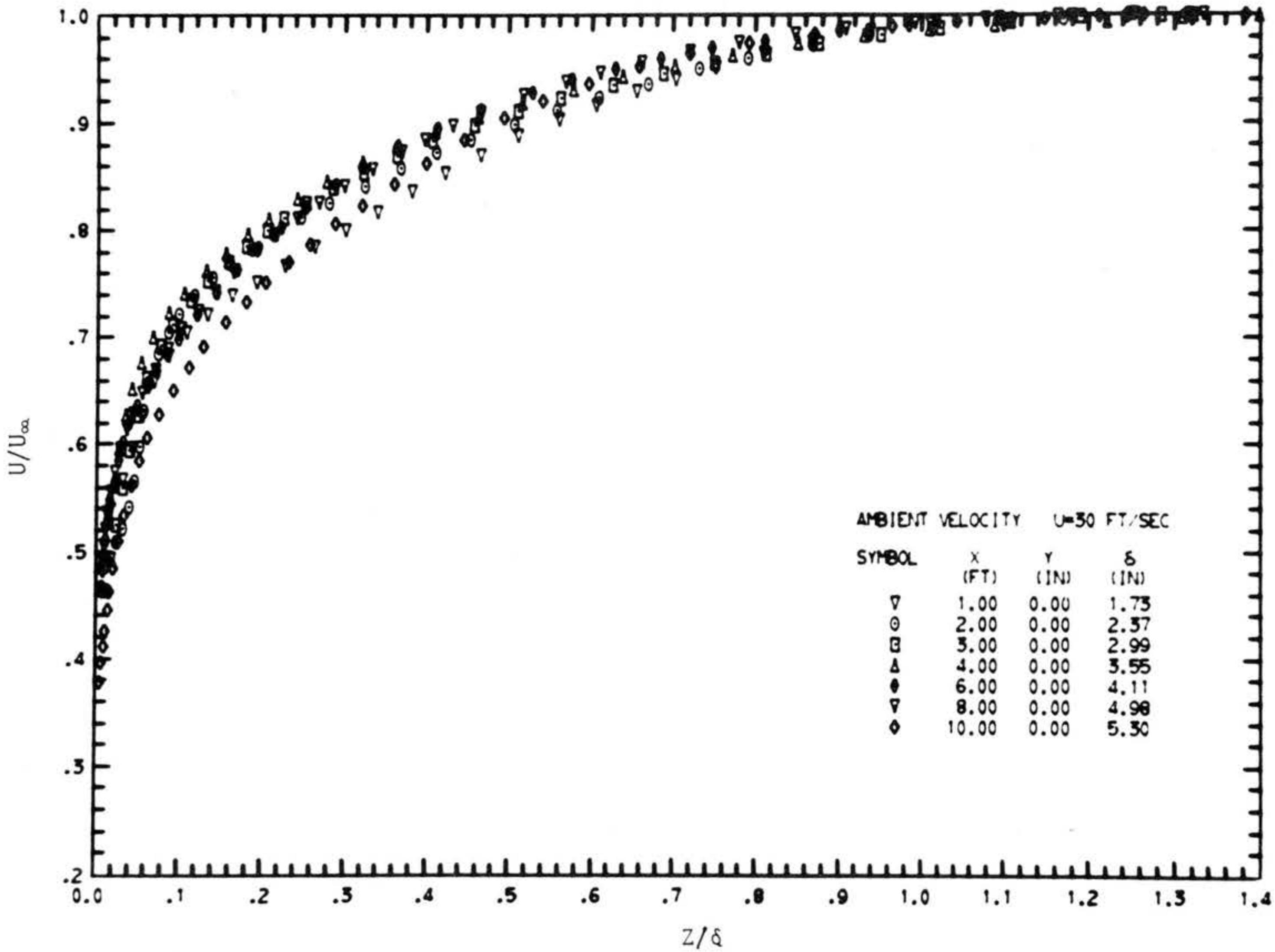

Fig. 5.7a Longitudinal plots of power law profiles (y = 0 in.)-- U/U_∞ vs. z/δ

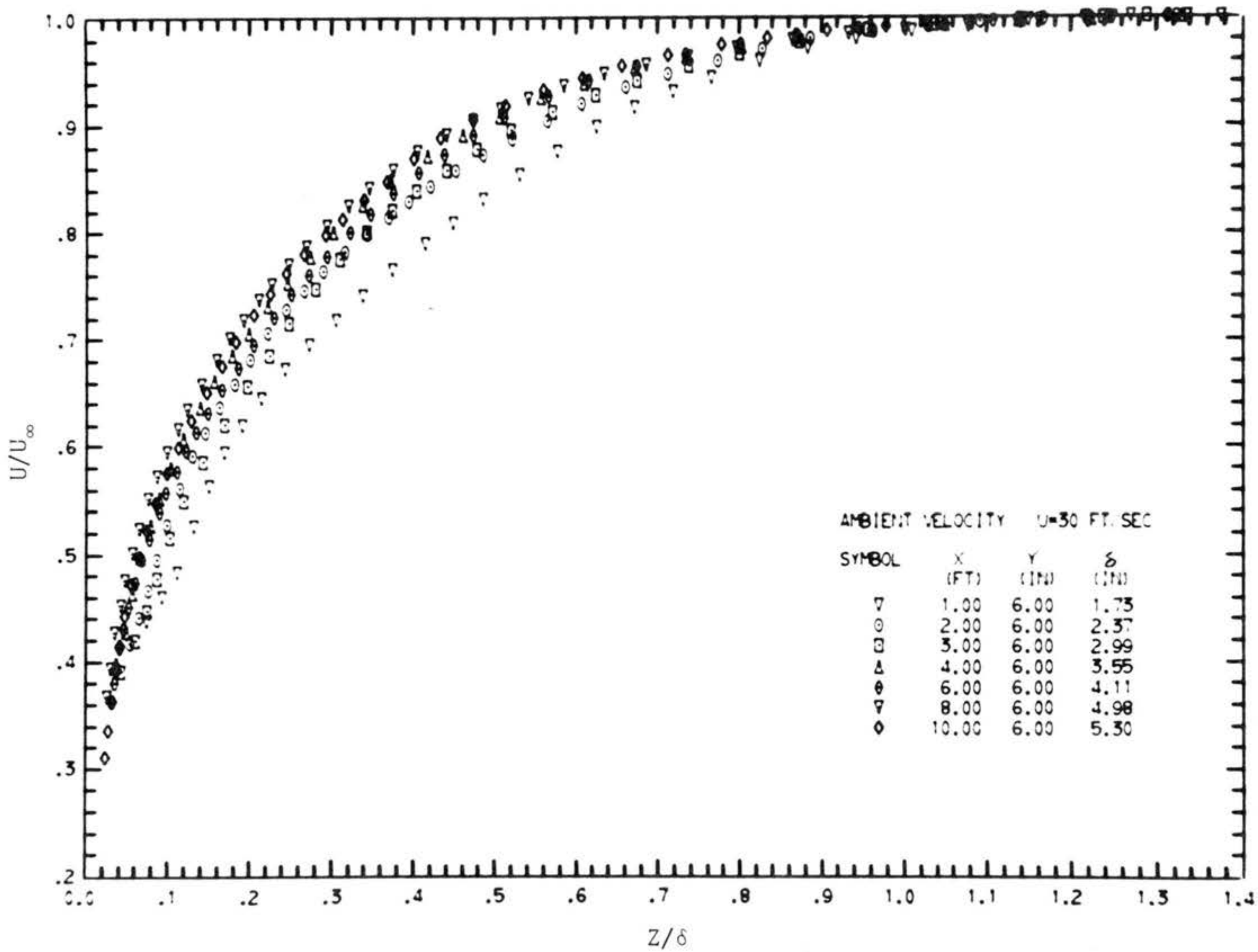

Fig. 5.7b Longitudinal plots of power law profiles (y = 6 in.)-- U/U_∞ vs. z/δ

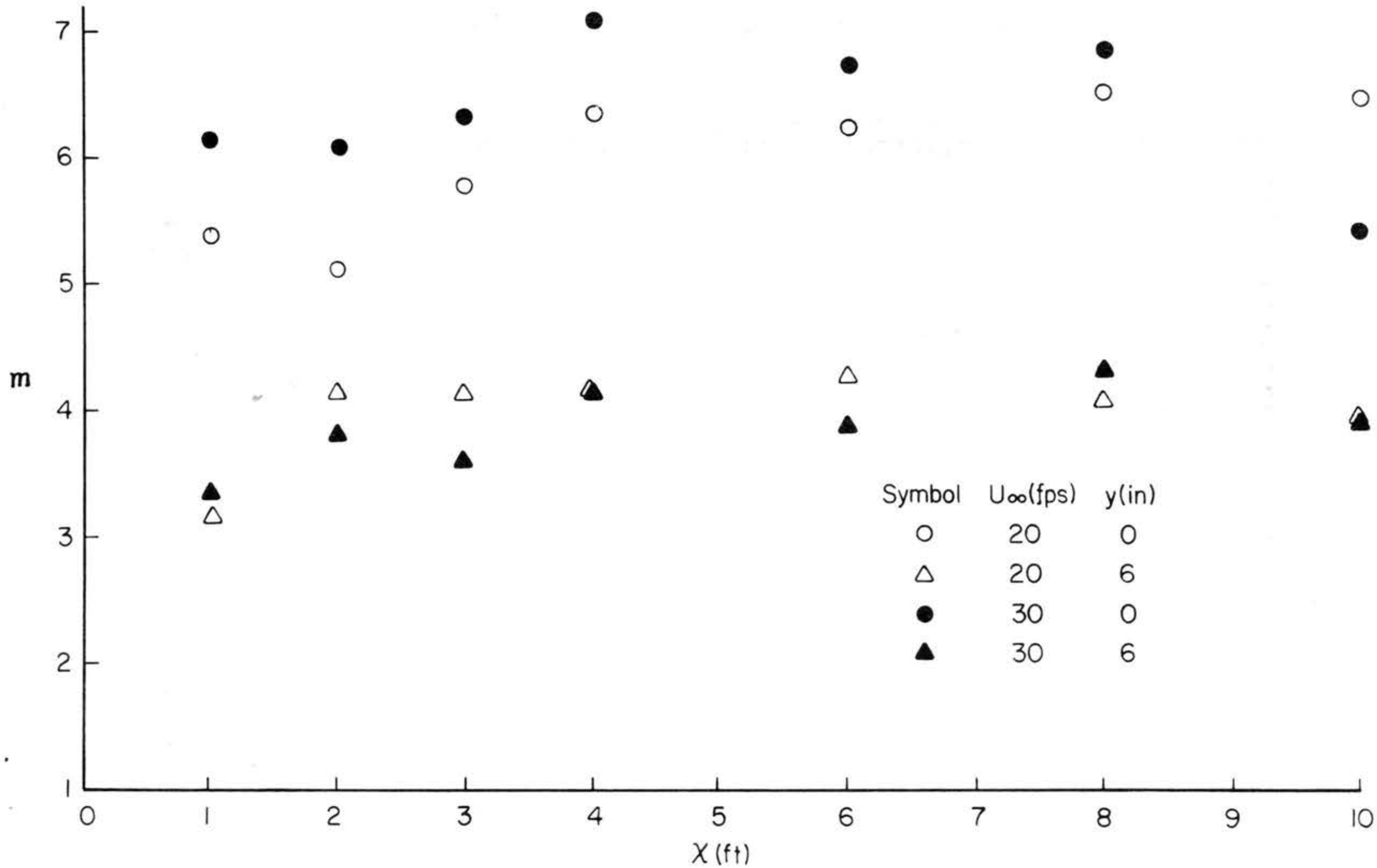

Fig. 5.8 The parameter m in power law profile as a function of x

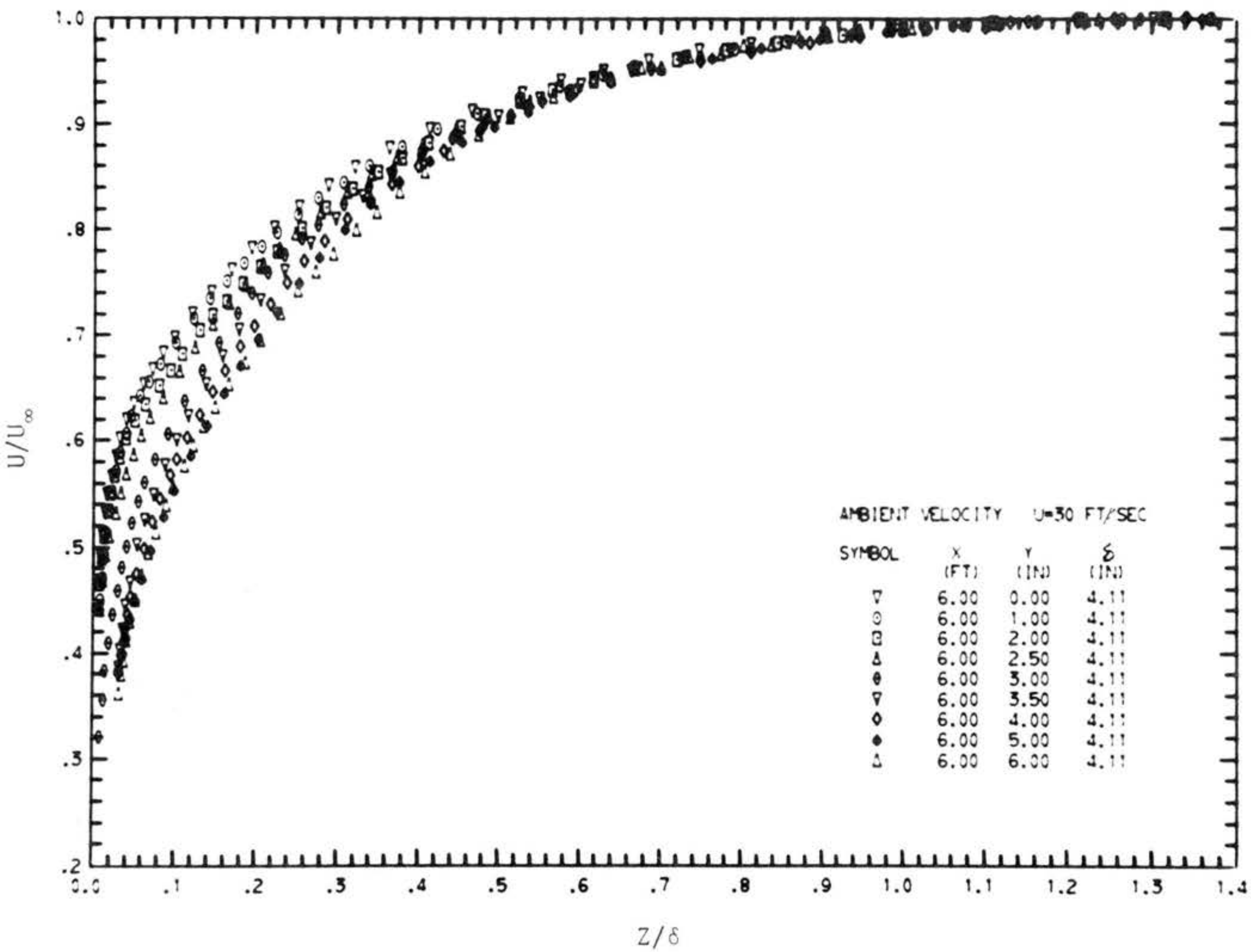

Fig. 5.9a Spanwise comparison of power law profiles at x = 6 ft.-- U/U_∞ vs. z/δ

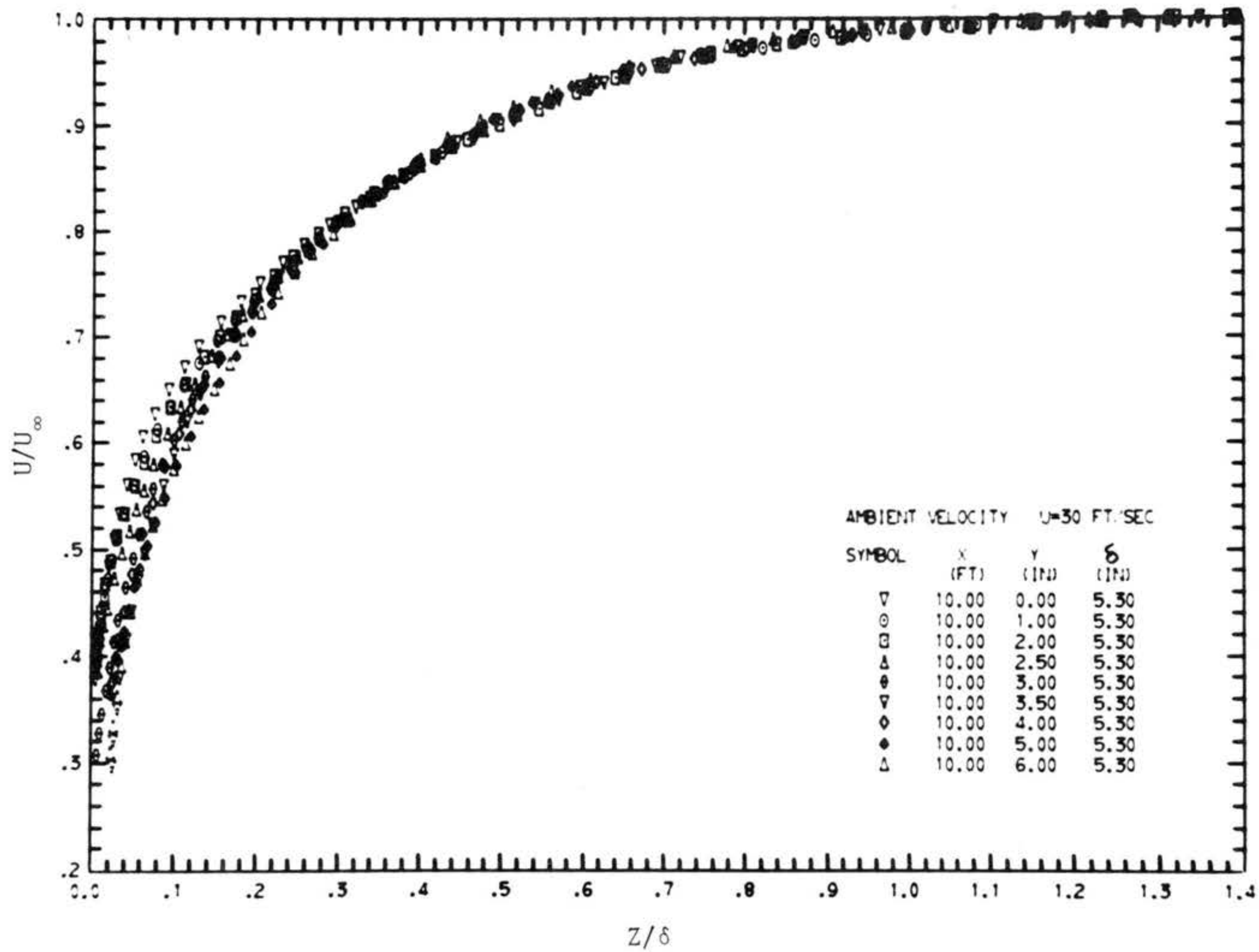

Fig. 5.9b Spanwise comparison of power law profiles at x = 10 ft.-- U/U_∞ vs. z/δ

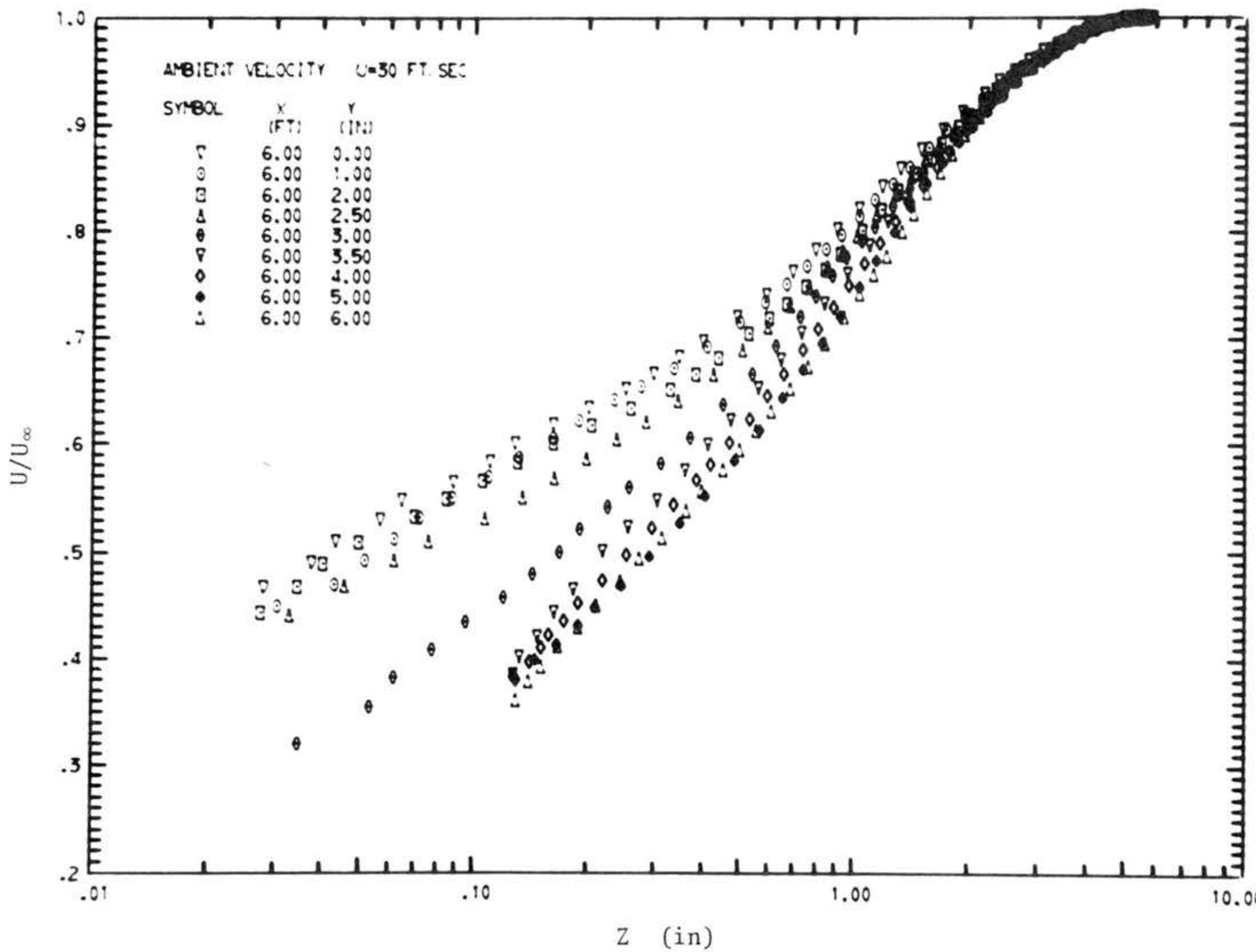

Fig. 5.10a Semi-logarithmic plots of mean velocity data at x = 6 ft.-- U/U_∞ vs. z

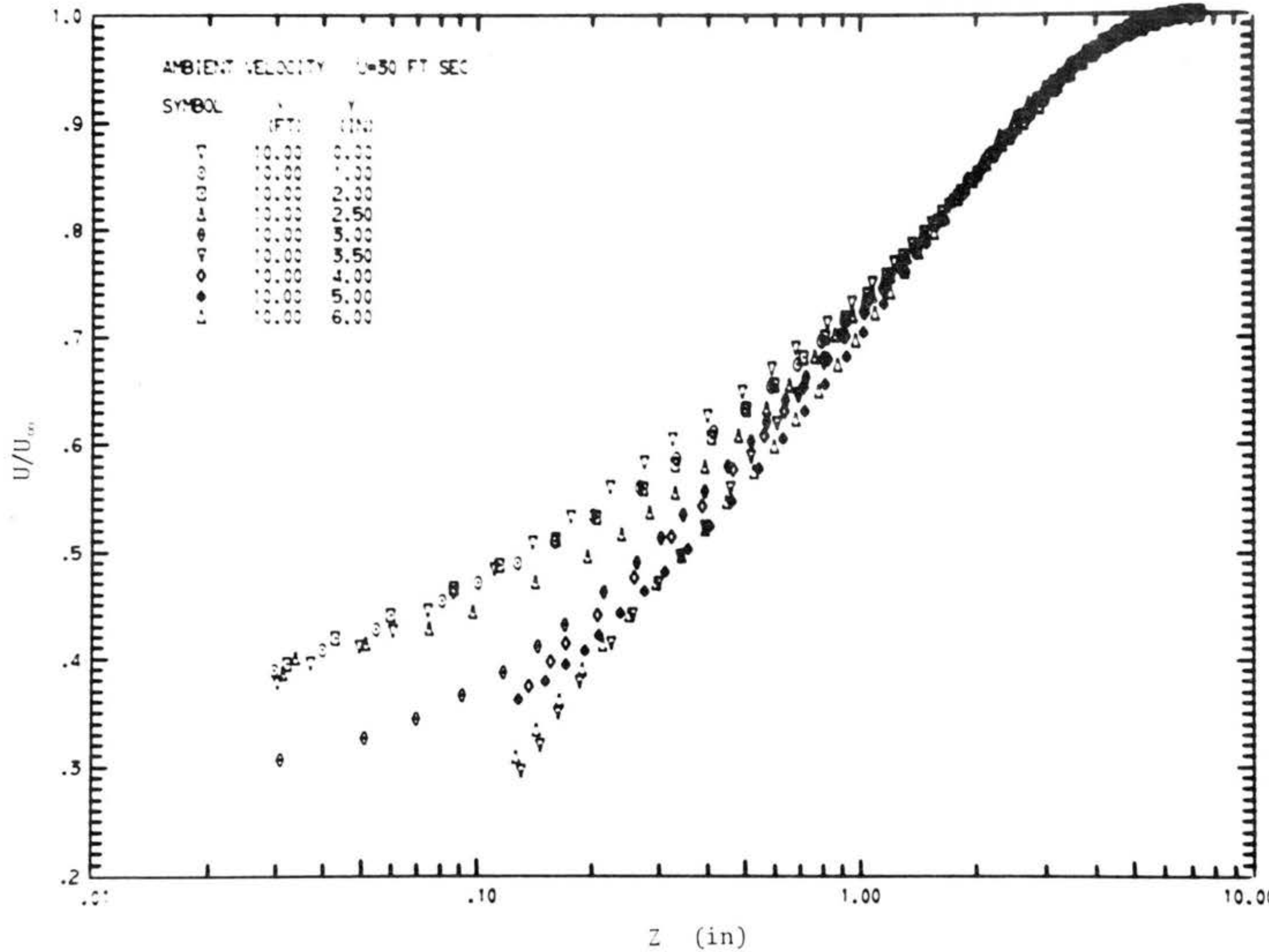

Fig. 5.10b Semi-logarithmic plots of mean velocity data at x = 10 ft.-- U/U_∞ vs. z

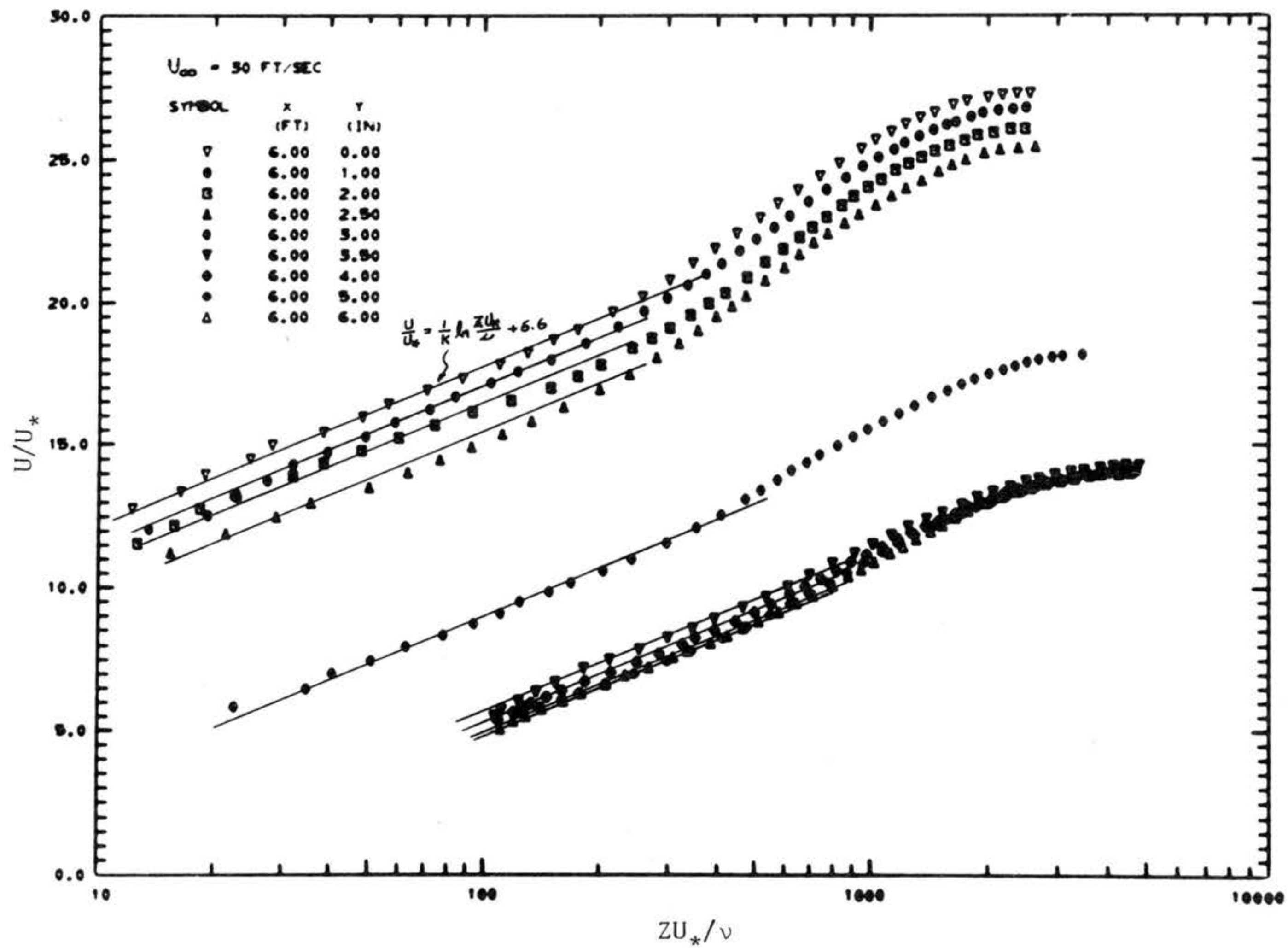

Fig. 5.11a Spanwise comparison of wall law profiles at x = 6 ft.-- U/U_* vs. zU_*/ν

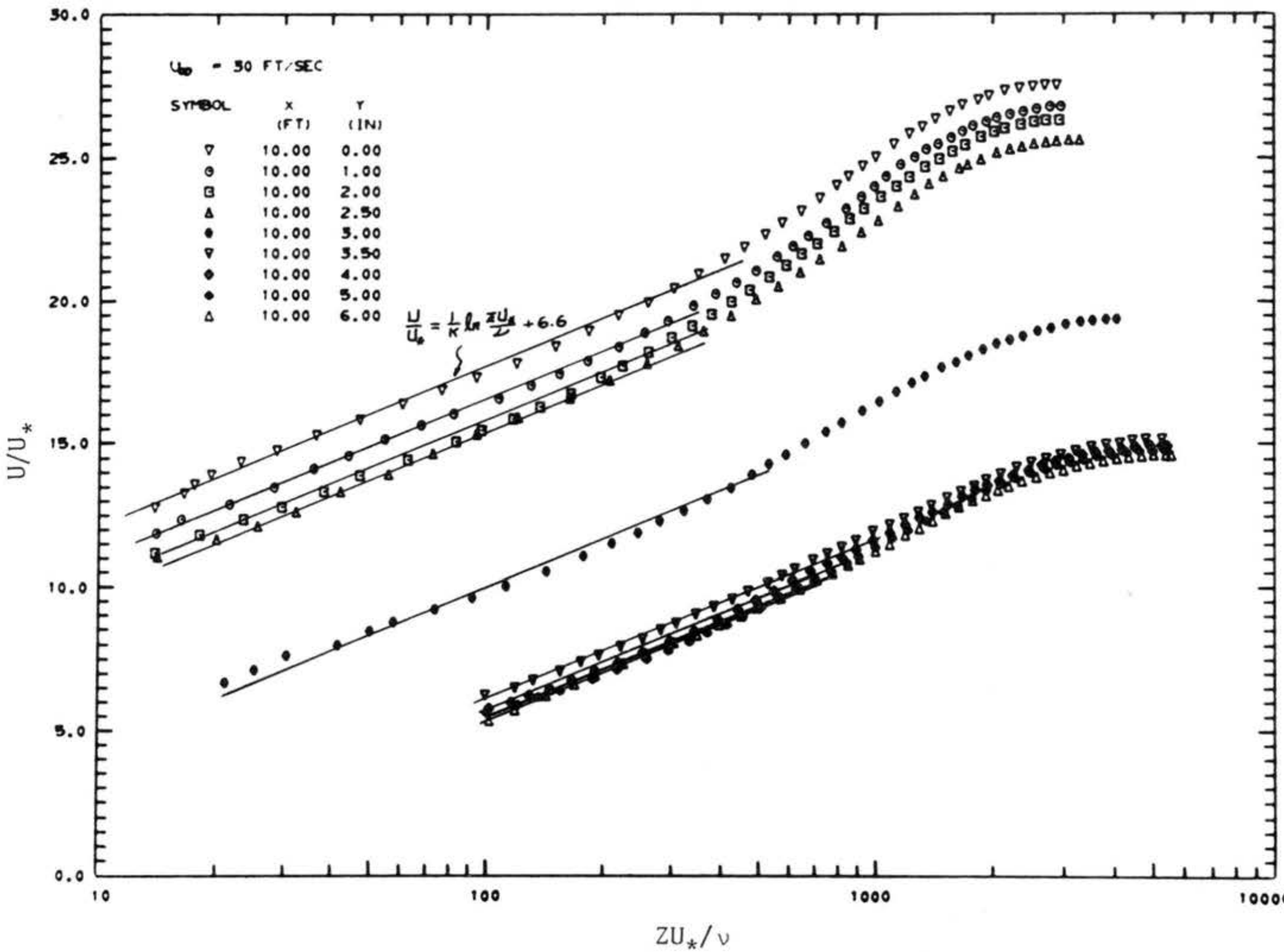

Fig. 5.11b Spanwise comparison of wall law profiles at x = 10 ft.-- U/U_* vs. zU_*/ν

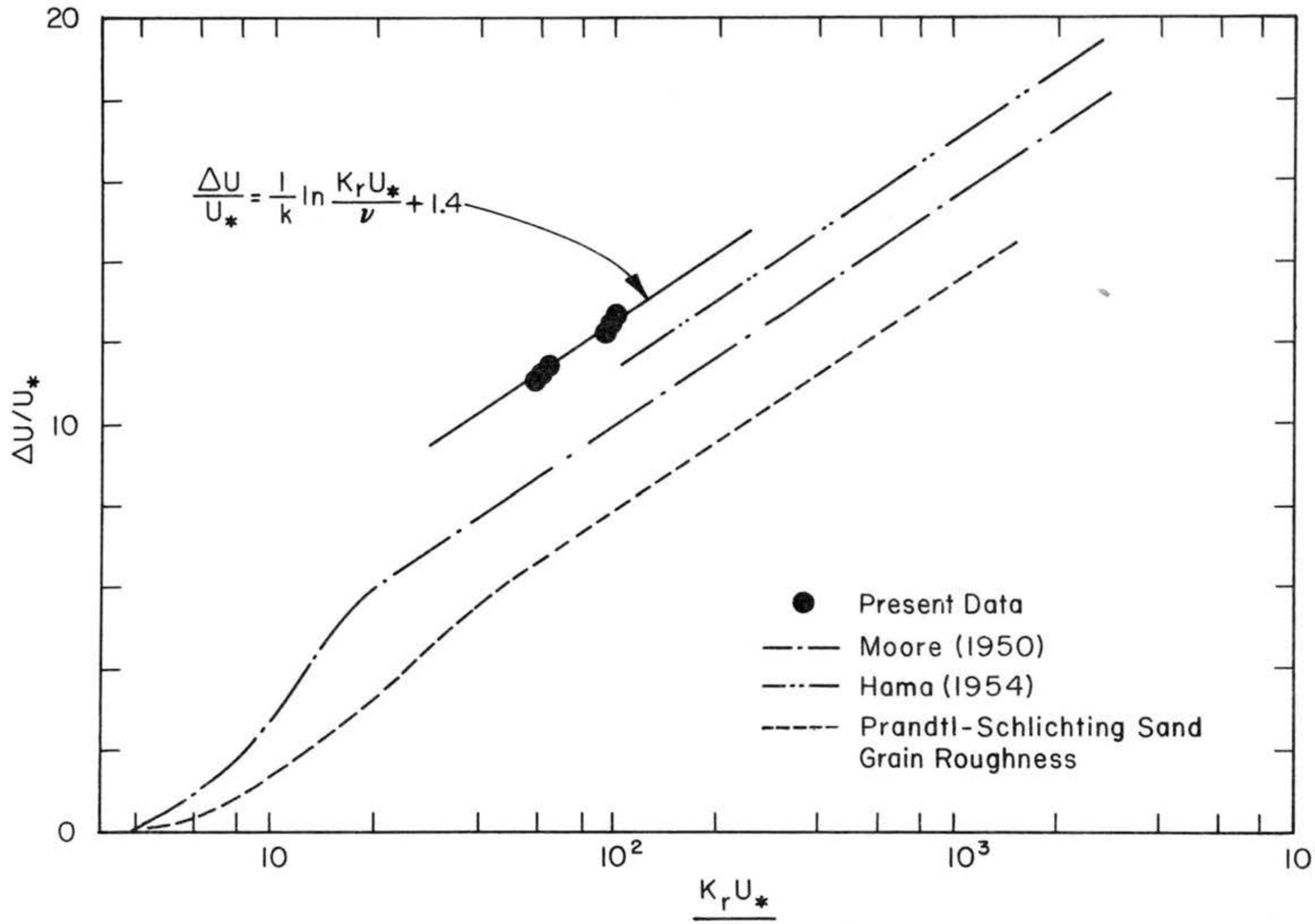

Fig. 5.12 Roughness effect $\Delta U/U_*$ vs. $k_r U_*/\nu$

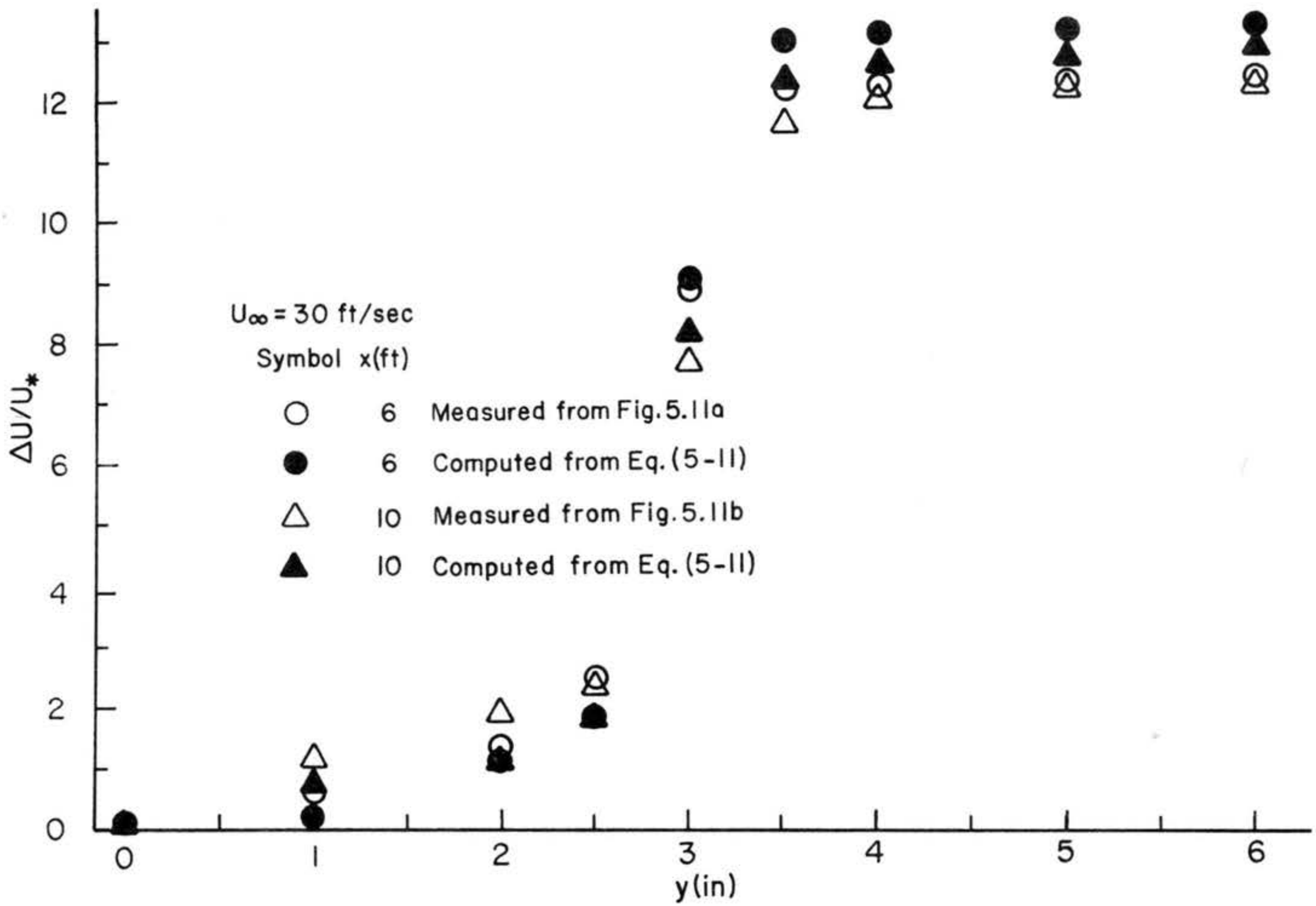

Fig. 5.13 Spanwise variation of $\Delta U/U_*$

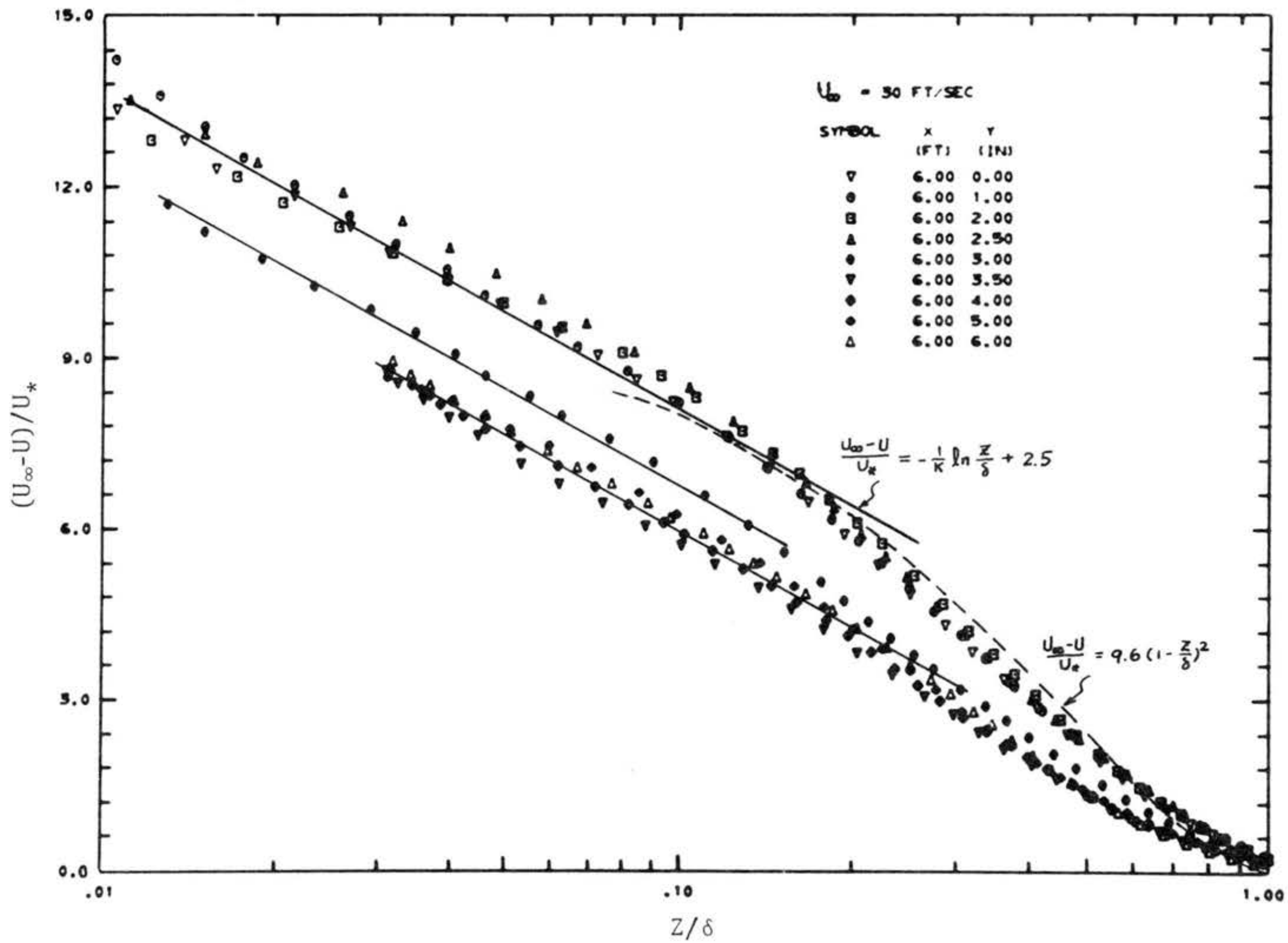

Fig. 5.14a Spanwise comparison of velocity-defect profiles at x = 6 ft.
-- $(U_\infty - U)/U_*$ vs. z/δ

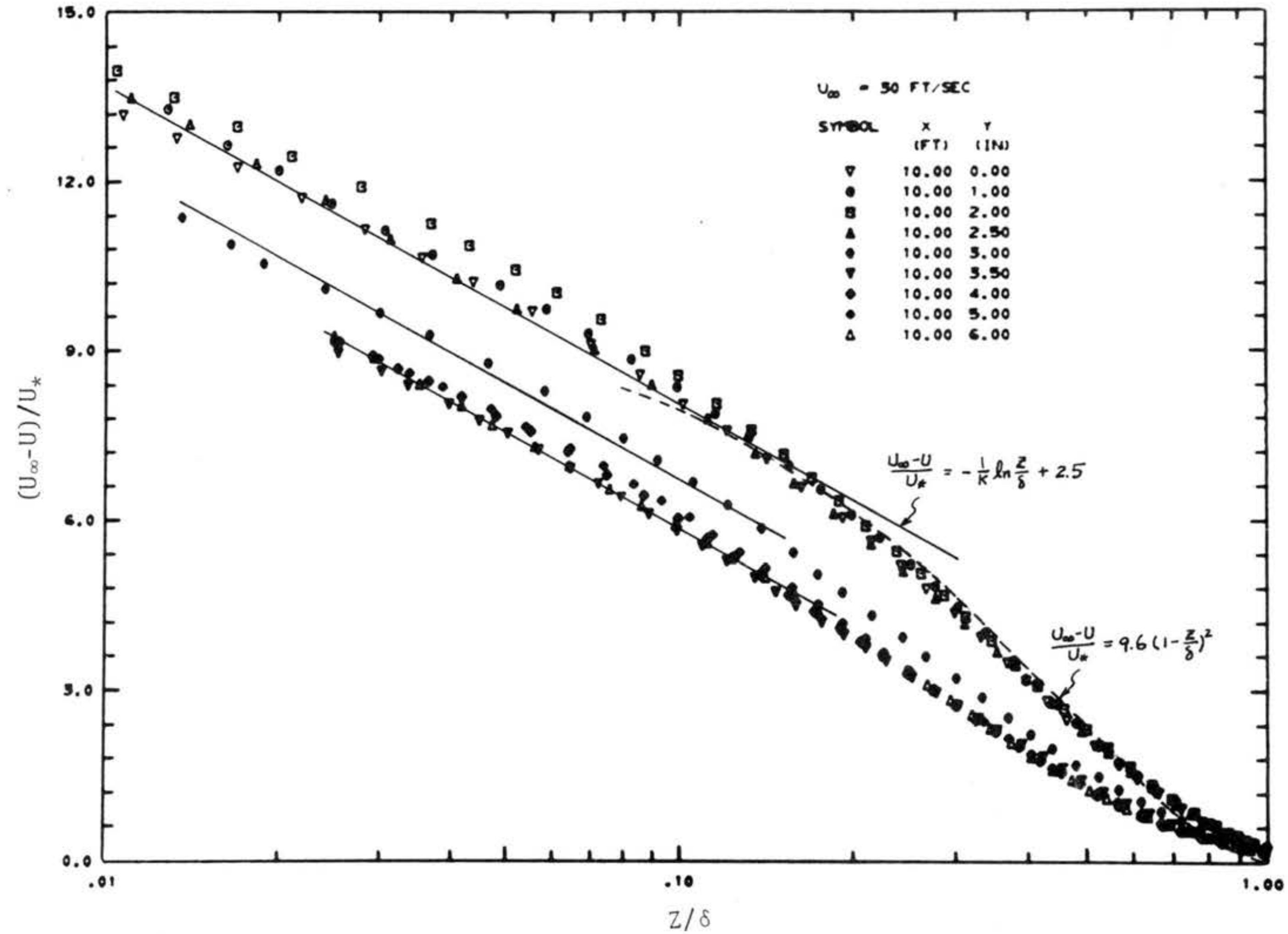

Fig. 5.14b Spanwise comparison of velocity-defect profiles at x = 10 ft.
-- $(U_\infty-U)/U_*$ vs. z/δ

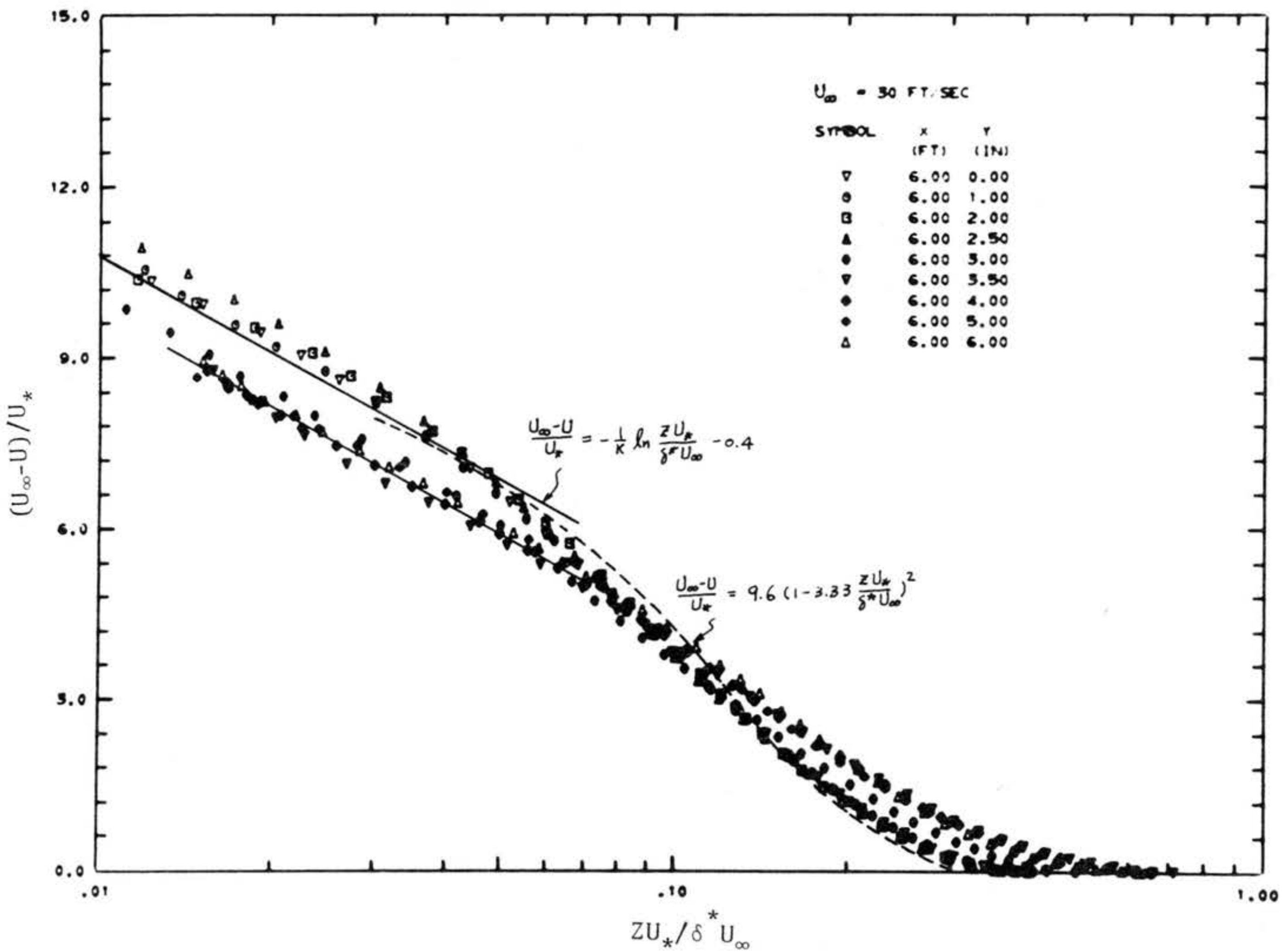

Fig. 5.15a Spanwise comparison of velocity-defect profiles at x = 6 ft. -- $(U_\infty - U)/U_*$ vs. $zU_*/\delta^* U_\infty$

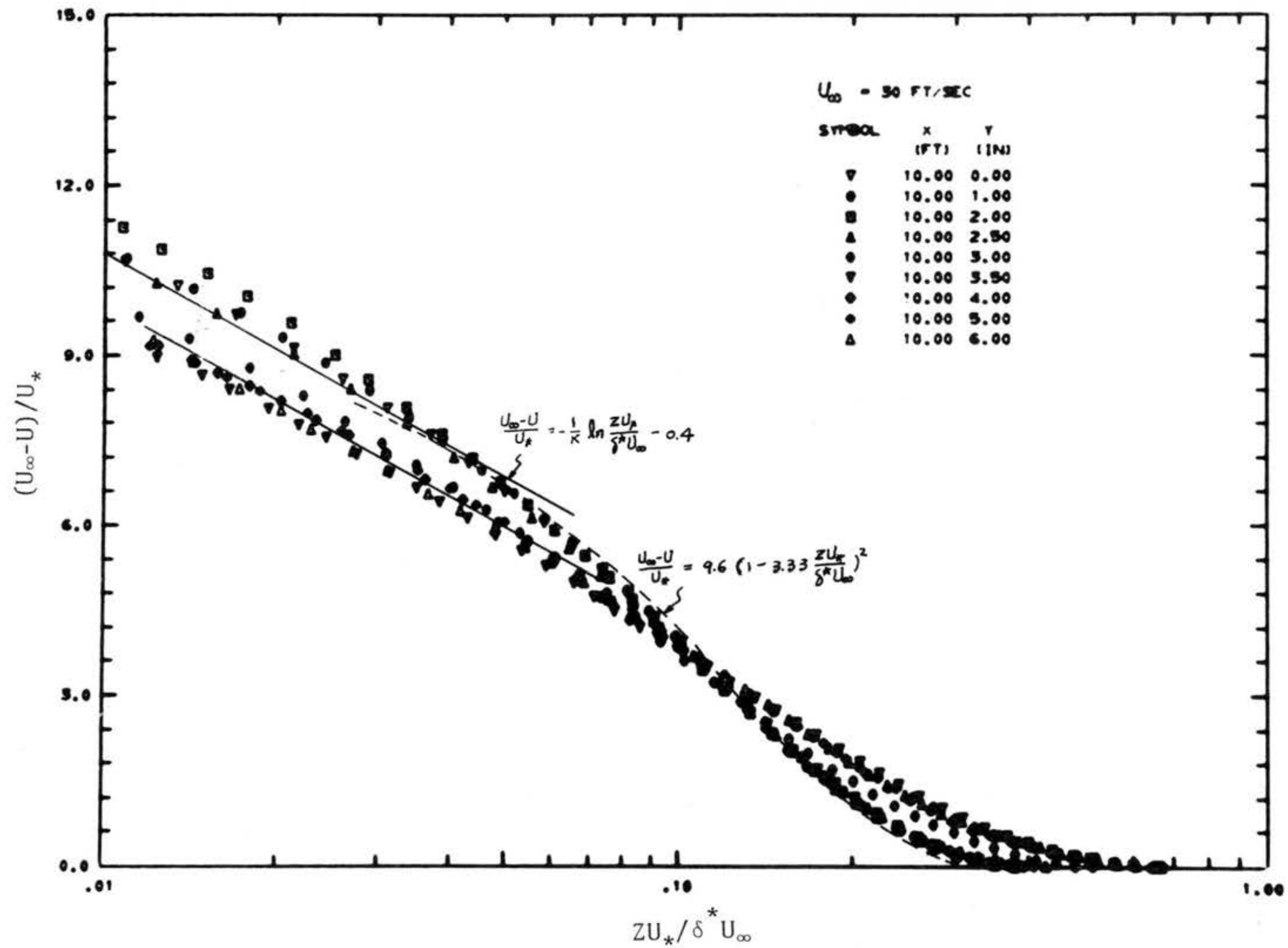

Fig. 5.15b Spanwise comparison of velocity-defect profiles at x = 10 ft. -- $(U_\infty - U)/U_*$ vs. $zU_*/\delta^* U_\infty$

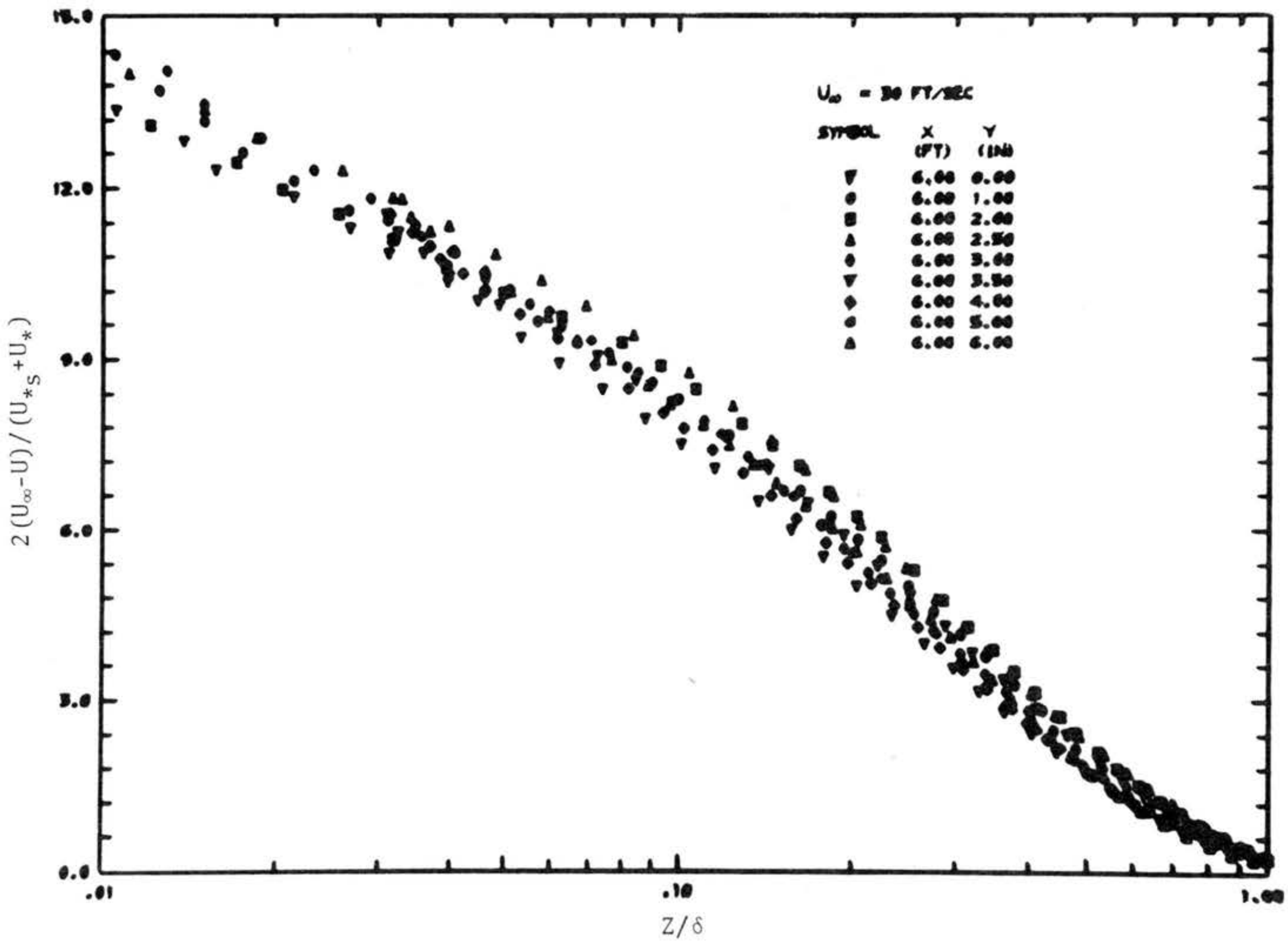

Fig. 5.16a Spanwise comparison of velocity-defect profiles at x = 6 ft.
-- $2(U_\infty-U)/(U_{*s}+U_*)$ vs. z/δ

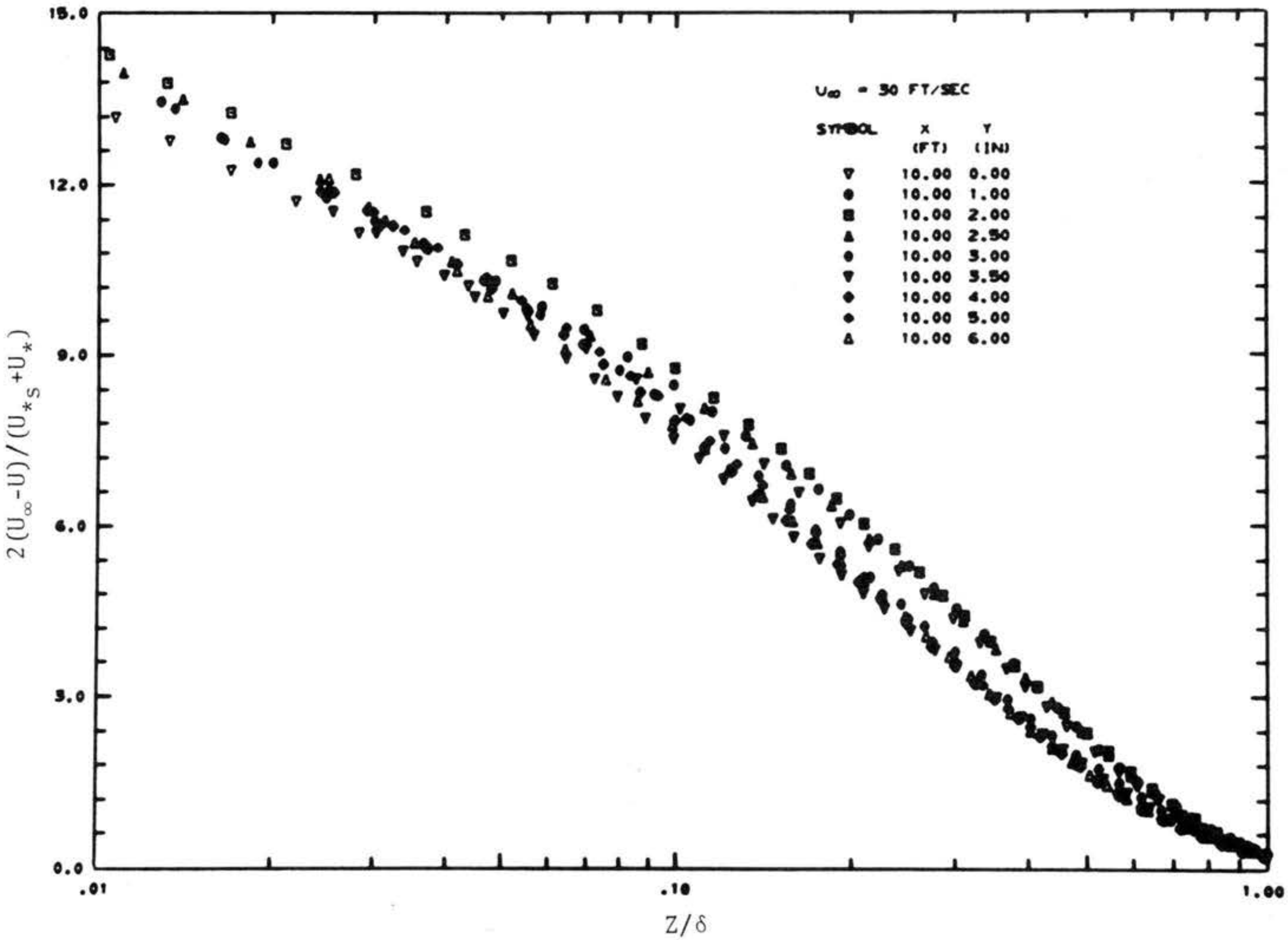

Fig. 5.16b Spanwise comparison of velocity-defect profiles at x = 10 ft.
-- $2(U_\infty-U)/(U_{*S}+U_*)$ vs. z/δ

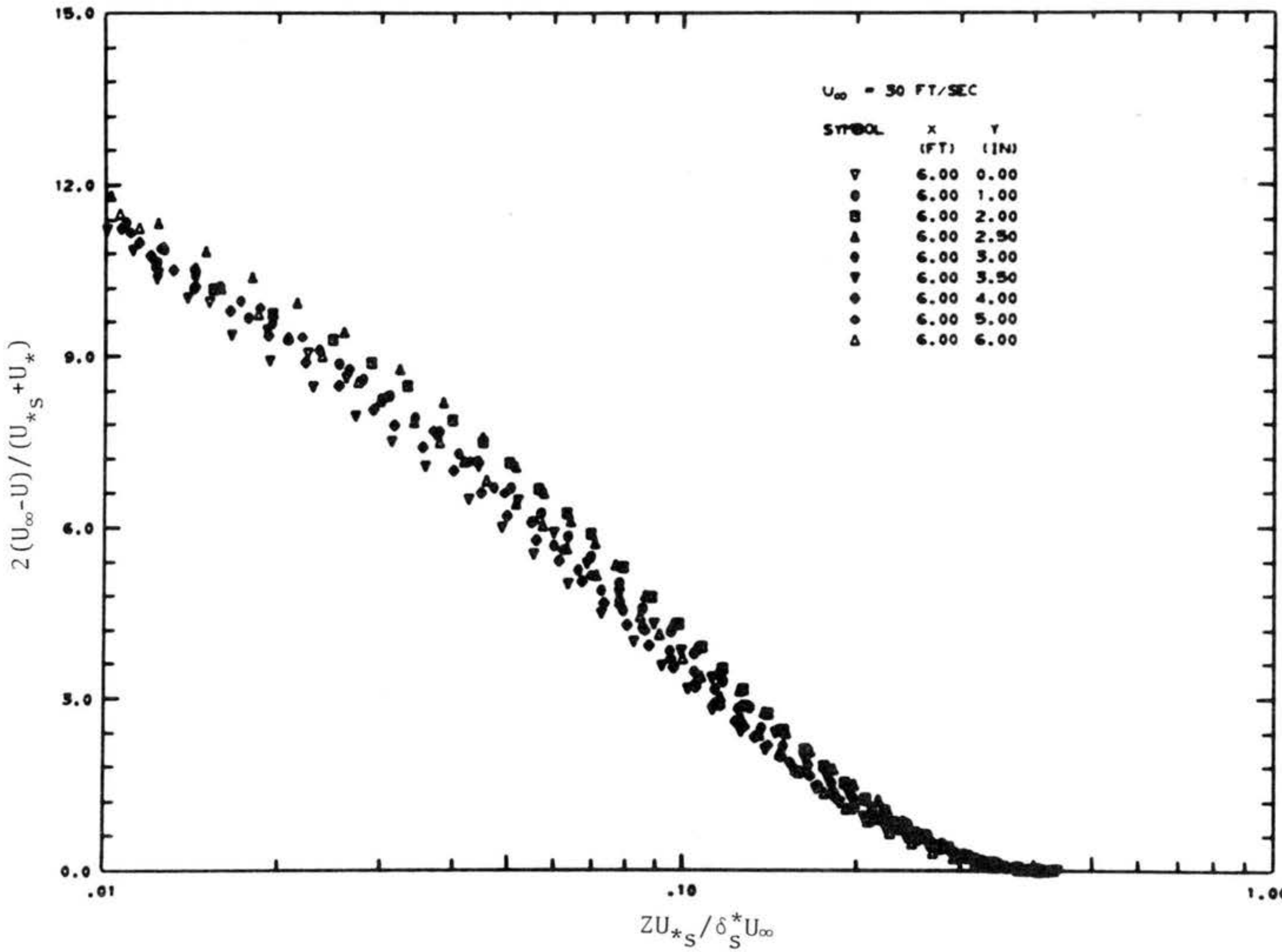

Fig. 5.17a Spanwise comparison of velocity-defect profiles at x = 6 ft.
-- $2(U_\infty-U)/(U_{*S}+U_*)$ vs. $zU_{*S}/\delta_S^*U_\infty$

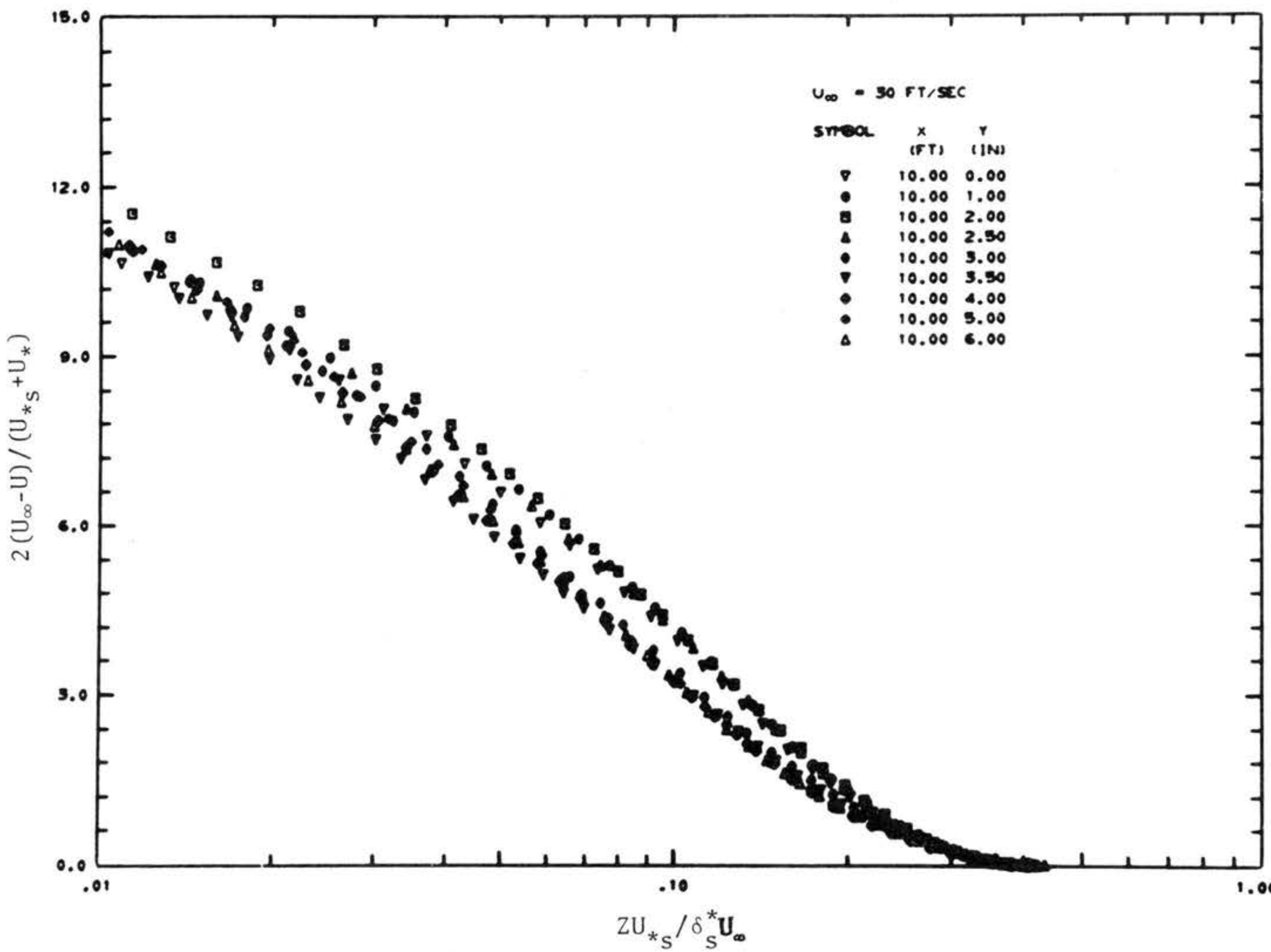

Fig. 5.17b Spanwise comparison of velocity-defect profiles at x = 10 ft. -- $2(U_\infty-U)/(U_{*s}+U_*)$ vs. $zU_{*s}/\delta_s^* U_\infty$

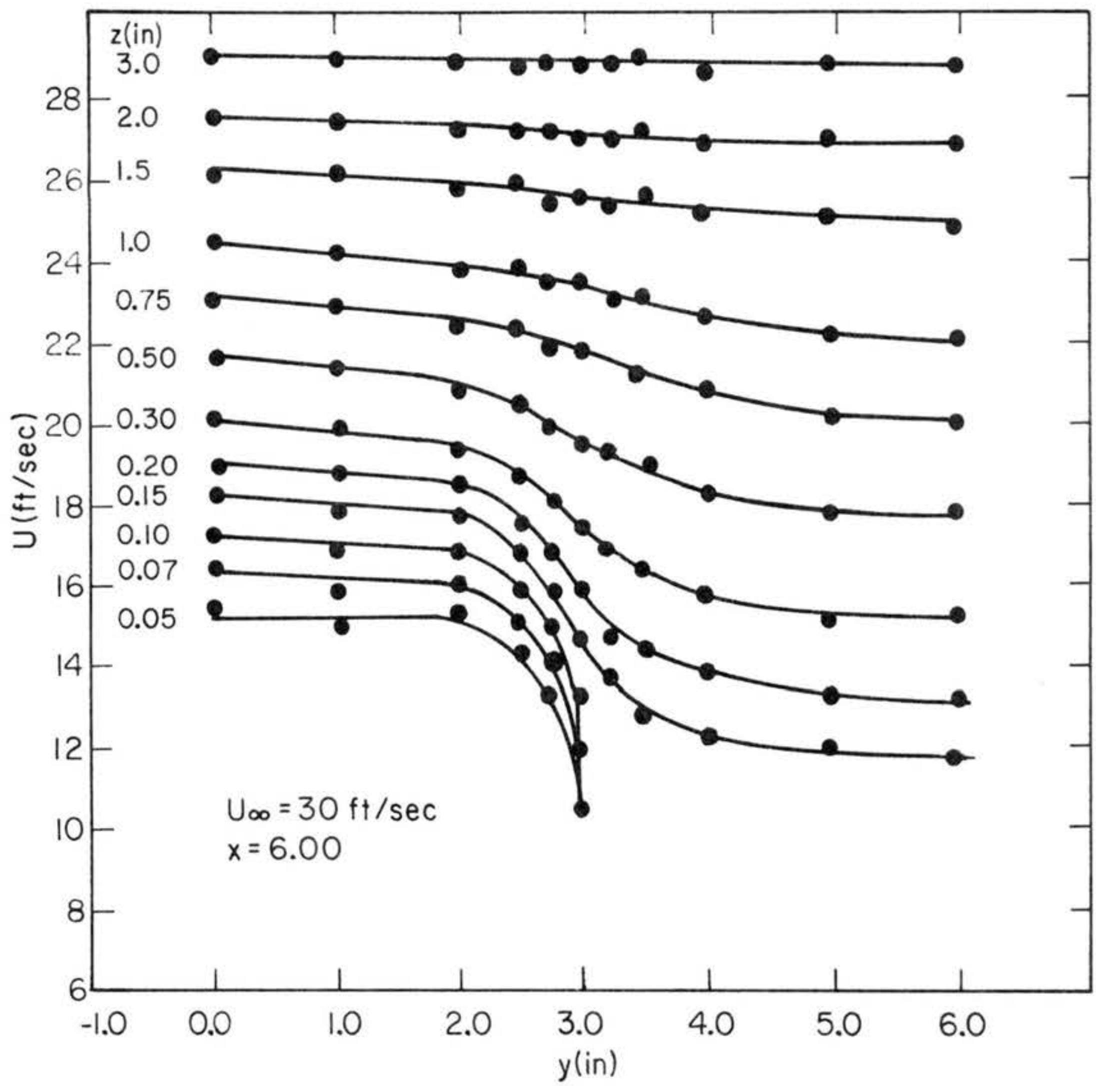

Fig. 5.18a Spanwise velocity distribution of constant height at x = 6 ft. for U_∞ = 30 ft/sec

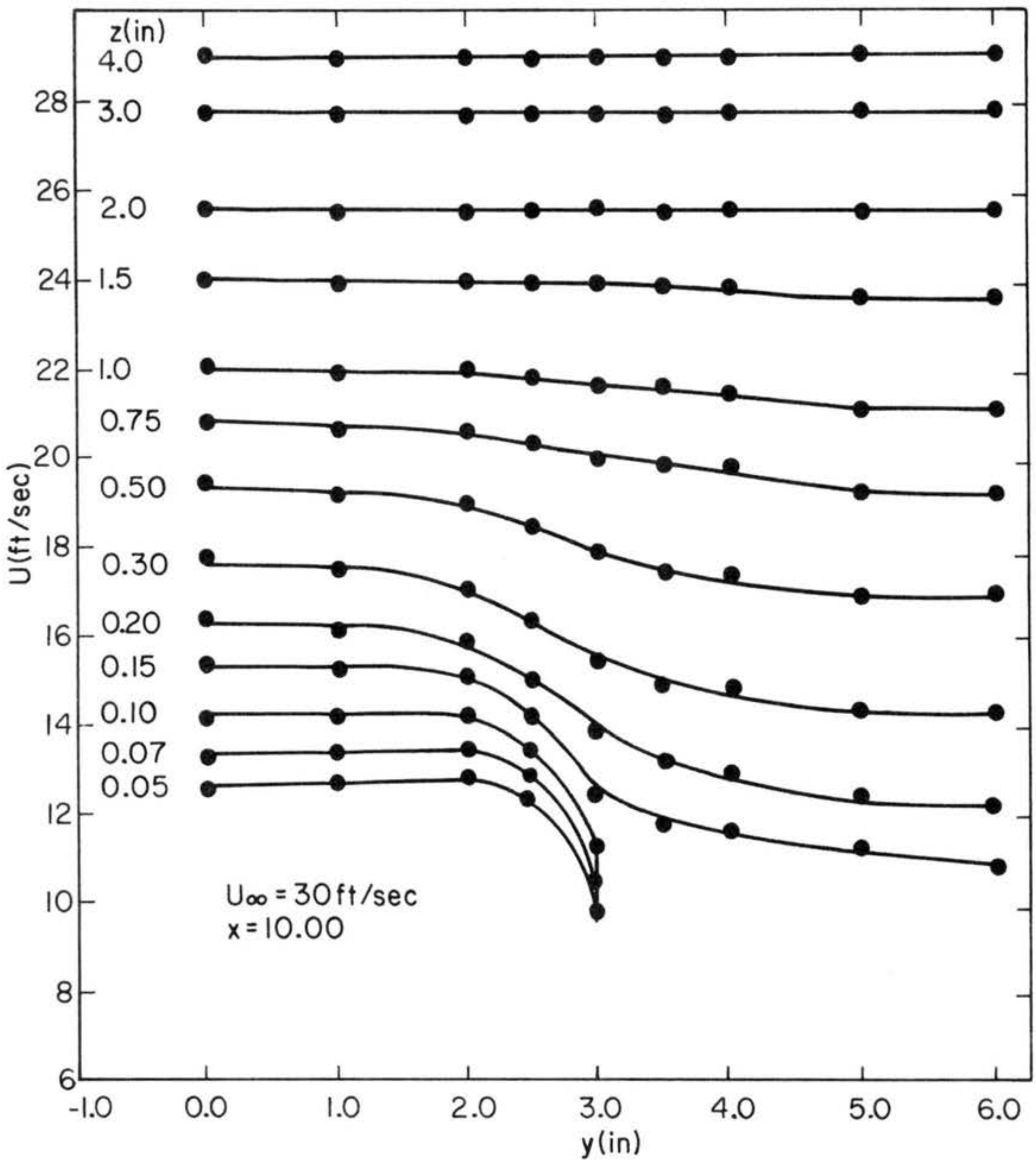

Fig. 5.18b Spanwise velocity distribution of constant height at x = 10 ft. for U_∞ = 30 ft/sec

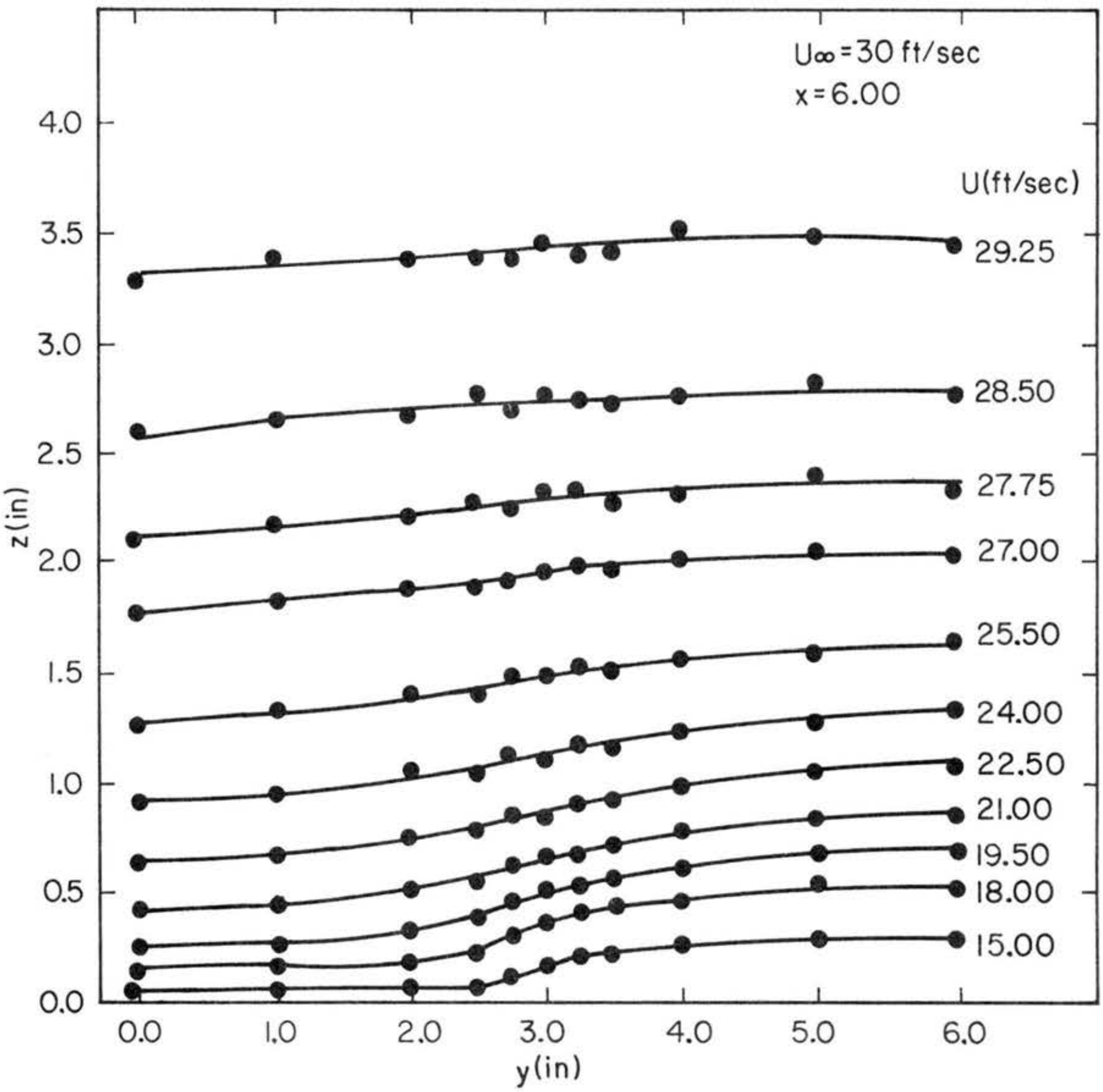

Fig. 5.19a Curves of constant velocity at x = 6 ft. for U_∞ = 30 ft/sec

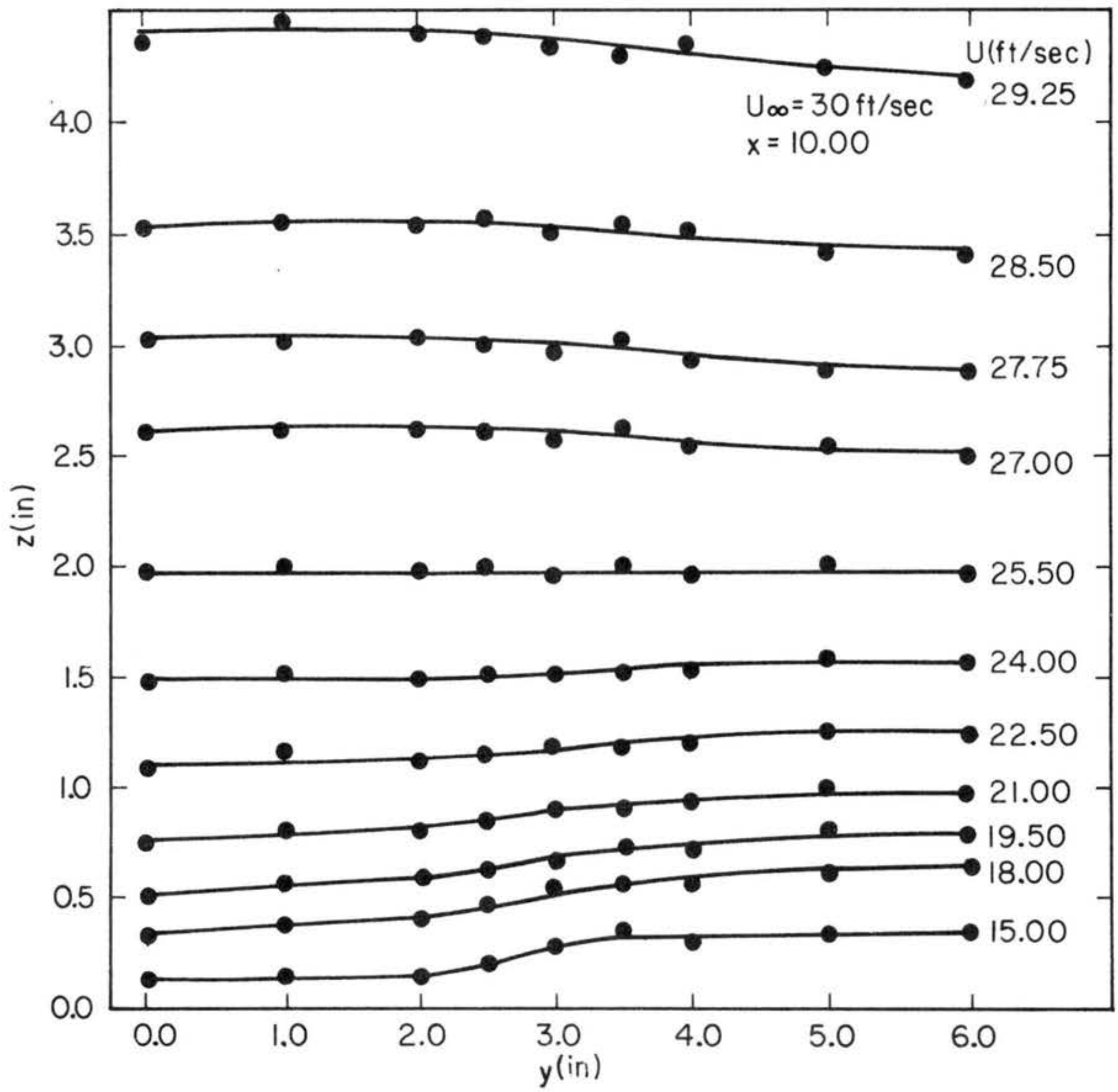

Fig. 5.19b Curves of constant velocity at x = 10 ft. for U_∞= 30 ft/sec

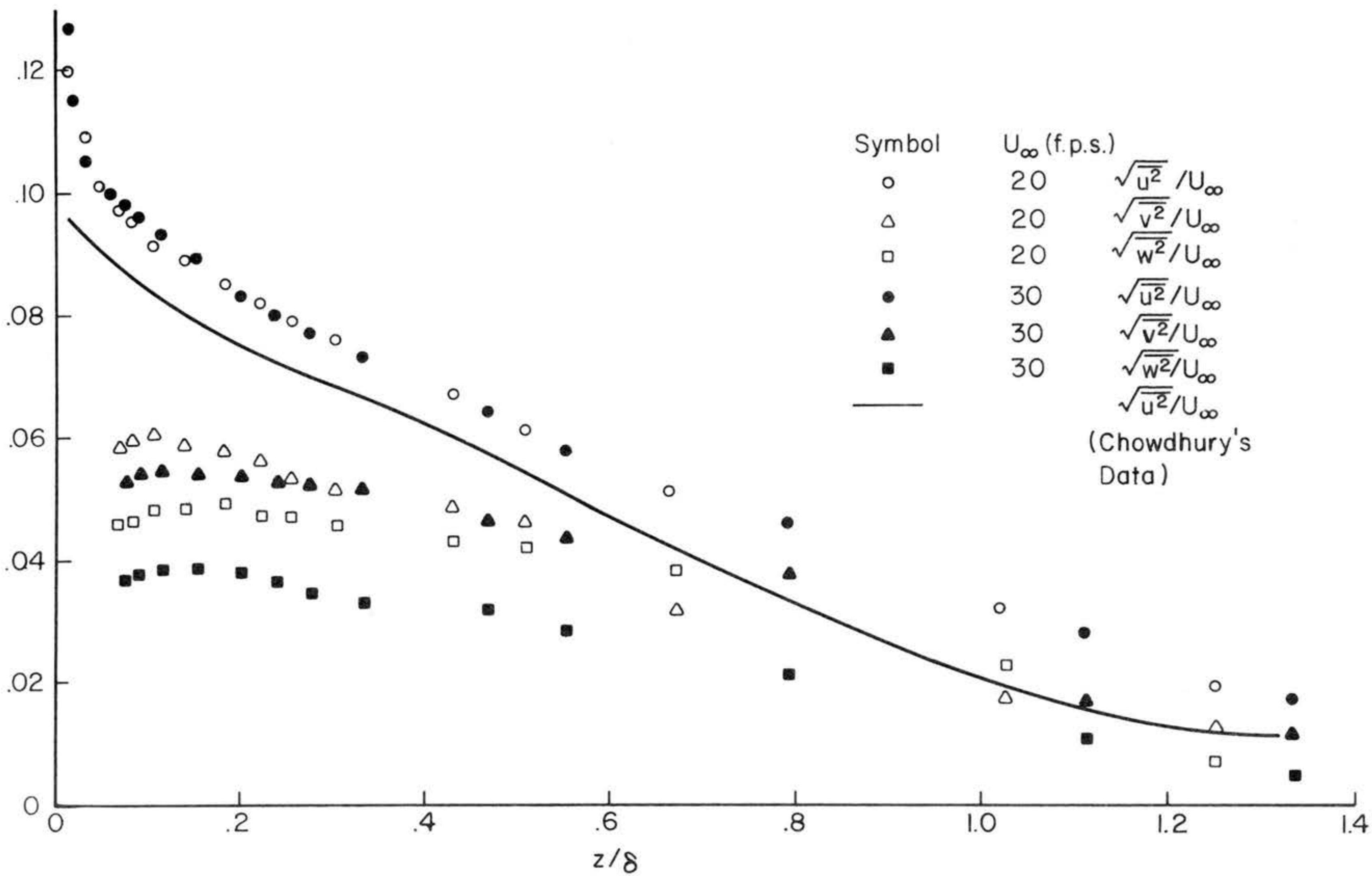

Fig. 5.20a Distribution of turbulent intensities at x = 6 ft. and y = 0 in.

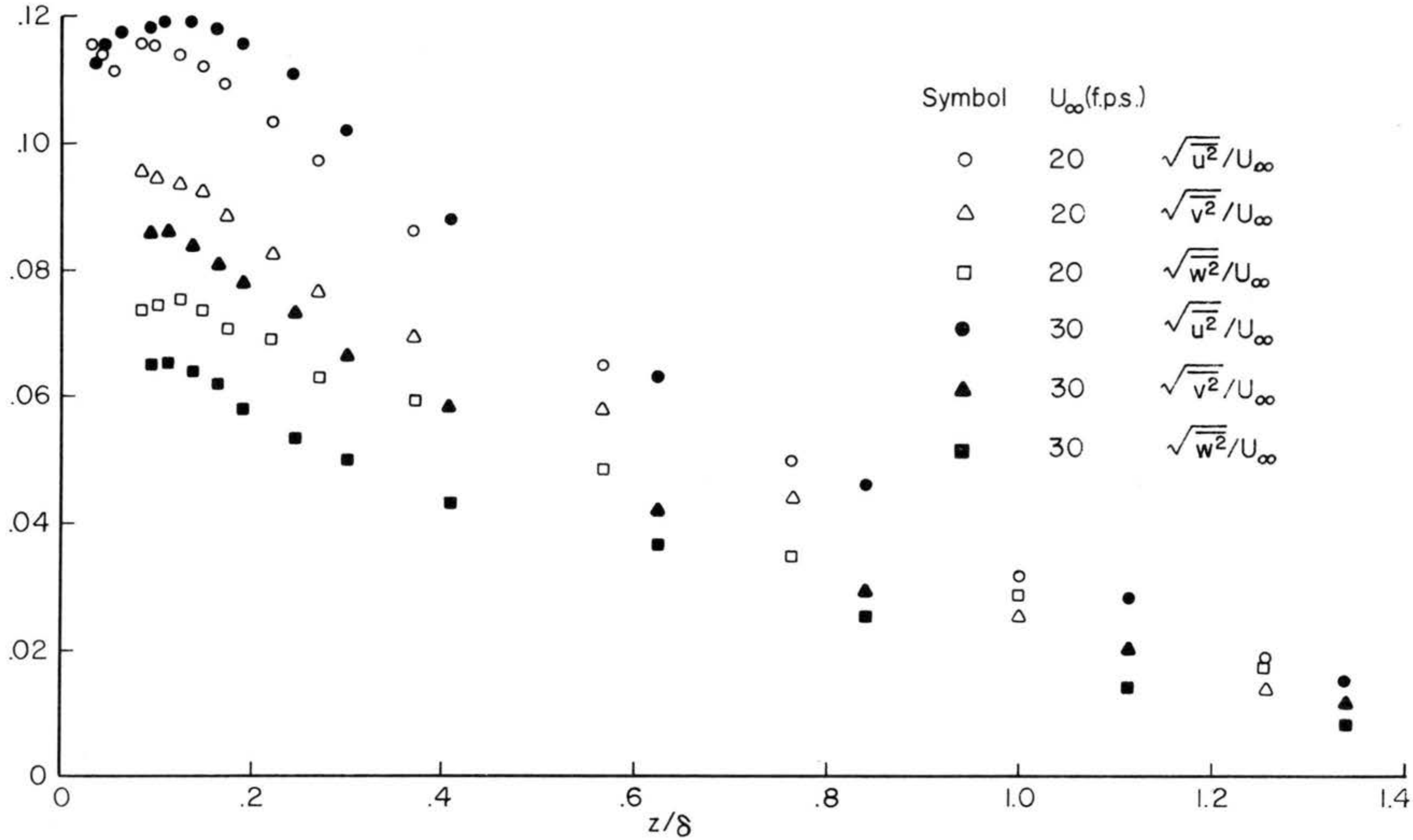

Fig. 5.20b Distribution of turbulent intensities at x = 6 ft. and y = 6 in.

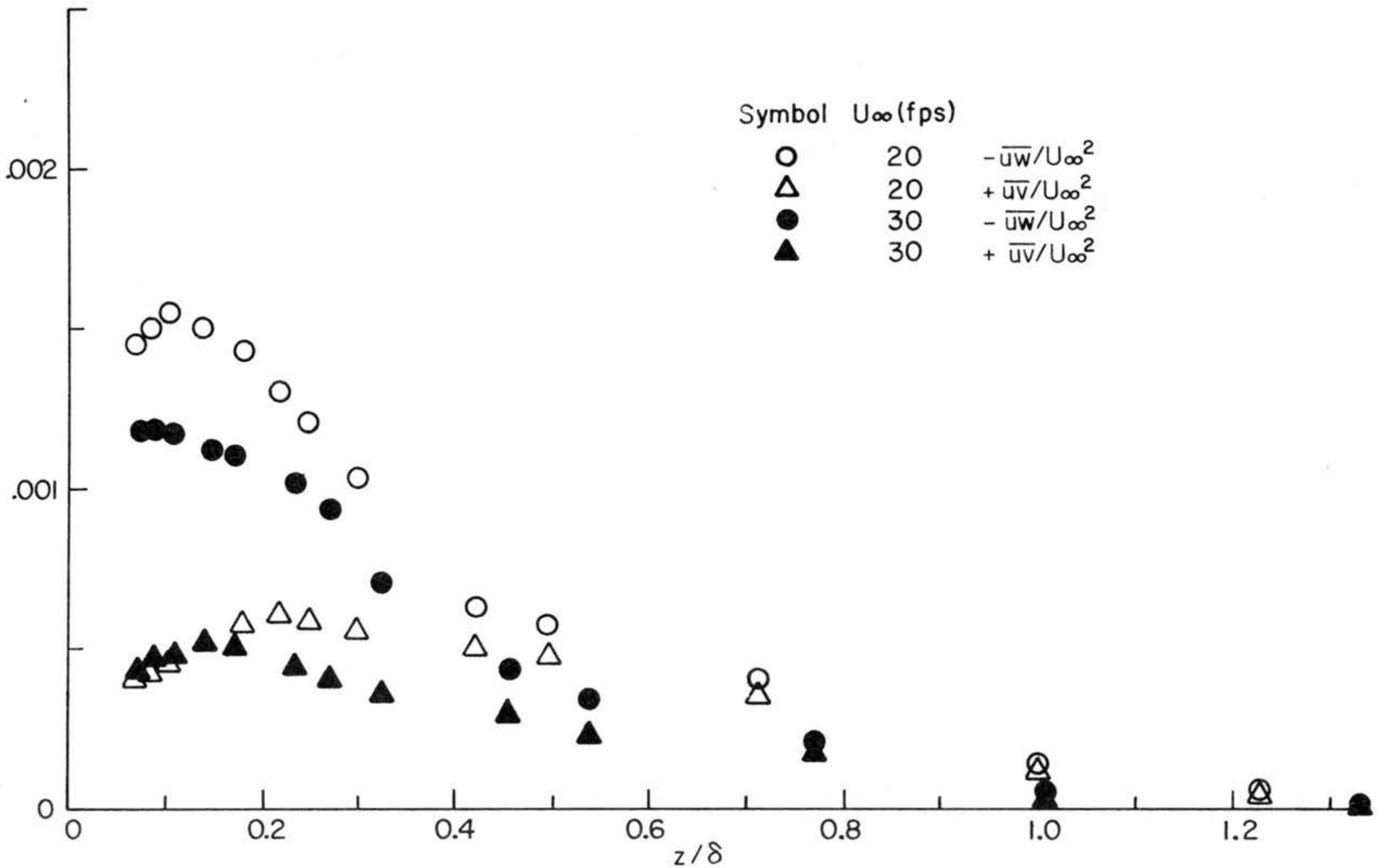

Fig. 5.21a Distribution of Turbulent shear stresses at x = 6 ft. and y = 0 in.

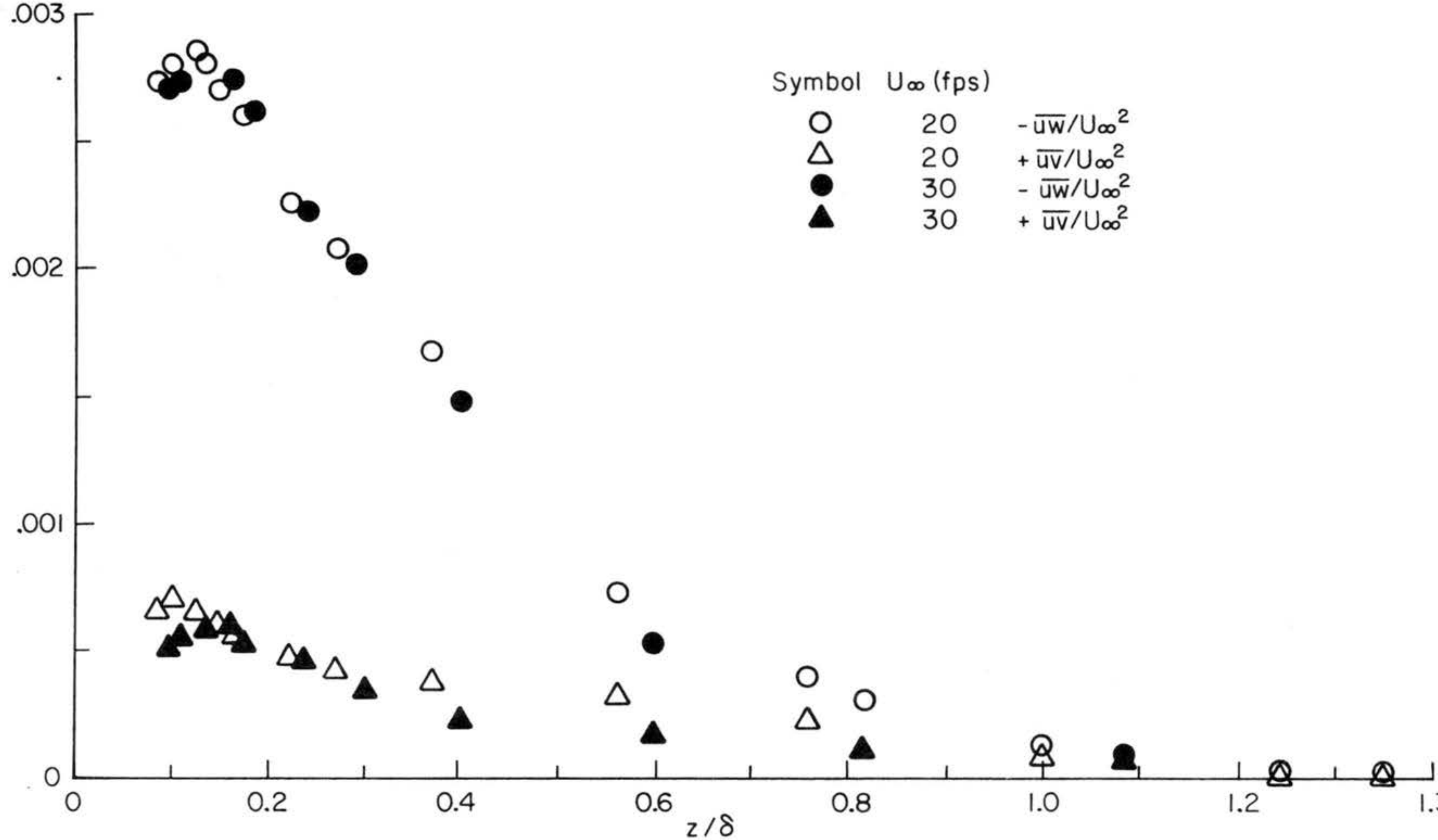

Fig. 5.21b Distribution of turbulent shear stresses at x = 6 ft. and y = 6 in.

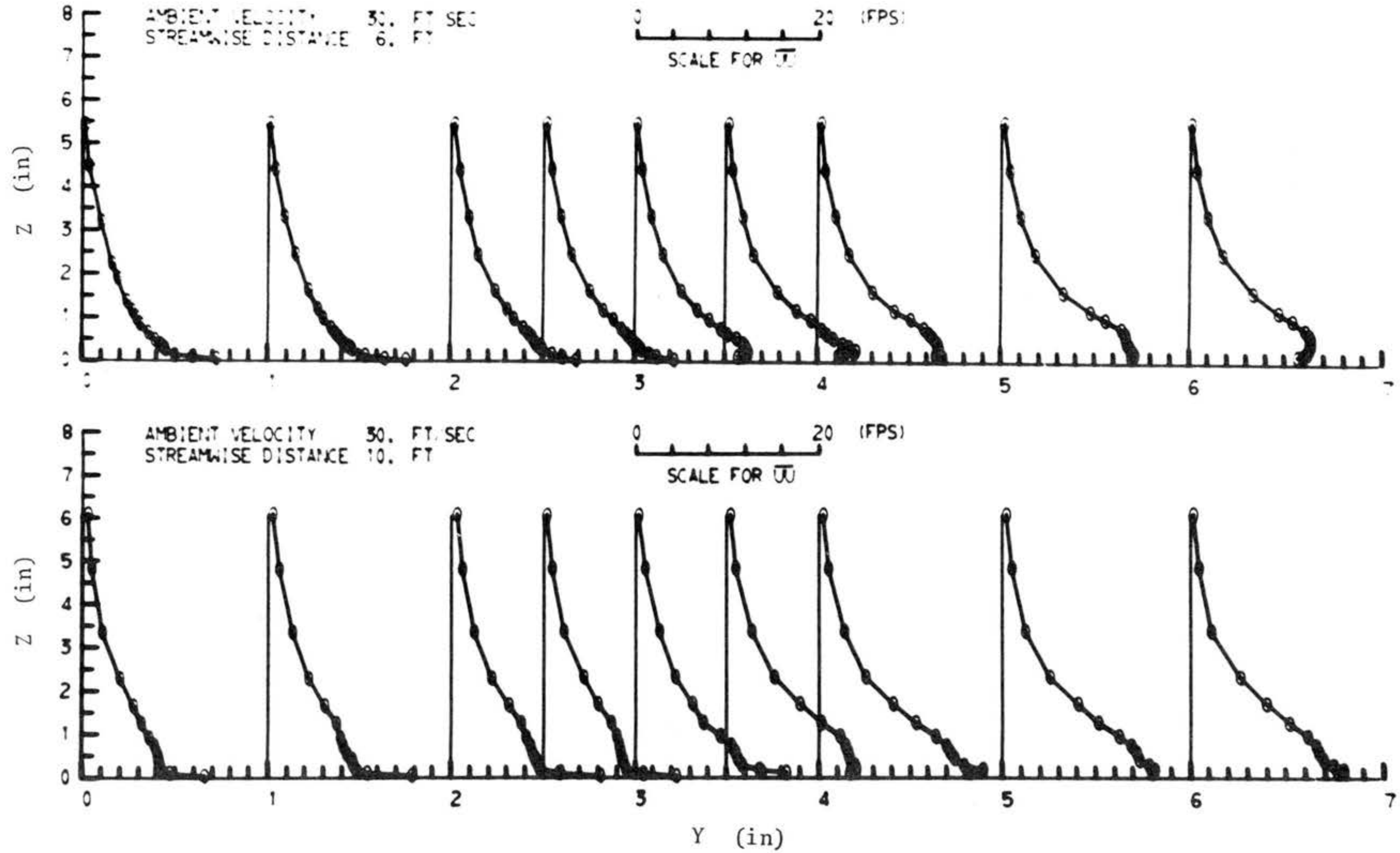

Fig. 5.22a Spanwise comparison of $\overline{u^2}$

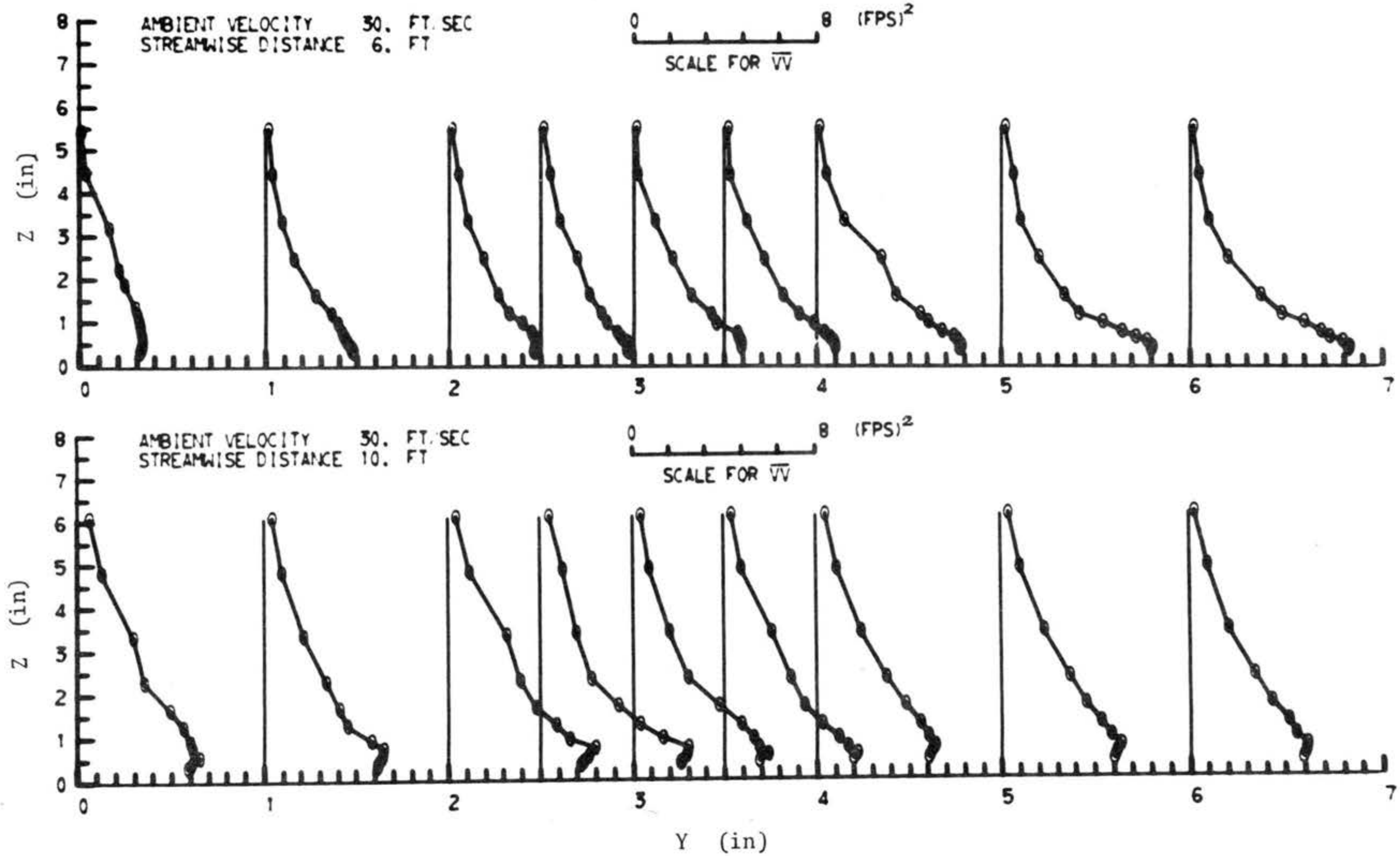

Fig. 5.22b Spanwise comparison of $\overline{v^2}$

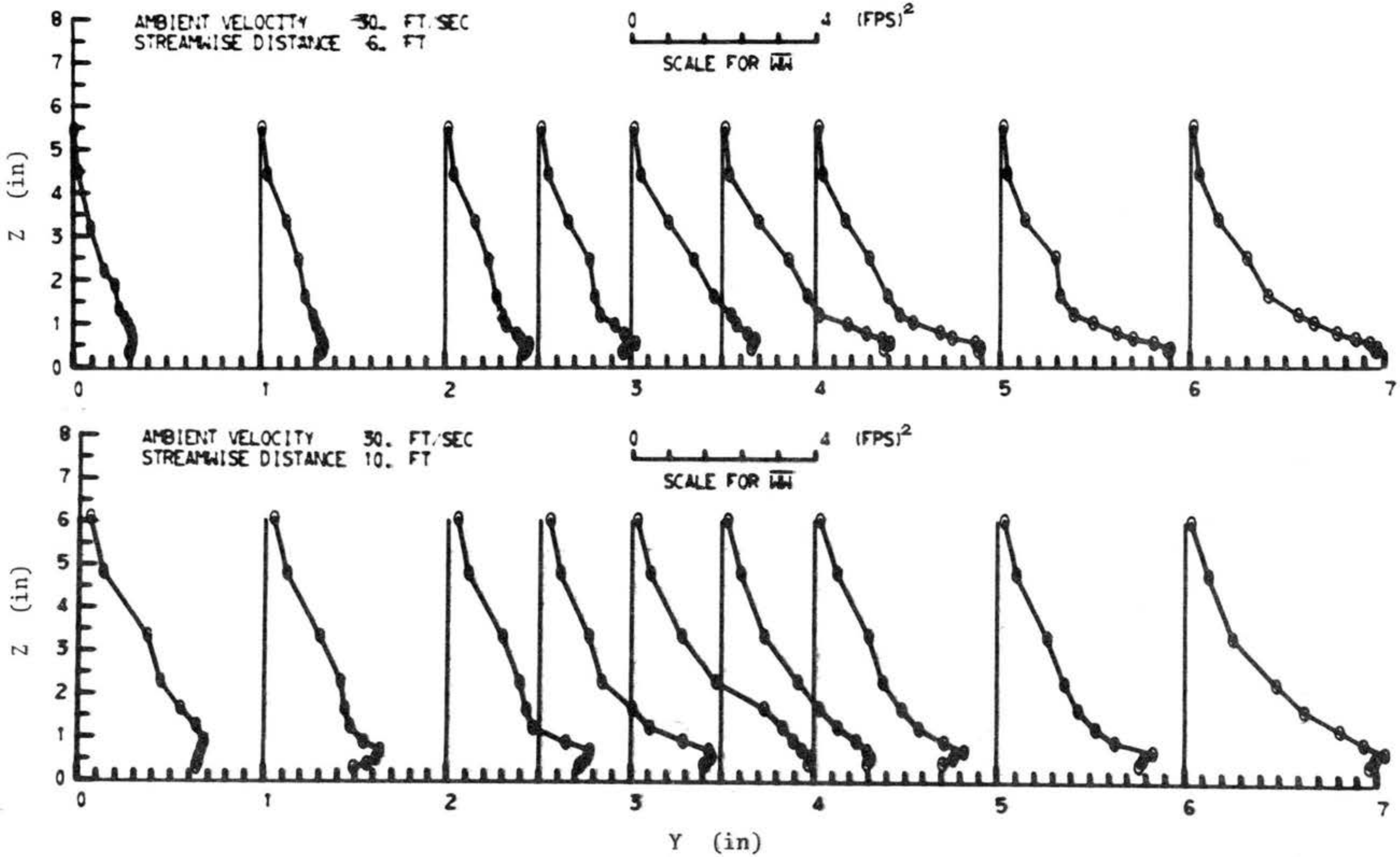

Fig. 5.22c Spanwise comparison of $\overline{w^2}$

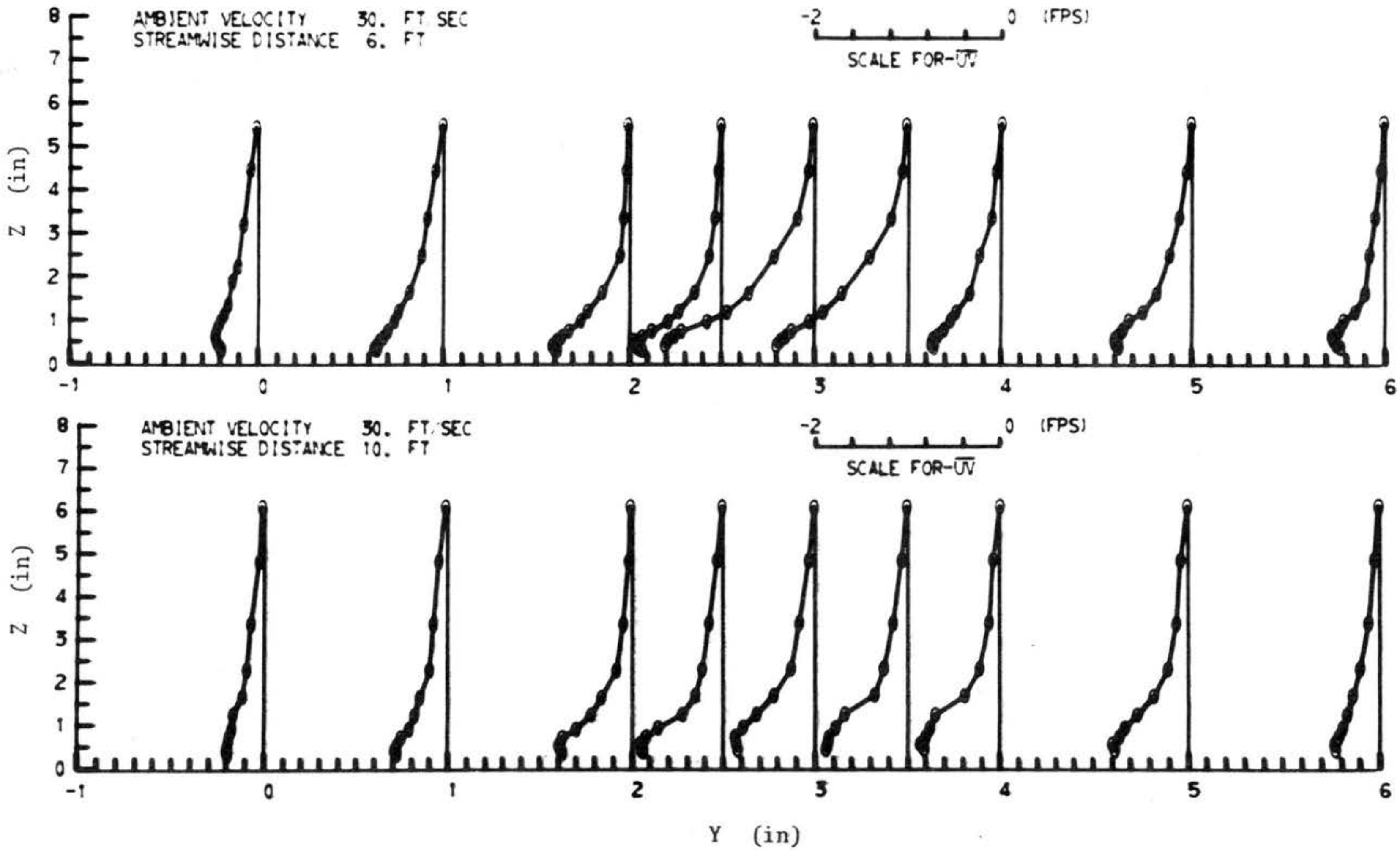

Fig. 5.22d Spanwise comparison of $-\overline{uv}$

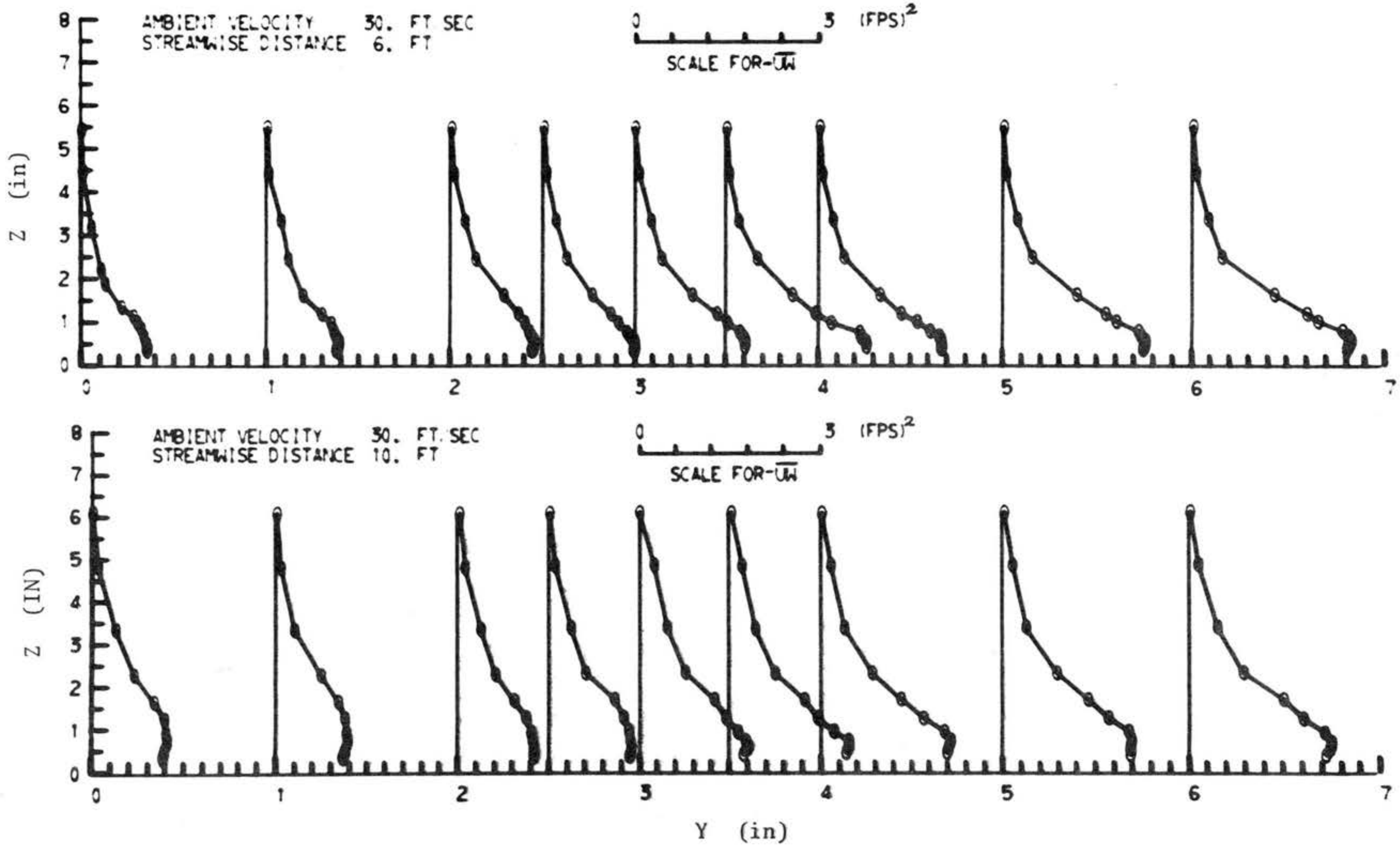

Fig. 5.22e Spanwise comparison of $-\overline{uw}$

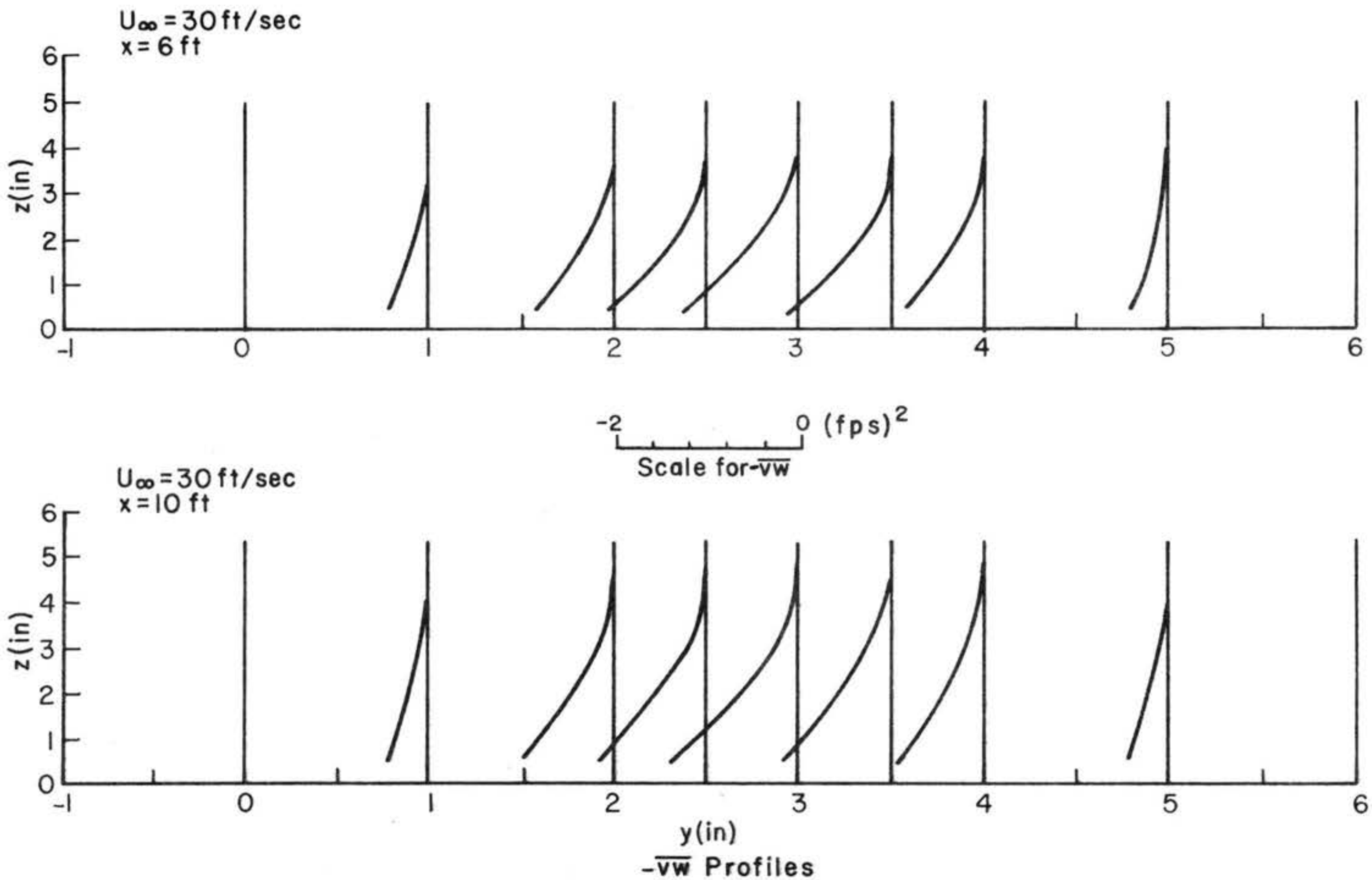

Fig. 5.22f Spanwise comparison of $-\overline{vw}$

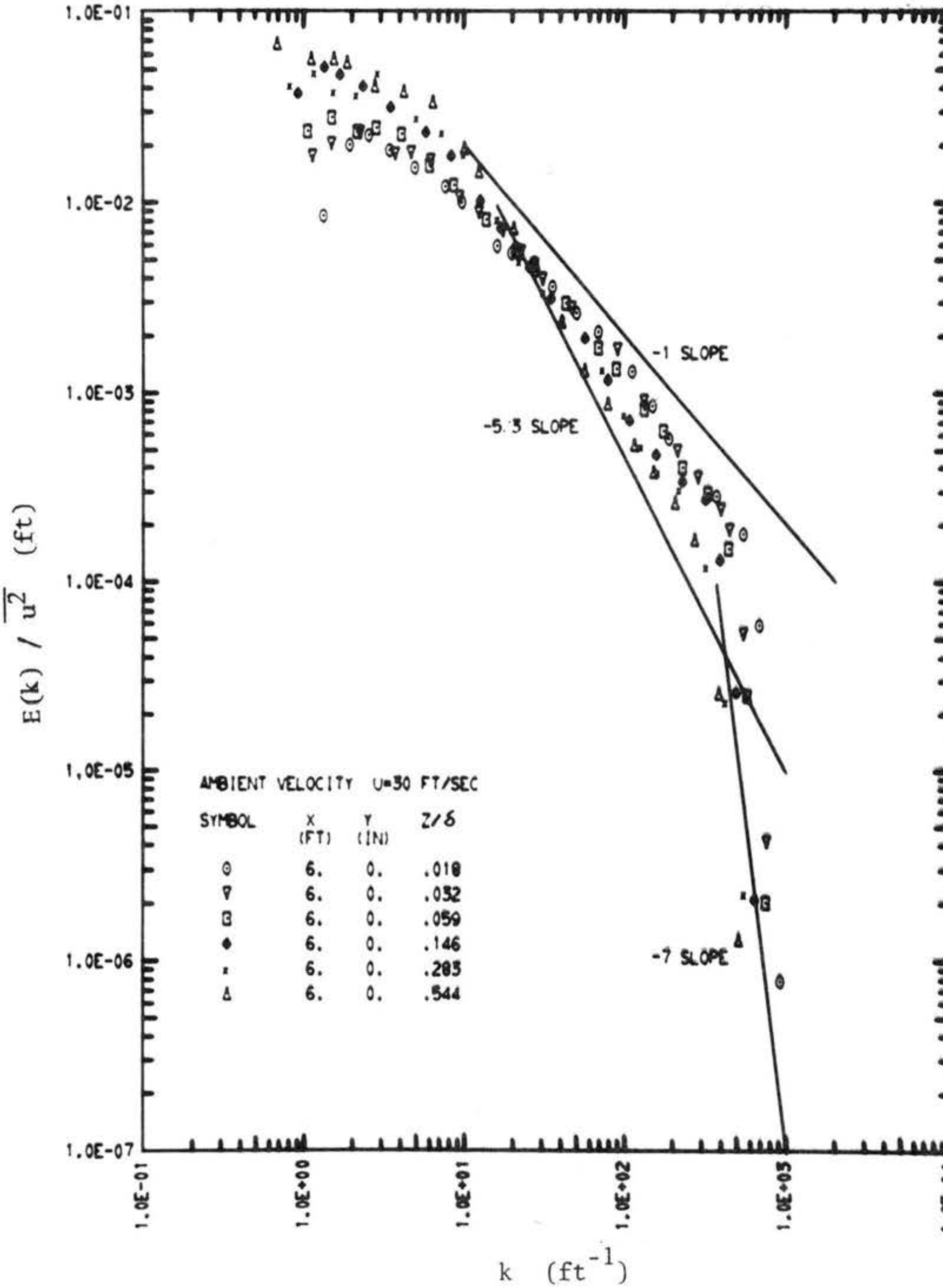

Fig. 5.23a Normalized spectra of streamwise turbulent velocity at x = 6 ft. and y = 0 in.

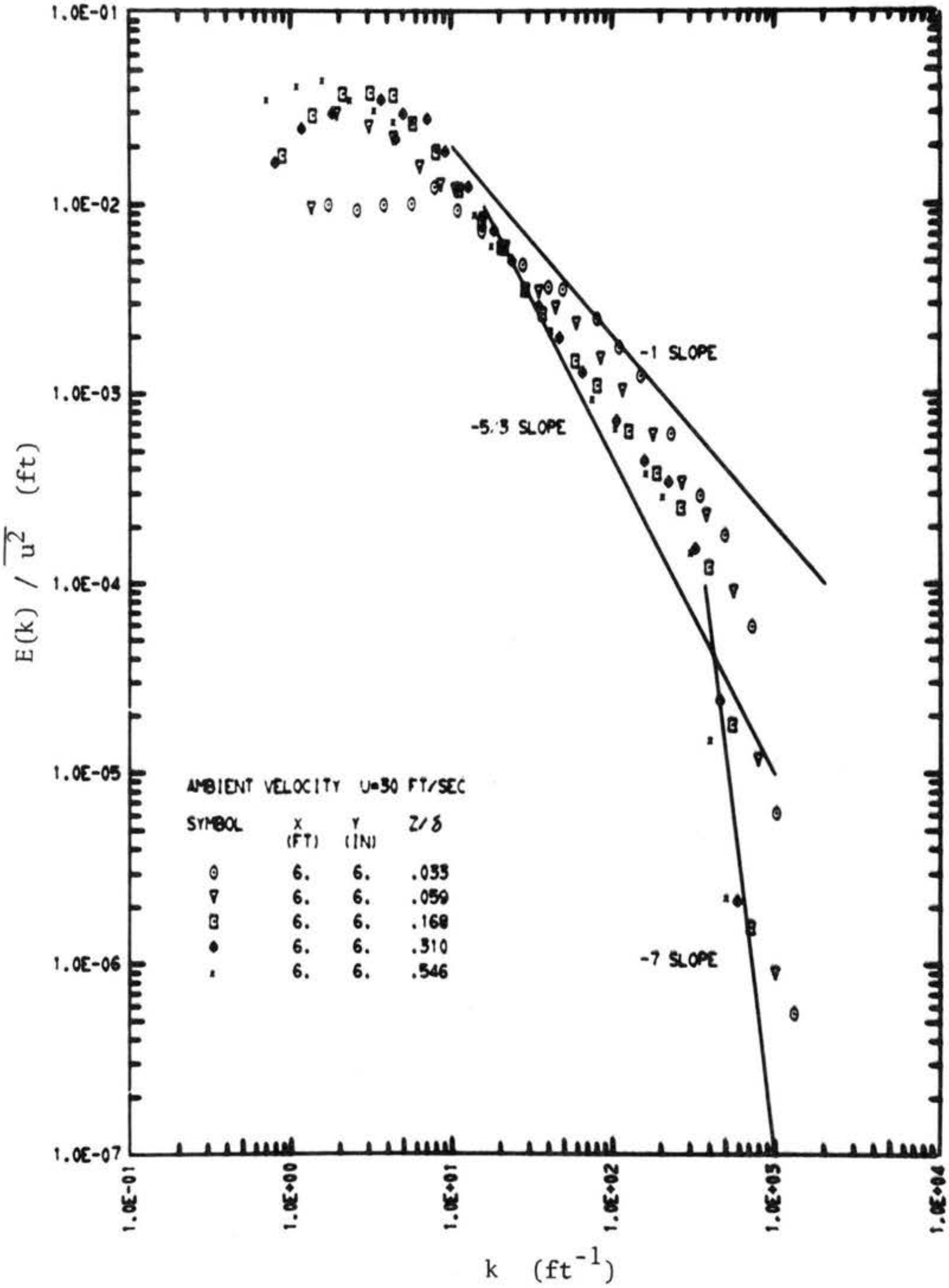

Fig. 5.23b Normalized spectra of streamwise turbulent velocity at x = 6 ft, and y = 6 in.

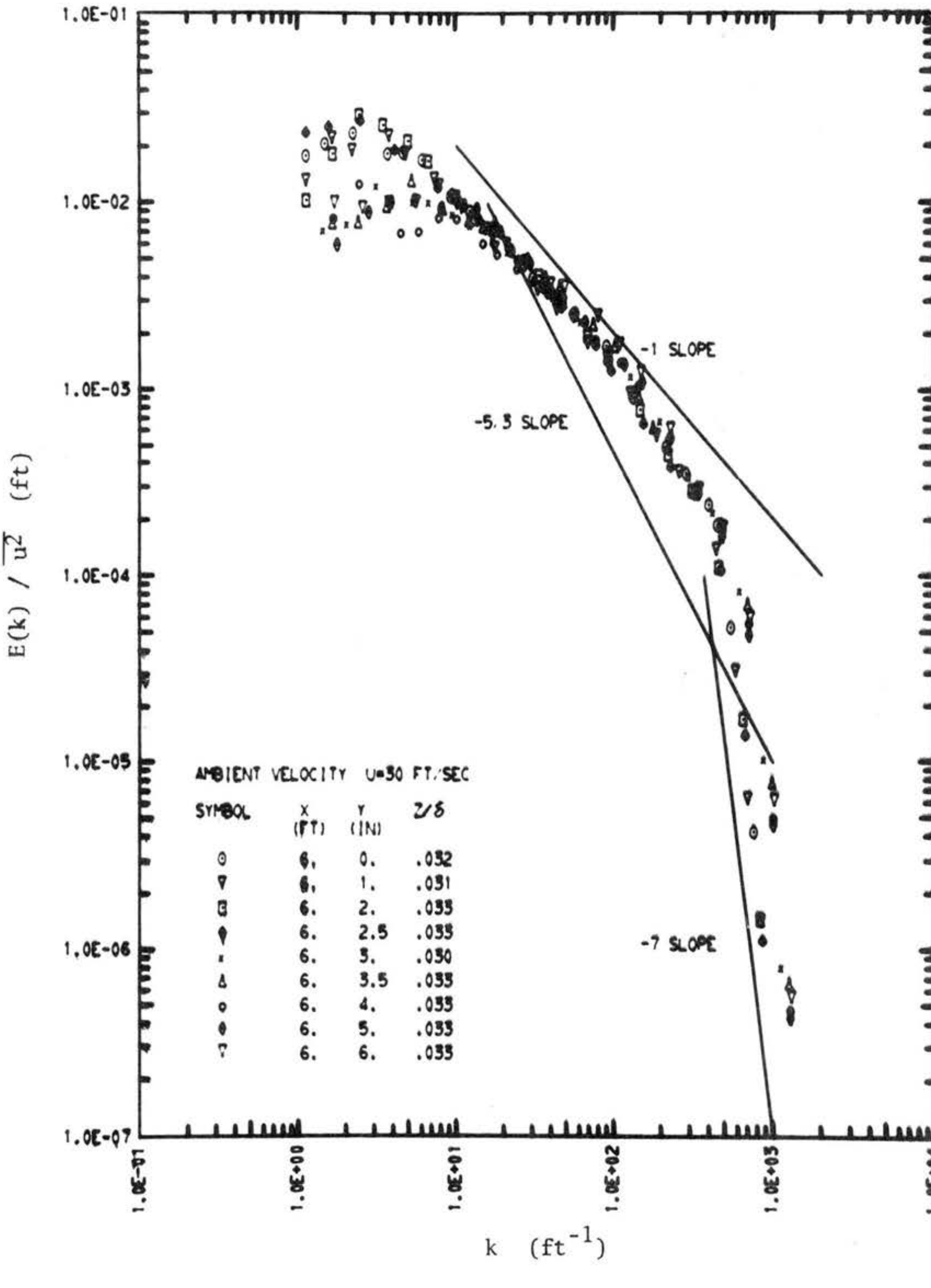

Fig. 5.24a Spanwise comparison of normalized spectra of streamwise turbulent velocity at x = 6 ft. and $z/\delta \simeq 0.03$

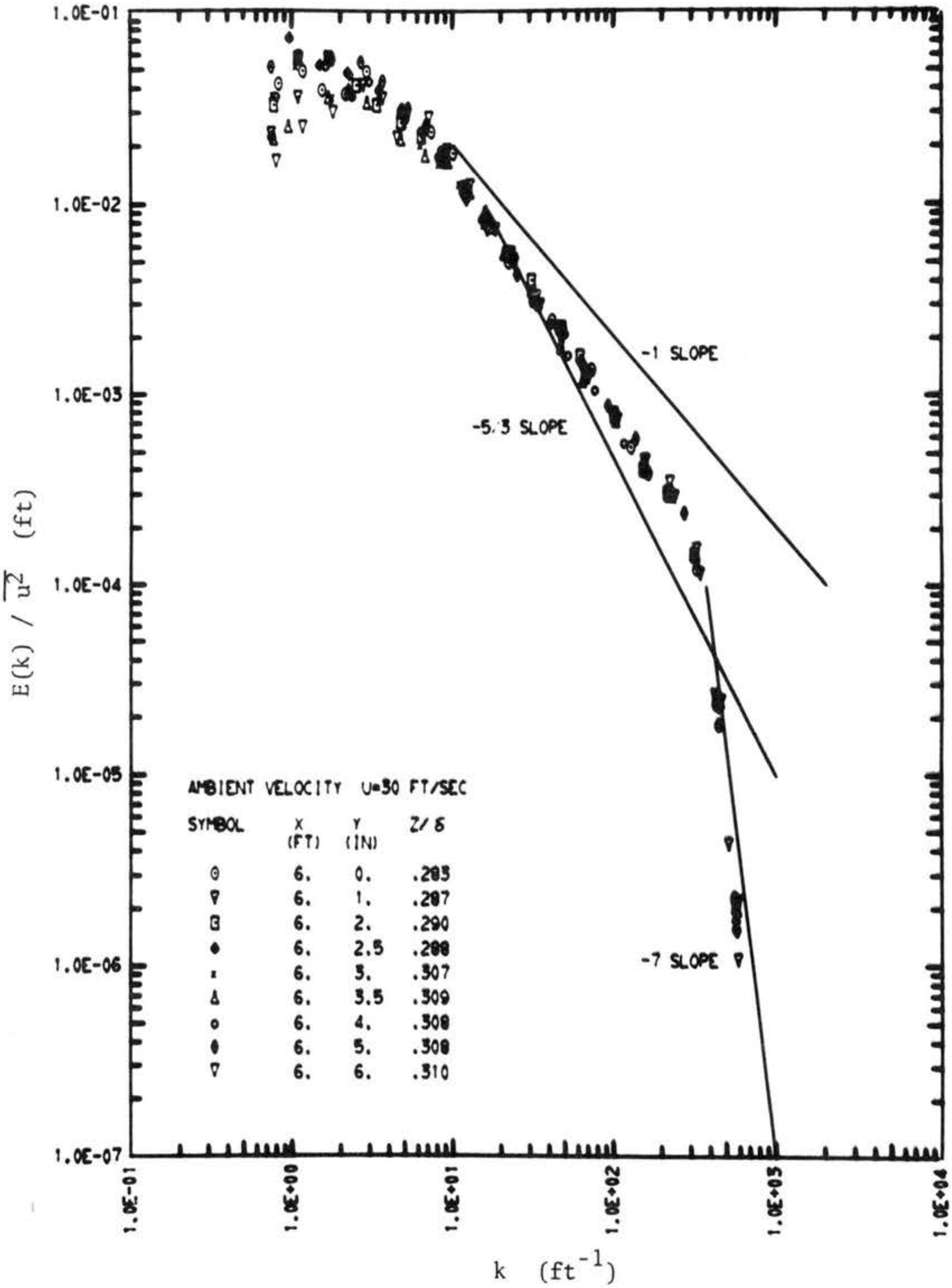

Fig. 5.24b Spanwise comparison of normalized spectra of streamwise turbulent velocity at x = 6 ft. and $z/\delta \simeq 0.30$

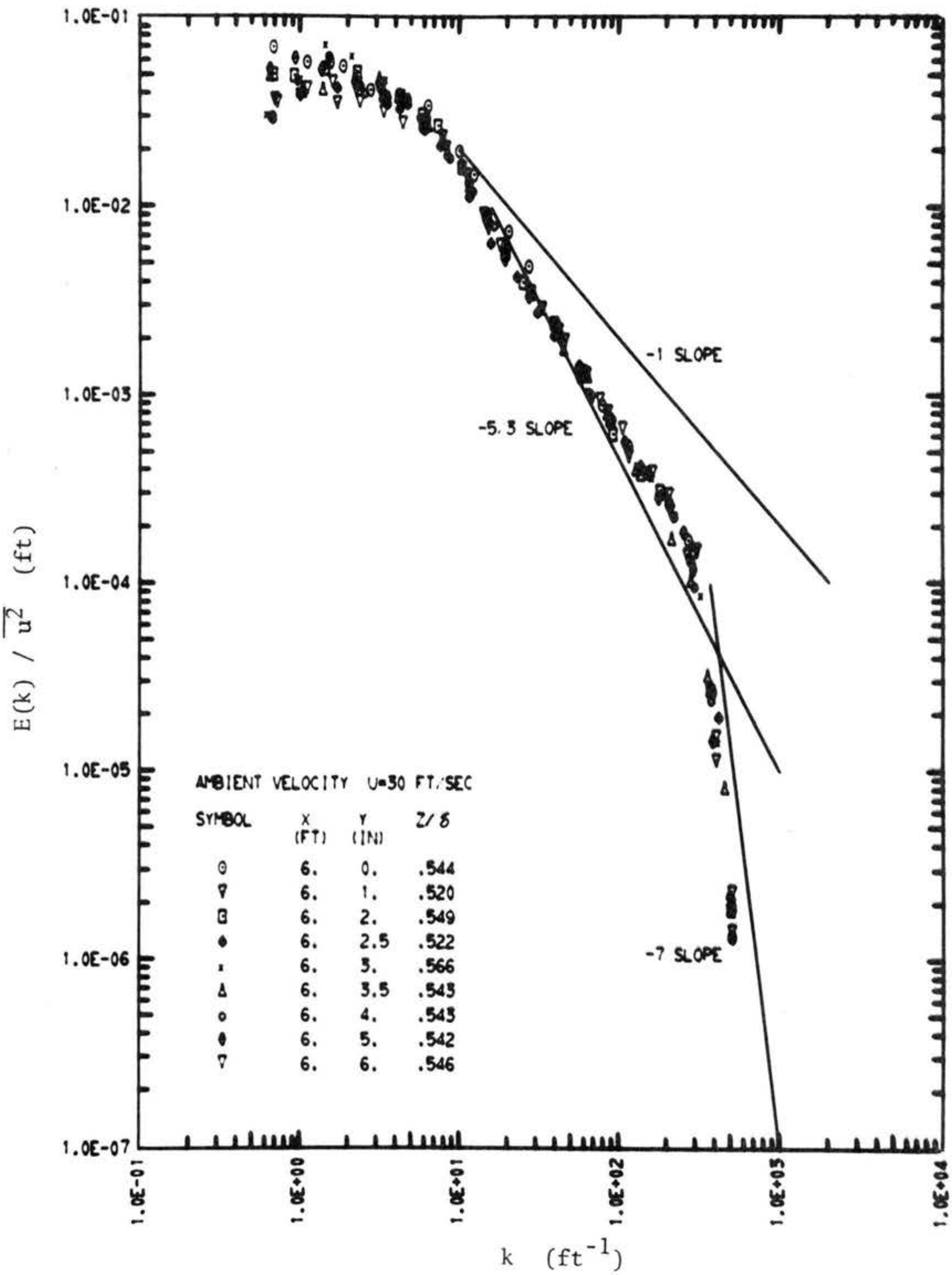

Fig. 5.24c Spanwise comparison of normalized spectra of streamwise turbulent velocity at x = 6 ft. and $z/\delta \simeq 0.54$

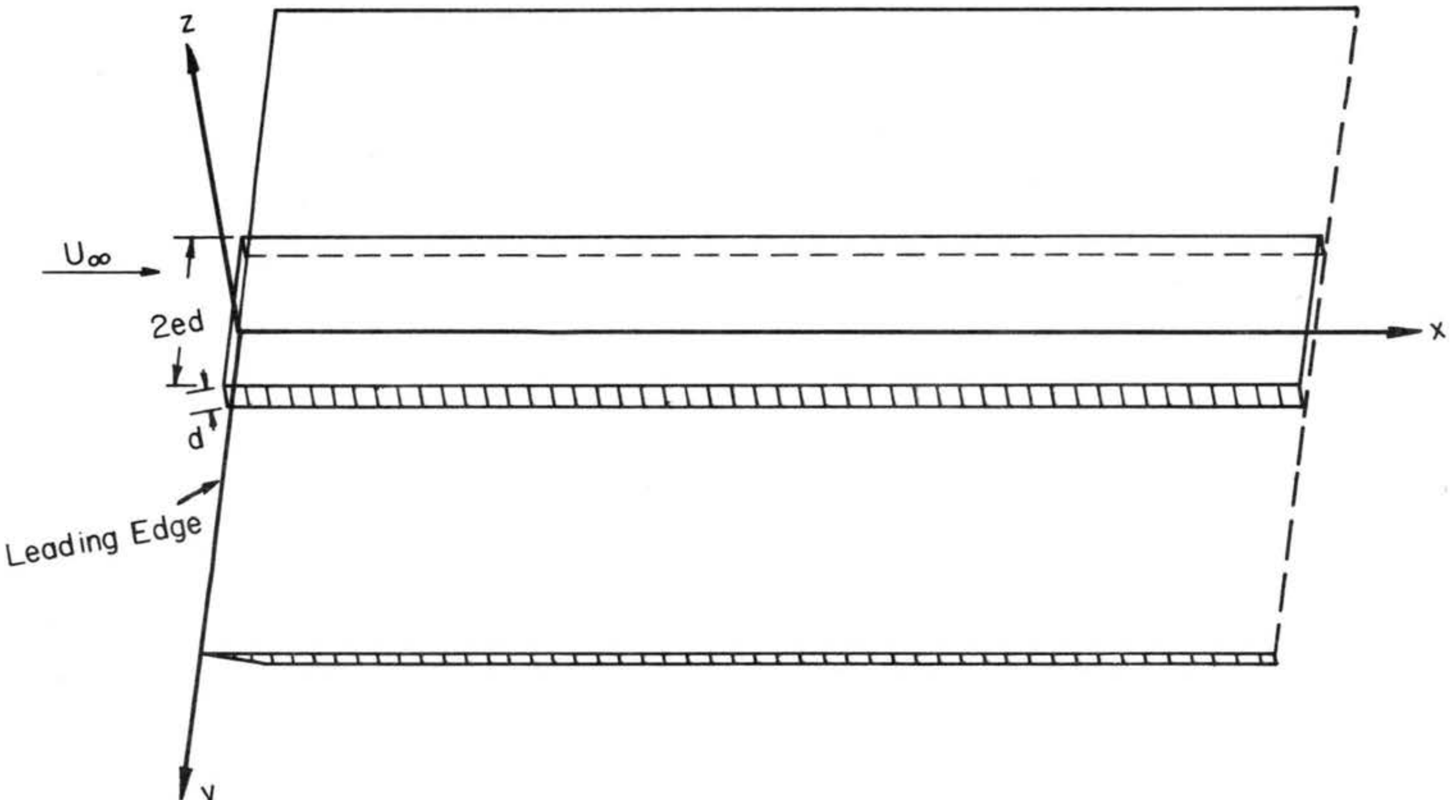

Fig. A.1 Coordinate system for boundary layer flow over a three-dimensional obdtscle

Unclassified

Security Classification

DOCUMENT CONTROL DATA - R & D

(Security classification of title, body of abstract and indexing annotation must be entered when the overall report is classified)

1. ORIGINATING ACTIVITY (Corporate author)	2a. REPORT SECURITY CLASSIFICATION
Fluid Dynamics and Diffusion Laboratory College of Engineering, Colorado State University Fort Collins, Colorado 80521	Unclassified 2b. GROUP

3. REPORT TITLE

Response of a Turbulent Boundary Layer to Lateral Roughness Discontinuity

4. DESCRIPTIVE NOTES (Type of report and inclusive dates)

Technical Report

5. AUTHOR(S) (First name, middle initial, last name)

Wang, H. and Nickerson, E. C.

6. REPORT DATE	7a. TOTAL NO. OF PAGES	7b. NO. OF REFS
July 1972	158	85

8a. CONTRACT OR GRANT NO.	9a. ORIGINATOR'S REPORT NUMBER(S)
14-01-0001	CER71-72HW-ECN51
b. PROJECT NO. N00014-68-A-0493-0001	
c.	9b. OTHER REPORT NO(S) (Any other numbers that may be assigned this report)
d.	THEMIS Technical Report No. 18

10. DISTRIBUTION STATEMENT

Distribution of this report is unlimited.

11. SUPPLEMENTARY NOTES	12. SPONSORING MILITARY ACTIVITY
	U.S. Department of Defense Office of Naval Research

13. ABSTRACT The structure of the turbulent boundary layer on a flat plate consisting of alternate, longitudinal strips of smooth and rough (Sand paper, Grit 4) surfaces parallel to the direction of the flow has been investigated. Measurements of mean velocity, wall shear stress, turbulent intensities, turbulent shear stresses and energy spectra of the streamwise turbulent velocity were obtained.

The flow field can be subdivided into three regions. These are: (a) the "smooth" region along the centerline of each smooth strip; (b) the "rough" region along the centerline of each rough strip; and (c) the "intermediate" region lying between the smooth and the rough regions. In both smooth and rough regions, the flow conditions are found to be nearly analogous to those in two-dimensional boundary layers over smooth and rough walls, respectively. In the intermediate region the wall shear stress was found to adjust itself very rapidly to the local conditions of the wall while going from the smooth to the rough region. The vertical distribution of mean velocity can satisfactorily be expressed by the two-dimensional descriptions for the law of the wall and the velocity-defect law. However, the two laws are not universal but form a family of curves depending on the local wall shear stress. The spanwise change from smooth-wall conditions to rough-wall conditions will induce a weak cross-flow directed from the rough to the smooth region near the wall. A theoretical description of the turbulent shear stress $-\rho\overline{vw}$ which is responsible for the generation of this cross-flow has been presented. The spanwise adjustment of turbulence quantities to local conditions of the wall takes place at a slower rate than does the wall shear stress. The normalized spectra of the streamwise turbulent velocity remains largely unaffected by the surface configuration investigated here.

DD FORM 1 NOV 65 1473

Security Classification

Unclassified
Security Classification

14 KEY WORDS	LINK A		LINK B		LINK C	
	ROLE	WT	ROLE	WT	ROLE	WT
Turbulent Boundary Layer						
Roughness Discontinuities						
Mean Velocity						
Turbulent Intensities						
Turbulent Shear Stresses						
Energy Spectra						

Security Classification

April 1971

DISTRIBUTION LIST FOR UNCLASSIFIED
TECHNICAL REPORTS ISSUED UNDER
CONTRACT N00014-68-A 0493-0001 TASK 000-414

Defense Documentation Center
Cameron Station
Alexandria, Virginia 22314 (12)

Technical Library
Naval Ship Research and Development Laboratory
Annapolis, Maryland 21402

Professor Bruce Johnson
Engineering Department
Naval Academy
Annapolis, Maryland 21402

Library
Naval Academy
Annapolis, Maryland 21402

Professor W.R. Debler
Department of Engineering Mechanics
University of Michigan
Ann Arbor, Michigan 48108

Professor W.P. Graebel
Department of Engineering Mechanics
University of Michigan
College of Engineering
Ann Arbor, Michigan 48108

Professor Finn C. Michelsen
Naval Architecture and Marine Engineering
445 West Engineering Building
University of Michigan
Ann Arbor, Michigan 48108

Dr. Francis Ogilvie
Department of Naval Architecture and Marine Engineering
University of Michigan
Ann Arbor, Michigan 48108

Professor W.W. Willmarth
Department of Aerospace Engineering
University of Michigan
Ann Arbor, Michigan 48108

Dr. S.A. Piacsek
Argonne National Laboratory
Applied Mathematics Division
9700 S. Cass Avenue
Argonne, Illinois 60439

AFOSR (REM)
1400 Wilson Boulevard
Arlington, Virginia 22204

Professor S. Corrsin
Mechanics Department
The Johns Hopkins University
Baltimore, Maryland 20910

Professor L.S.G. Kovasznay
The Johns Hopkins University
Baltimore, Maryland 20910

Professor O.M. Phillips
The Johns Hopkins University
Baltimore, Maryland 20910

Librarian
Department of Naval Architecture
University of California
Berkeley, California 94720

Professor Israel Cornet
Department of Mechanical Engineering
University of California
Berkeley, California 94720

Professor M. Holt
Division of Aeronautical Sciences
University of California
Berkeley, California 94720

Professor E.V. Laitone
Department of Mechanical Engineering
University of California
Berkeley, California 94720

Professor P. Lieber
Department of Mechanical Engineering
University of California
Institute of Engineering Research
Berkeley, California 94720

Professor J.R. Paulling
Department of Naval Architecture
University of California
Berkeley, California 94720

Professor J.V. Wehausen
Department of Naval Architecture
University of California
Berkeley, California 94720

Professor E.R. van Driest
Virginia Polytechnic Institute and University
Department of Aerospace Engineering
Blacksburg, Virginia 24061

Commander
Boston Naval Shipyard
Boston, Massachusetts 02129

Director
Office of Naval Research Branch Office
495 Summer Street
Boston, Massachusetts 02210

Commander
Puget Sound Naval Shipyard
Bremerton, Washington 98314

Professor J.J. Foody
Chairman, Engineering Department
State University of New York
Maritime College
Bronx, New York 10465

Dr. Alfred Ritter
Assistant Head, Applied Mechanics Department
Cornell Aeronautical Laboratory, Inc.
Buffalo, New York 14221

Dr. J.W. Morris
Manager, Material Sciences Section
Advanced Materials Research
Bell Aerospace Company
P.O. Box 1
Buffalo, New York 14240

Professor G.H. Carrier
Department of Engineering and Applied Physics
Harvard University
Cambridge, Massachusetts 02138

Commanding Officer
NROTC Naval Administrative Unit
Massachusetts Institute of Technology
Cambridge, Massachusetts 02139

Professor M.A. Abkowitz
Department of Naval Architecture and Marine Engineering
Massachusetts Institute of Technology
Cambridge, Massachusetts 02139

Professor A.T. Ippen
Department of Civil Engineering
Massachusetts Institute of Technology
Cambridge, Massachusetts 02139

Professor L.N. Howard
Department of Mathematics
Massachusetts Institute of Technology
Cambridge, Massachusetts 02139

Professor E.W. Merrill
Department of Mathematics
Massachusetts Institute of Technology
Cambridge, Massachusetts 02139

Professor E. Mollo-Christensen
Room 54-1722
Massachusetts Institute of Technology
Cambridge, Massachusetts 02139

Professor N. Newman
Department of Naval Architecture and Marine Engineering
Massachusetts Institute of Technology
Cambridge, Massachusetts 02139

Professor A.H. Shapiro
Department of Mechanical Engineering
Massachusetts Institute of Technology
Cambridge, Massachusetts 02139

Commander
Charleston Naval Shipyard
U.S. Naval Base
Charleston, South Carolina 29408

A.R. Kuhlthau, Director
Research Laboratories for the Engineering Sciences
Thorton Hall, University of Virginia
Charlottesville, Virginia 22903

Director
Office of Naval Research Branch Office
536 South Clark Street
Chicago, Illinois 60605

Library
Naval Weapons Center
China Lake, California 93555

Professor J.M. Burgers
Institute of Fluid Dynamics and Applied Mathematics
University of Maryland
College Park, Maryland 20742

Professor Pai
Institute for Fluid Dynamics and Applied Mathematics
University of Maryland
College Park, Maryland 20740

Acquisition Director
NASA Scientific & Technical Information
P.O. Box 33
College Park, Maryland 20740

Technical Library
Naval Weapons Laboratory
Dahlgren, Virginia 22448

Computation & Analyses Laboratory
Naval Weapons Laboratory
Dahlgren, Virginia 22448

Dr. C.S. Wells, Jr.
Manager - Fluid Mechanics
Advanced Technology Center, Inc.
P.O. Box 6144
Dallas, Texas 75222

Dr. R.H. Kraichnan
Dublin, New Hampshire 03444

Commanding Officer
Army Research Office
Box CM, Duke Station
Durham, North Carolina 27706

Professor A. Charnes
The Technological Institute
Northwestern University
Evanston, Illinois 60201

Dr. Martin H. Bloom
Polytechnic Institute of Brooklyn
Graduate Center, Dept. of Aerospace
Engineering and Applied Mechanics
Farmingdale, New York 11735

Technical Documents Center
Building 315
U.S. Army Mobility Equipment
Research and Development Center
Fort Belvoir, Virginia 22060

Professor J.E. Cermak
College of Engineering
Colorado State University
Ft. Collins, Colorado 80521

Technical Library
Webb Institute of Naval Architecture
Glen Cove, Long Island, New York 11542

Professor E.V. Lewis
Webb Institute of Naval Architecture
Glen Cove, Long Island, New York 11542

Dr. B.N. Pridmore Brown
Northrop Corporation
NORAIR-Div.
Hawthorne, California 90250

Dr. J.P. Breslin
Stevens Institute of Technology
Davidson Laboratory
Hoboken, New Jersey 07030

Dr. D. Savitsky
Stevens Institute of Technology
Davidson Laboratory
Hoboken, New Jersey 07030

Mr. C.H. Henry
Stevens Institute of Technology
Davidson Laboratory
Hoboken, New Jersey 07030

Dr. J.P. Craven
University of Hawaii
1801 University Avenue
Honolulu, Hawaii 96822

Professor E.L. Resler
Graduate School of Aeronautical Engineering
Cornell University
Ithaca, New York 14851

Professor John Miles
c/o I.G.P.P.
University of California, San Diego
La Jolla, California 92038

Director
Scrippe Institution of Oceanography
University of California
La Jolla, California 92037

Professor A. Ellis
University of California, San Diego
Department of Aerospace & Mechanical Engineering
La Jolla, California 92037

Dr. B. Sternlicht
Mechanical Technology Incorporated
968 Albany-Shaker Road
Latham, New York 12110

Dr. Coda Pan
Mechanical Technology Incorporated
968 Albany-Shaker Road
Latham, New York 12110

Mr. P. Eisenberg, President
Hydronautics, Inc.
Pindell School Road
Howard County
Laurel, Maryland 20810

Mr. M.P. Tulin
Hydronautics, Inc.
Pindell School Road
Howard County
Laurel, Maryland 20810

Mr. Alfonso Alcedan L.,Director
Laboratorio Nacional De Hydraulics
Antigui Cameno A. Ancon
Casilla Jostal 682
Lima, Peru

Commander
Long Beach Naval Shipyard
Long Beach, California 90802

Professor John Laufer
Department of Aerospace Engineering
University Park
Los Angeles, California 90007

Professor J.M. Killen
St. Anthony Falls Hydraulic Lab.
University of Minnesota
Minneapolis, Minnesota 55414

Lorenz G. Straub Library
St. Anthony Falls Hydraulic Lab.
Mississippi River at 3rd Avenue S.E.
Minneapolis, Minnesota 55414

Professor J. Ripkin
St. Anthony Falls Hydraulic Lab.
University of Minnesota
Minneapolis, Minnesota 55414

Dr. W. Silberman
St. Anthony Falls Hydraulic Lab.
Mississippi River at 3rd Avenue S.E.
Minneapolis, Minnesota 55414

Superintendent
Naval Postgraduate School
Library Code 0212
Monterey, California 93940

Professor A.B. Metzner
University of Delaware
Newark, New Jersey 19711

Technical Library
Naval Underwater Systems Center
Newport, Rhode Island 02840

Professor Dudley D. Fuller
Department of Mechanical Engineering
Columbia University
New York, New York 10027

Professor V. Castelli
Department of Mechanical Engineering
Columbia University
New York, New York 10027

Professor H. Elrod
Department of Mechanical Engineering
Columbia University
New York, New York 10027

Professor J.J. Stoker
Institute of Mathematical Sciences
New York University
251 Mercer Street
New York, New York 10003

Society of Naval Architects and Marine Engineering
74 Trinity Place
New York, New York 10006

Engineering Societies Library
345 East 47th Street
New York, New York 10017

Office of Naval Research
New York Area Office
207 W. 24th Street
New York, New York 10011

Miss O.M. Leach, Librarian
National Research Council
Aeronautical Library
Montreal Road
Ottawa 7, Canada

Technical Library
Naval Ship Research and Development Center
Panama City, Florida 32401

Technical Library
Naval Undersea R & D Center
Pasadena Laboratory
3202 E. Foothill Boulevard
Pasadena, California 91107

Dr. Andrew Fabula
Naval Undersea Research & Development Center
Pasadena Laboratory
3202 E. Foothill Boulevard
Pasadena, California 91107

Dr. J.W. Hoyt
Naval Undersea R & D Center
Pasadena Laboratory
3202 E. Foothill Boulevard
Pasadena, California 91107

Professor A. Acosta
Department of Mechanical Engineering
California Institute of Technology
Pasadena, California 91109

Professor H. Liepmann
Department of Aeronautics
California Institute of Technology
Pasadena, California 91109

Professor M.S. Plesset
Engineering Division
California Institute of Technology
Pasadena, California 91109

Professor A. Roshko
California Institute of Technology
Pasadena, California 91109

Professor T.Y. Wu
Department of Engineering
California Institute of Technology
Pasadena, California 91109

Director
Office of Naval Research Branch Office
1030 E. Green Street
Pasadena, California 91101

Naval Ship Engineering Center
Philadelphia Division
Technical Library
Philadelphia, Pennsylvania 19112

Technical Library
Philadelphia Naval Shipyard
Philadelphia, Pennsylvania 19112

Professor R.C. Mac Camy
Department of Mathematics
Carnegie Institute of Technology
Pittsburgh, Pennsylvania 15213

Dr. Paul Kaplan
Oceanics, Inc.
Plainview, Long Island, New York 11803

Technical Library
Naval Missile Center
Point Mugu, California 93441

Technical Library
Naval Civil Engineering Laboratory
Port Hueneme, California 93041

Commander
Portsmouth Naval Shipyard
Portsmouth, New Hampshire 03801

Commander
Norfolk Naval Shipyard
Portsmouth, Virginia 23709

Professor F.E. Bisshopp
Division of Engineering
Brown University
Providence, Rhode Island 02912

Dr. William A. Gross, Vice President
Ampex Corporation
401 Broadway
Redwood City, California 94063

Dr. H.N. Abramson
Southwest Research Institute
8500 Culebra Road
San Antonio, Texas 78228

Editor
Applied Mechanics Review
Southwest Research Institute
8500 Culebra Road
San Antonio, Texas 78206

Office of Naval Research
San Francisco Area Office
50 Fell Street
San Francisco, California 94102

Library
Pearl Harbor Naval Shipyard
Box 400
FPO San Francisco, California 96610

Technical Library
Hunters Point Naval Shipyard
San Francisco, California 94135

Librarian
Naval Ordnance Laboratory
White Oak
Silver Spring, Maryland 20910

Fenton Kennedy Document Library
The Johns Hopkins University
Applied Physics Laboratory
8621 Georgia Avenue
Silver Spring, Maryland 20910

Professor E.Y. Hsu
Department of Civil Engineering
Stanford University
Stanford, California 94305

Dr. Byrne Perry
Department of Civil Engineering
Stanford University
Stanford, California 94305

Dr. R.L. Street
Department of Civil Engineering
Stanford University
Stanford, California 94305

Professor Milton Van Dyke
Department of Aeronautical Engineering
Stanford University
Stanford, California 94305

Professor R.C. Di Prima
Department of Mathematics
Rensselaer Polytechnic Institute
Troy, New York 12180

Professor J. Lumley
Ordnance Research Laboratory
Pennsylvania State University
University Park, Pennsylvania 16801

Dr. M. Sevik
Ordnance Research Laboratory
Pennsylvania State University
University Park, Pennsylvania 16801

Dr. J.M. Robertson
Department of Theoretical and Applied Mechanics
University of Illinois
Urbana, Illinois 61803

Technical Library
Mare Island Naval Shipyard
Vallejo, California 94592

Code 438
Office of Naval Research
Department of the Navy
Arlington, Virginia 22217 (3)

Code 461
Office of Naval Research
Department of the Navy
Arlington, Virginia 22217

Code 463
Office of Naval Research
Department of the Navy
Arlington, Virginia 22217

Code 472
Office of Naval Research
Department of the Navy
Arlington, Virginia 22217

Code 468
Office of Naval Research
Department of the Navy
Arlington, Virginia 22217

Code 473
Office of Naval Research
Department of the Navy
Arlington, Virginia 22217

Code 481
Office of Naval Research
Department of the Navy
Arlington, Virginia 22217

Code 2627
Naval Research Laboratory
Washington, D.C. 20390 (6)

Library, Code 2620 (ONRL)
Naval Research Laboratory
Washington, D.C. 20390 (6)

Code 6170
Naval Research Laboratory
Washington, D.C. 20390

Code 4000
Director of Research
Naval Research Laboratory
Washington, D.C. 20390

Code 8030 (Maury Center)
Naval Research Laboratory
Washington, D.C. 20390

Code 8040
Naval Research Laboratory
Washington, D.C. 20390

Code 031
Naval Ship Systems Command
Washington, D.C. 20390

Code 0341
Naval Ship Systems Command
Washington, D.C. 20390

Code 03412B (L. Benen)
Naval Ship Systems Command
Washington, D.C. 20390

Code 03412 (J. Schuler)
Naval Ship Systems Command
Washington, D.C. 20390

Code 2052
Naval Ship Systems Command
Washington, D. C. 20390

Code 6034
Naval Ship Engineering Center
Center Building
Prince George's Center
Hyattsville, Maryland 20782

Code 6110
Naval Ship Engineering Center
Center Building
Prince George's Center
Hyattsville, Maryland 20782

Code 6113
Naval Ship Engineering Center
Center Building
Prince George's Center
Hyattsville, Maryland 20782

Code 6114
Naval Ship Engineering Center
Center Building
Prince George's Center
Hyattsville, Maryland 20782

Code 6120E
Naval Ship Engineering Center
Center Building
Prince George's Center
Hyattsville, Maryland 20782

Code 6136
Naval Ship Engineering Center
Center Building
Prince George's Center
Hyattsville, Maryland 20782

Dr. A. Powell
Code 01
Naval Ship Research and Development Center
Washington, D.C. 20034

Mr. W.M. Ellsworth
Code 0H50
Naval Ship Research and Development Center
Washington, D.C. 20034

Central Library
Code L42
Naval Ship Research and Development Center
Washington, D.C. 20034

Dr. W.E. Cummins
Code 500
Naval Ship Research and Development Center
Washington, D.C. 20034

Mr. S.F. Crump
Code 513
Naval Ship Research and Development Center
Washington, D.C. 20034

Mr. R. Wermter
Code 520
Naval Ship Research and Development Center
Washington, D.C. 20034

Dr. P. Pien
Code 521
Naval Ship Research and Development Center
Washington, D.C. 20034

Dr. W.B. Morgan
Code 540
Naval Ship Research and Development Center
Washington, D.C. 20034

Mr. P. Granville
Code 541
Naval Ship Research and Development Center
Washington, D.C. 20034

Mr. J.B. Hadler
Code 560
Naval Ship Research and Development Center
Washington, D.C. 20034

Dr. H.R. Chaplin
Code 600
Naval Ship Research and Development Center
Washington, D.C. 20034

Mr. G.H. Gleissner
Code 800
Naval Ship Research and Development Center
Washington, D.C. 20034

Dr. M. Strasberg
Code 901
Naval Ship Research and Development Center
Washington, D.C. 20034

Mr. J. McCarthy
Code 552
Naval Ship Research and Development Center
Washington, D.C. 20034

Code 03
Naval Air Systems Command
Washington, D.C. 20360

AIR 5301
Naval Air Systems Command
Department of the Navy
Washington, D.C. 20360

Code ORD 03
Naval Ordnance Systems Command
Washington, D.C. 20360

Code ORD 035
Naval Ordnance Systems Command
Washington, D.C. 20360

Code ORD 05413
Naval Ordnance Systems Command
Washington, D.C. 20360

Code ORD 9132
Naval Ordnance Systems Command
Washington, D.C. 20360

Oceanographer of the Navy
Washington, D.C. 20390

Commander
Naval Oceanographic Office
Washington, D.C. 20390

Chief Scientist (CNM PM-1)
Strategic Systems Project Office
Department of the Navy
Washington, D.C. 20360

Technical Division (CNM PM 11-20)
Deep Submergence Systems Project Office
Department of the Navy
Washington, D.C. 20360

Dr. A.L. Slafkosky
Scientific Advisor
Commandant of the Marine Corps (Code AX)
Washington, D.C. 20380

Librarian Station 5-2
Coast Guard Headquarters
NASSIF Building
400 7th Street, S.W.
Washington, D.C. 20591

Office of Research and Development
Maritime Administration
441 G. Street, N.W.
Washington, D.C. 20235

Division of Ship Design
Maritime Administration
441 G. Street, N.W.
Washington, D.C. 20235

National Science Foundation
Engineering Division
1800 G. Street, N.W.
Washington, D.C. 20550

Dr. G. Kulin
National Bureau of Standards
Washington, D.C. 20234

Science & Technology Division
Library of Congress
Washington, D.C. 20540

Chief of Research & Development
Office of Chief of Staff
Department of the Army
The Pentagon, Washington, D.C. 20310

Professor A. Thiruvengadam
Department of Mechanical Engineering
The Catholic University of America
Washington, D.C. 20017

Professor G. Birkhoff
Department of Mathematics
Harvard University
Cambridge, Massachusetts 02138

AIR 604
Naval Air Systems Command
Department of the Navy
Washington, D.C. 20360

Dr. A.S. Iberall, President
General Technical Services, Inc.
451 Penn Street
Yeadon, Pennsylvania 19050

Professor J.F. Kennedy, Director
Iowa Institute of Hydraulic Research
State University of Iowa
Iowa City, Iowa 52240

Professor L. Landweber
Iowa Institute of Hydraulic Research
State University of Iowa
Iowa City, Iowa 52240

Dr. Lee Segel
Department of Mathematics
Rensselaer Polytechnic Institute
Troy, New York 12180

Code 6101E
Naval Ship Engineering Center
Center Building
Prince George's Center
Hyattsville, Maryland 20782